ISSN: 2067-3809

Universitatea Politehnica Timișoara

ACTA TECHNICA CORVINIENSIS – Bulletin of Engineering

Tome XII [2019]
Fascicule 1
[January – March]

Editura POLITEHNICA

Edited by:

UNIVERSITY POLITEHNICA TIMISOARA

with kindly supported by:

THE GENERAL ASSOCIATION OF ROMANIAN ENGINEERS (AGIR) – branch of HUNEDOARA

Editor / Technical preparation / Cover design:

Assoc. Prof. Eng. KISS Imre, PhD.
UNIVERSITY POLITEHNICA TIMISOARA,
FACULTY OF ENGINEERING HUNEDOARA

Commenced publication year:
2008

ASSOCIATE EDITORS and REGIONAL COLLABORATORS

The Editor and editorial board members do not receive any remuneration. These positions are voluntary. The members of the Editorial Board may serve as scientific reviewers.

We are very pleased to inform that our journal ACTA TECHNICA CORVINIENSIS – Bulletin of Engineering is going to complete its ten years of publication successfully. In a very short period it has acquired global presence and scholars from all over the world have taken it with great enthusiasm. We are extremely grateful and heartily acknowledge the kind of support and encouragement from you.

ACTA TECHNICA CORVINIENSIS – Bulletin of Engineering seeking qualified researchers as members of the editorial team. Like our other journals, ACTA TECHNICA CORVINIENSIS – Bulletin of Engineering will serve as a great resource for researchers and students across the globe. We ask you to support this initiative by joining our editorial team. If you are interested in serving as a member of the editorial team, kindly send us your resume to redactie@fih.upt.ro.

ISSN: 2067-3809

INTERNATIONAL SCIENTIFIC COMMITTEE MEMBERS and SCIENTIFIC REVIEWERS

MANAGER & CHAIRMAN

ROMANIA 

Imre KISS, University Politehnica TIMISOARA, Faculty of Engineering HUNEDOARA, Department of Engineering & Management, General Association of Romanian Engineers (AGIR) – branch HUNEDOARA

INTERNATIONAL SCIENTIFIC COMMITTEE MEMBERS & SCIENTIFIC REVIEWERS from:

ROMANIA 

Viorel–Aurel ŞERBAN, University Politehnica TIMIŞOARA – TIMIŞOARA
Teodor HEPUŢ, University Politehnica TIMIŞOARA – HUNEDOARA
Caius PĂNOIU, University Politehnica TIMIŞOARA – HUNEDOARA
Mircea BEJAN, Tehnical University of CLUJ-NAPOCA – CLUJ-NAPOCA
Liviu MIHON, University Politehnica TIMIŞOARA – TIMIŞOARA
Ilare BORDEAŞU, University Politehnica TIMIŞOARA – TIMIŞOARA
Corneliu CRĂCIUNESCU, University Politehnica TIMIŞOARA – TIMIŞOARA
Liviu MARŞAVIA, University Politehnica TIMIŞOARA – TIMIŞOARA
Nicolae HERIŞANU, University Politehnica TIMIŞOARA – TIMIŞOARA
Dumitru TUCU, University Politehnica TIMIŞOARA – TIMIŞOARA
Valer DOLGA, University Politehnica TIMIŞOARA – TIMIŞOARA
Ioan VIDA-SIMITI, Technical University of CLUJ-NAPOCA – CLUJ-NAPOCA
Csaba GYENGE, Technical University of CLUJ-NAPOCA – CLUJ-NAPOCA
Sava IANICI, "Eftimie Murgu" University of REŞIŢA – REŞIŢA
Ioan SZÁVA, "Transilvania" University of BRASOV – BRASOV
Liviu NISTOR, Technical University of CLUJ-NAPOCA – CLUJ-NAPOCA
Sorin VLASE, "Transilvania" University of BRASOV – BRASOV
Horatiu TEODORESCU DRĂGHICESCU, "Transilvania" University of BRASOV – BRASOV
Maria Luminiţa SCUTARU,"Transilvania" University of BRASOV – BRASOV
Iulian RIPOŞAN, University Politehnica BUCUREŞTI – BUCUREŞTI
Ioan DZITAC, Agora University of ORADEA – ORADEA
Daniel STAN, University Politehnica TIMIŞOARA – TIMIŞOARA
Adrian STUPARU, University Politehnica TIMIŞOARA – TIMIŞOARA
Corina GRUESCU, University Politehnica TIMIŞOARA – TIMIŞOARA
Carmen ALIC, University Politehnica TIMIŞOARA – HUNEDOARA

SLOVAKIA 

Štefan NIZNIK, Technical University of KOŠICE – KOŠICE
Karol VELIŠEK, Slovak University of Technology BRATISLAVA – TRNAVA
Juraj ŠPALEK, University of ŽILINA – ŽILINA
Ervin LUMNITZER, Technical University of KOŠICE – KOŠICE
Miroslav BADIDA, Technical University of KOŠICE – KOŠICE
Milan DADO, University of ŽILINA – ŽILINA
Ladislav GULAN, Slovak University of Technology – BRATISLAVA
Ľubomir ŠOOŠ, Slovak University of Technology in BRATISLAVA – BRATISLAVA
Miroslav VEREŠ, Slovak University of Technology in BRATISLAVA – BRATISLAVA
Milan SAGA, University of ŽILINA – ŽILINA
Imrich KISS, Institute of Economic & Environmental Security – KOŠICE
Michal CEHLÁR, Technical University KOSICE – KOSICE
Pavel NEČAS, Armed Forces Academy of General Milan Rastislav Stefanik – LIPTOVSKÝ MIKULÁŠ
Vladimir MODRAK, Technical University of KOSICE – PRESOV
Michal HAVRILA, Technical University of KOSICE – PRESOV

CROATIA 

Drazan KOZAK, Josip Juraj Strossmayer University of OSIJEK – SLAVONKI BROD
Predrag COSIC, University of ZAGREB – ZAGREB
Milan KLJAJIN, Josip Juraj Strossmayer University of OSIJEK – SLAVONKI BROD
Miroslav CAR, University of ZAGREB – ZAGREB
Antun STOIĆ, Josip Juraj Strossmayer University of OSIJEK – SLAVONKI BROD
Ivo ALFIREVIĆ, University of ZAGREB – ZAGREB

GREECE 

Nicolaos VAXEVANIDIS, University of THESSALY – VOLOS

The Scientific Committee members and Reviewers do not receive any remuneration. These positions are voluntary.

We are extremely grateful and heartily acknowledge the kind of support and encouragement from all contributors and all collaborators!

ACTA TECHNICA CORVINIENSIS – Bulletin of Engineering is dedicated to publishing material of the highest engineering interest, and to this end we have assembled a distinguished Editorial Board and Scientific Committee of academics, professors and researchers.

ACTA TECHNICA CORVINIENSIS – Bulletin of Engineering publishes invited review papers covering the full spectrum of engineering. The reviews, both experimental and theoretical, provide general background information as well as a critical assessment on topics in a state of flux. We are primarily interested in those contributions which bring new insights, and papers will be selected on the basis of the importance of the new knowledge they provide.

ACTA TECHNICA CORVINIENSIS – Bulletin of Engineering encourages the submission of comments on papers published particularly in our journal. The journal publishes articles focused on topics of current interest within the scope of the journal and coordinated by invited guest editors. Interested authors are invited to contact one of the Editors for further details.

ACTA TECHNICA CORVINIENSIS – Bulletin of Engineering accept for publication unpublished manuscripts on the understanding that the same manuscript is not under simultaneous consideration of other journals. Publication of a part of the data as the abstract of conference proceedings is exempted.

Manuscripts submitted (original articles, technical notes, brief communications and case studies) will be subject to peer review by the members of the Editorial Board or by qualified outside reviewers. Only papers of high scientific quality will be accepted for publication. Manuscripts are accepted for review only when they report unpublished work that is not being considered for publication elsewhere. The evaluated paper may be recommended for:

- ✓ **Acceptance without any changes** – in that case the authors will be asked to send the paper electronically in the required .doc format according to authors' instructions;
- ✓ **Acceptance with minor changes** – if the authors follow the conditions imposed by referees the paper will be sent in the required .doc format;
- ✓ **Acceptance with major changes** – if the authors follow completely the conditions imposed by referees the paper will be sent in the required .doc format;
- ✓ **Rejection** – in that case the reasons for rejection will be transmitted to authors along with some suggestions for future improvements (if that will be considered necessary).

The manuscript accepted for publication will be published in the next issue of ACTA TECHNICA CORVINIENSIS – Bulletin of Engineering after the acceptance date.

All the authors and the corresponding author in particular take the responsibility to ensure that the text of the article does not contain portions copied from any other published material which amounts to plagiarism. We also request the authors to familiarize themselves with the good publication ethics principles before finalizing their manuscripts

ISSN: 2067-3809

TABLE of CONTENTS

The ACTA TECHNICA CORVINIENSIS – Bulletin of Engineering, Tome XII [2019], Fascicule 1 [January–March], includes scientific papers presented in the sections of:

– The ISB-INMA TEH' 2017 International Symposium (Agricultural and Mechanical Engineering), organized by University "POLITEHNICA" of Bucharest – Faculty of Biotechnical Systems Engineering, National Institute of Research-Development for Machines and Installations Designed to Agriculture and Food Industry – INMA Bucharest, Scientific Research and Technological Development in Plant Protection Institute (ICDPP), National Institute for Research and Development for Industrial Ecology – INCD ECOIND, Research and Development Institute for Processing and Marketing of the Horticultural Products "HORTING" and Hydraulics, Pneumatics Research Institute INOE 2000 IHP, University of Agronomic Sciences and Veterinary Medicine of Bucharest (UASVMB) – Faculty of Horticulture and Romanian Society of Horticulture (SRH), in Bucharest, ROMANIA, between 26–28 October, 2017. The current identification number of the papers are the #11–12, #15–19 and #21–24, according to the present contents list.

Also, the ACTA TECHNICA CORVINIENSIS – Bulletin of Engineering, Tome XII [2019], Fascicule 1 [January–March] includes original papers submitted to the Editorial Board, directly by authors or by the regional collaborators of the Journal.

ISSN: 2067-3809

[1.]Mike GOVERNMENT RABBONI, [2.]Onyekachi Stanley AGU, [3]John Ariyo OLOWOKERE

THE USE OF FLAME OF FOREST POD FLOUR IN HIGH DENSITY POLYETHYLENE COMPOSITE

[1.]Nnamdi Azikiwe University, Faculty of Engineering, Department of Chemical Engineering, Awka, NIGERIA
[2.]Enugu State University of Science & Technology, Faculty of Engineering, Department of Chemical Engineering, Enugu, NIGERIA
[3.]Federal University of Technology, Faculty of Engineering, Department of Chemical Engineering, Minna, NIGERIA

Abstract: Polymer composites are known to have improved outstanding properties compared to pure materials. Polymeric material based composite was compounded from flame of forest pod flour (FFPF) and high density polyethylene (HDPE). The manufactured flame of forest pod flour-high density polyethylene (FFPF-HDPE) composite was studied based on the influence of particle size and content of FFPF on its mechanical properties. The pure HDPE, FFPF and FFPF-HDPE composite was examined using Fourier Transform Infrared (FTIR) to know the functional group/bonds characteristics present. The results obtained from this work shows that the particle size and mass content of FFPF influenced the properties of the FFPF-HDPE composite. With this outcome, this composite can be applied for domestic purposes based on the limit of its properties.
Keywords: FFPF, FFPF-HDPE, mechanical properties, FTIR

INTRODUCTON

Studies have shown that, different natural local fibres which have been neglected over time, are becoming perfect substitute for inorganic fillers for use as reinforcement in composite [1], [2], [3], [4]. Bearing this in mind, it seems most Africa countries are not doing much in following the western world in the drive of converting local resources in their domain into source of wealth. Moreover, the availability of organic fibers in nature will help to reduce the cost of composite production as they also help in complementing the properties of polymer composite [5], [6], [7], [8]. This means that the search for suitable fibers is pivotal to upgrading the performance of fiber-plastic composites which is one of the qualities of a good researcher in solving societal problems. Ultimately, qualities of fiber to be use as an additive are function of internal characterization of the filler [9]. Presently, there are thousands of low cost fibres/fillers found in nature that are wasting away as composite manure and being burnt as a means of fuel for heating and cooking purposes. The burning process discharges emission and pollutants to the environment. It is on this note that the world health organization (WHO) and other environmental agencies are looking for ways to curb this menace. There is much emphasis to utilize these organic fillers as a constituent in polymer composite to create wealth and to reduce environmental challenges. Recently, some of the natural fillers have been explored in polymeric based composites to produce light product at lowest cost which displays comparable specific strength and minimal density than metallic components for domestic and industrial products [10], [11], [12], [13]. A good Plastic composite is a function of filler/fibre composition, aspect ratio of the filler, polymer matrix, chemical modification and the process technology employed [14], [15]. Therefore, particle size distribution and mass content of lignocellulose as presented in this work are the major parameters influencing plastic based composites. Lately, some scholars have carried out tremendous works on how these factors determine the final properties of composite using other natural fibres. Some of them include oil palm [16], walnut shell [17], saw-dust [18], coconut shell [19], corn cob flour [20], raphia palm [21], and peanut shell [22] have been researched into by these researchers in relation to plastic composites. Interestingly, flame of forest plant is found in some residential areas and in the forest as well, but its prospect and potentials has been ignored over the years. It is on this basis that the use of flame of forest pod flour (FFPF) as reinforcement in polymer based composite is researched into as a novel initiative that has not been worked on to the best of my knowledge.

MATERIALS AND METHODS

— FFPF PREPARATION AND SOURCING

The flame of forest pod (FFP) was obtained at Park Avenue G.R.A Enugu. The FFP was dried for 18 hours in the sun. The FFP was subjected to grinding and sieving, respectively. The FFPF was sieved into a particle size distribution of 425 µm, 850 µm and 2000 µm.

— PURCHASING OF HDPE

HDPE was bought in Owada, Onitsha Anambra State.

— COMPOSITE PREPARATION AND TESTING

The HDPE was reinforced by FFPF at 10, 20, 30, 40 percentage by weight and compounded through injection molding machine (HUICHON/5SON10/500×1000 model no.6241 1990/6) at the above three variation particle sizes. The composites manufactured were tested by the aid of universal tensile (BSS1610 model no. 8889) and simple Charpy impact equipments (LOS LOSENHAUSENWERK DUSSELDORFER MASCHINENBAU AG. DUSSELLDORF, model no.17562/1963). The properties determined were ultimate tensile strength, elongation, Young's modulus, Brinell's hardness and impact

strength. These mechanical properties were evaluated based ASTM procedure [23].

— FOURIER INFRA RED TEST (FTIR)

The analysis for FFPF, HDPE and FFPF-HDPE composite was determined using Shimazdu FTIR machine (model no 8400S).

RESULTS AND DISCUSSION

— FTIR CHARACTERIZATION

The FTIR of raw HDPE, FFPF and FFPF-HDPE composite were captured in Figure 1, Figure 2, Figure 3, respectively.

There are many display of OH group found in 3878.73-3362.51 cm^{-1}, 3868.08-3390.34 cm^{-1}, 3616.84-3362.64 cm^{-1}, for Figure 1, Figure 2 and Figure 3, respectively. For the HDPE, FFPF and FFPF-HDPE composite, the transmittance took a shift from 9.589 to 10.38 %, 8.403 to 3.519% and 5.579 to 5.506%, respectively. This is the conditions of the peaks when HDPE and FFPF are in their raw state, and both combinations also leads to the reduction of intensity during the formation of composite as shown in the Figure 1-3.

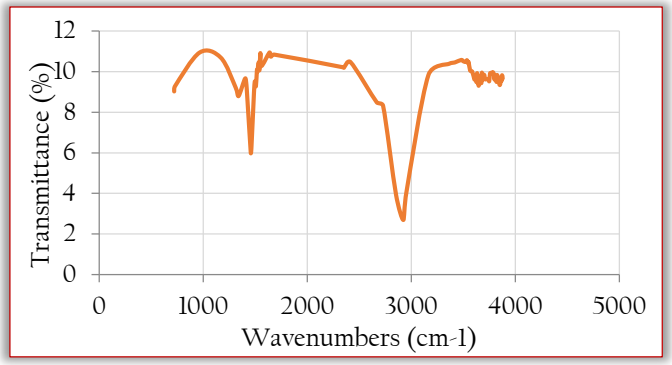

Figure 1. FTIR FOR HDPE

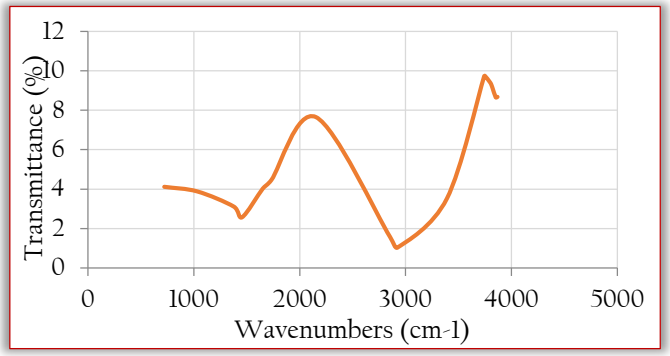

Figure 2. FTIR FOR FFPF

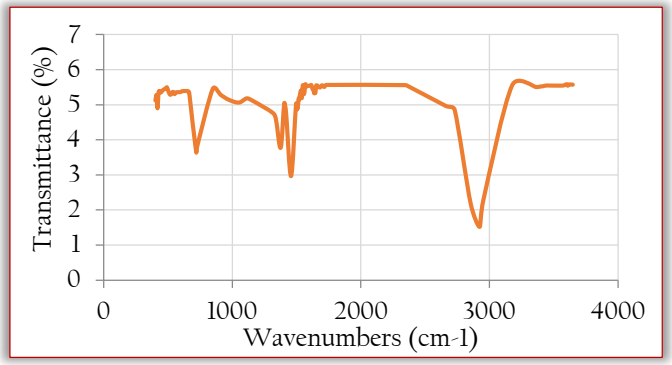

Figure 3. FTIR FOR FFPF-HDPE COMPOSITE

There are crests of the wavelength from 2923.32-2663.97 cm^{-1} that distribute COOH active group for HDPE, FFPF and the composite. The peaks from 2415.79-2145.79 represented P-OH stretching compounds as shown in Figure 1-3.

The Figure 2-3 gives the attribute of C=O stretching aliphatic which transmits from the wavelength of 1732.46 to 1732.86 cm^{-1} at 4.458 to 5.567% during the inclusion of FFPF into HDPE for production of FFPF-HDPE but invisible in Figure 1. The availability for C=O stretching aromatic is discovered at peak of 1698.26-1682.82 cm^{-1} from 10.833 to 5.496% in Figure 1 to Figure 3. The NH_2 bending was domiciled in FFPF to FFPF-HDPE at 1651.63 to 1622.34 cm^{-1} with a displacement in the intensity of transmission, this is totally unavailable in the raw HDPE. The features of the crests dormant at 1645.83-1607.74cm^{-1} formed C=H stretching found in the Figure 1-3. The influence of C-Cl radicals was dominating in the peaks of 592.07-402.3 cm^{-1} in Figure 3 was completely absence in Figure 2 and 1.

— MECHANICAL CHARACTERIZATION OF THE COMPOSITE

Figure 4 (a) shows a graphical description of the impact of the FFPF content and particle size distribution on the tensile strength of FFPF-HDPE composite. The tensile strength of FFPF-HDPE depreciated from the crude HDPE when the FFPF content is added. A similar situation occurred when the FFPF particle size is increased. This reason may be due to the influencing increasing large particle size of FFPF resulting to non-uniform distribution of FFPF and HDPE phase.

Similar report was presented by the following researchers [2], [9], [11]. The elongation of FFPF-HDPE composite variation with FFPF content was also highlighted in Figure 4(b). The incorporation of FFPF content in HDPE thoroughly reduced elongation of the crude polymer. The elongation at breaks of FFPF-HDPE composite was lowest at 2000 µm, followed by 850 µm and 450 µm. This was firmly attributed to bigger size of FFPF particles which will generate more spaces at the union of FFPF and HDPE, thereby reducing the ductility of the composite. This trend was also previously reported by these researches in their works [2], [9], [24].

Figure 4(c) expresses the graphical changes between the tensile modulus of FFPF-HDPE composite and FFPF content. The modulus of elasticity of FFPF-HDPE composite rises as the FFPF content was infused in HDPE. This occurrence is due to the amalgamation of FFPF content into HDPE, causing the FFPF–HDPE composite ductile ability to cutback, leading to the enhancement of the stiffness nature of the composite. Nevertheless, the utmost young's modulus was attained at FFPF size of 850 µm. These were reported as follows [2], [9], [18].

Figure 4(d) describes the impact strength of FFPF-HDPE composite versus the FFPF content. The impact strength of FFPF-HDPE composite absolutely increased as the FFPF content was continuously added in the HDPE matrix with the lessening of the size of FFPF. This attribution is in association of adding FFPF content into polymeric substances, triggering

more energy to formalize cracks promulgation at lower sizes of FFPF. Though, the most Impact strength occurred at minimal size of FFPF. These were related to the trend as reported by previous studies [16], [18], [25], [26]. Figure 4 (e) features Brinell hardness number of FFPF-HDPE composite as a function of FFPF content. It was obviously observed that the insertion of FFPF content in the HDPE generally swells Brinell hardness number of FFPF-HDPE composite by 1107 %, 718 % and 292% as the size of FFPF increases from 425-2000 µm. Conversely, reducing FFPF size favoured the Brinell hardness of FFPF-HDPE composite. The motivation for this trend of results is absolutely due to introduction of FFPF content into HDPE matrix completely resisting the possibility of indentation. Previously, these researchers also discussed this pattern of report [24], [27].

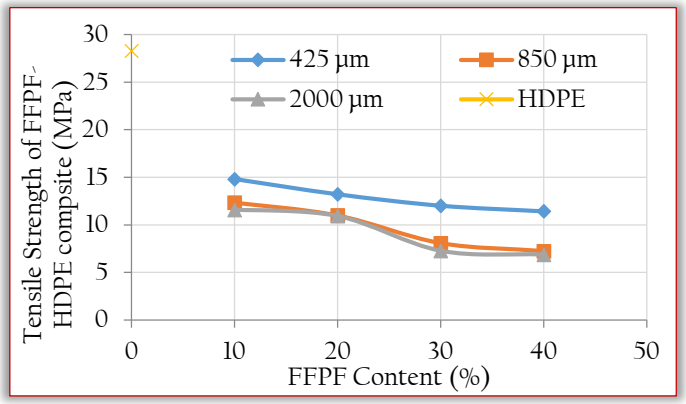

(a)

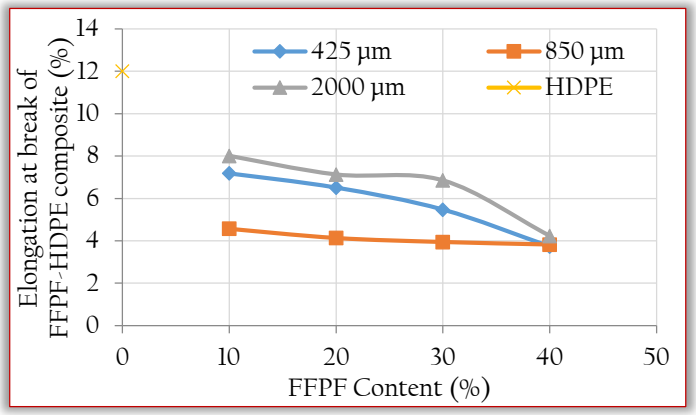

(b)

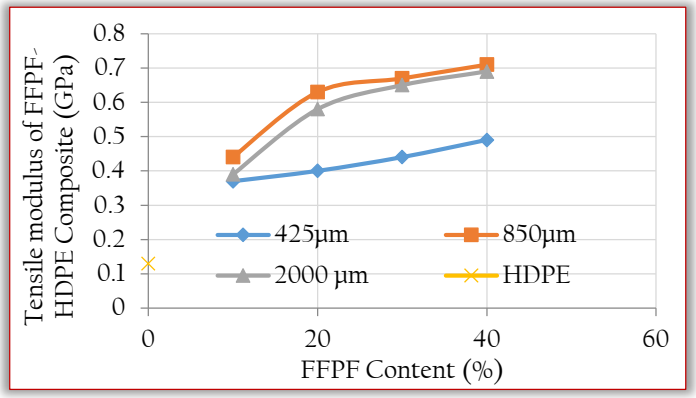

(c)

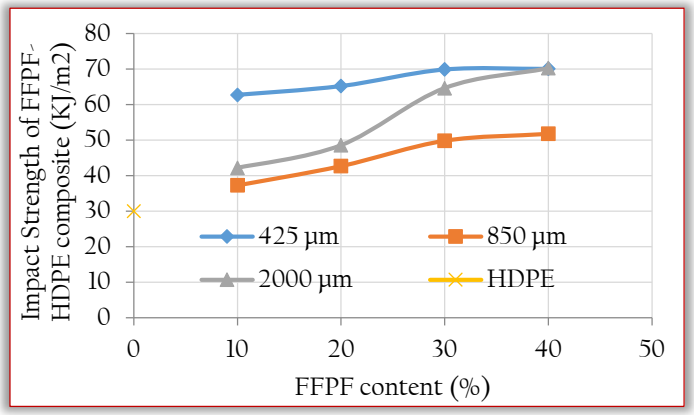

(d)

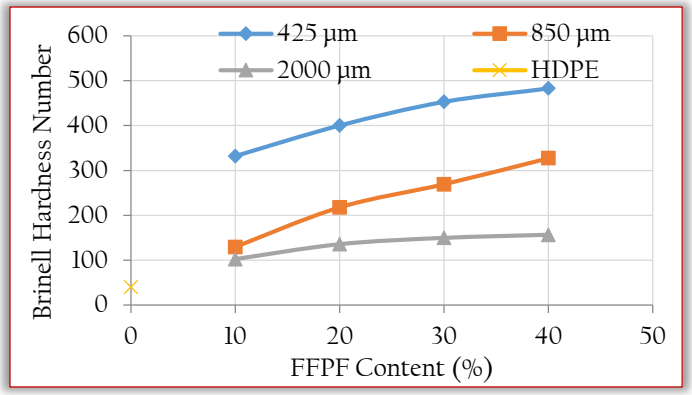

(e)

Figure 4. FFPF content on the (a) tensile strength (b) elongation (c) Young's modulus (d) impact strength (e) Brinell hardness number of FFPF-HDPE composite.

CONCLUSIONS

This novel filler from FFPF was used as a reinforcing agent for the development of FFPF-HDPE composite, and the FFPF was fully exploited in this research. The FTIR analysis of the crude FFPF, HDPE and FFPF-HDPE composite presents distinguishing structural properties for the raw fiber, thermoplastic and the composite, with displaying evidence of changes in transmittances percentage, disappearances of radicals and visible presence of additional new bonds in the output product which is totally absence in the input. The FFPF content and size had a great influence on the mechanical properties of the FFPF-HDPE composite. Specifically, the introduction of FFPF into HDPE polymer has tremendously improved the mechanical-characteristics of FFPF-HDPE composite with exception of elongation and tensile strength. The data and information realized in this work indicates that the composite can be recommended for domestic use.

References

[1] Brent, T; Louis, R; David, G; and Gowrishanker, S: Effect of particle size, coupling agent and DDGS additions on paulownia wood polypropylene composites, Journal of Reinforced Plastics and Composites, Vol.33,(No.14), 1279-1293, 2014,

[2] Obidiegwu, MU.; Nwanonenyi, SC; Eze, IO and Egbuna, IC: The Effect of Walnut Shell Powder on the Properties of Polypropylene Filled Composite, The International Asian Research Journal, Vol.2, (No.1), 22-29, 2014.

[3] Government, RM; Onukwuli, OD and Amechi, AK: Chemically treated avocado wood flour-LLDPE composite, Usak University Journal of Material Sciences, 27-40, 2017.
[4] Ikhlef, S; Nokka, S; Guessoum, M. and Haddaoui, N: Effects of alkaline treatment on the mechanical and rheological properties of low-density polyethylene/Spartium Junceum flour composite, Biocomposite, Vol. 2, 1-7, 2012.
[5] George, J; Sreekala, MS; and Thomas S: A review on interface modification and Characterization of a natural fiber reinforced plastic composites, Journal of Polymer Engineering and Science, Vol.41, (No.9), 1471-1485, 2001.
[6] Wang, X; and Wendy, H: Mechanical properties of irregular fiber (invited review paper)." *International Journal of Engineering-Transactions A: Basics*, Vol.16, (No.1), 99.31, 2003.
[7] Kona, S and L.N.A: Experimental study of the mechanical properties of banana fiber and groundnut shell ash reinforced epoxy hybrid composite, International Journal of Engineering-Transactions A, Vol.31, (No.3), 212-219, 2017.
[8] Khamedi, R; Ahmadi, M; Hashemi, M; and Ahmaditabar, K: Stiffness prediction of beech wood flour polypropylene composite by using proper fiber orientation distribution function, International Journal of Engineering-Transactions A, Vol.31, (No.3), 582-590, 2017.
[9] Hassine, B; Ahmed, K; Patrick, P and Alain, C: Effects of fiber characteristics on the physical and mechanical properties of wood plastic composites," Composite Part A: Applied Science and Manufacturing, Vol. 40, (No.12), 1975-1981, 2009.
[10] Kord, B: Influence of maleic anhydride on the flexural, tensile and impact characteristics of sawdust flour reinforced polypropylene composite, World Applied Sciences Journal, Vol.12, (No. 7), 1014-1016, 2011.
[11] Lee, S; Lee, BH; Kim, HJ, Kim, S and Eom, Y.G: Properties evaluation of bio-composite by content and particle size of bamboo flour," Mokchae Konghak, Vol. 37, (No.4), 310-319, 2009.
[12] Zabihzabeth, S.M: Water uptake and flexural properties of natural filler/pp composites, Bioresource, Vol. 5, 316-323, 2010.
[13] Chanda, B; Kumar, R: and Kumar, KI: Optimization of the mechanical properties of wood dust-reinforced epoxy composite using grey relational analysis, Proceedings of fourth international conference on soft computing for problem solving, 2015.
[14] Netral, B; Sabu, T; Chapal, KD and Rameshwar, A: Analysis of morphology and mechanical behaviours of bamboo flour reinforced polypropylene composites, Nepal Journal of Science and Technology, Vol.13, (No.1), 95-100, 2012,.
[15] Bogoeva-Gaceva, G; Avella, M; Malinconico, M; Buzarovska, A; Grozdanov, A. and Erica, ME; Natural fiber eco-composites, Polymer Composites, Vol.28, (No.1), 98-107, 2007.
[16] Zaini, MJ; Fuad, MYA; Ismail, Z: Mansor, MS and Mustafah, J: The effect of filler content and size on the mechanical properties of polypropylene/oil palm wood flour composites, Polymer International, 0959-8103/96 (Great Britain), 1995.
[17] Obidiegwu, MU; Nwanonenyi, SC; Eze, IO and Egbuna, IC: The effect of walnut shell powder on the properties of polypropylene filled composite, The International Asian Research Journal, Vol.2, No.1, 22-29, 2014.
[18] Stark, NM and Rowlands, RE: Effects of wood fiber characteristics on mechanical properties of wood/polypropylene composites, Wood and Fiber Sciences, Vol.35, (No.2), 165-174, 2003.
[19] Salmah, H; Marliza, M and Tel, PL: Treated coconut shell reinforced unsaturated polyester composites, International Journal of Engineering and Technology, IJET-IJENS, Vol.13, 94-103, 2005.
[20] Obasi, HC: Studies on biodegradability and mechanical properties of high density polyethylene/corncob flour based composites, International Journal of Scientific and Engineering Research, Vol.3, 8-17, 2012.
[21] Obasi, HC: Properties of raphia palm interspersed fiber filled high density polyethylene, Journal of Advances in Material Science and Engineering, Article ID932143, 1-5, 2013.
[22] Obasi, HC: Peanut filled poltetheylene composites; effects of filler content and compatibilizer on properties, Journal of Polymer Science, http//dx.doi.org/10.1155/2015/189289, 1-9, 2015.
[23] ASTM: Annual book of ASTM standard, Vol.8.Philadelphia, PA; American Society for Testing and Materials, 1990.
[24] Nwanonenyi, SC; Obidiegwu, MU; and Onuegbu, GG: Effect of particle size, filler content and compactibilization on the properties of linear low density polypropylene filled periwinkle shell powder, The International Journal of Engineering and Science, Vol. 2, (No.2), 1-8, 2013.
[25] Stark, NM and Berger, MJ: Effect of particle size on the properties of wood flour reinforced polypropylene composites," Fourth International Conference on Woodfiber-Plastic Composite Madison, Wisconsin, USA. May 12-14,134-143, 1997a.
[26] Stark, NM and Berger, MJ: Effect of species and particle size on the properties of wood flour-filled polypropylene composites, In Proceedings: Functional Filler for Thermoplastics and Thermosets. Intertech Conference. San Diego, California December 8-10, 1-16, 1997b.
[27] Atunaya, CU and Nwigbo, S: Evaluation of the mechanical properties of recycled polyethylene/Iroko wood saw dust particulate composites, Journal of Basic Applied Science and Resources, Vol.1, (No.2), 28006-28010, 2011.

ISSN: 2067-3809

[1.]Lissette CONCEPCIÓN MAURE, [2.]Félix Abel GOYA VALDIVIA,
[3.]Norge Isaias COELLO MACHADO, [4.]Elke GLISTAU

METHODOLOGY FOR THE MANAGEMENT OF RISK IN THE STORAGE AND TRANSPORT OF HAZARDOUS SUBSTANCES

[1-3.]Central University "Marta Abreu" from Las Villas, CUBA
[4.]Institute of Materials Flow and Logistics, Otto Von Guericke University, GERMANY

Abstract: The decision making has great importance in the formulation of prevention and recovery policies against technological accidents in the chemical process industry and companies that handle hazardous substances. The main objective of management of technological risks in storage and transport activities along the supply chain, is the search of alternatives to reduce or mitigate the major hazards without eliminating the obtaining of benefits. The objective of this research is to develop a general procedure and its methodological instruments for the management of risks of major accidents in activities of storage and distribution of hazardous substances. It includes multicriteria analysis, risk measurement methods and control tools to identify, characterize and hierarchize the storage areas and distribution routes of greater danger. The application of the procedure enables the reorientation of organizational efforts supported by information technologies and ensures a continuous improvement approach. This research takes as case of practical study the logistics network of Fuel Trading Company of Villa Clara and uses the strategy of multiple explanatory cases in different companies that operate with hazardous substances in the province. As a result, a ranking was obtained of the activities where dangerous substances are manipulated, for the execution of evaluation and mitigation actions.
Keywords: risk management; hazardous substances; multicriteria analysis; control tools

INTRODUCTION

Modern industry is characterized by continuous growth of the unitary power on its plants, to obtain better performance[6]. Regardless of the scientific technical development, the increase in the complexity`s degree of technological processes generates risk conditions in society and natural environment that acts as support for it [1, 7]. Given this reality, the paradigm of technological risk management and the conceptual approach (social, economic and environmental) that underlies it, have evolved from the theoretical point-of-view in a remarkable way [10].

The importance of risks management in the handling of hazardous substances is given by the following aspects: production increase on products of high added value, which require industrialized processes with narrow safety margins [11]; increase of inventories [5]; diversity of distribution routes, change in risk profiles of the supply chain as a result of changes in their business models [9]; population growth that leads to an unplanned urbanization near the industrial sector [12]; the inclusion in the organizational performance of the sustainable development concept [3]; the need to ensure the efficient and optimal allocation of limited resources in processes of evaluation and risk management [12].

On the literature review, the research problem was defined as the lack of a prescriptive theory for analysis of major hazards in logistic activities of storage, processing and distribution of dangerous substances.

The decision making in the logistic processes when hazardous substances are handled requires that the risk is measured and represented by models, maps and indices. These should consider the existing dangers, the vulnerability of the system, the expected physical damage and the possible aggravation of the impact according to social, economic and environmental conditions.

Reference [2, 13] consider that the main objective of the management of technological risks within the logistics process is the search of alternatives to reduce or mitigate the major hazards without eliminating the obtaining of benefits. In this regard, a multicriteria analysis is necessary to manage the uncertainty regarding a threat and the vulnerability of the system. This must be done through a sequence of activities that include the identification of triggering events, prevention and mitigation actions, levels of acceptability, disaster management, governance and transfer.

Despite the importance given by the government, the academic circles and the business sector, Cuba recognizes the lack of a framework that analyzes the complexity of the major technological risks in the supply chains. The absence of a holistic conception and a systemic and continuous improvement approach, which addresses all dimensions of risk management, limits a modification of the situation reflected.

The present research shows a procedure for the management of technological risks in activities of storage and distribution of hazardous substances as support for the decision making process. This document is structured in five sections. In the next section, a research background of the models and indices of evaluation of technological risk, and a discussion about its advantages and limitations is presented. Section 3 proposes a methodology for management of technological risks in logistics processes where hazardous substances are handled. Results and conclusions are presented in section 4 and 5.

RESEARCH BACKGROUND

Several methodologies have been developed to study technological risks in logistics processes. According to different probable risk scenarios and their interaction with the environment, those methodologies have progressed towards a dynamic direction [8].

Technological risk management depends on the measurement of the level of risk associated with the identified hazards. It also depends on the degree of precision with which the variables that condition it and its synergy are determined [11]. The risk profiles should show the existing situation and allow the classification and prioritization of activities.

The choice of risk metrics is critical since it selects the type of information included in the study and legitimizes the results [9]. Consequently, the assessment of risk level must be deployed by various levels of analysis: risk activities, logistics processes and supply chains. Some advantages reported in the reference [3, 4, 11, 13] of use of risk indexes in security management systems are:

- Reducing the complexity of risk management at the company level and make it possible to measure their social and environmental performance. The information is synthesized and expressed by a numerical value including parameters and/or variables of risk management.
- Evaluate and support decisions regarding environmental and social impact allowing the observation of evolution in the time and study trends about disaster situation.
- Fulfillment of accomplish with social and environmental laws.
- Operability of the strategies. It shows the limits for acceptable operations that can lead to better efficiency of process and serve as basis for planning inspections and establishing prevention measures.
- Improvement of performance. It facilitates internal communication and helps to maintain a high degree of awareness about prevention of major accidents. Facilitates the efficient and optimal allocation of limited resources for risk assessment around the classification and prioritization of different scenarios.

Reference [2] states that determining the level of risk requires the use of different mathematical and empirical models. Reference [8] provides an explanatory overview of risk metrics related to the study of major accidents.

At the same time, it shows in most cases these are conditioned to estimate certain variable within the risk assessment process, making it difficult to prioritize the sources of technological risks within a supply chain.

METHODOLOGY TO DETERMINE THE LEVEL OF TECHNOLOGICAL RISK IN LOGISTICS PROCESSES

In this section we will show how to determine the current risk level in the logistics processes. To achieve this goal we will follow the procedure shown in figure 1.

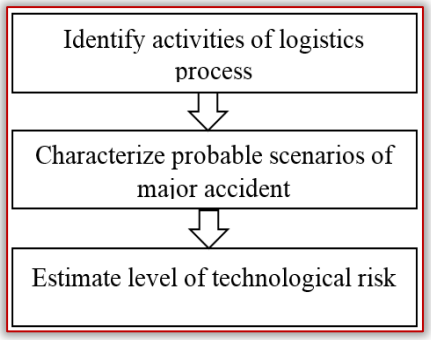

Figure 1. Methodology to determine the level of technological risk

Identify activities of logistics process

This step constitutes the basis to determinate the scenarios of major accident occurrence considering the hazard of technological risk. All activities and relations between different organizations belonging to the supply chain are delimited. Once the flows of existing materials have been analyzed, a unique inventory of hazardous substances is made. This inventory relates all substances with potential to trigger a major accident, causing damage to people (workers and surrounding communities), industrial or public property and environmental components.

The experts will assess the physical-chemical nature of inventoried substances and type of potential damage (explosives, flammable-toxic liquids, and flammable-toxic gases), forms of containment, associated activities (storage, processing, and distribution), possible initiating events, disasters events that can be triggered and routes of propagation.

Characterize probable scenarios of major accident

In this step, the group of experts must establish a sequence of accidents that can be triggered considering the occurrence of an initiating event:

- Spillage of toxic liquids: due to loss of fluid containment, it can generate toxic effects, fires and/or explosions, depending on the nature of the substances.
- Exhaust of gases: due to loss of fluid containment, it can generate toxic effects, fires and/or explosions, depending on the nature of the substances.
- Fire: combustion of multiple forms of the contained or emitted fluids generates harmful thermal radiation, when the substances are flammable.
- Explosion: prior to the emission or after the fire, generates pressure or overpressure waves, and the propagation of projectiles.

The process is supported by the software ALOHA (Areal Locations of Hazardous Atmospheres). This computer program designed for models key hazards-toxicity, flammability, thermal radiation (heat), and overpressure (explosion blast force) - related to chemical releases that result in toxic gas dispersions, fires, and/or explosions. Its chemical library contains information about the physical properties of approximately 1 000 common hazardous chemicals.

ALOHA allows to determinate the radius of affectation in the event of a major accident taking into account: type of substance, form of containment and description of how the chemical is escaping from containment, and weather conditions. The software will display the threat zones in red, orange, and yellow. The red threat zone represents the worst hazard and the orange and yellow threat zones represent areas of decreasing hazard.

Estimate level of technological risk

In this step, the level of technological risk will be assessed in logistics activities. The risk level estimation must quantify the damage caused within the affected radius, delimited in the previous step. A holistic assessment of risk takes into account: 1) the physical damage: number of victims and economic and environmental losses (first-order effects) 2) the conditions related to the social fragility and the resilience lack of communities that favor the occurrence of accident or aggravate the impact of these (second-order effects).

The analytical structure of indicators systems for holistic evaluation of technological risk *(IRT)* in an activity *i* is expressed as the sum for each possible event *e* (fire, explosion, spill, escape), considering their occurrence probability p_e and probable physical consequences C_e within the radius of affectation. It is affected by a coefficient of aggravation of the impact Cai, which depends on conditions of socioeconomic fragility and lack of resilience of the community (equation 1).

$$\mathrm{IRT_i} = (1 + \mathrm{Cai_i}) \sum(\mathrm{p_{ei}} * \mathrm{C_{ei}}) \quad (1)$$

The consequences respond to the determination of the physical damage before an event e in activity i. This is evaluated using the equation 2.

$$\mathrm{C_{ei}} = \sum_{n=1}^{p} \mathrm{w_{XC_{ne}}} * \mathrm{X_{C_{ne}}} \quad (2)$$

where $\mathrm{X_{C_{ne}}}$ represents the physical risk factors, $\mathrm{w_{XC_{ne}}}$ the weights of these factors and p is the total number of factors to be considered in the calculation. We propose the quantification of victim's number, economic losses and environmental damage, with an equivalent weight.

The coefficient of aggravation $\mathrm{Cai_i}$ depends on the weighted sum of a set of aggravating factors in the social, economic, ecological, structural, nonstructural and functional perspective; associated with the fragility of community $\mathrm{X_{FSi}}$ and the resilience lack of context $\mathrm{X_{FRj}}$, being $\mathrm{w_{XFSi}}$ and $\mathrm{w_{XFRj}}$ the weights of each factors.

$$\mathrm{Cai} = \sum_{i=1}^{m}(\mathrm{w_{XFSi}} * \mathrm{X_{FSi}}) + \sum_{j=1}^{n}(\mathrm{w_{XFRj}} * \mathrm{X_{FRj}}) \quad (3)$$

The evaluation results of analysis units are presented in terms of relative indexes of physical risk, socioeconomic fragility, resilience lack of and total risk. The set of descriptors used in the multicriteria evaluation corresponds to qualitative or quantitative data that are derived from previous studies, damage scenarios and socio-economic information of the context to be analyzed.

The descriptors proposal was made based on a bibliographic compilation of risk indicators proposed by other methodologies to assess physical risk, socioeconomic fragilities and resilience lack (table 1).

Table 1. Descriptors of socioeconomic fragility and lack of resilience

Perspective	Descriptors	Criteria
Social	Population density	X_{FS}
	Presence of community areas	X_{FS}
	Level of human development	X_{FR}
	Reaction capacity	X_{FR}
	Perception of risk	X_{FS}
Ecological	Vulnerable environmental receptors	X_{FS}
	Reversibility of damage – recovery	X_{FR}
Economic	Potential losses	X_{FS}
	Financial resilience	X_{FR}
	Institutions within the radius of affectation	X_{FS}
Structural	Physical condition of constructions	X_{FS}
	Nearby facilities that handle hazardous substances	X_{FS}
	Protection of facilities	X_{FS}
	Evacuation system	X_{FR}
	Structural reconstruction	X_{FR}
Not structural	Presence of aggravating non-structural units	X_{FS}
	High density traffic routes	X_{FS}
	Non-structural reconstruction	X_{FR}
Functional	Security practice	X_{FR}
	Emergency plans (internal and external)	X_{FR}
	Operability the emergency	X_{FR}
	Firefighting brigades	X_{FR}
	Hospital services	X_{FR}

These descriptors used in holistic risk assessment have different units. To standardize the gross value of the descriptors, transforming them into commensurable values, must be used transformation functions with the pattern shown is Figure 2.

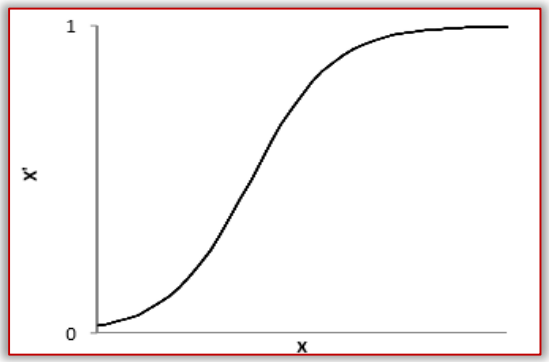

Figure 2: Sigmoidal transformation function for the normalization of risk indicators

The previous function responds to the equation 4.

$$X' = \frac{1}{1 + e^{-\beta\left(\frac{X-m}{M-m} - \mu\right)}} \quad (4)$$

where,
X: Initial value of the indicator
X': Normalized value of the indicator
e: Base of natural logarithm
β: Parameter - slope of the curve
M: Maximum value of parameters (table 1)
m: Minimum value of parameters (table 1)
μ: Point of inflection of the curve
The parameters valuesused for the transformation of each descriptors are obtained from the reference values established by experts, bibliographic review, observations made in major accidents and examination of descriptor statistics along the chain.
The weights of the descriptors represent the relationships of hierarchy (relative importance) in the aggregation process through a multicriteria evaluation. The evaluation of these coefficients is carried out through the analytical hierarchical process (AHP). This is based on the comparison between pairs of descriptors to establish the relative importance (quantitatively). These comparisons generate a matrix that allows to calculate the weight factors and verify the exercise consistency. As a result, we obtain a set of weight factors that are less sensitive to judgment errors.
A network can be generated from a hierarchy by gradually increasing the interconnections. This allows to generate a network, taking into account all existing relationships between levels (perspectives) and between alternatives (descriptors) without assuming the axiom of dependence. At the same time, it generates maps of causal relationships, with a solid mathematical foundation. The figure 3 shows the analytical network modeled in the SuperDecisions software.

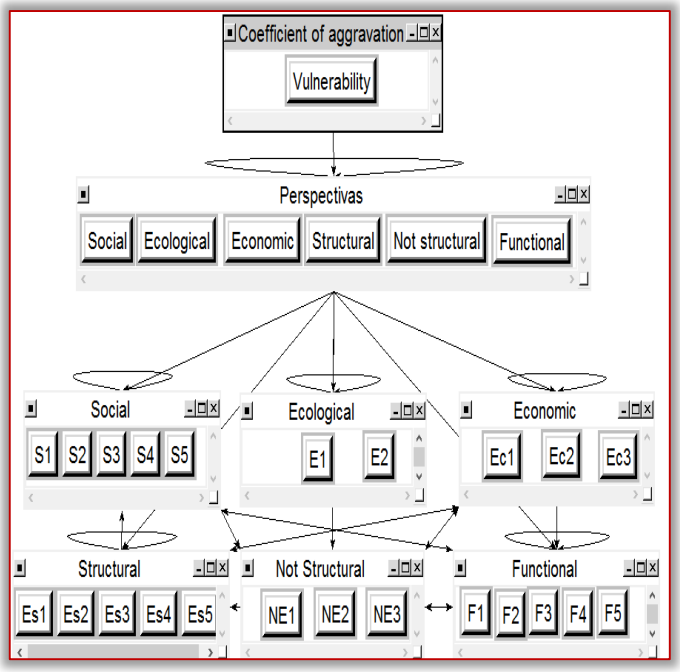

Figure 3: Weight`s network of socioeconomic fragility descriptors and resilience lack descriptors

The table 2 presents the results of application of AHP method.

Table 2: Weight`s coefficients network of socioeconomic fragility descriptors and resilience lack descriptors

Perspective	Weighting coefficient from the perspective	Weighting coefficient	Equivalent Weighting coefficient *WI*
Social	0.240	S1 0.326	0.078
		S2 0.246	0.059
		S3 0.108	0.026
		S4 0.160	0.038
		S5 0.160	0.038
		∑ 1.000	
Ecological	0.124	E1 0.660	0.082
		E2 0.324	0.042
		∑ 1.000	
Economic	0.196	Ec1 0.493	0.098
		Ec2 0.196	0.039
		Ec3 0.311	0.062
		∑ 1.000	
Structural	0.144	Es1 0.215	0.031
		Es2 0.140	0.020
		Es3 0.287	0.041
		Es4 0.252	0.036
		Es5 0.106	0.015
		∑ 1.000	
Not structural	0.078	Ne1 0.493	0.039
		Ne2 0.311	0.024
		Ne3 0.196	0.015
		∑ 1.000	
Functional	0.216	F1 0.326	0.070
		F2 0.143	0.031
		F3 0.212	0.046
		F4 0.108	0.023
		F5 0.212	0.046
		∑ 1.000	
∑	1.000		1.000

RESULTS

In this section the results will be shown according the methodology established in the previous section. This model uses the strategy of multiple explanatory cases in different companies that operate with hazardous substances in the province of Villa Clara. The provincial is subdivided into 13 municipalities, with a total of 124 evaluated facilities.
The inventory of hazardous substances in the province and the evaluation of the activities carried out (storage, processing and distribution) allowed the analysis of 240 potential hazards. The total risk is evaluated in each analysis units as a function of exposure factor, (social, economic and environmental consequences) and the aggravating factor through Equation 1.
The figure 4 shows the results of the evaluation carried out in companies located in Villa Clara, divided by municipalities. In this the possible radio of affectation is delimited, and the evaluation of the level of risk is expressed in low, medium and high scale (green, yellow and red). When comparing the results of technological risk in four possible scenarios of major accident, it is observed that Santa Clara municipalities have

the highest technological risk index. On the other hand, the municipalities of Quemado de Güines, Camajuaní and Ranchuelo are those exposed to a lower level of technological risk. The figure 4-7 shows the affectation radio of different possible accident.

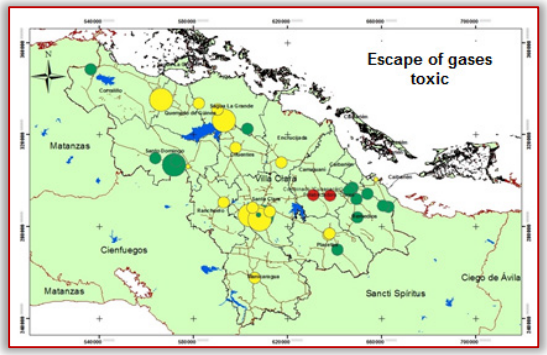

Figure 4: Radio of affectation and level risk. Exhaust of toxic gases[4]

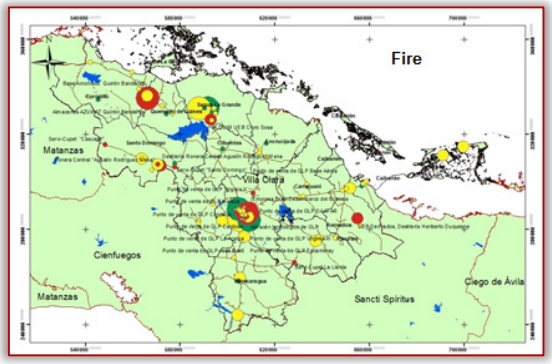

Figure 5: Radio of affectation and level risk. Fire [4]

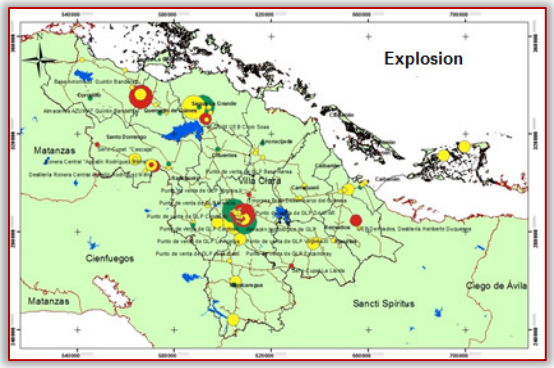

Figure 6: Radio of affectation and level risk. Explosion [4]

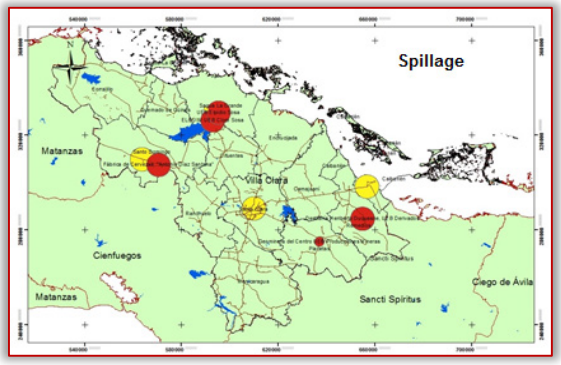

Figure 7: Radio of affectation and level risk. Spillage [4]

This research takes as case study the logistics network in Fuel Trading Company of Villa Clara. This logistics network includes the Fuel Trading Company and the technological warehouse of liquefied petroleum gas (LPG), 53 gas station, 11 stores the sell gas (LPG). These analyzed entities constitute fuel storage and sale centers. This logistics network includes a total of 22 routes by highways and 2 routes by railways.

The highest risk index in storage activities is in the storage area from the Fuel Trading Company, and the most dangerous route is the RFC-02 route corresponding to the transportation of fuel by trains from the Camilo Cienfuegos Refinery in Cienfuegos, to warehouse of the Fuel Trading Company in Santa Clara. This route crosses the center of the town of Cruces, which increases the index of associated vulnerability factor. These results are shown in figure 8 and 9 of technological risk level.

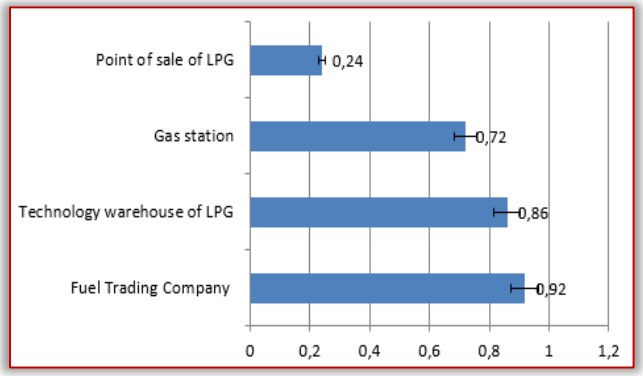

Figure 8: Technological risk index in storage activities [4]

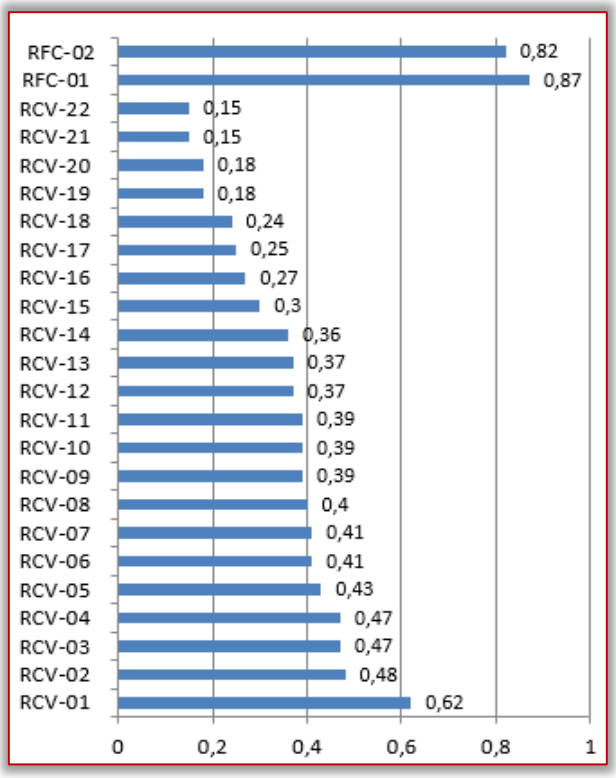

Figure 9: Technological risk index by distribution route [4]

This analysis allows us to index those logistic activities that constitute a major danger in their execution, being necessary to establish disaster prevention and mitigation measures.

CONCLUSIONS

The proposed technological risk index considers the effect of existing physical risk given the occurrence of a destabilizing event, as well as the worsening of the impact due to socioeconomic conditions and the resilience lack of the involved area. It provides a scientific basis for risk-based approach and the development of a proactive culture of prevention, improvement and protection.

The indexing of the technological areas and plants depends on existing risk level in the occurrence of major technological accidents. At same time, facilitates the documentation of involved processes in risk management and decision making for the planning of preventive actions.

The analysis of technological risk level in storage and transport activities supports the decision making process. This analysis is based on the characterization and hierarchization of storage areas and distribution routes of greater danger. The application of the procedure allows the reorientation of the organizational efforts and guarantees an approach of continuous improvement.

References

[1] Abrahamsen, E; Milazzo, M; Selvik, J: Using the ALARP principle for safety management in the energy production sector of chemical industry. Reliability Engineering and System Safe. 169, 160–165, 2018

[2] Arunraj, N: A methodology for overall consequence modeling in chemical industry. Journals of Hazardous Materials, 169, 556–574, 2009

[3] Bellamy, L.: Exploring the relationship between major hazard, fatal and non-fatal accidents through outcomes and causes. Safety Science.71, 93–103, 2015

[4] Concepción, L: Support methodology for decisional assistance in the Technological Risk management process. XI International Conference of Business Sciences. Editorial Samuel Feijóo ISBN: 978-959-312-258-0. Central University "Marta Abreu" of Las Villas, 2017

[5] Fyffe, L: A preliminary analysis of Key Issues in chemical industry accident reports. Safety Science. 82, 368–373, 2016

[6] Gruden, D: Umweltschutz in der Automobilindustrie Motor, Kraftstoffe, Recycling, 2008

[7] Hirst, I.; Carter, D: A "worst case" methodology for obtaining a rough but rapid indication of the societal risk from a major accident hazard installation. Journals of Hazardous Materials, 92, 223–237, 2002

[8] Johansen, I.; Rausand, M: Foundations and choice of risk metrics. Safety Science, 62, 386–399, 2014

[9] Li, C.; Ren, J.; Wang, H: A system dynamics simulation model of chemical supply chain transportation risk management systems. Computers and Chemical Engineering, 89, 71–83, 2016

[10] Marulanda, M.; Cardona, O; Barbat, A: Robustness of the holistic seis-mic risk evaluation in urban centers using the USRi. Journal International Society for the Prevention of Hazards, 49, 501–516, 2009

[11] Meel, A.; Seider, W: Real-time risk analysis of safety systems. Computers and Chemical Engineering, 32, 827–840, 2008

[12] Sujan, M: How can health care organizations make and justify decisions about risk reduction? Lessons from a cross-industry review and a health care stakeholder consensus development process. Reliability Engineering and System Safety, 161, 1–11, 2017

[13] Tixier, J.; Dusserre, G.; Salvi, O.; Gaston, D: Review of 62 risk analysis methodologies of industrial plants. Journal. Loss Prevention Process Industries, 15,291–303, 2002

ISSN: 2067-3809

[1.] P. MANIKANDAN, [2.] Faheem Ahmed KHAN

DETERMINATION OF STRESS ON TURBINE GENERATOR SHAFT DUE TO SUBSYNCHRONOUS RESONANCE USING FINITE ELEMENT METHOD

[1.]Christ (Deemed to be University), Department of EEE, Bangalore, INDIA
[2.]Ghousia College of engineering, Department of EEE, Ramanagaram, INDIA

Abstract: Power Capacitors plays a vital role in reactive power compensation. When the capacitors are connected to the transmission line, it improves the reactive power. Although the reactive power is improved, there is a possibility for sub synchronous resonance created by this capacitors in the transmission line can travel to the generator side. The sub synchronous resonance causes electro-mechanical stress in the generator shaft which ultimately leads to malfunction of the entire system. It is necessary to find out operating modes of the generator and turbine when the line is compensated with capacitors. Once the operating modes are clear, torsion analysis will give the weak points in the turbine generator shaft which is encountered immediately when sub synchronous resonance arises. It is possible to damp the sub synchronous resonance when the weak points are monitored continuously. In this paper, three phase generator is coupled with a prime mover and the line is compensated with the series capacitors. The stress on the turbine is analyzed based on the torque of two rotating machines. Finite element method gives the weak points in the turbine generator shaft system.

Keywords: finite element method, ANSYS, Capacitors, fatigue, MATLAB, shaft, series compensation

INTRODUCTION

Misalignment of shafts in the turbine generator system is one among the most common trouble of any drives in a power generating station. Alignment of shaft without any deviation is not practical to achieve since it handles a several tons of mass on it. Couplings connected to the shaft creates parallel and angular misalignment, in several cases it may also create axial and lateral misalignment.

Cost of operating a turbine during the tenure is compared with the power generation. Most of the industry follows reactive maintenance where they fix the system when it breaks and preventive maintenance where the operator follows the manual. In order to operate the power generating unit, predictive maintenance is preferred [1]. Natural frequency of the rotating machine with mechanical load is not constant and the frequency which is calculated is not accurate [2]. When the pulsating torque arises in the system, it leads to increasing stress in the shaft of the turbine generator.

Weak points in the shafts get damages first and further torque will result in permanent damage. It is ideal to have a method which offers a technical and logical solution to monitor the operation of the turbine which will focus on the alignment. Misalignment arises in the system due to several reasons, one such reason is sub synchronous resonance which comes in to the system due to the series compensation which is essential to have the reactive power under control.

Series capacitors connected in the power transmission line to compensate the reactive power requirement. The high-power capacitors are rated up to 100MVAR till 132kV transmission line [3]. When these high rated capacitors are connected to the transmission line, it injects a frequency into the transmission line which can be either sub synchronous frequency or super synchronous frequency.

Several literature survey have recorded that sub synchronous resonances arises in both the generator terminal and also at substation. The main objective of this research is focused on determining the weak points in the shaft which connects turbine generator system when it has pulsating torque due to the addition of series capacitors. Experiments are carried over on two rotating mass having electrical load and series capacitors.

SIMPLIFIED SHAFT ASSEMBLY MODEL

In a large-scale machine, there is a coupler connected between the generator and the turbine. In case of thermal power plants, the turbines are separated based on the load that takes from the system. High pressure turbine, low pressure turbine and intermediate pressure turbine are involved in the power generation. Including the generator and exciter, there are six masses in the total turbine shaft system.

When the shaft is loaded with external torque, decoupled Newton's law can be applied to explain the system and circumstances [7]. So even for a small torque, the amplitude will increase over time. Figure 1 represents a simplified shaft model and Figure 2 represents the experimental set up which is analogous to the same model represented in figure 1.

If there is no damping or enough protection, the shaft will be stressed more and it gets damaged. It can be extended when the system has multiple masses especially in thermal power plants and hydro power plants. Figure 2 represents two rotating mass in the experimental set up.

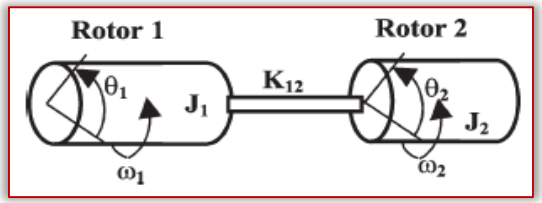

Figure 1. Simplified flexible shaft with two rotors

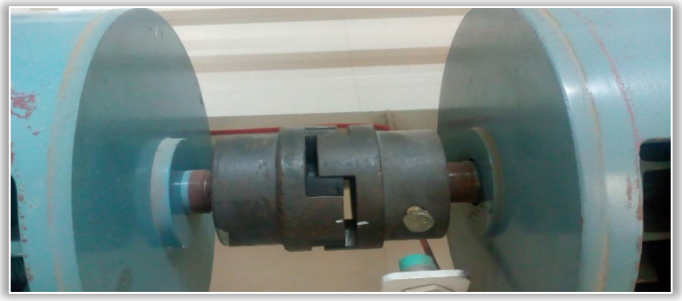

Figure 2. Experimental set up for stress determination

EXPERIMENTAL SETUP

In this research paper, experimental set up denotes generation of power using a turbine. The generated power is transferred the load. Capacitors are added to the system to compensate the reactive power. It is clear from the experimental set up, Generation, Transmission, Distribution and Reactive power compensation is covered in the experiment. The machines are not high power machines which are used in the power plants and it is not possible to test in the machine which is online in the power system. To overcome the problem, a prototype is made in the laboratory using low power machines. Setup consists of a two rotating machines, resistive load and capacitors the ratings of the machines are given in table 1.

Figure 3. Experimental set up

Table 1: Machine Parameters

Machine 1		Machine 2	
Source	AC	Source	DC
Output power	2.2kW	Output power	3.7kW
Max speed	1500rpm	Max speed	1500rpm
Voltage (Max)	415V AC	Voltage (Max)	220V DC
Current (Max)	4A	Current (Max)	19A
Insulation class	F	Insulation class	F

The two rotating machines are connected through the same shaft using a coupler. The shaft is made of stainless steel and the coupler is made with galvanized iron.

The coupler ensures that misalignments in the machines are minimum. It also helps in transmission of mechanical power and torque between the two rotating shafts. DC motor in the system drives the three-phase synchronous generator. When the dc excitation is given to the synchronous generator, it starts generating power. The electric power is transferred to the load. Capacitors are connected to the system to improve the reactive power requirement [6].

The experimental results are tabulated in table 2. The experimental results show that the torque produced in the machine keeps increasing when the compensation increases. Increase in torque causes more stress on the shaft which leads to misalignment.

Table 2. Output parameters –i

Results				
Degree of compensation (%)	Voltage induced (volts)	Current generated (amps)	Speed of the shaft (rpm)	Torque induced in the machine (Nm)
10%	448	2.1	1543	3821
20%	481	3.4	1560	7643
30%	514	3.8	1597	9461
Predicted results (ratio method)				
40%	547	4.2	1627	10981
50%	607	4.5	1786	12234

As the compensation increases, torque produced by the machine increases. Since the machine is given F class insulation [4], the temperature rise must not go beyond 155 degree Celsius. The compensation in any transmission line will be in the range of 10%-70%. Line current increases by 42% for every 10% increase in the compensation. The synchronous generator in the experimental setup is rated till 4 amperes. It was not possible to increase the compensation by more than 30%. Based on the linear range of increase the torque, current and speed was predicted.

During the operation, it was identified that the illumination of the lamp increases as well as the vibration in the machine mounts increases when the compensation increases. Since the work of the turbine is done by the DC Motor, the stress on the motor increases even for 10% compensation. Brush in the Dc motor started giving sparks when the compensation increases beyond 30%.

SIMULATION RESULTS & DISCUSSION

Finite element method started with analyzing static, deformation and elastic problems. Technology has improved which made finite element method to analyze the dynamic problems where both vibration and transient condition are studied in the system. It is used to study the fluid flow and heat transfer in various non-structures. In finite element method, the simulation is carried on large structures which have complex geometry.

The simulation software breaks the complex structure into tiny parts that interacts which each other. Modelling of the static or dynamic structure is the first step in the analysis. Boundary conditions are marked and the equilibrium equations are solved. From the values of the nodal displacement, the stress and strain are analyzed. In this research paper ANSYS software package is used for modelling and analysis for the parameters identified in the experimental set up. The shaft which connects the two machines in the experimental set up is modelled in SOLID WORKS with the exact dimension. The coupler is designed in such a way it improves mechanical strength and also it automatically adjust the misalignment.

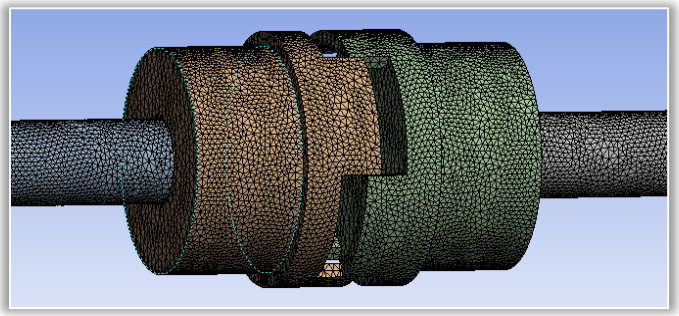

Figure 4. Meshing of the coupler

Material property of stainless steel is given as input while modelling in the SOLIDWORKS. The model is tested for the total deformation, equivalent elastic strain, equivalent stress & strain energy. It is clear from the results, the stress and the strain in increasing when the torque is increasing. Experimental results shows that when the compensation increases, torque between the two running machine increases. Minimum deformation occurs in the coupler as it enhances the mechanical strength and it damps the misalignment when the rotating shaft deviates from the equilibrium. Figure 5 shows that the equivalent stress on the coupler is minimum when compared to the shaft and damage caused by series compensation directly impact the shaft more when compared to coupler. The weak points in the entire set up will have more stress when compared to others.

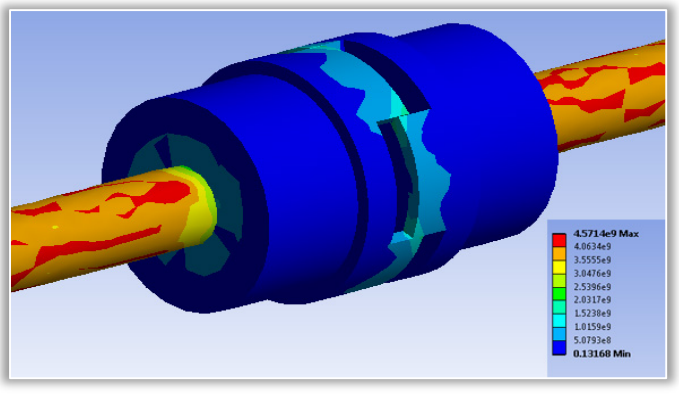

Figure 5. Equivalent stress on the coupler when torque 12234 N.m

Figure 6 shows the equivalent stress happening between the rotating mass and the point which connects the shaft and rotating mass. The stress originates from the center of the circular rotating mass and flows circularly towards the edge. The shaft which connects the rotating mass gets more stresses when compared to the rotating mass.

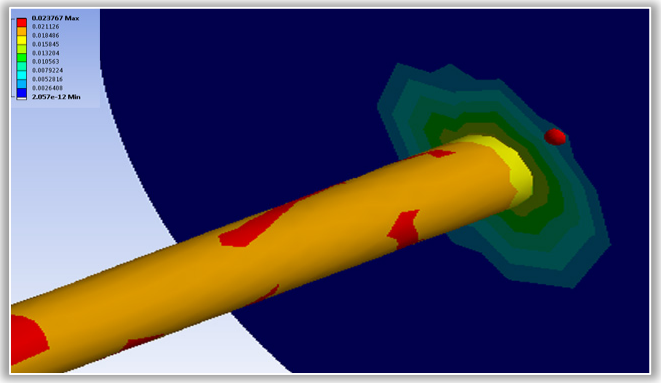

Figure 6. Equivalent stress on the rotating shaft of the generator

Table 3. Output parameters –II

Torque	Total deformation		Equivalent elastic strain	
	Maximum	Minimum	Maximum	Minimum
3821	$1.772e^{-5}$	$1.4493e^{-15}$	.00742	$6.424e^{-13}$
7643	$3.546e^{-5}$	$2.899e^{-15}$	.01484	$1.285e^{-12}$
9461	$4.389e^{-5}$	$3.588e^{-15}$	.01838	$1.590e^{-12}$
10981	$5.094e^{-5}$	$4.165e^{-15}$	.02133	$1.843e^{-12}$
12234	$5.676e^{-5}$	$4.640e^{-15}$	.02376	$2.057e^{-12}$

Table 4. Output parameters –III

Torque	Equivalent stress		Strain energy	
	Maximum	Minimum	Maximum	Minimum
3821	$1.427e^{9}$	.04112	2.5129	$4.79e^{-21}$
7643	$2.855e^{9}$	.08226	10.054	$1.91e^{-20}$
9461	$3.535e^{9}$	.10183	15.406	$2.94e^{-20}$
10981	$4.103e^{9}$	.11819	20.754	$3.96e^{-20}$
12234	$4.571e^{9}$	.13168	25.761	$4.91e^{-20}$

CONCLUSION

Capacitors are used in transmission lines for reactive power compensation. When capacitors are connected along the line, it leads to resonance. Resonance in the line may create sub synchronous frequency or super synchronous frequency which leads to fatigue in the turbine generator shaft system. In this research paper, an experimental set up which demonstrates generation, transmission and distribution with low power rated machine is experimented. Capacitors are connected for reactive power management.

It is observed that the capacitors improve the reactive power and at the same time it causes stress in the turbine generator shaft system due to the frequency change in between the turbine and generator. The vibration caused in the turbine generator mount increases when the capacitors are added to the line. These vibrations are the result of the frequency mismatch.

The torque which is obtained in the experimental set up is analysed using finite element method. It shows that the

coupler in the machine helps in improving the misalignment and continuous operation may lead to severe damage in the turbine generator shaft system.

Acknowledgement

The authors are grateful to Christ (Deemed to be) University – Department of EEE, Faculty of engineering for providing the laboratory facilities and Department of EEE, Ghousia College of engineering Ramanagaram (Affiliated to Visvesvaraya Technological University), Karnataka India.

References

[1] S. Sim, W. So and H. G. Yeh, "Real-time Monitoring of Wind Turbine Generator Shaft Alignment using Laser Measurement", 2nd International Through-life Engineering Services Conference- Springer, 2013 pp. 291 – 295.

[2] J. Song-Manguelle, J. M. Nyobe-Yome and G. Ekemb, "Pulsating Torques in PWM Multi-Megawatt Drives for Torsional Analysis of Large Shafts," in IEEE Transactions on Industry Applications, vol. 46, no. 1, pp. 130-138, Jan.-Feb. 2010

[3] M. Hernandez, J. L. Guardado, V. Venegas, E. Melgoza and L. Rodriguez, "Analysis of the torsional modes of the turbine-synchronous generator group," 2008 IEEE/PES Transmission and Distribution Conference and Exposition: Latin America, Bogota, 2008, pp. 1-7.

[4] T. Sebastian, "Temperature effects on torque production and efficiency of PM motors using NdFeB magnets," Conference Record of the 1993 IEEE Industry Applications Conference Twenty-Eighth IAS Annual Meeting, Toronto, Ont., 1993, pp. 78-83 vol.1

[5] Adrees and J. V. Milanović, "Optimal Compensation of Transmission Lines Based on Minimisation of the Risk of Subsynchronous Resonance," in IEEE Transactions on Power Systems, vol. 31, no. 2, pp. 1038-1047, March 2016

[6] N. Aspragathos and A. D. Dimarogonas, "Fatigue damage of turbine-generator shafts due to fast reclosing," in IEE Proceedings C - Generation, Transmission and Distribution, vol. 129, no. 1, pp. 1-9, January 1982.

[7] Assenkamp, R. Hoffmann, C. Kreische and S. Exnowski, "Simulative analyses of dynamical behavior of steam-powered turbo generators during power system incidents with a higher rate of change of frequency," IET International Conference on Resilience of Transmission and Distribution Networks (RTDN 2017), Birmingham, 2017, pp. 1-6

[8] Liu C, Jiang D. "Fatigue Damage Evaluation of Turbine Generator Due to Multi-Mode Sub Synchronous Oscillation" ASME. International Design Engineering Technical Conferences and Computers and Information in Engineering Conference, Volume 3: 30th Computers and Information in Engineering Conference, Parts A and B

[9] T. Maricic, D. Haber and S. Pejovic, "Standardization as Prevention of Fatigue Cracking of Hydraulic Turbine-Generator Shaft," 2007 IEEE Canada Electrical Power Conference, Montreal, Que., 2007, pp. 103-110.

[10] IEEE Sub synchronous resonance working group, "Second benchmark model for computer simulation of sub synchronous resonance," IEEE Transactions on Power Apparatus and Systems, vol. PAS-104, no. 5, 1985, pp. 1057-1066.

[11] IEEE Sub synchronous resonance working group, "Terms, definitions and symbols for sub synchronous resonance oscillations" IEEE Transactions on Power Apparatus and Systems, vol. PAS-104, no. 6, 1985, pp. 1326-1334.

[12] IEEE Sub synchronous resonance working group, "Readers guide to sub synchronous resonance oscillations" IEEE Transactions on Power Apparatus and Systems, vol. no. 7, 1992, pp. 150-157.

[13] P. Kundur, Power System Stability and Control. New York, NY, USA: McGraw-Hill, 1994

[14] Padiyar K.R, Power System Dynamics: Stability and Control, BS Publications, 2002

ISSN: 2067-3809

[1.]Habib BENBOUHENNI

SIX SECTORS DTC CONTROL OF IM DRIVES BASED ON ANN WITH REGULATION SPEED USING ANFIS CONTROLLER

[1.]Ecole Nationale Polytechnique d'Oran Maurice Audin, Oran, ALGERIA

Abstract: In this paper, an adaptive neuro fuzzy inference (ANFIS) based neural direct torque control (DTC-ANN) controlling of an induction machine (IM) is proposed. In this method control the Artificial Neural Network (ANN) used to replace the switching table and the speed of the IM is controlled by using the ANFIS controller. The entire proposed system is implemented in MATLAB/SIMULINK environment. And simulation results are also presented to demonstrate the attractive performance of the proposed ANFIS based DTC-ANN speed control of the induction machine. The comparison between proposed scheme control and classical DTC, show the proposed control reduced the torque ripple, stator flux ripple and Total Harmonic Distortion value (THD) of stator current of IM drives.

Keywords: IM, DTC, ANFIS, ANN, THD

INTRODUCTION

Adaptive neuro-fuzzy inference system (ANFIS) is the grouping of artificial neural network (ANN) and fuzzy logic regulator (FLC). This mixture combination enables to decrease the difficulty of power intelligent structure [1]. In the designed ANFIS system, ANN techniques are used to choose a proper rule base, which is achieved by the back propagation algorithm.

This incorporated approach improves the classification performance. Cost-effectiveness, efficiency, dynamism, reliability of the designed regulator [2].

Since, the IM has been widely used in industry due to its relative cheapness, low maintenance and high reliability [3]. The apparition of the field oriented control (FOC) made IM drives a most important candidate in high performance motion command applications. However, the difficulty of FOC algorithms led to the development in recent years of many studies to find out diverse solutions for the IM command having the features of exact and rapid torque response. The DTC command proposed by I. Takahashi and M. Depenbrock in the mid-eighties has been standard to be a viable solution to attain these requirements [4].

DTC command is characterized by its simple realization and a quick dynamic response. In addition, the inverter is directly regulated by the algorithm, i.e. a modulation method for the inverter is not needed. The major advantages of DTC command are absence of coordinate conversion and current controller, absence of divide voltage modulation block [5]. Though, DTC has high dynamic performance, it has few drawbacks such as high undulation in torque, flux, current and variant in switching frequency of the inverter [6].

This paper is presented a neural direct torque command of IM using PI controller based on ANFIS regulator. ANFIS neural direct torque control is used to improve dynamic response performance and decrease the ripples of stator flux, torque and THD value of stator current.

DIRECT TORQUE CONTROL SCHEMA

It is well recognized that DTC command operators to command the stator flux and the torque directly by selecting the parallel inverter switching situation [7]. The DTC command consisted of torque and flux controllers (hysteresis controllers), electromagnetic torque and flux estimator and switching table. It is very much simpler than the vector command system due to the existence of synchronize conversion between immobile frame and synchronous frame and PI regulators [8]. Figure 1 shows a simple structure of the classical DTC for IM drives.

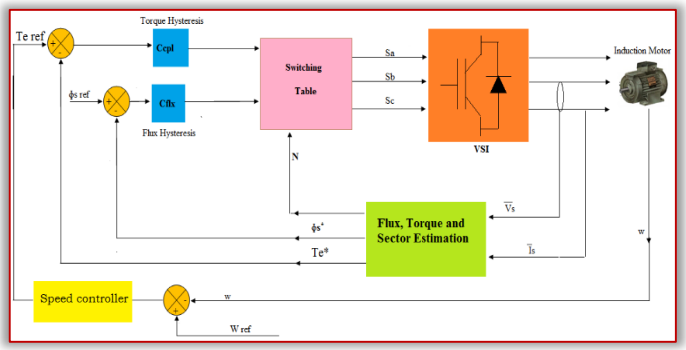

Figure 1. Basic DTC control scheme for IM.

The flux can be evaluated by integrating from the stator electrical energy equation [9]:

$$\Phi_S = \int_0^t (v_S - R_S i_S)dt \quad (1)$$

The electromagnetic torque is expected from the stator flux and stator current information as:

$$Te = \frac{3}{2} p\left[\Phi_{s\alpha} i_{s\beta} - \Phi_{s\beta} i_{s\alpha}\right] \quad (2)$$

The flux angle θs is calculated by:

$$\theta_S = \operatorname{arctg}\left(\frac{\Phi_{\beta s}}{\Phi_{\alpha s}}\right) \quad (3)$$

A two-level conventional electrical energy inverter can attain 7 divide positions in the phase corresponding to the 8 sequences of the electrical energy inverter. These positions are illustrated in Figure 2. In the accumulation, Table. 1 shows the sequences for each situation, such as: Si= 1,…,6, Si are the areas of localization of stator flux vector [10].

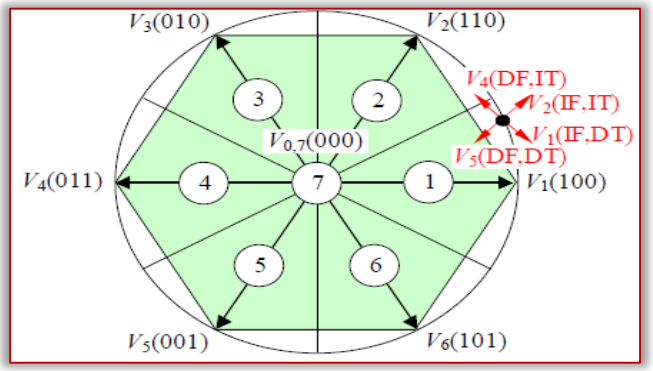

Figure 2. Different vectors of stator voltages provided by a two levels inverter, (100): (1: inverter switch is ON, 0: for OFF) I(D) F: increase (decrease) of flux magnitude, I(D) T: increase (decrease) of torque

TABLE 1. SWITCHING TABLE FOR CLASSICAL DTC WITH ZERO VOLTAGE

N							
Cflx	Ccpl	1	2	3	4	5	6
1	1	2	3	4	5	6	1
	0	7	0	7	0	7	0
	-1	6	1	2	3	4	5
0	1	3	4	5	6	1	2
	0	0	7	0	7	0	7
	-1	5	6	1	2	3	4

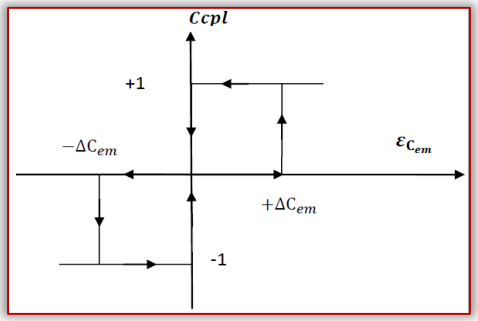

Figure 3. Torque hysteresis comparator

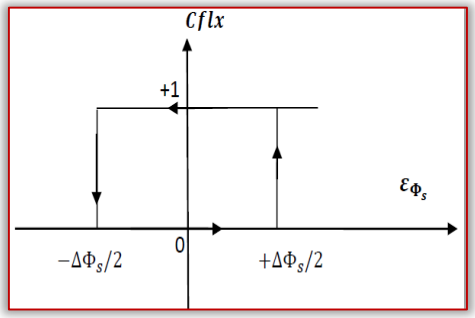

Figure 4. Flux hysteresis comparator.

Figures 3 and 4 illustrate the torque and stator flux controllers, respectively. The output of torque hysteresis comparator are (-1, 0, 1) and the output of stator flux hysteresis comparator are (0, 1).

DTC-ANN CONTROL WITH ANFIS SPEED CONTROLLER

The essential of DTC-ANN command with ANFIS speed regulator for IM drives is shown in Figure 5. ANN have self-adapting compatibilities which makes them well suited to handle non-linarites, uncertainness and parameter modifications. A multilayer feed forward ANN constructs a global expertises to non- linear input-output mapping. ANN are capable of generalization in regions of the input space, where little or no training data are available [11]. The principle of ANN techniques DTC command is similar to traditional DTC command. However, the switching table is replaced by the ANN controller.

The structure ANN has three layers. Input layer has 3 neuron, output layer has only 3 neuron and hidden layer has 30 neurons.

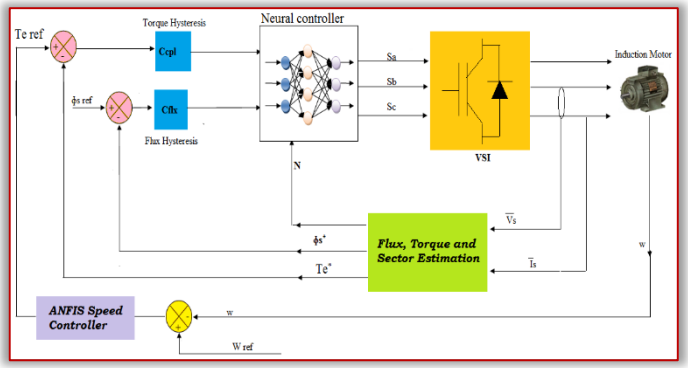

Figure 5. DTC-ANN with ANFIS speed controller.

The construction of the proposed ANN used in this command, is shown in Figure 6.

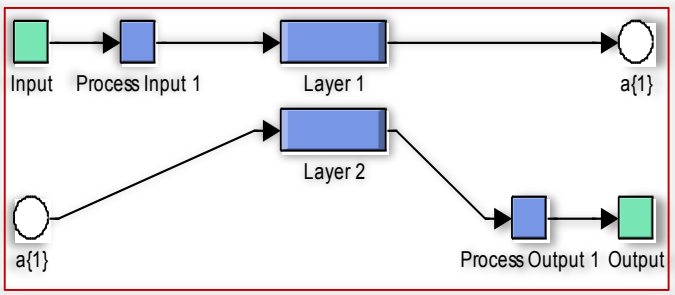

Figure 6. Structure of proposed artificial neural networks

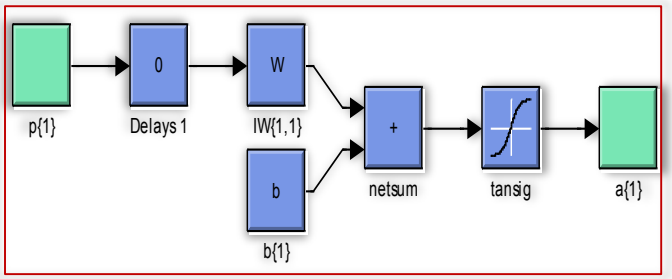

Figure 7. Structure of layer 1

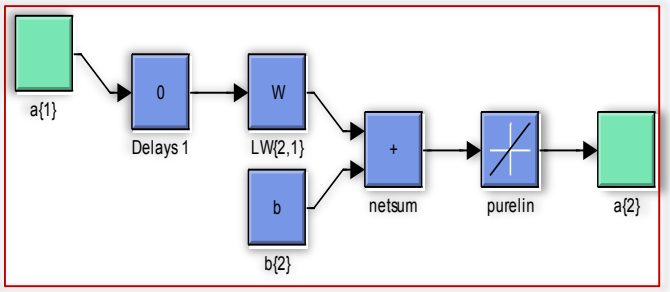

Figure 8. Structure of layer 2

In this paper, the PI controller of speed is replaced by the ANFIS regulator. The Adaptive Neuro-Fuzzy Inference System (ANFIS) controller is one of the popular neuro-fuzzy techniques that is the mixture combination of ANN and is based on Takagi–Sugeno fuzzy inference system (FIS) [12]. The ANFIS is urbanized using Matlab ANFIS editor [13]. The block diagram for ANFIS based PI regulator is shown in Figure 9.

Then the designed ANFIS has 2 inputs namely, the reference speed (w ref) and speed of motor (w) while the output is the Cem ref. The construction of ANFIS PI regulator is shown in Figure 10.

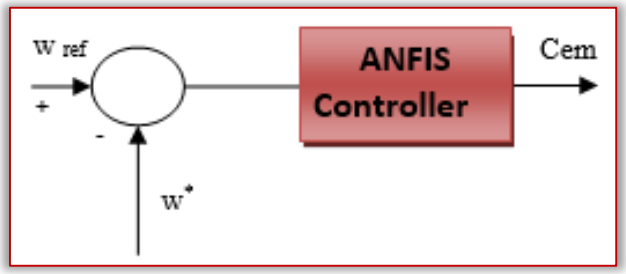

Figure 9. ANFIS control of PI regulator

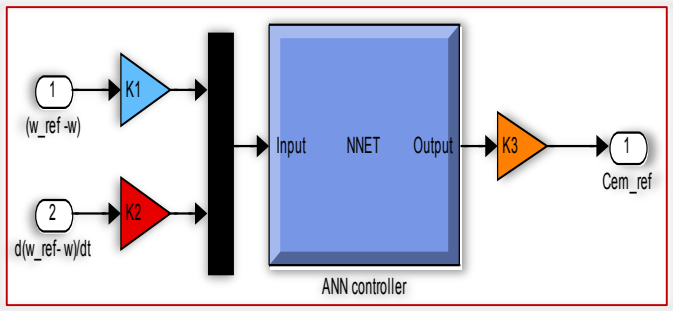

Figure 10. ANFIS construction for PI regulator.

Table 2. Fuzzy rules of speed regulator

e / Δe	NL	NM	NP	EZ	PS	PM	PL
NL	NL	NL	NL	NL	NM	NP	EZ
NM	NL	NL	NL	NM	NP	EZ	PS
NP	NL	NL	NM	NP	EZ	PS	PM
EZ	NL	NM	NP	EZ	PS	PM	PL
PS	NM	NP	EZ	PS	PM	PL	PL
PM	NP	EZ	PS	PM	PL	PL	PL
PL	EZ	PS	PM	PL	PL	PL	PL

The fuzzy regulator design is based on connaissance and simulation. These values compose a training set which is used to obtain the table rules [14]. On possible initial rule base, that can be used in drive systems for a fuzzy regulator, consist of 49 linguistic rules, as shown in Table 2 [15, 16], and gives the change of the produit of fuzzy regulator in borne of two input: the error (e= w_{ref} – w) and change of error (Δe).

SIMULATION RESULTS

The simulations of the neural DTC with ANFIS regulator of IM drive are compared with classical DTC command. A 3-phase, 1MW, 3 pole, IM with parameters of Rs=0.228Ω, Rr=0.332Ω, Ls=0.0084H, Lr=0.0082H, Lm=0.0078H, J=20 Kg.m2 are considered.

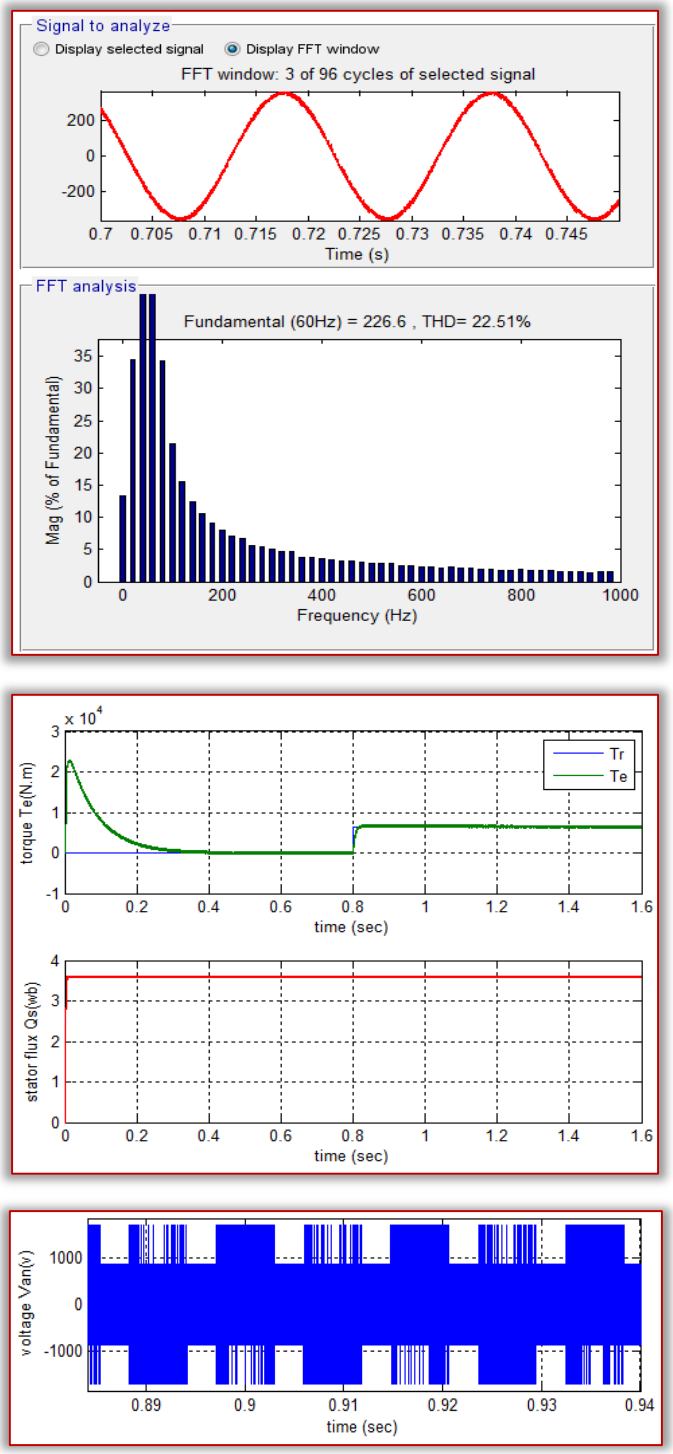

Figure 11. Performances of classical DTC command

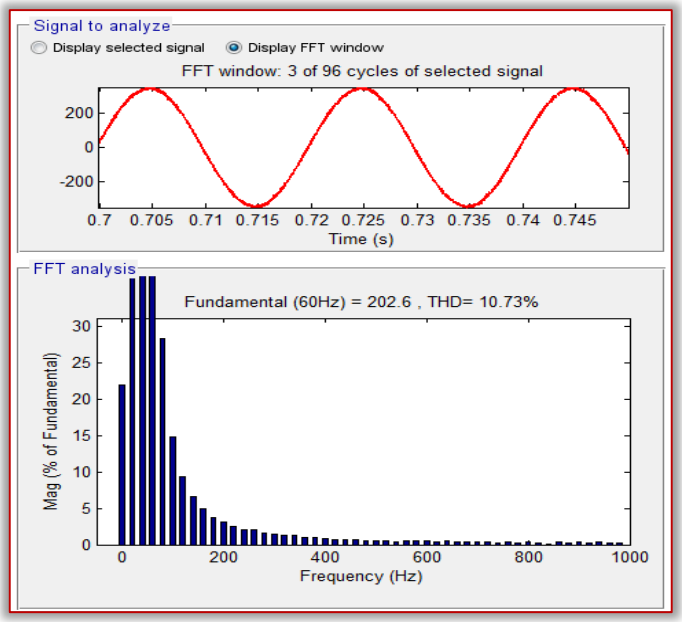

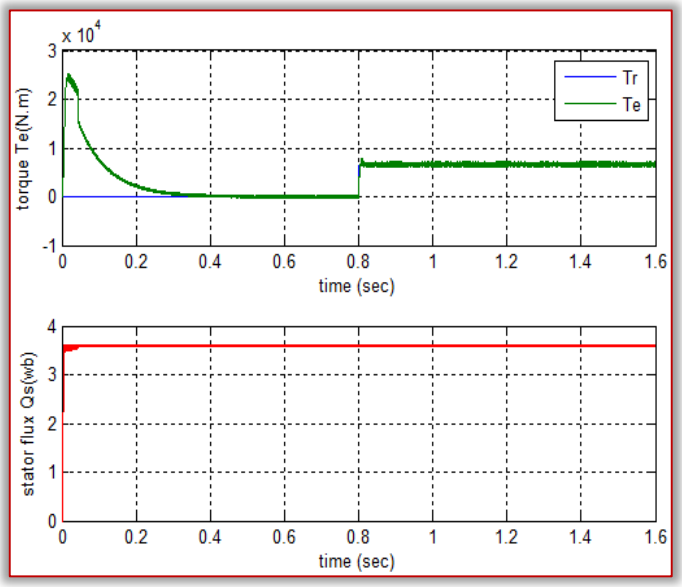

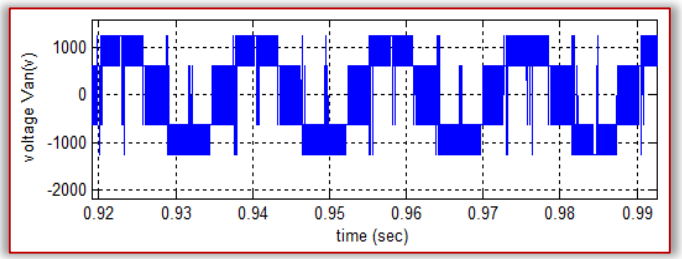

Figure 12. Performances of classical DTC-ANN with ANFIS speed controller

Figures 11-12 shows the harmonic spectrum of one phase stator current (las) of the IM obtained using FFT technique for classical DTC command and DTC-ANN with ANFIS regulator one respectively. It can be clear observed that the THD is reduced for DTC-ANN with ANFIS regulator (THD=10.73 %) when compared to the classical DTC command one (THD = 22.51 %). In the other hand, the dynamics of the components of the stator flux are not affected by the application of these load guidelines.

Electromagnetic torque response comparing curves are shown in Figure 13. See figure the electromagnetic torque ripple is significantly reduced when the intelligent techniques is in use.

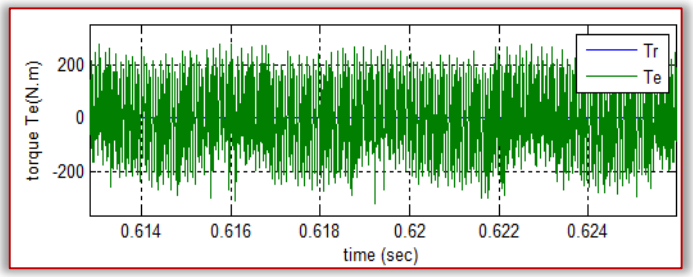

a) Classical DTC

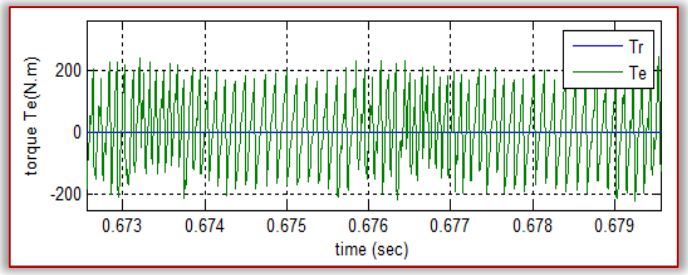

b) Neural DTC with ANFIS speed controller
Figure 13 Zoom in the torque.

Figure 14 shows that the DTC-ANN with the ANFIS PI regulator significantly reduces the ripple of the stator flux compared to that of the classical DTC command.

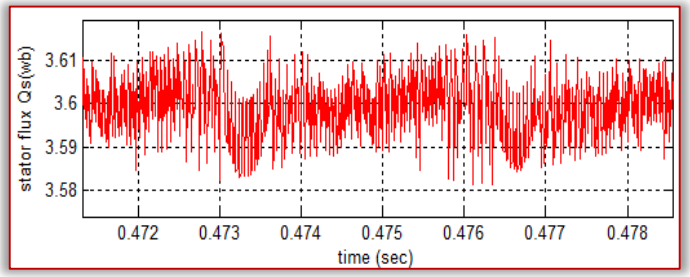

a) Classical DTC command

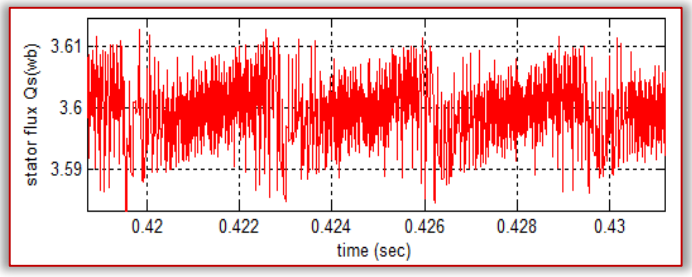

b) DTC-ANN with ANFIS speed regulator
Figure 14 Zoom in the stator flux.

CONCLUSION

In this paper, the DTC command of IM drives using intelligent techniques is presented. This intelligent technique (ANN and ANFIS) determinates the desired amplitude of switching table and classical PI regulator of speed.

The proposed DTC command schemes improve considerably the drive performance in terms of reduced electromagnetic torque, stator flux pulsations and THD value of stator current.

Therefore, proposed DTC command is an excellent solution for general purpose IM drives.

References

[1] D. C. Sekhar, G. V.0 Marutheshwar, « Modeling and field oriented control of induction motor by using an adaptative neuro fuzzy interference system control technique, » International Journal of Industrial Electronics and Electrical Engineering, Vol. 2, Issue 10, 2014, pp. 75-81.

[2] A. Kusagur, S. F. Kodad, B. V. Sankar Ran, « Modeling, Design & Simulation of an Adaptative Neuro-Fuzzy inference Système (ANFIS) for speed control of induction motor, » International Journal of Computer Applications, Vol. 6, No. 12, 2010, pp. 29-44.

[3] S. Allirani, V. Jagannthan, « Direct torque control technique in induction motor drives-A review, » Journal of Theoretical and Applied Information Technology, Vol. 60, No. 3, 2014, pp. 452-475.

[4] Eid Al-radadi, « Direct torque neuro fuzzy speed control of an induction machine drive based on a new variable gain PI controller, » Journal of Electrical Engineering, Vol. 59, No. 4, 2008, pp. 2010-2015.

[5] A. H. Adel, S. Abo-Zaid, A. Refky, « Improvement of direct torque control of induction motor drives using neuro-fuzzy controller, » Journal of Multidisciplinary Engineering Science and Technology, Vol. 2, Issue 10, 2015, pp. 2913-2918.

[6] A. Idir, M. Kidouche, « Direct torque control of three phase induction motor drive using fuzzy logic controllers for low torque ripple, » Proceedings Engineering & Technology, Vol. 2, 2013, pp. 78-83.

[7] Md. Habibullah, Md. Jahirul Islam, Md. Abdur Rafiq, Kalyan Kumar Halder, B. C. Ghosh, « A new DTC-SVM based control of field oriented position sensorless induction motor drive with reduced torque and flux ripple, » International Journal of Computer and Electrical Engineering, Vol. 3, No. 3, 2011, pp. 327-334.

[8] H. G. Zaini, M. K. Metwally, M. Ahmed, « Direct torque control of induction motor drive fed from hybrid multilevel inverter, » International Journal of Electrical & Computer Sciences, Vol. 14, No. 3, 2014, pp. 6-11.

[9] F. Kadri, S. Drid, F. Djeffal, « Direct torque control of induction motor fed by three-level NPC inverter using fuzzy logic, » International Conference on Systems and Processing Information, May 15-17, 2011, Guelma, Algeria.

[10] A. Ameur, L. Mokrani, B. Mokhtari, N. Essounbouli, A. Azoui, « Intelligent DTC of PMSM, fed by a three-phase NPC three-level inverter, » Acta Electrotehnica, Vol. 55, No. 1-2, 2014, pp. 3-9.

[11] N. Vahdatifar, Ss. Mortazavi, R. Kianinezhad, «Neural network based predictive DTC algorithm for induction motors, » International Journal of Computer, Electrical, Automation, Control and Information Engineering, Vol. 4, No. 11, 2011.

[12] M. Yucel, F. V. Celebi, M. Torun, H. H. Goktas, « Adaptive neuro-fuzzy based gain controller for erbium-doped fiber amplifiers, » Advances in Electrical and Computer Engineering, Vol. 17, No. 1, 2017, pp. 16-20.

[13] S. Darwin, M. Murugan, J. J. Gnana Chandran, « A comparative investigation on DTC of B4-inverter-fed BLDC motor drives using PI and intelligent controllers, » International Journal of Advanced Research in Electrical, Electronics and Instrumentation Engineering, Vol. 4, Issue 3, 2015, pp. 1486-1494.

[14] L. Youb, A. Craciumescu, "Direct torque control of induction motors with fuzzy minimization torque ripple," Proceedings of the World Congress on Engineering and Computer Science, Vol. 2, 2009.

[15] M. Abdelhafidh, "Stratégies de commande DTC-SVM et DPC appliquées à une MADA utilisée pour la production d'énergie éolienne," Thèse de Doctorat, Ecole Nationale Polytechnique, Alger, 2014.

[16] H. Benbouhenni, "Nouvelle approche de la commande DTC modifié par les techniques de l'intelligence artificielle d'une machine asynchrone," Journal of Advanced Research in Science and Technology, Vol. 4, No. 2, 2017, pp. 509-528.

ISSN: 2067-3809

Fascicule 1

[January - March]

t o m e XII

[2019]

ACTA Technica CORVINIENSIS
BULLETIN OF ENGINEERING

ISSN: 2067-3809

[1.] S.E. UWADIAE, [2.]O.M. EDOKPIAWE

MODELLING AND OPTIMIZATION OF LEAD ADSORPTION FROM AQUEOUS SOLUTION USING GROUNDNUT SHELL

[1,2]Department of Chemical Engineering, Faculty of Engineering, University of Benin, Benin City, Edo State, NIGERIA

Abstract: In this study, the design of experiment for response surface methodology (RSM) was used to analyse and optimise the simultaneous effect of adsorbent dose, contact time and pH of solution during the removal of Pb(II) ion from aqueous solution using activated carbon developed from groundnut shell as adsorbent. Groundnut shells were collected from a dust bins and thoroughly washed with distilled water; sun-dried and pulverized. It was thereafter carbonated using a muffle furnace at 500°C for 1 hour, after which the carbonated groundnut shell was sieved to attain 0.425mm or less before activation using nitric acid. A three-variable and three-level Box-Behnken factorial design was used to develop a statistical model to describe the relationship between percentage removal of Pb^{2+} and the selected independent variables. The selected parameters were then optimised using RSM. The model was statistically significant ($p<0.0001$) with a low standard deviation of 0.76 and did not show lack of fit ($R^2=0.9768$). The optimum values of adsorbent dose, contact time and pH of the solution obtained from RSM were 0.94 g, 5115.36 min and 5.42 respectively. The observed results indicate the viability of activated carbon from groundnut shell for removal of Pb^{2+} from aqueous solution and industrial wastewater.

Keywords: Groundnut-shell, activation, Box-Behnken design, Response surface methodology, Optimization

INTRODUCTION

Because of advancement and industrialization in numerous nations, the levels of modern contamination have been relentlessly rising. Thusly, the treatment of dirtied mechanical wastewater remains a point of worldwide worry since wastewater gathered from regions, groups, and enterprises should, at last, come back to getting water or to the land. In addition, sullying of groundwater is today a noteworthy worry in the administration of water assets (Weber, 1991). Natural contamination because of the release of substantial metals from different businesses, including metal plating, mining, painting and horticultural sources, for example, manures and fungicidal showers are of noteworthy concern in view of their danger and risk to human life, particularly when resilience levels are surpassed (Gupta *et al*., 2009). Various treatment techniques for the expulsion of metal particles from fluid arrangements have been accounted for. This incorporates diminishment, particle trade, electrodialysis, electrochemical precipitation, dissipation, solvent extraction, reverse osmosis, substance precipitation and adsorption (Gupta *et al*., 2009). Adsorption processes are not sophisticated and also not complicated hence it has found wide usage for treatment of wastewater (Mabrouk *et al.,* 2009). Since it is highly efficient, commercial activated carbon (CAC) is a commonly used adsorbent in the adsorption process for the treatment of wastewater but it is however expensive (Aksu, 2005).

Because of the high cost of CAC and misfortune amid recovery, alternative low-cost adsorbents have pulled in the consideration of a few researchers to give a contrasting option to the costly CAC. The low-cost adsorbents include banana and orange peels (Annadurai and Lee, 2002); Sheep Hoofs (Touaibia and Benayada, 2006); *Luffa Cylindrica* (Oboh *et al*., 2011) and sawdust (Šćiban *et al*., 2006).

Regular and classical techniques for concentrate a procedure by keeping up different elements required at determined steady levels don't delineate the consolidated impact of the considerable number of components included. This strategy is likewise tedious and requires various tests to decide ideal levels (Chaisongkroh *et al.,* 2012). Apart from being a tool that is employed to optimize and study interactions among factors, response surface methodology (RSM) likewise the relative importance of different variables engaged with complex collaborations can be assessed (Saha *et al*., 2009). The general objective of the study was to investigate the effectiveness of activated carbon formulated from locally available groundnut shell for the removal of lead ions from aqueous solution.

MATERIALS AND METHODS

— Preparation of Activated Carbon

The groundnut shells were collected from a dustbin in a local market in Benin City, Nigeria. They were then thoroughly washed with distilled water so as to remove all adhering particles before sun-drying for 5 days. The dried samples were pulverized and weighed on a digital weighing balance. The measured groundnut shell was placed in the muffle furnace at 500°C for 1 hour, after which the carbonated groundnut shell was sieved to attain 0.425 mm or less before activation. The activation was done by soaking the sieved carbonated groundnut shell in the solution of nitric acid, at a ratio of 1:4 by mass of groundnut shell to nitric acid, for 24 hours for activation purposes. Then the activated groundnut shells were removed from the solution and placed in the oven for 2 hours, at 60°C; it was then left to cool in a desiccator. After cooling, the groundnut shell was washed with distilled water and placed in a container, and dried in the oven for another 4.5 hours, at 105°C.

— Preparation of Aqueous Solution

Stock solution of Pb (II) ion was prepared by dissolving analytical grade $Pb(NO_3)_2$ in an appropriate amount of distilled water. From this stock solution a working solution of 100 mg/L of Pb (II) ion was prepared which was used for the batch adsorption process.

— Adsorption Experiment

Batch adsorption experiments were carried out for the removal of Pb^{2+} from aqueous solutions onto the adsorbent to study the effect of some specific process parameters. The effects of adsorbent dosage, contact time and pH were investigated for the adsorption onto groundnut shell. 100mg/l of concentration of lead(II) ions was used as the working solution. The adsorption was carried out at ambient temperature and shaking speed of 250 rpm in an orbital shaker. After filtrations, the residual concentrations of Pb(II) were determined using atomic adsorption spectrophotometer (AAS).

The percentage removal of Pb^{2+} is defined as:

$$\text{Re}\ \% = \frac{\text{Ci}-\text{Cf}}{\text{Ci}} \times\ 100 \qquad (1)$$

where: Re (%) is percentage removal of Pb(II) ions, C_i is the concentration of Pb(II) ions before adsorption (mg/l); C_f is the concentration of Pb(II) ions after adsorption (mg/l)

— Experimental Design

A 3-stage-three-element Box-Behnken factorial layout was accomplished using design Expert, version 7.1.6 (Stat-Ease Inc., Minneapolis, MN, USA) to determine the best combination of adsorption variables for the yields of Pb(II) ions.

The variable input parameters were pH of the solution, contact time and adsorbent. As shown in Table 1, independent variables had three levels which were based on preliminary experiments.

Table 1: Independent variables and their levels for BBD experimental design

Independent Variable	Symbols	Coded and Actual Levels		
		-1	0	1
Adsorbent dose (g)	X_1	0.2	0.6	1
Contact time (min)	X_2	10	65	120
Ph	X_3	2	4	6

The response was percentage removal of Pb(II) ions. The relation between the coded values and actual values are described as follows:

$$\text{x}_\text{i} = \frac{\text{X}_\text{i}-\text{X}_0}{\Delta\text{X}} \qquad (2)$$

where x_i and X_i are the coded and actual values of the independent variable respectively. X_o is the actual value of the independent variable at the centre point and ΔX_i is the step change in the actual value of the independent variable. The following generalized second order polynomial equation was used to estimate the response of the dependent variables.

$$\text{Y} = \text{b}_0 + \sum \text{b}_\text{i}\text{X}_\text{i} + \sum \text{b}_\text{ii}\text{X}_\text{i}^{\,2} + \sum\sum \text{b}_\text{ij}\text{X}_\text{i}\text{X}_\text{j} + \text{E} \qquad (3)$$

where Y_i is the predicted response, X_i and X_j are the independent variables, b_o is offset term, b_i and b_{ij} are the single and interaction effect coefficients and E is the error term.

Based on RSM, this equation was used to evaluate the linear, quadratic and interactive effects of independent variables on the chosen response. For the model, the calculations from the linear and cross regression were performed. The R^2 value, the residual error, the pure error calculated from the repeated measurements and the lack of fit were calculated. ANOVA was utilized to estimate the measurable attributes of the model fitting. The total test outline and results comprising of coded levels, real factors, and responses are given in Table 2. Keeping in mind the end goal to guarantee a good model, a test for criticalness of the relapse model and individual model coefficients was performed together with the absence of-fit test. Regularly, the huge components can be positioned in light of the F-value or p-value. The bigger the extent of the F-value and correspondingly the smaller the p-esteem, the more critical is the comparing coefficient (Yi *et al.*, 2010).

RESULTS AND DISCUSSION

The complete experimental design and results consisting of coded levels, actual variables, predicted and experimental responses are given in Table 2.

Table 2: Box Behnken design matrix for the optimization of variables and the response values

Run No.	Factors						Response	
	Coded values			Actual values			Percentage Pb(II) ion removal	
	x_1	x_2	x_3	X_1	X_2	X_3	Experimental	Predicted
1	0	0	0	0.6	65	4	90	91.66
2	0	1	1	0.6	120	6	99.1	99.11
3	-1	-1	0	0.2	10	4	98	98.02
4	0	-1	1	0.6	10	6	98.8	98.88
5	1	-1	0	1	10	4	96.65	96.55
6	0	0	0	0.6	65	4	91.5	91.66
7	0	0	0	0.6	65	4	92	91.66
8	0	0	0	0.6	65	4	92.5	91.66
9	0	-1	-1	0.6	10	2	97.75	97.74
10	1	0	1	1	65	6	99.8	99.82
11	1	0	-1	1	65	2	98.4	98.5
12	1	1	0	1	120	4	99.02	98.996
13	0	0	0	0.6	65	4	92.3	91.66
14	-1	1	0	0.2	120	4	96.79	96.89
15	-1	0	1	0.2	65	6	99	98.9
16	-1	0	-1	0.2	65	2	98.8	98.78
17	0	1	-1	0.6	120	2	98.9	98.82

As appeared in Table 2, the entire plan comprised of 17 trial focuses, and five duplicates (run 13– 17) at the focal point of the outline were utilized for evaluating the trial blunder entirety of squares.

Investigation of fluctuation (ANOVA) is a measurable strategy that subdivides the aggregate variety in an arrangement of information into segment parts related with particular wellsprings of variety to test speculations on the parameters of the model (Francesc and Julia, 2014).The results of the analysis of variance (ANOVA) which are given in Table 3.

Table 3: ANOVA table for quadratic model

Sources	Sum of squares	Degree of freedom	Mean square	F value	P value prob>F
Model	171.11	9	19.01	32.73	<0.0001
X_1	0.2	1	0.2	0.35	0.5714
X_2	0.85	1	0.85	1.47	0.2653
X_3	1.02	1	1.02	1.75	0.2277
X_1X_2	3.2	1	3.2	5.52	0.0512
X_1X_3	0.36	1	0.36	0.62	0.457
X_2X_3	0.18	1	0.18	0.31	0.5945
X_1^2	42.01	1	42.01	72.32	<0.0001
X_2^2	32.92	1	32.92	56.67	0.0001
X_3^2	73.61	1	73.61	126.71	<0.0001
Residual	4.07	7	0.58		
Lack of fit	0.0055	3	0.018	0.018	0.9961
Pure Error	4.01	4	1		
Cor Total	175.18	16			
Std dev	0.76		R^2		0.9768
Mean	96.43		Adjusted R^2		0.9469
C.V (%)	0.79		Predicted R^2		0.9592
PRESS	7.14		Adequate precision		13.952

ANOVA table proposes whether the condition is sufficient to depict the connection amongst reaction and other autonomous factors. The model can be considered as factually noteworthy, if the estimation of p is lower than 0.05 with a bigger F-value (Ravikumar *et al.*, 2013. From the ANOVA table it is observed that the model fitted well with the information created and can be considered as factually noteworthy since the F-value is large. (32.73) and p value is lesser than 0.0001. The goodness of the model was assessed through the lack of fit test. The P-values for the lack of fit test was not significant (p>0.05) demonstrating that the model was fit for predicting the adsorption of Pb(II) ions onto activated carbon planned from groundnut shell. A good fit means that the generated models adequately explained the data variation.

An R^2 value of 0.9768 means that 97.68 % of the variations for percent lead ion adsorption are explained by the independent variables and this also means that model does not explain only 2.32 % of the variation. Predicted R^2 is a measure of how good the model predicts a response value.

The predicted R^2 value of 0.9592 is in reasonable agreement with an adjusted R^2 value of 0.9469. The coefficient of variation, C.V. obtained was 0.79 %. . C.V is an indication of the degree of precision with which the treatments were carried out. A low value of C.V suggests a high reliability of the experiment (Montgomery, 2005; Mason *et al.*, 1989). "Adeq Precision" measures the signal to noise ratio. A ratio greater than 4 is desirable (Cao *et al.*, 2009), therefore the ratio of 13.952 indicates an adequate signal

Design Expert software was used to calculate the coefficients of the second-order fitting equation and the model suitability was tested using the ANOVA test. Therefore, the second order polynomial equation should be expressed by Eq. (4`)

$$\mathrm{Re} = 120.04394 - 27.43494X_1 - 0.13092X_2 - 8.28381X_3 + 0.040682X_1X_2 + 0.37500X_1X_3 - 1.93182X10^{-3}X_2X_3 + 19.7421X_1{}^1 + 9.24380X10^{-4}X_2{}^2 + 1.04531X_3{}^2 \quad (4.)$$

According to the monomial coefficient value of regression model Eq. (4), X_1 = ´-27.4349; X_2= ´-0.13092 and X_3 = -8.28381 (pH), and the order of priority among the main effect of impact factors is $X_1 > X_3 > X_2$

The created information was examined to decide the connection between's the genuine and anticipated esteems as appeared in Figure 1.

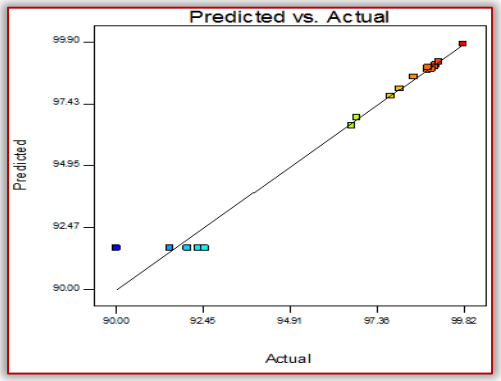

Figure 1: Plot of predicted against actual lead ion percentage removal.

From Figure 1 it is watched that the information focuses are conveyed close to the straight line showing that the quadratic model could be utilized as the noteworthy model for anticipating lead (II) ions removal over the autonomous information factors.

The effects of contact time and adsorbent dose, pH of solution and contact time, and pH of the solution and adsorbent dose on Pb(II) ions percentage are shown in the response surface plots presented in Figures 2- 4.

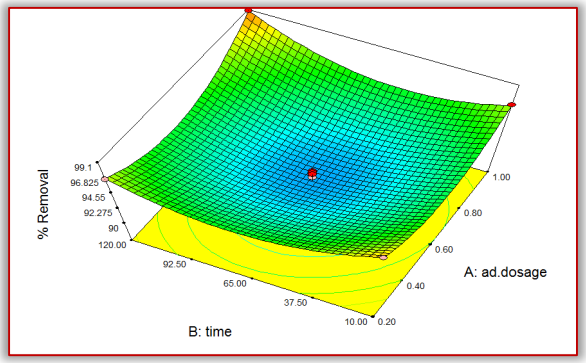

Figure 2: Response surface plots showing the effect of adsorbent dosage and time on Pb(II) ion removal

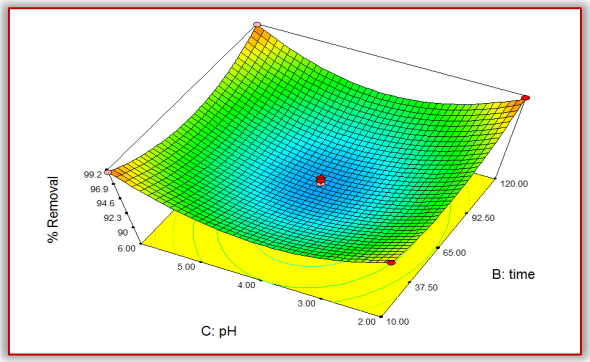

Figure 3: Response surface plots showing the effect of time and solution pH on Pb(II) ion removal

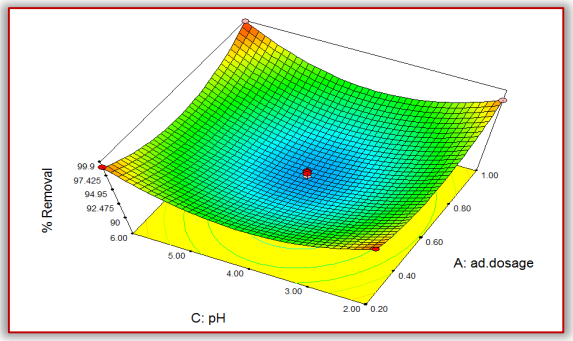

Figure 4: Response surface plots showing the effect of adsorbent dosage and pH of the solution on Pb(II) ion removal

The association between contact time and adsorbent dosage and the cooperation between contact time and pH had a general beneficial outcome on removal the of Pb(II) from the aqueous solution; as contact time and the adsorbent dose increased, removal of Pb(II) ion likewise increased. A comparative pattern was noticed when contact time and pH increased. Be that as it may, as both adsorbent measurement and pH increased, the removal of Pb(II) from aqueous solution diminished.

Following the optimization step, corresponding optimum conditions for optimum values of Pb(II) ion removal were obtained thus; adsorbent dosage (0.94 g), contact time (115.36 min), and pH (5.42).

CONCLUSION

The production of activated carbon from groundnut shell which is an agricultural waste/by-product is a value addition to the groundnut residue. The formulated activated carbon from groundnut shell was used in the removal of Pb(II) ion from aqueous solution. The effects of adsorbent dose, contact time and pH of the solution on the sorption of Pb(II) onto the activated carbon was investigated, Furthermore, statistical methodology, employing Box-Behnken Response Surface Design was used to determine the optimal conditions for the adsorption of Pb(II) ion onto the developed activated carbon from groundnut shell. The optimal conditions for Pb(II) ion removal from aqueous solution is identified as adsorbent dose of 0.94 g, contact time of 115.36 min and pH value of 5.42. It can be concluded that groundnut shell can serve as ready raw material for the development of affordable and effective activated carbon which can serve as a good adsorbent for the removal of Pb(II) ion from wastewater.

References

[1] Aksu, Z: Application of biosorption for the removal of organic pollutants: a Review, Process Biochemistry, 40, 997–1026, 2005
[2] Annadurai, G and Lee, J. F: Equilibrium studies on the adsorption of acid dye into chitin, Environmental Chemistry Letters, 6, 77–81, 2002.
[3] Cao, G.; Ren, N; Wang, A; Lee, D.J.; Guo, W.; Liu, B.; Feng, Y. and Zhao, Q.: Acid hydrolysis of corn stover for biohydrogen production using Thermoanaerobacterium thermosaccharolyticum W16, International Journal of Hydrogen Energy, 34, 7182–7188, 2009.
[4] Chaisongkroh, N.; Chungsiriporn, J and Bunyakan, C.: Modeling and optimization of ammonia treatment by acidic biochar using response surface methodology, Songklanakarin Journal of Science and Technology, 34 (4), 423-432, 2012.
[5] Francesc, T. and Julia, G.M.: Using central composite experimental design to optimize the degradation of real dye wastewater by Fenton and photo-Fenton reactions, Dyes Pigment, 100, 184–189, 2014.
[6] Gupta, N.; Prasad, M.; Singhal, N. and Kumar.V.: Modeling the Adsorption Kinetics of Divalent Metal Ions onto Pyrophyllite Using the Integral Method, Industrial and. Engineering Chemistry Research, 48(4), 2125-2128, 2009.
[7] Mabrouk, E.; Ikram, J. and Mourad, B. : Adsorption of Copper Ions on Two Clays From Tunisia: pH and Temperature Effects, Applied Clay Science, 46, 409–413, 2009.
[8] Mason, R.L.; Gunst, R.F. and Hess, J.L.: Statistical Design and Analysis of Experiments, New York, John Wiley & Sons, Inc., 1989.
[9] Montgomery, D.C. : Design and Analysis of experiments, 6th ed., New York, John Wiley & Sons, Inc., 2005.
[10] Oboh, I. O.; Aluyor, E.O. and Audu, T.O.K. 2011. Application of *Luffacylindrica* in natural form as biosorbent to removal of divalent metals from aqueous solutions - Kinetic and equilibrium study, In: Waste Water Treatment and Reutilization, Rueka, Croatia, InTech, 2011.
[11] Ravikumar, R.; Renuka, K.; Sindhu,V. and Malarmathi, K.B.: Response Surface Methodology and Artificial Neural Network for Modeling and Optimization of Distillery Spent Wash Treatment Using *Phormidium valderianum* BDU 140441, Polish Journal of Environmental Studies, 22 (4),1143-1152, 2013.
[12] Saha, B.C.; Iten, L.B.; Cotta, M.A. and Wu, Y.V.:Dilute acid pretreatment, enzymatic saccharification and fermentation of wheat straw to ethanol, Process Biochemistry, 40(12),3693–3700, 2005.
[13] Šćiban M., Klašnja, M. and Škrbić, B. Modified softwood sawdust as adsorbent of heavy metal ions from water, Journal of Hazardous materials, 136 (2), 266-271, 2006
[14] Touaibia, D. and Benayada, B.: Removal of mercury (II) from aqueous solution by adsorption on keratin powder prepared from Algerian sheep hooves, Desalination, 186, 75-80, 2006.
[15] Weber J Jr: Physiochemical processes for water quality control,. Adsorption Science and Technology, 28 (10), 913-921, 1991.
[16] Yi, S.; Su, Y.; Qi, B.; Su, Z. and Wan, Y. : Application of response surface methodology and central composite rotatable design in optimization; the preparation condition of vinyltriethoxysilane modified silicalite/ polydimethylsiloxane hybrid pervaporation membranes, Separation and Purification Technology, 71, 252-262, 2010.

ISSN: 2067-3809

[1.] Flavius BUCUR

RESEARCH ON THE FACTORS INFLUENCING THE QUALITY OF PHOSPHOROUS CAST IRONS

[1.] University Politehnica Timisoara, Department of Engineering and Management, Hunedoara, ROMANIA

Abstract: This paper focuses on the influence of chemical composition upon the hardness mechanical characteristics of phosphorous cast irons. The casting of the parts is done by meeting specific chemical and mechanical parameters. Data collected from a cast iron foundry has been used for analysis, resulting in a series of graphic and analytical correlations created with the Matlab application. The resulting regression areas and level curves allow the identification of the optimal areas of variation in chemical composition of the cast irons with the purpose of obtaining an optimal hardness degree.
Keywords: phosphorous cast iron, hardness, brake block, quality

INTRODUCTION

When manufacturing brake blocks intended for rolling stock, phosphorous cast irons P10 are most widely used. These brake blocks have limited usage as their friction coefficient decreases notably when braking at high speed, and the wear caused by the tendency to jam increases as the temperature in the friction coupler rises [1,2].

The size of the eutectic particles and the distribution of the phosphide network in the structure, the shape, size and distribution of the graphite network, as well as the quantity of graphite expelled during graphical crystallization, all play an important part in the resulting quality of the cast iron used for producing brake blocks.

The chemical elements found in the structure of the cast iron from which brake blocks are made have a different influence on crystallization. The rise in manganese content favours cementitious crystallization. Manganese neutralises the harmful influence of sulphur by forming manganese sulphide, which leads to increased hardness and tear resistance. On the other hand, as the manganese content increases, the fluidity of the cast iron and its casting capacity decreases. A rise in silicon content favourises the graphical crystallization. By modifying the silicon content, the relation between carbon, bound as cementite (Fe_3C), and the free carbon found as graphite, changes. In industrial practice, the sum (C+Si) is taken into account, but it depends on the cast iron structure required and the thickness of the part shell. The silicon enhances cast iron fluidity, thus improving its casting properties [3,4].

The sulphur and the iron form iron sulphide (FeS) which, upon solidification, forms with the iron an easily fusible eutectic (Fe–FeS) that melts at 950^0 C. This eutectic has a delayed solidification, thus favouring the production of intercrystalline segregations which lead to decreased mechanical properties of cast irons. This effect is a consequence of the redistribution of alloying elements in between the liquid and solid phases during the primary structure formation. The micro–segregation occurs as a consequence of mass shift by short distance diffusion [5,6]. The sulphur also prevents graphitization, favouring the formation of cementite, leading to increased hardness and fragility, increased contraction, decreased fluidity and a higher tendency to form cracks in the cast iron.

Brake blocks are made by the casting of second–fusion cast iron. The process of obtaining cast iron is performed according to the requirements provided by the supplier of brake blocks for motor and towed rolling stock, and also needs to follow the tender specifications no. 1/SFMR/SDT/2000 [7].

Types of brake blocks for engines and freight/ passenger wagons (figure 1) [8]:

- S_1 – brake blocks size 1 for freight/ passenger wagons;
- S_2 – brake blocks size 2 for freight wagons;
- LDH – brake blocks for 1250 HP Diesel hydraulic engines;
- LDE – brake blocks for 2100 HP Diesel electric engines;
- LE – brake blocks for 5100 kW and 3400 kW electric engines.

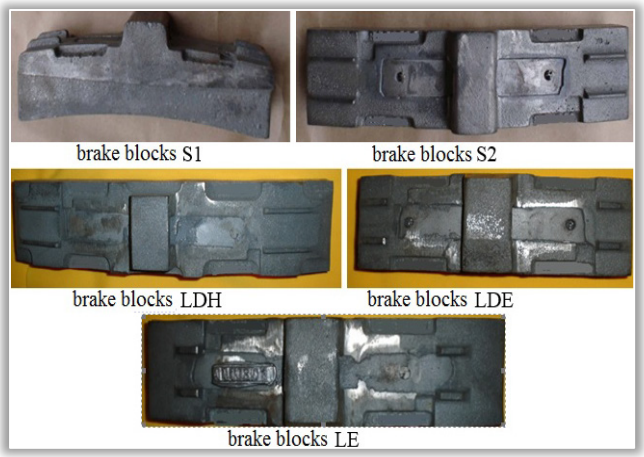

Figure 1. Types of brake blocks for engines and freight/ passenger wagons [8]

Phosphorous cast irons are frequently used in manufacturing brake blocks for rolling stock [9]. It is required to determine the influence of different chemical elements found in the

structure upon the hardness of the cast iron in order to avoid obtaining a phosphorous cast iron which would be too hard and which would prematurely wear the wheel dressing of the train. However, a too soft phosphorous cast iron would lead to increased consumption of brake blocks due to premature wear [9,10].

DESCRIPTION OF MANUFACTURING AND CONTROL PROCESSES

— Manufacturing Brake Blocks

In order to analyse the influence of chemical composition on the hardness quality characteristics of brake blocks, a number of 70 charges of cast iron have been observed in the industrial practice, which were produced by a company that manufactures cast iron parts. The brake blocks manufacturing process involves obtaining phosphorous cast iron and then casting it. Scrap, cast iron waste and worn brake blocks are used to obtain cast iron. The load at the charging points that were analysed was: 10–20% first–fusion cast iron; 30–60% cast iron waste (worn brake blocks); 20–30% steel waste. The cutting–to–dimension of the load plays an important role in its production in induction furnaces, which means that the load needs to be cut according to the size and melting capacity of the furnace. The recharging of the furnace is done periodically, usually by bucket, ensuring a continuous melting process, with a minimum energy consumption. When using small waste metal parts (chips, splinters), these are briquetted (pressed) or minced and a continuous line load is ensured. The cast iron thus obtained is poured into casts on the manual casting line, as shown in figure 2.

Figure 2. Manual brake blocks casting line [4]

The research has been done in order to determine the influence of the chemical composition of the cast iron on the hardness of brake blocks. The chemical composition, as well as the physical and mechanical characteristics have been analysed.

— Brake Blocks Control

The quality control for brake blocks is done according to the tender specifications no.1/SFMR/SDT/2000 [3]. The first parameters checked are the percentages of chemical elements found in the cast iron. For this check, samples from the melting pot are taken and checked with a spectrometer (figure 3).

Figure 3: Determining the chemical composition of analysed samples [4]

Hardness checking [3] is done at both ends and through the cross section, in three points, as shown in figure 4.

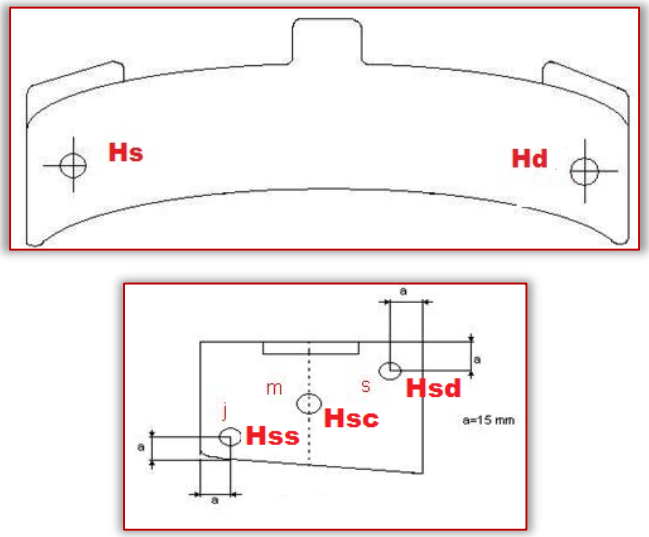

Figure 4. Areas of brake blocks hardness sampling [3].

Also, for each charge, a mechanical shock resistance test is performed and the metallographic structure is checked.

SOLUTIONS AND APPROACHES

The data obtained from industrial practice has been processed through Matlab and Excel software. Charts of variation in hardness by carbon, manganese, phosphorus and silicon have been created for all points in which hardness was measured. By calculating an average, charts of variation in average hardness for the outside and cross section of the part have been created. These charts have been done using Microsoft Excel and have been represented using second degree polynomial functions. Then, using Matlab and a second degree equation, three–dimensional charts with regression areas and level curves for hardness variation by combination of two chemical elements have been created for analysis, for all the points. The equation is as follows:

$$z = a(1)\cdot x^2 + a(2)\cdot y^2 + a(3)\cdot x\cdot y + a(4)\cdot x + a(5)\cdot y + a(6) \quad (1)$$

RESULTS

The following correlations obtained for the average hardness in the cross section of the brake block are presented here as example – $H_{sm} = (H_{ss}+H_{sc}+H_{sd})/3$.

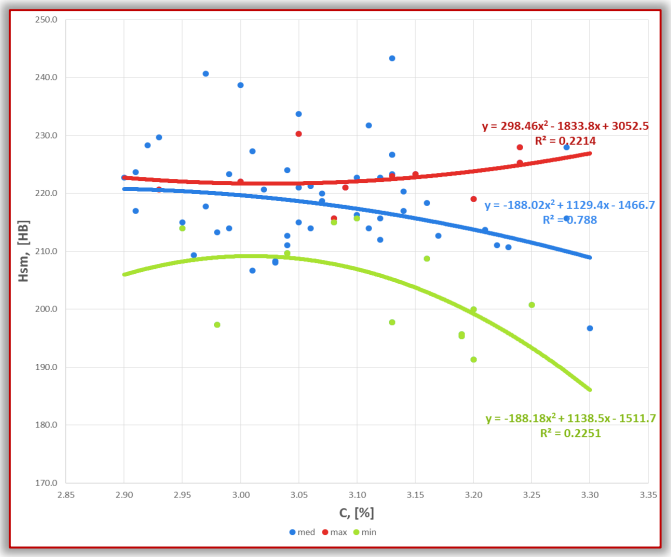

Figure 5. The variation of average hardness in the cross section by carbon percentage

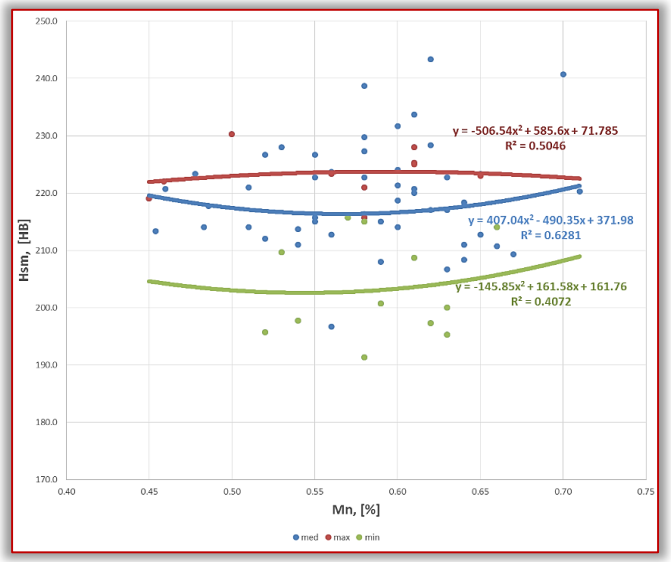

Figure 6: The variation of average hardness in the cross section by manganese percentage

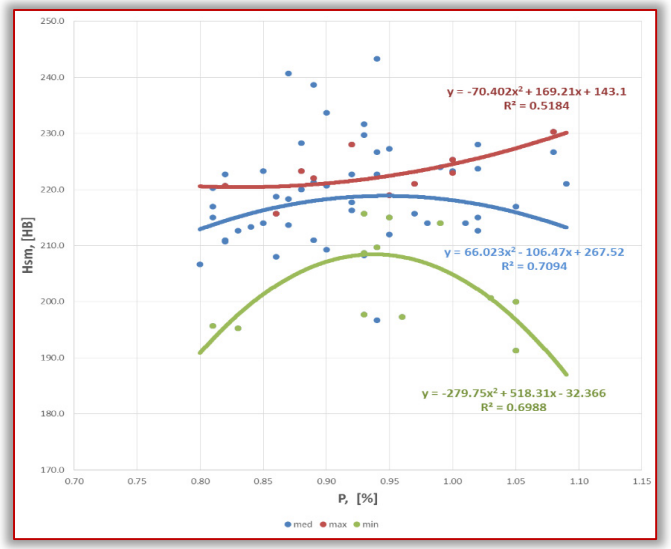

Figure 7: The variation of average hardness in the cross section by phosphorus percentage

Figures 5–7 show the variation in average hardness calculated for the three cross section measurements by carbon, manganese and phosphorus percentages.
Figures 8–9 show the regression areas and level curves for average hardness variation in the cross section by carbon, manganese and phosphorus content.

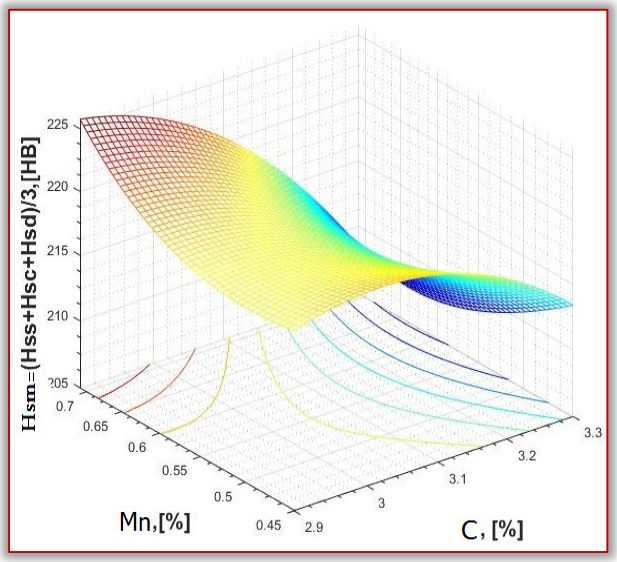

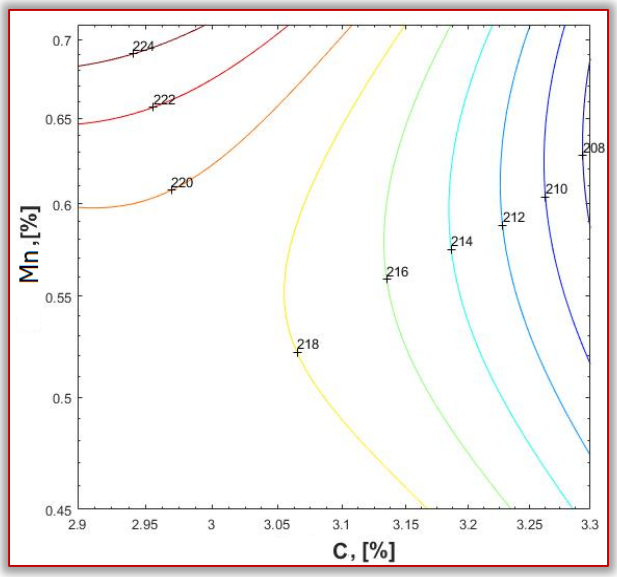

Figure 8: $H_{sm} = f(C, Mn)$

In case of the average hardness variation in the cross section by carbon and manganese content, the equation becomes:

$$H_{sm} = -80.75 \cdot C^2 + 165.42 \cdot Mn^2 - 115.06 \cdot C \cdot Mn + 539.02 \cdot C + 168.92 \cdot Mn - 624.68 \quad (2)$$

The correlation coefficient is R^2=0.2912 and the coordinates of the inflection point are: H_{sm} = 218.7914 HB; C = 2.9663%; Mn = 0.5210%.

In case of the average hardness variation in the cross section by carbon and phosphorus content, the equation becomes:

$$H_{sm} = -67.20 \cdot C^2 - 267.72 \cdot P^2 + 52.48 \cdot C \cdot P + 338.15 \cdot C + 349.21 \cdot P - 427.99 \quad (3)$$

The correlation coefficient is R^2 = 0.3294 and the calculation reveals a point of local maximum for the following values: H_{sm} = 222.2430; C = 2.8807%; P = 0.9345%.

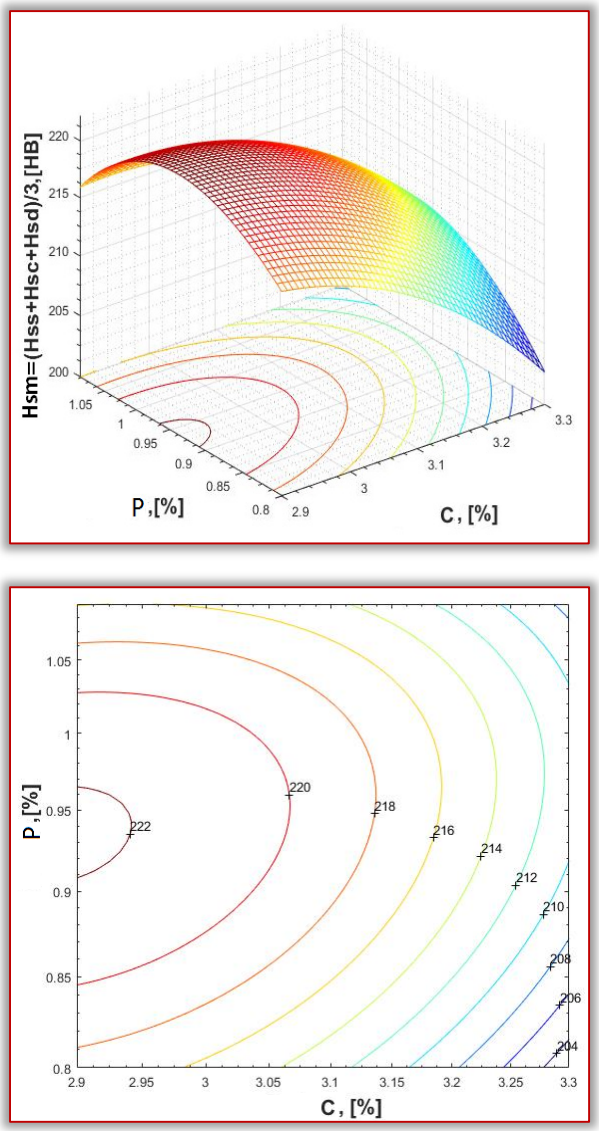

Figure 9: $H_{sm} = f(C, P)$

CONCLUSIONS

The rise in carbon concentration leads to negative outcomes due to graphitization increase and a decrease in tear resistance. The increase in hardness with manganese content addition is translated using a second degree polynomial equation. As the manganese content rises, so do the complex carbides proportions, and a dissolution of iron in the solid solution takes place (ferrite).

The phosphorus contributes to the formation of a phosphorous eutectic. The increase in phosphorus content leads to increased hardness, both at the surface and in the cross section of the brake block.

After analysing the results of the experimental research performed on a number of 70 phosphorous cast iron charges produced in a brake block foundry, the following conclusions can be drawn:

- the chemical composition of the cast iron used in manufacturing brake blocks ensures the necessary hardness to comply with standards;
- the correlations presented above reveal a clear influence of carbon and manganese content upon hardness;
- there is a difference in hardness between the brake block cross section extremities and its cross section centre, due to solidifying conditions;
- the level curves presented in the charts allow choosing independent parameters (C, Mn and P) so as to obtain a desired hardness value.

Bibliography

[1] M. Stoica, Braking trains, ASAB House, Bucharest, 2002.
[2] Carlan, B., Constantinescu, D., Constantin, N., Study regarding the thermal properties of the iron oxides and their application in the process of the heat transfer from the furnace hearth to the ingot, University Politehnica of Bucharest Scientific Bulletin Series B–Chemistry and Materials Science, 78(4), pp. 169–180, 2016
[3] Mincu, V., Negru, M., Constantin, N., Increase the ingots quality cast in vacuum, Solid State Phenomena 188, pp. 339–345, 2012
[4] V. Cojocaru, C. Filipiu, Preparing for developing iron load in induction furnaces, Samia Publishing, Science, 2006.
[5] Rucai, V., Constantin, N., Dobrescu, C., Experimental research program regarding the influence of thermo–time treatment of multicomponent Ni–base melting on their properties in solid phase, University Politehnica of Bucharest Scientific Bulletin Series B–Chemistry and Materials Science, 77(4), pp. 359–364, 2015
[6] Butnariu, I., Constantin, N., Dobrescu, C., Heput, T., Research on the recycling of pulverulent waste from the ferrous and non–ferrous industry in order to reduce the pollution, Revista de Chimie, 69(5), pp.1066–1070, 2018
[7] xxx, Specificication, no.1 /SFMR/SDT/2000, Brake shoes for tractors and trailers rolling
[8] www.tef.ro.
[9] Pascu L., Socalici A., Popa E., Crisan E., Influence of chemical composition on hardness of brake blocks for rolling stock, 12th International Conference of Numerical Analysis and Applied Mathematics, Mathematical Methods in Economics and Engineering, Rhodes, Greece, 22–28 September 2014.
[10] Pascu L., Researches on improving the quality of brake shoes meant for use with the rolling stock, PhD Thesis, Politehnica, 2015.

ISSN: 2067-3809

[1.]Oana LUPU

PULVEROUS FERROUS WASTE PROCESSING BY PELLETIZATION

[1.] Politehnica University of Timisoara, Department of Engineering and Management, Hunedoara, ROMANIA

Abstract: From the iron and steel industry always results a series of waste that are not capitalized enough with the rest of them being stored in stockpiles and ponds. Considering the fact that these waste contain iron and that – being unrecycled – they represent a polluting factor to the environment, it is imperial to find solutions to process them in a manner that will make them useful as raw or auxiliary material in manufacturing or other branches of the economy. The current paper presents the experimental research made in laboratory regarding the processing of pulverous ferrous waste through pelletizing with the purposes of making a new product that can be used as raw material in the iron and steel industry.
Keywords: waste, sludge, capitalizing, pellets

INTRODUCTION

The handling of industrial waste lies in capitalization, stockage, final storage and incineration. In Romania, the storage of waste on an open surface represents the most important means to eliminate industrial waste. In this manner, over the years a huge quantity of waste has been reached [1,2].

From the total amount of industrial waste landfills, a great deal do not have any facilities for protecting the environment and in most times, they are just cornered through fences. Some of these landfills have one or more of the special facilities (waterproofing, drainage, culvert, supervision drilling), but very few can be deemed as benefiting from all the conditions necessary to protect the environment. The cinder waste dumps are the storages that have most facilities: waterproofing with mineral layer, a drainage system that collects leachate, stability terraces, supervision drilling for the phreatic waters, splutter systems for surfaces.

Generally, as a consequences of the lack of facilities and the lean exploitation, the landfills also count as risk and impact generators for the environment and public health. The main impact and risk forms are (in the order perceived by the population):

- scenery modification and visual discomfort,
- the pollution of air and water,
- the decrease of soil fertility and
- the alteration of biocenosis composition in the neighbouring terrains [3].

The problems that waste management in Romania is dealing with can be summarized in the following way [4–7]:

- the storage on an open terrain being the most important way to eliminating waste;
- the existing waste being stored in inappropriate locations (near housing units, surface waters and vacation land);
- the landfills are not facilitated properly for environmental protection and lead to the pollution of water and soil in that area;
- the area occupied by the landfills now is considered a degraded area that cannot be used anymore in agricultural purposes; currently, in Romania, more than 12000ha of land are affected by the storage of domestic and industrial waste.

All these lead to the conclusion that the waste management sector needs to adopt certain specific measures that are fitting to each phase of waste elimination into the environment. Following these specific measures must be the objective of environmental risk factor monitoring that are related to wastes [8–10].

In this sense, the pelletizing is a method of agglomeration, or particle size enlargement, in which material fines are processed into pellets or granules. Pelletizing is used throughout a multitude of industries to process thousands of materials from difficult to handle powders and fines, into easy to handle pellets. Unlike pressure methods of agglomeration, such as compaction granulation or briquetting, pelletizing is considered a wet process, because moisture (in the form of a binding agent) is used to agglomerate the fines into larger particles, as opposed to the extreme pressure used in compaction or briquetting. Pelletizing a material can offer a number of benefits. Because of this, it has become a popular method of improving product performance, easing handling challenges, and even targeting desired product characteristics. In fact, the pelletizing is an incredibly diverse and flexible process, lending itself to thousands of materials, and nearly any material in powder or slurry form can be transformed into a dry, granular product.

Pelletizing, particularly on a disc pelletizer, is a highly flexible process, allowing for a significant amount of product customization to occur. Additives can be included to improve product formulations, and a number of variables can be adjusted to target specific end product parameters, such as particle size distribution, crush strength, flowability, and more. In essence, pelletizing allows producers to create a granular product that suits their exact needs.

For the many reasons (reduced dust, reduced attrition, faster product breakdown, and customization), products created via pelletizing are considered a premium product. With many benefits, and a highly customizable process, pelletizing has become a staple in many industries, with new applications for this valuable process constantly on the rise.

LABORATORY EXPERIMENTS

In this paper, there are presented the capitalization methods of pulverous ferrous waste that are the result of water depuration, this being: ferrous sludge (10.02.2018 – waste from the cooling water depuration). It comes from a plant that produces metallic powders. Choosing the procedure and technology of capitalization must have in view the features of the waste, the destination of the resulting product and the existing processing facilities in the waste area [11].

The ferrous sludge samples have been put laboratory research. The chemical composition presented in table 1 and the granulometric composition have been determined. Analysing the chemical and granulometric composition of the pulverous ferrous waste we determined it can be processed through classic technologies like: briquetting, pelletizing and agglomeration.

Table 1. The chemical composition of ferrous sludge

Chemical composition [%] ASTM E 1479/2016						
Al	Cd	Cu	Cr	Mg	Mn	Ni
0.003	0.003	0.70	0.54	0.003	0.079	0.046
Pb	Fe	Sn	Sb	Zn	Other	
0.008	84.40	0.016	0.003	0.003	14.196	

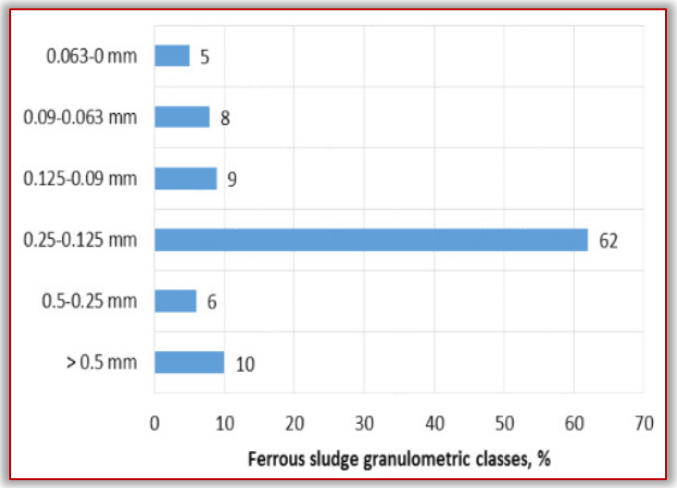

Figure 1. Ferrous sludge granulometric classes

In this paper there are presented the processing through pelletizing (micro–pelletizing). A processing method was chosen that requires the addition of bonding materials in order to capitalize the waste as pellets/micro–pellets and as raw materials in the steel ovens [11,12].

There has been an experiment of 5 recipes and as bonding materials bentonite 5–10% and slag LF 5–10%. The flow sheet of processing the pellets/micro–pellets is presented in figure 2.

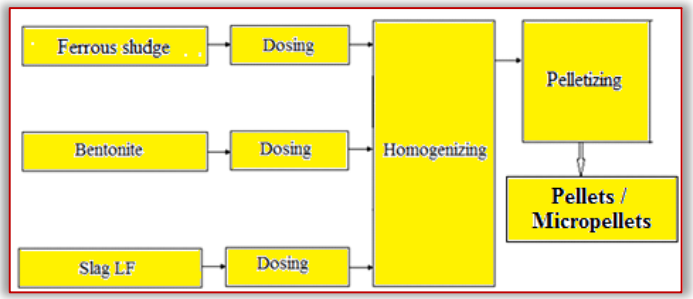

Figure 2. Technological flux of pelleting/micro–pelleting

Figure 3. Aspects during laboratory experimentation

The steps from the processing procedure and the procurence of sub–products are presented in figure 3. The experimental pellets/micro–pellets were put under hot–tempering in the oven according to figure 4. The chemical composition of the obtained pellets/micro–pellets is shown in table 2.

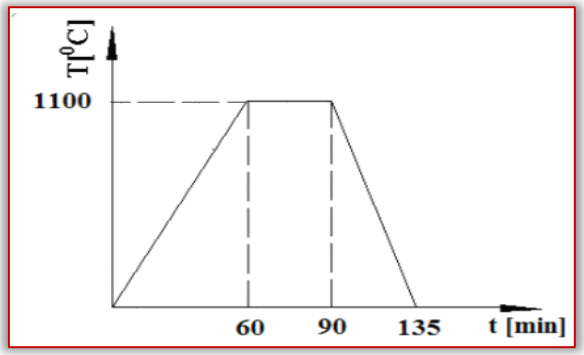

Figure 4. The pellets hardening diagram
(T– hardening temperature, [°C]; t – hardening time,[min])

Table 2. The chemical composition of the pellets

Chemical composition, [%] ASTM E 1479/2016						
Al	Ca	Cu	Cr	Mg	Mn	Ni
1.16	3.44	0.13	0.06	0.63	0.41	0.03
Si	Fe	W	S	Na	Anothers	
3.13	75.18	1.68	0.13	0.26	13.76	

From each batch of pellets we chose pellets sized 12–15 mm in diameter for which we tested compression strength of pellets. The result of the experiment are presented in table 3.

Table 3. Compressive strength of pellets

Compressive strength of pellets [daN/pellet]				
R1	R2	R3	R4	R5
178	172	167	157	175

The results show that compressive strength of pellets for raw and burnt pellets confirm the fact that the waste can be capitalized through pelletizing since the obtained pellets have the necessary astriction for manipulation and transportation from the manufacturing agent to the ovens at the steel plant.

FINAL RESULTS AND CONCLUSIONS

This paper present the obtained by–products (pellets/micro–pellets) while processing the analysed waste. After laboratory experiments a balance pan device was used and as binding agent bentonite and slag LF (max 10%).

The pulverous, small sized waste can be capitalized in the contemporary iron and steel industry and there is a need to continue research in order to establish the most performing procedures, capitalization methods that are good both from an economical and an ecological point of view.

The constant preoccupation to respect legal norms regarding the environmental protection and the need to harmonize them with the requirements of economic progress, the reasonable segmentation of material and energetic resources should lead to the capitalization of waste through technologies that can be deemed as the optimal solution economically and ecologically.

The laboratory experiments we performed lead to the procurance of experimental by–products – pellets that can be used as raw material in the siderurgy.

The main benefit of a granular product over raw fines is the improved product performance. In this sense, the pellets performance can be improved in a variety of ways as a result of agglomeration. Granular soil amendments, for example are more likely to deliver targeted results over their powdered form, because they do not become windblown and are much easier to accurately apply. Also, the pelletized products are much easier to handle and apply over raw material fines. Pellets are easier to feed, due to improved and more consistent flowability. Moreover, the pellet products are also much less dusty. Some materials may even be pelletized prior to landfilling in order to reduce dust loss during transport and handling, as well as to avoid material becoming windblown.

The production of pellets from different wastes can be made according to the range of recyclable waste available, the addition of binding substances, water and the granulometric finesse of the waste. The values obtained at the test for resistability at astriction for the raw and burnt pellets show that the product has the necessary resistance for being manipulated and transported to the iron processing plant. Reintroduction these ferrous materials in the economic circuit represents an advantage from an economic and ecological point of view.

References

[1] Costoiu, M., Ioana, A., Semenescu, A., Constantin, N., Florea, B., Rucai, V., Dobrescu, C., Polifroni, M., Păunescu, L., Environmental performance indicators for decision making and stakeholder interests, Environmental Engineering And Management Journal, Vol. 15, Nr. 10, pp. 2279–2284, 2016.

[2] Constantin, N., Stanasila, O., Stanasila, C., Alternative iron making technologies, Metalurgia International, Vol. 14, Nr. 7, pp. 5–7, 2009.

[3] Buzduga, R., Constantin, N., Ioana, A., Solutions to reduce the environmental pollution by the producers of refractories, University Politehnica Of Bucharest Scientific Bulletin Series B–Chemistry And Materials Science, Vol. 80, Nr. 1, pp. 231–244, 2018.

[4] Rucai, V., Constantin, N., Dobrescu, C., Experimental research program regarding the influence of thermo–time treatment of multicomponent ni–base melting on their properties in solid phase, University Politehnica Of Bucharest Scientific Bulletin Series B–Chemistry And Materials Science, Vol. 77, Nr. 4, pp. 359–364, 2015.

[5] Costoiu M, Ioana A, Semenescu A, Constantin N, Florea B, Rucai V, Dobrescu C, Polifroni M, Păunescu L 2016 Environmental performance indicators for decision making and stakeholder interests, Environmental Engineering and Management Journal, 15(10) 2279–2284

[6] Buzduga R, Constantin N, Ioana A 2018 Solutions to reduce the environmental pollution by the producers of refractories, University Politehnica Of Bucharest Scientific Bulletin Series B–Chemistry And Materials Science, 80(1) 231–244

[7] Rucai V, Constantin N, Dobrescu C 2015Experimental research program regarding the influence of thermo–time treatment of multicomponent ni–base melting on their properties in solid phase, University Politehnica Of Bucharest Scientific Bulletin Series B–Chemistry And Materials Science, 77(4) 359–364.
[8] Buzduga R V, Constantin N and Lazar E A 2015 Research on uses plant ashes in processing powders for classical moulding of steel, IOP Conf. Ser.: Mater. Sci. Eng. 85 012008
[9] Andrei V, Hritac M and Constantin N 2017 Experimental research on the behavior of the pneumatic transport of fine–grained iron, IOP Conf. Ser.: Mater. Sci. Eng. 163 012011
[10] Ioana A, Constantin N and Dragna E C 2017 EAF optimal managing elements, IOP Conf. Ser.: Mater. Sci. Eng. 163 012004
[11] Project no. 31–098/2007 Prevention and fighting pollution in the steel making, energetic and mining industrial areas through the recycling of small–size and powdering wastes Program PN2 Consortium CO Responsable Heput T, Beneficiary CNMP Romania
[12] Project no. BC 13/2018, Procesarea deşeurilor feroase pulverulente şi mărunte, Director proiect Ardelean, M., Beneficiar Johnson Solution SRL Deva.

ISSN: 2067-3809

[1.]A M RAJESH, [2.]Mohamed KALEEMULLA, [3.]Saleemsab DODDAMANI

EFFECT OF ADDITION OF SIC AND AL_2O_3 ON WEAR BEHAVIOR OF HYBRID ALUMINUM METAL MATRIX COMPOSITES

[1.]Department of Mechanical Engineering, SJM Institute of Technology, Davangere, Karnataka, INDIA
[2.]Department of Studies in Mechanical Engineering, U B.D.T. College of Engineering, Karnataka, INDIA
[3.]Department of Mechanical Engineering, Jain Polytechnic, Davangere, Karnataka, INDIA

Abstract: In the present investigations, wear test is conducted on pin on disc device at room temperature for both the age hardening and without age hardening conditions. Al7075 has chosen as the matrix material. HMMCs are produced utilizing stir casting route for enhancing the wear behavior and hardness number. The reinforcement used is silicon carbide with 5%, 10% and 15% weight percentage and Al_2O_3 as the reinforcement in 5%, 10% and 15% weight percentage. In the aluminum matrix Microstructural characterization reveals the homogeneous mixing of reinforcements. This investigation shows the enhanced in wear resistance is due to the increment weight fraction of reinforcement. By raising the sliding speeds there is a reduction in the rate of wear and it reduces with increment in sliding distance. As an increase in weight fraction there is decrement in rate of wear of composites. In general tribological property enhances because of the addition of the two reinforcements.
Keywords: Al7075/SiC–Al_2O_3, Dry sliding wear, wear rare, HAMMCs

INTRODUCTION

MMCs comprise of an alloy or a metal as the matrix and a reinforcement such as the particles, short fibre or whisker and/or long fibre. MMCs were a group of material with perspective for a broad collection of applications in structural management. Their properties such as light in weight, superior strength and resistance to wear are the requirement for the aviation and automobile industries.

Discontinuously reinforced MMCs are much less expensive to fabricate than continuously reinforced composites. Consequently, performance enhancement of the matrix comes at lower additional costs with discontinuous reinforcements compared with aligned reinforcements. Particulate reinforced MMCs are not expensive to manufacture than reinforced composites. Accordingly, performance improvement of the matrix comes at lesser expenses with particulate reinforcements compared with fiber aligned reinforcements. In addition, particulate reinforced composites exhibit the isotropic properties [1], whereas the properties of composites with fiber aligned reinforcements are highly anisotropic.

Hybrid aluminum metal matrix composite (HAMMC) materials are an excellent substitute to conventional materials, because of the enhanced hardness, specific strength and creep resistance properties. Based on the literature survey made, one can consider the Al7075–SiC/alumina particulate MMC for automobile applications such as: pistons, cam shafts, brake components, Bearing surfaces, cylinder liners, etc., and aerospace applications such as wing and fuselage (main body) of aircraft structure, internal aerospace engine components, exhaust systems.

A surface phenomenon referred as wear will occurs by relocation & separation of material. It generally suggests a progressive loss of material and change of measurements over some undefined time frame.

The principle tribological considerations that manage the wear and friction properties of discontinuously reinforced aluminium (DRA) composite can be categorized into two types (i) Mechanical and physical properties: such as loads, speeds, surface finish, sliding distance, orientation of reinforcement, temperature and environment etc. (ii) Material factors: for instance the type, size, and size distribution, shape, reinforcement's weight fraction, and the matrix microstructure [2].

The important parameter which influences the wear of materials is the microstructure. According to research reports, microstructure and mechanical properties have a correlation. On the other hand, to relate the wear techniques with microstructural characteristics only limited reports were used. The wear surface exhibits microstructural heterogeneity which influences wear procedure since constituent, for example, incorporations, intermetallics, and scattered phases have properties not quite the same as those of the matrix. The most imperative part of the microstructure is the distribution of second phase particles [3].

AMCs are majorly impacted by the characters of the matirx and reinforcement material. The worn surface of the material, in dry sliding wear, is subjected to considerable work hardening. The layer, mechanically mixed layer (MML) is produced during wear of aluminum alloys, sliding against ferrous alloy. Due to the shift and combination of materials, under definite load and velocity range, MML is formed. The generated MML consists of materials from both contact surfaces. It was also reported that the hardness of the generated MML is greater than the bulk hardness of the composite. The generated MML is majorly responsible for the decrement of wear rate and holding–up of transition to severe wear.

The literature survey gives the survey of the published material accessible on the influence of different types of

reinforcements, volume/weight fractions, aging behaviour and size with aluminium based MMCs are a blend of two phases: one is referred as matrix, and the other as the reinforcement. Singla et al [4] developed aluminium alloy/ SiC_p composites of varying weight fractions of silicon carbide (5–30%) by stir casting techniques using a two step–mixing method. Results showed that impact strength and hardness increased with an increment in weight percentage of silicon carbide. Rajesh A M et al [5–7] conducted experimentations like hardness, wear behavior at as–cast and age hardened conditions etc on aluminum hybrid metal matrix composites. The matrix material considered is Al7075, and reinforcement material is SiC and alumina. From the results it is clear that the HAMMCs have better properties as compared to unreinforced aluminum alloy.

M K Surappa et al [8] studied the Al–Si composite for their tribological behavior. For the study, they considered the automobile brake in pin on disc tribometer. Aluminum metal matrix composites were utilized as a disc whereas brake pad material forms the pin. Form the outcomes it is observed that the coefficient of wear and the fraction is varied with the load. Also as the coefficient of fraction decreases wear rate increases. R. L. Deuis et al [9] surveyed the wear behaviour of the materials and the development of fine equiaxed wear debris is related with a stable tribo–layer on the worn surfaces. The critical parameters for adhesive wear are applied load, sliding velocity, the surface hardness of worn surface and morphology in relative to the theories of wear encuontered by the materials.

Radhika et al. [10,11] has conducted the experiments to evaluate the wear characteristics of Al/Gr/Al_2O_3 hybrid MMC and suggested that the graphite reinforcement has boost up the resistance to wear. This increment is due to the forming a protective layer between the counterface & pin. Addition of the reinforcement Al_2O_3 has considerable influence in reducing rate of wear of the composite. Saleemsab Doddamani et al [12] conducted experimentation on wear behaviour of Aluminum–graphite MMC. From the results it is found that the adding of particles of graphite has increased the resistance to wear of the MMC. Also it is reported that addition of particles of graphite in aluminum reduces the friction then that of the base alloy.

Heat treated material demonstrate the resistance to wear [13]. Because of the higher ductility and strength of the aluminum matrix, the effectual stress connected on material surface along with the wear progression is less on account of the heat–treated alloys. This occurrence caused a reduction in the cracking propensity of the material surface when contrasted with the as–cast alloy [14]. The heat treatment didn't drastically modify the morphology, but rather the matrix hardening by age hardening occurred, which prompted greater strength & hardness [15]. The yield strength and higher hardness of the material after this heat treatment condition may have the benefit of keeping generation of aluminium debris & reduction in its exchange to the steel surface [16]. Amro M. Al–Qutub et al [17] investigated the properties of Al6061 matrix reinforced with 10% volume fraction of Al_20_3. Cui Y Geng et.al [18] observed that, an aluminum matrix composite was viably gotten using the self proliferating high temperature silicon carbide particles. The composite was seen to be better in mechanical exhibitions to those of the composite with the normal status evaluation silicon carbide particles. From the outcome it is reported that between aluminum–SiC their exist a high strength interfacial bond.

It is noticed from the literature that more research conducted on the wear characteristics of Al–SiCp, Al–Li/SiC MMCs. In this background, the research gaps indicate that there is a lot of scope for current researchers for investigation with the use of a combination of silicon carbide and aluminium oxide as reinforcement. Therefore this research work will focus on wear behaviour of aluminum hybrid metal matrix reinforced MMCs. Main aim of the proposed research work is to develop the hybrid MMC in–order to improve the strength and wear resistance characteristics of the material that generate Mechanically mixed layer.

MATERIALS AND PROCESSING

— Materials

Al–7xxx alloys, for instance, 7075 are commonly used as a part of applications including transport, automobile, marine and also in aerospace, because of their high strength and low weight. The main constituents in the Al7075 are Si=0.4%, Zn = 6.1%, Mg=2.9%. The properties of the Al7075 are density = 2.85g/cc, ultimate strength = 480MPa, elastic modulus = 75GPa, Poissons' ratio = 0.33, melting point = 650^{0}C.

Silicon carbide is a ceramic material also known as carborundum, denoted as SiC. It is a blend of silicon and carbon. It is an outstanding abrasive material utilized to prepare grinding wheel and other abrasive parts. Now a day, the SiC material is formed into a technical grade better quality ceramic with excellent mechanical/physical properties. Some of the key properties of silicon carbide utilized here are Density –3.1 g/cc, melting point –2730^{0}c, molecular mass –40.10 g/mol, grit size –16–100grit, Appearance –Black in color. Aluminum oxide, commonly known as alumina (Al_2O_3) is corundum in its crystalline form is widely used in industry. The alumina (Al_2O_3) as a reinforcement is steadier with aluminium and withstand higher temperatures. Some of the key properties of aluminum oxide utilized here are density=3.69g/cc, melting point –2072^{0}C, mesh size=100–200 mesh, appearance – White in color.

— Processing

Al7075–SiC/Al_2O_3 samples are formed at varied weight fractions of SiC/Al_2O_3 (5%, 10% and 15%) utilizing stir casting technique. The aluminum slabs were melted in the furnace. In the wake of liquefying, liquid aluminum was superheated to 750^{0}C temperature [5,6]. The required measures of SiC/Al_2O_3 particles were added to the liquid aluminum while mixing with a stirrer at 600rpm speed. The liquid Al7075–SiC/Al_2O_3 was filled a permanent mold and it was permitted

to set. The Al7075–SiC/Al_2O_3 composite bars were taken out from the mold. The samples were set up from as–cast combinations for investigation of required properties. Shearing temperature (620^{0}C) and shearing speed (600 rpm) were the two process parameters which affect the composites. To examine the effect of processing parameters tests were conducted. The different process parameters were chosen to exert a hydrodynamic force on the molten material and to retain best possible fluidity for the casting.

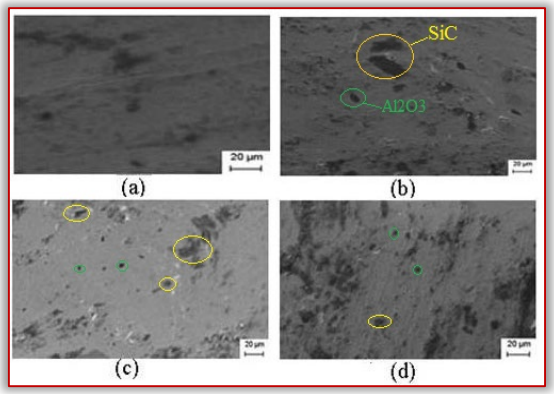

Figure 1. Scanning Electron Micrograph shows a uniform distribution of particles of SiC/Al_2O_3 (a) As cast Al7075 (b) 5% SiC/Al_2O_3 (c) 10% SiC/Al_2O_3 (d) 15% SiC/Al_2O_3

In the microstructure, shown in Figure 1, of the Al7075–SiC/Al_2O_3 particulate composite confirms uniform distribution of the reinforcement. In the process of the mixing, a whirling of molten material is formed from the rotation of the stirrer through which the SiC/Al_2O_3 particles are drained into the melt. The force gave by mixing the molten material with a mechanical stirrer beats the surface vitality hindrance because of poor wettability of SiC/Al_2O_3 by Al composite. Once the SiC/Al_2O_3 particles are moved into the molten aluminium, the dissemination is firmly influenced by certain flow transitions. From the momentum transfer and the outspread flow of melt, lifting of SiC/Al_2O_3 particles will take place and also causes prevention of particle settling in the matrix. Meanwhile, local hydrodynamic forces are induced on the particle grouping of SiC/Al_2O_3 particulates. These forces induced are capable of separating the clustering of SiC/Al_2O_3 particles which in turn leads to homogeneous microstructure all through the cast segment.

A strong homogeneous microstructure between the reinforcement and matrix helps in the load exchange from the reinforcement to the matrix. Thus, the break happens in the composite via the reinforcement and not along the interface. Despite the fact that the SiC/Al_2O_3 is a non–load bearing ingredient, a solid particle/matrix interface helps the SiC/Al_2O_3 particles install themselves into the matrix legitimately, enhancing the crack resistance. It has been reported that during solidification, an enhancement in the interfacial relationship between the aluminum matrix and SiC/Al_2O_3. By reason of the uniform distribution and good bonding of SiC/Al_2O_3 particles in the aluminium matrix, Al7075–SiC/Al_2O_3 particulate composites have greater tribological properties such as the good machinability, low wear rate, high damping capacity, and their outstanding properties.

— Age Hardening

The as–cast composite specimens were heat treated at a temperature of 465^{0}C for 02 hrs taken after by quickly quenched in cool water. After quenching the specimens, these are subjected to an age (precipitation hardening) by heat–treatment the specimens to 120^{0}C, maintaining this temperature for 05 hrs and after that taken after cooling in air to room temperature.

EDX ANALYSES

To determine the chemical composition of the Al7075–SiC, alumina composites, EDX measurements are carried out in the SEM on individual specimens. The EDX analysis indicates the foremost composition of Al7075–SiC, alumina composites silicon, magnesium, Fe, carbon and aluminum. Small amount of oxygen are also observed. The signals of oxygen may arise from the contamination of the aluminum oxide. Table in the Figure 2 describes the atom percentage of Si, magnesium, carbon, and aluminum. These outcomes specified that the chemical compositions of the Al7075–SiC, alumina is consistent. The atomic percentage of carbon is high than compared to silicon and magnesium. The presence of carbon indicates the adding up of SiC, alumina reinforcement with the Al7075 matrix. The content of Silicon (0.63 to 0.91) and Magnesium (0.6 to 2.54) indicates that the presence of Si and Mg in the Al7075 alloy.

From the EDX analysis (Figure 2), it is found that Al7075– SiC, alumina MMCs are rich in both Si and Mg. The existence of $MgAl_2O_4$ at interfaces was confirmed in a detailed study on the interfaces in discontinuously reinforced metal–matrix composites. In all the compositions of Al7075– SiC, alumina, oxygen (O) content has been obtained. The content of O is due to the formation of Al_2O_3 on the top of the pits as the main compound on the surface. The analysis of mechanically mixed layer was carried out by utilizing EDX to study the degree of exchange of material from the disc to pin. O–mapping, in addition, is performed to know if any sample of oxidation tested at Along with Fe, O was likewise in age hardened Al7075 reinforced with Sic and alumina specimens. The O presents in an O_2, though, no clarity though it is a FeO_2 or Alumina.

WEAR ANALYSIS

The dry sliding wear behaviour of Al7075/SiC–Al_2O_3 HAMMCs and heat treated (T6) Al7075/SiC–Al_2O_3 HAMMCs conducted according to ASTM G–99 standard testing procedure. Dry sliding wear experiments were conducted using a computerized Pin–On–Disc (POD) wear apparatus (Model: Wear & Friction Monitor TR–20) supplied by DUCOM. The dry sliding wear tests are conducted by weight loss measurement technique and data obtained from the experimentation for different loads, speeds and different compositions for as–casted and age hardened conditions.

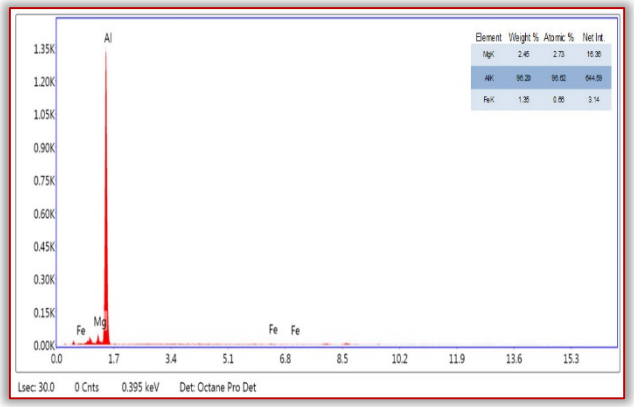

(a) 0% reinforcement

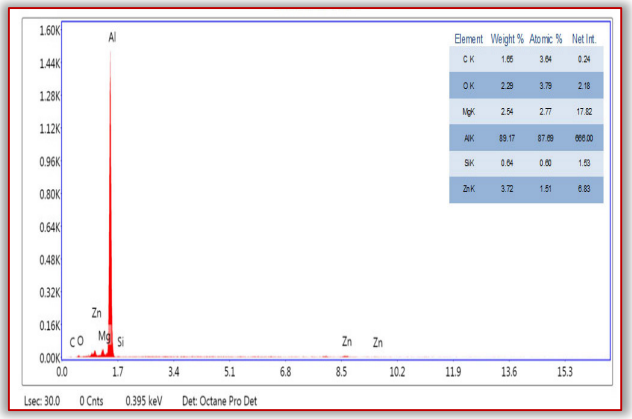

(b) 5% reinforcement

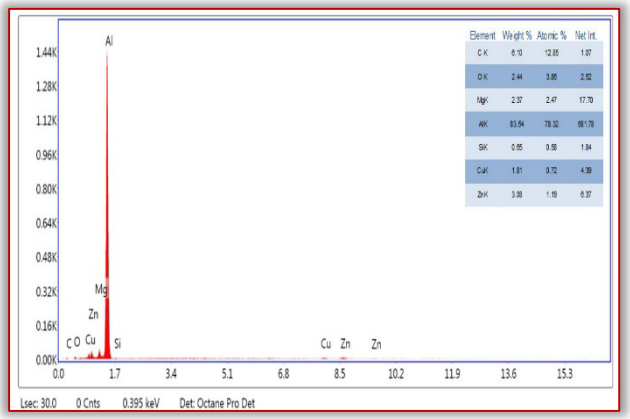

(c) 10% reinforcement

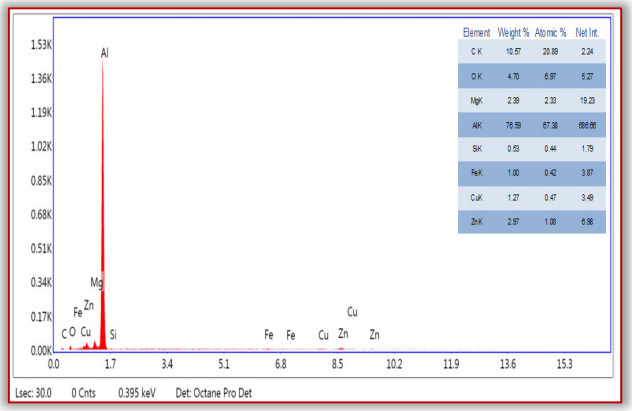

(d) 15% reinforcement

Figure 2. EDX profile analysis for the surfaces

SEM was carried out to understand the changes in worn surfaces with the addition of SiC and Al_2O_3 reinforcements. The dry sliding wear behavior of Al7075 base Alloy–Sic– Al_2O_3, HAMMCs and heat treated (T6) Al7075 base Alloy–SiC– Al_2O_3 HAMMCs conducted according to ASTM G–99 standard testing procedure. Dry sliding wear experiments were conducted using a computerized Pin–On–Disc (POD) wear apparatus(Model: Wear & Friction Monitor TR–20) supplied by DUCOM The machine comprises of high carbon EN–31steel disc and a wear track diameter of 90 mm. The cylindrical specimen of 10 mm diameter and 30 mm height were utilized for wear tests. Wear tests conducted for 3 different normal loads i.e. 2kg, 4kg, 6kg, at a fixed sliding velocity of 0.942m/s, 1.8849m/s, 2.82m/s for 200, 400, 600rpm respectively for about 5minutes.During the wear test, height loss of the specimen was recorded and the corresponding volume loss, wear rate, were calculated. Before and after the test, both disc and specimen were cleaned.

After the sliding wear test the volumetric wear loss was calculated over a Sliding distance of 282.47m, 565.48m, and 848.23m for 200, 400, 600rpm respectively for about 5minutes at a load of 2kg (19.62N), 4kg (39.24N), 6kg (58.86N). It was observed that the volumetric wear loss increased linearly with the increase in sliding distance in all the investigating composites. The volumetric wear loss reduced with increment in content of SiC and Al_2O_3 reinforcements in MMCs when compared with base alloy. It shows the increased wear resistance of the composites. In HAMMCs the reduced wear loss was observed when compared with as–cast 7075 because of the existence of Sic and alumina, which act as solid lubricant [19]. At higher in sliding distances the temperature of the sliding surfaces increases, which consequences in soften of the pin surface which is in contact with the disc, leading to heavy deformation and results in advanced volumetric wear loss of the pin.

From the analysis minimum wear loss was observed in Al7075–10wt%SiC–10wt% Al_2O_3 HAMMCs. Dry sliding wear tests on hybrid aluminum matrix composites, reinforced with silicon carbide and graphite particle and show that graphite particles were useful agents in rising resistance of dry sliding wear of Al2219–SiCp composites [20]. Graphite particles effect on distribution on wear behavior of aluminum composites with a weight percentage of graphite content. They found that the existence of graphite particulate could enhance the wear resistance in composites. When compared with base matrix alloy lower wear loss was observed in composites. Increased loads resulted in delamination leading to high volumetric wear of both the matrix alloy.

— Impact of sliding distance on the volumetric wear rate

The volumetric wear rate varies with the sliding distance as shown in Figure 3(a–c) as–cast and Figure 4(a–c) with age hardening, by incrementing the sliding distances rate of wear reduces. The high temperature effect led to deformation instead of wear in softer material. This outcome is seen in each composites which reduces the rate of wear.

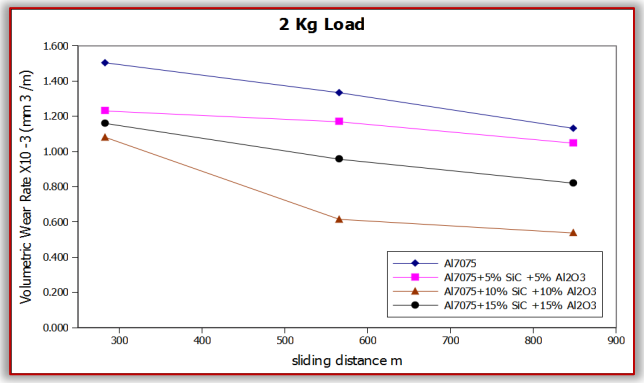

Figure 3a. Volumetric wear rate vs sliding distance Al7075 HAMMCs at load of 2kg [as–cast]

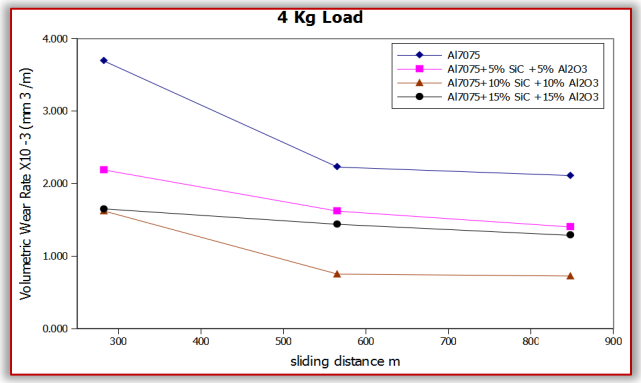

Figure 3b. Volumetric wear rate vs sliding distance Al7075 HAMMCs at a load of 4kg [as–cast]

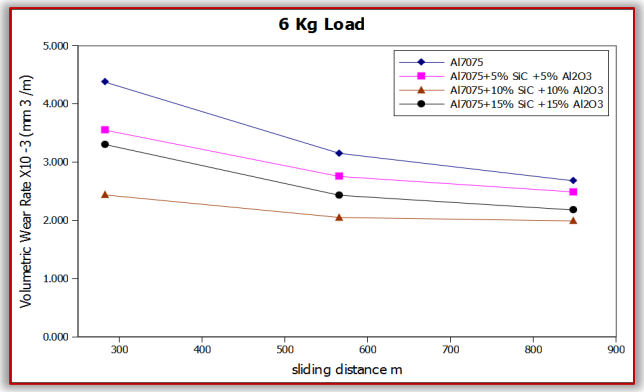

Figure 3c. Volumetric wear rate vs sliding distance Al7075 HAMMCs at a load of 6kg [as–cast]

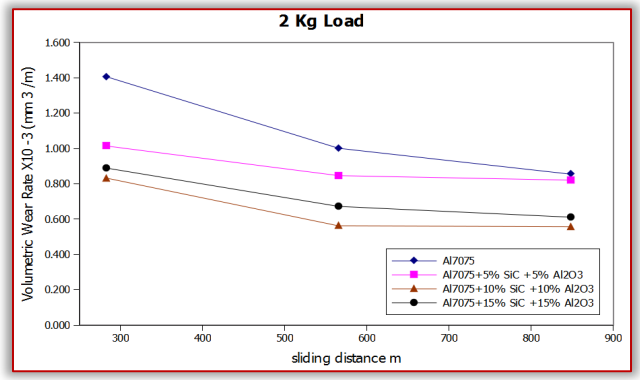

Figure 4a. Volumetric wear rate vs sliding distance Al7075 HAMMCs at a load of 2kg [age hardening]

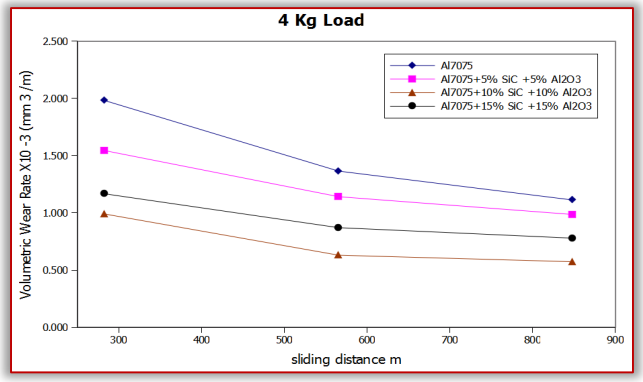

Figure 4b. Volumetric wear rate versus sliding distance Al7075 HAMMCs at 4kg load [age hardening]

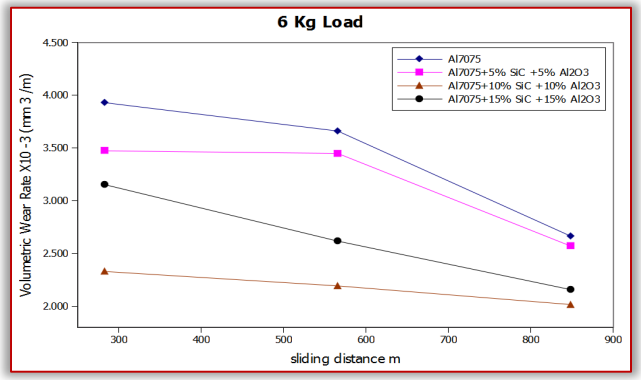

Figure 4c. Volumetric wear rate versus sliding distance Al7075 HAMMCs at 6kg load [age hardening]

From Figure 3 to 4 it was observed that the volumetric wear loss decreased in heat treated 7075 HAMMCs increased Sic and Al_2O_3 reinforcement (10%). When compared with the 7075 HAMMCs.

In aged HAMMCs the volumetric wear loss was further reduced when compared with 7075 HAMMCs. Remarkably the lowest volumetric wear loss was observed in heat treated Al7075–10%SiC + 10%Al_2O_3– with ageing when compared to 7075 HAMMCs. Wear behavior of AA6092–SiC composite which is heat treated, highlighted the improvement in hardness due to T6 heat treatment, which lead to the improved wear resistance of MMCs.

— Outcome of functional load on the volumetric wear rate

The wear properties of 7075 HAMMCs and heat treated 7075 HAMMCs were discussed on the basis of volumetric wear rate with applied load. From Figure 5 to Figure 6 it was observed that, with an increase in load from 2 kg (19.62N), 4 kg (39.24N) and 6 kg (58.86N) the volumetric wear rate increased in 7075 HAMMCs and heat treated 7075 HAMMCs proportionately. In heat treated 7075 HAMMCs, the volumetric wear rate was less when compared with the 7075 HAMMCs Also the lowest volumetric wear rate was observed at Al7075–10%SiC + 10%Al_2O_3, at a load of 2 kg(19.62 N). The cumulative volume loss increases with increasing applied normal load [96]. The parameters like time 5minutes, track diameter 90mm is considered for all the wear specimens without heat treatment and age hardening.

From Figure 5a, for sliding velocity 0.9424m/s, the volumetric wear rate will increases as there is increase in applied load. Also the lowest volumetric wear rate was seen at Al7075+10%Sic + 10%Al_2O_3, from Figure 5b, sliding velocity is 1.884 m/s the Volumetric wear rate will be less for 10% reinforcement at a speed of 400 RPM is applied. From Figure 5c, for sliding velocity2.827 m/s, the volumetric wear rate will decreases for 15% reinforcement when load is applied and it is less for 10% reinforcements.

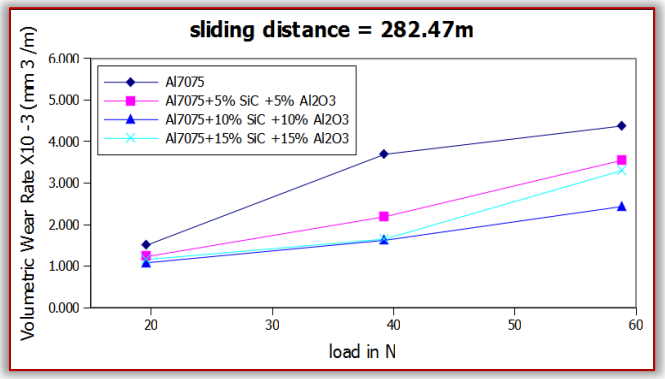

Figure 5a: Volumetric wear rate at an applied of speed 200 RPM in Al7075 HAMMCs [as–cast]

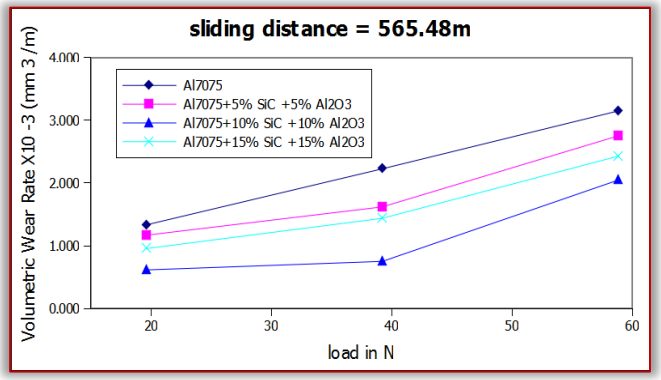

Figure 5b: Volumetric wear rate at an applied of speed 400 RPM in Al7075 HAMMCs [as–cast]

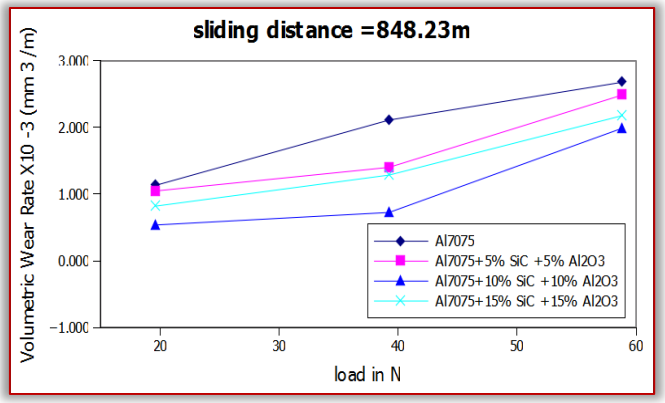

Figure 5c: Volumetric wear rate at an applied of speed 600 RPM in Al7075 HAMMCs [as–cast]

The inclusion of ceramic materials in an aluminium alloys incremented the load bearing capacity. The investigation of wear behaviour of Aluminum Matrix Composites against friction materials is receiving particular attention because of the possibility of using these materials for disc brakes in automotive application [89]. The addition of reinforcement in an aluminium matrix increases the load bearing capacity and higher wear resistance. The role of silicon carbide and alumina are responsible for improving the wear resistance of the hybrid composites. Because of increase in load rate of wear incremented as material contacting pressure is more. Pressure raise influenced the wear depth this is seen from the Figure 5 to 6.

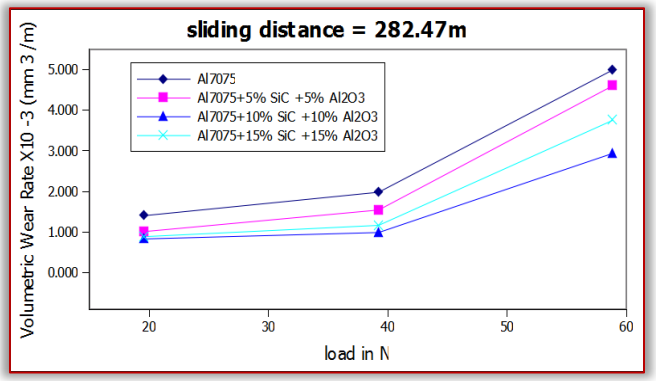

Figure 6a: Volumetric wear rate at an applied of speed 200 RPM in Al7075 HAMMCs [age hardening]

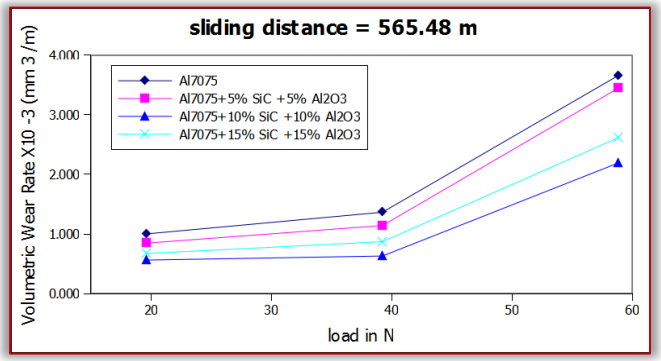

Figure 6b: Volumetric wear rate at an applied of speed 400 RPM in Al7075 HAMMCs [age hardening]

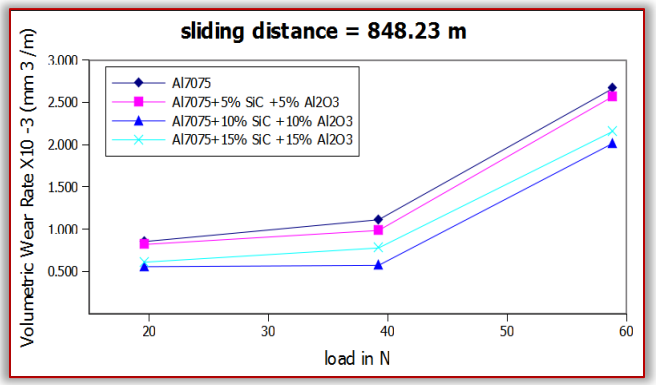

Figure 6c: Volumetric wear rate at an applied of speed 600RPM in Al7075 HAMMCs [age hardening]

From Figure 6a,sliding velocity 0.9424m/s the Volumetric wear rate will increases as the load increases to 4kg and again increases as the load increases to 6kg and it is observed From Figure 6b, sliding velocity 1.884 m/s, the Volumetric wear rate will be less for 5% reinforcement when a load of 6kg is applied. From Figure 6c, for sliding velocity 2.827m/s, the volumetric wear rate will decreases for 5% reinforcement

when 4kg load is applied and it is less for 15% reinforcement when 6kg load is applied. Silicon carbide reinforced aluminum alloy composite observed that the useful effect of particle reinforcement is reduced with load increment. The effect of each reinforcement particle is able to carry a bigger portion of load.

— Result of sliding distance (sliding speed) on wear rate

In the Metal Matrix Composites (MMCs) increase wt% of SiC and Al_2O_3 reinforcement improves the hardness. At larger sliding distances, the rise of the sliding surface temperature is unavoidable. Addition of hard particulate reinforcement in the composites restricts the composites from getting soft which results in the reduction in wear rate. A Similar trend was observed in case of Al7075–Sic–Al_2O_3HAMMCs as shown in Figure 7 to Figure 8.

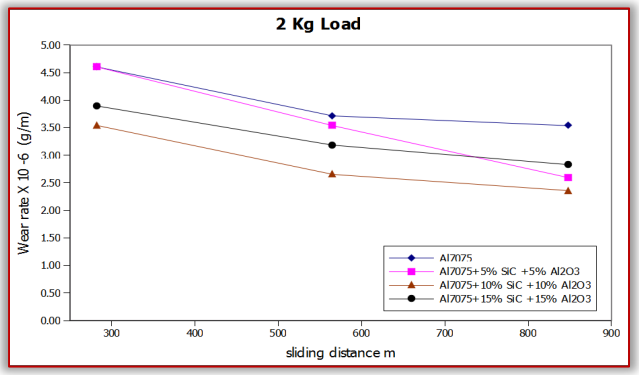

Figure 7a: Wear rate vs sliding distance for HAMMCs at a load of 2kg, after a sliding–distances of 848.23 m [as–cast]

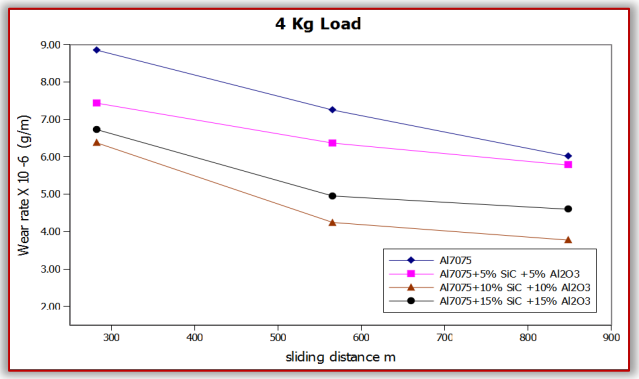

Figure 7b: Wear rate vs sliding distance for HAMMCs at a load of 4kg, after a sliding– distance of 848.23 m [as–cast]

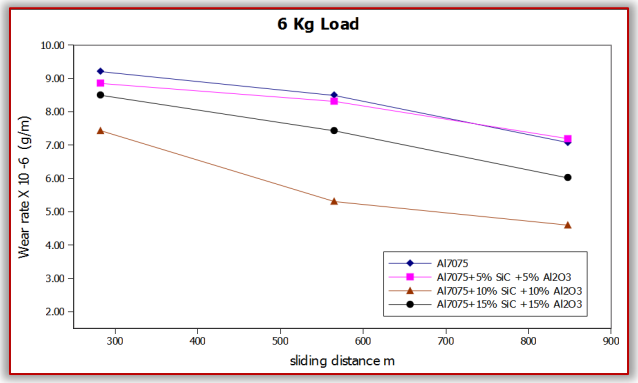

Figure 7c: Wear rate vs sliding distance for HAMMCs at applied load of 6kg, after a sliding distance of 848.23 m [as–cast]

In Al7075–10%Sic–10%Al_2O_3 HAMMCs reported the least wear rate at 58.86 N load. From Figure 7a to Figure 7c it was seen that the wear rate reduced drastically with sliding distance from 282.47m, 565.48m, and 848.23m for 200, 400, 600rpm in base alloy Al7075 HAMMCs and heat treated Al7075 HAMMCs Further increase in sliding distance, the wear rate reduces gradually, beyond sliding distance of around 848.23 m, the wear rate remains almost unchanged. This clearly reflects that the wear stabilization called critical point and the corresponding sliding distance and wear rate are considered to be critical, beyond which the wear stabilization was observed.

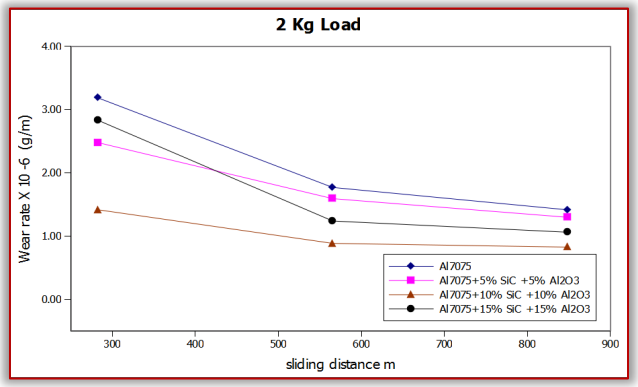

Figure 8a: Wear rate vs sliding distance for HAMMCs at a load of 2kg, after a sliding distance of 848.23 m [age hardening]

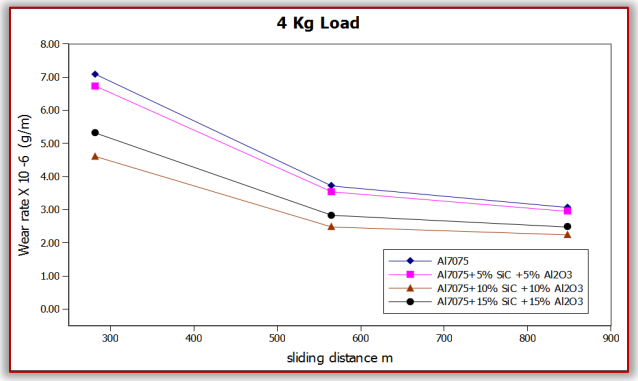

Figure 8b: Wear rate vs sliding distance for HAMMCs at a load of 4kg, after a sliding– distances of 848.23m [age hardening]

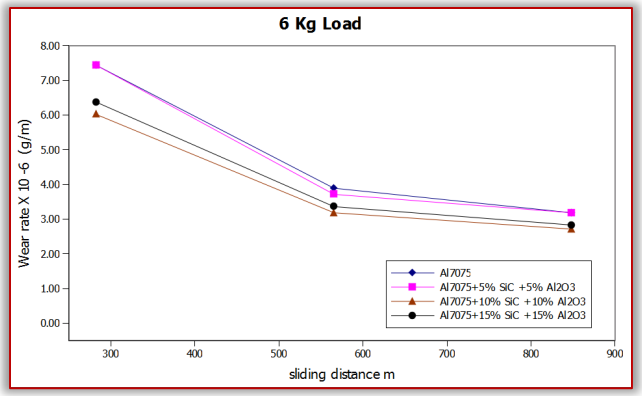

Figure 8c: Wear rate vs sliding distance for HAMMCs a load of 6kg, after a sliding distance of 848.23 m [age hardening]

The reduced wear rate was observed in heat treated HAMMCs with increment in SiC and Al_2O_3 reinforcements as shown in

Figure 8(a–c). The improvement in hardness number of the composite represents the reduced rate of wear as noticed by researcher. The minimum wear rate was observed for all loading conditions in Al7075–10%SiC–10%Al_2O_3 HAMMCs with T6 heat treatment also observed the least wear rate at 58.86N.Minimum wear rate was observed that in Heat treated HAMMCs at 58.86 N loads.

At higher loads the temperature of the sliding surfaces increases which leads to higher wear rates. But due to hard particulate reinforcement in the composites, it restricts the composites from getting soft. Further increased sliding distance reduces the wear rate and after a particular sliding distance.

The wear rate remains almost unchanged as shown in Figure 7 to Figure 8. This clearly reflects that the wear stabilization occurs at a critical point and such corresponding sliding distance and the wear rate are considered as critical, beyond which the wear stabilization occurs.

— Effect of applied load on wear rate

The applied load is the most dominating factor which controls the wear behavior. Figure 9 to Figure 10 shows the effect of applied on the wear rate of 7075 HAMMCs and heat treated 7075 HAMMCs. The wear rate varies with the normal load. It was seen that at high loads the wear rate was increased in both 7075 HAMMCs and heat treated 7075 HAMMCs with the increase in load the wear rate was increased. The decrease in wear rate was observed with the increase in the percentage of SiC and Al_2O_3 reinforcement up to 10 wt%.

The wear rate was significantly lower in heat treated 7075 HAMMCs when compared with the 7075 HAMMCs, from Figure 9a, for sliding velocity 0.9424 m/s. Wear rate decreases as the % of reinforcement increases up to 10%. From Figure 9b, for sliding velocity of 1.884 m/s. Wear rate will be less for 10% reinforcement of silicon carbide and aluminium oxide. From Figure 9c, for sliding velocity 2.827 m/s, wear rate will be less for 15% reinforcement. But when 6kg load is applied the wear rate will decreases for 10% reinforcement sic and alumina. According to several authors with an increase in load, increase in wear rate was observed. At higher loads the contact surface temperature increases.

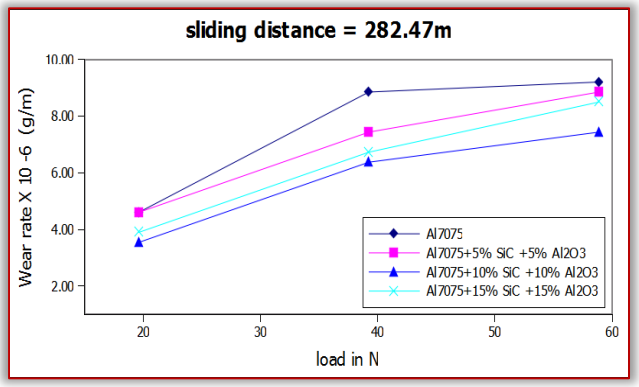

Figure 9a. Effect of load on rate of wear of HAMMCs for a speed of 200 RPM [as–cast]

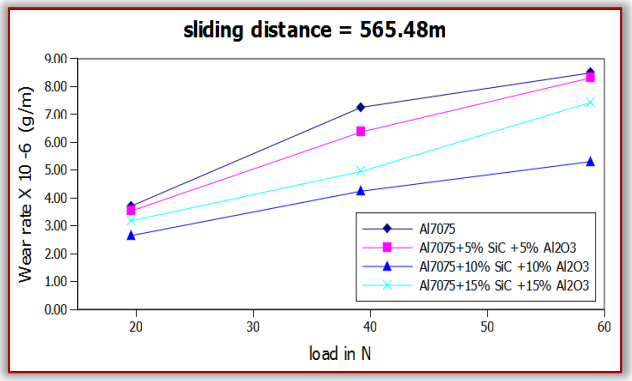

Figure 9b. Effect of load on the rate of wear of HAMMCs for a speed of 400 RPM [as–cast]

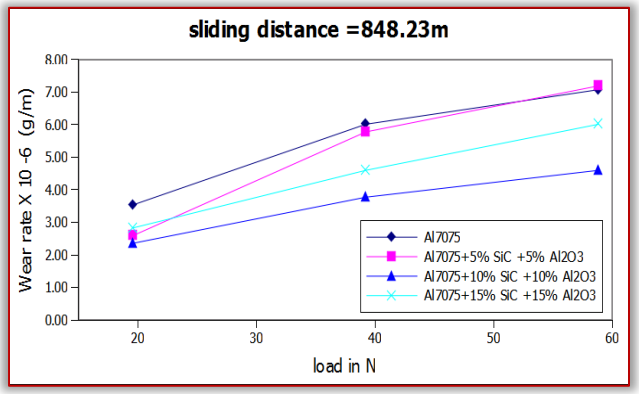

Figure 9c. Effect of load on the rate of wear of HAMMCs for a speed of 600 RPM [as–cast]

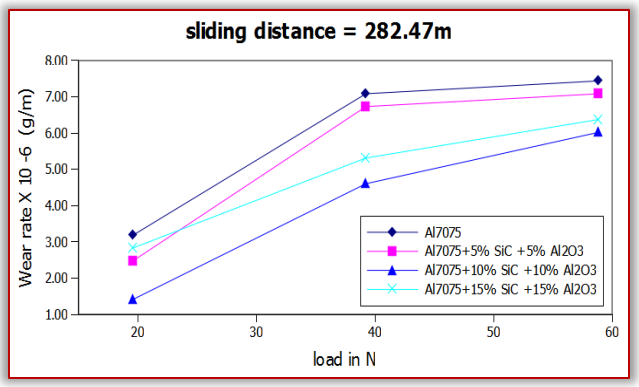

Figure 10a. Result of load on the rate of wear of HAMMCs for a speed of 200 RPM [age hardening]

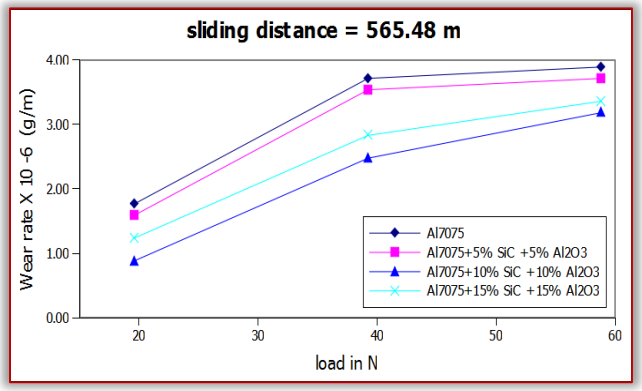

Figure 10b. Cause of load on the rate of wear of HAMMCs for a speed of 400 RPM [age hardening]

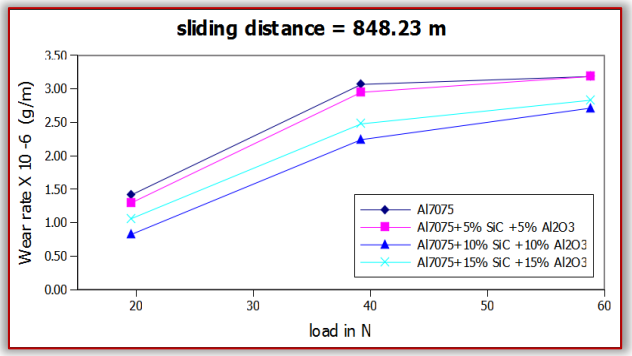

Figure 10c. Cause of load on the wear rate of HAMMCs for a speed of 600 RPM [age hardening]

From Figure 10a, for, sliding velocity 0.9424m/s, wear rate decreases as the % of reinforcement increases up to 10%.From Figure 10b, for, sliding velocity 1.884 m/s Wear rate will be less for 10% reinforcement of silicon carbide and aluminium oxide. From Figure 10c, for, sliding velocity 2.827 m/s wear rate will be less for 5% reinforcement at 4kg of load. But when 6kg load is applied the wear rate will decreases for 10% reinforcement. In the present investigation similar trend was observed. The enhancement of hardness of the composites in improvement of wear and seizure resistance.

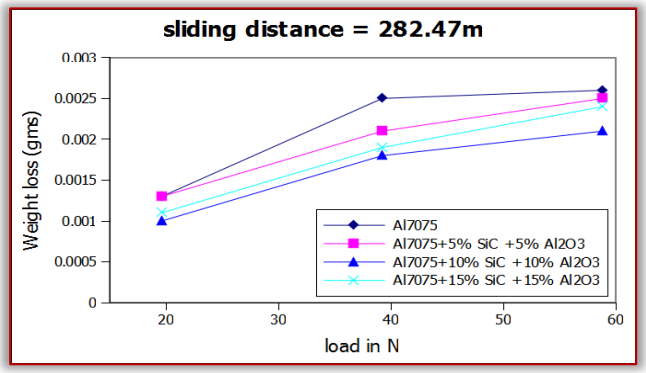

Figure 11a. Result of load on weight–loss of HAMMCs for a speed of 200 RPM [as–cast]

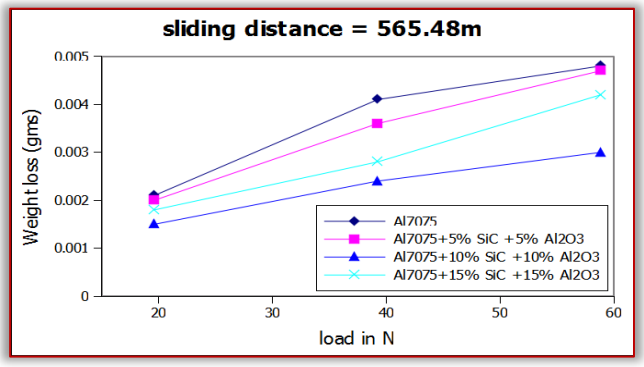

Figure 11b. Outcome of load on weight– loss of HAMMCs for a speed of 400 RPM [as–cast]

From Figure 11a, for sliding velocity 0.9424m/s, the weight loss will be less for 10% reinforcement when speed of 200 RPM is applied. From Figure 11b, for sliding velocity 1.884 m/s, the weight loss will be less for 10% reinforcement compared to other percentages of reinforcement when 6kg load is applied. From Figure 11c, for sliding velocity=2.827m/s. The weight loss will be less for 15% reinforcement when 4kg of load is applied but when the load is increased to 6kg the weight loss is reduced for 10% reinforcement.

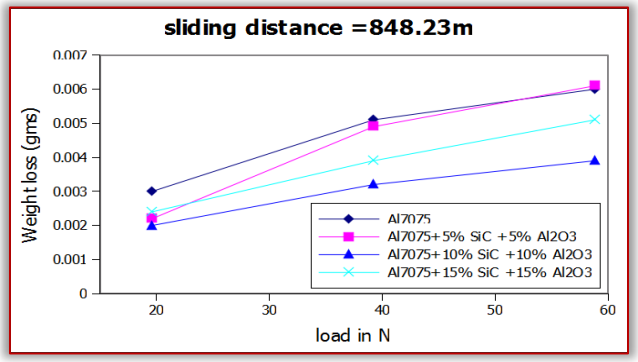

Figure 11c. Outcome of load on weight loss of HAMMCs for a speed of 600 RPM [as–cast]

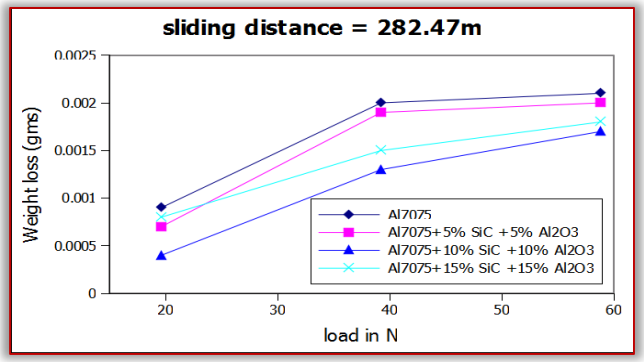

Figure 12a. Outcome of load on weight loss of HAMMCs for a speed of 200 RPM [age hardening]

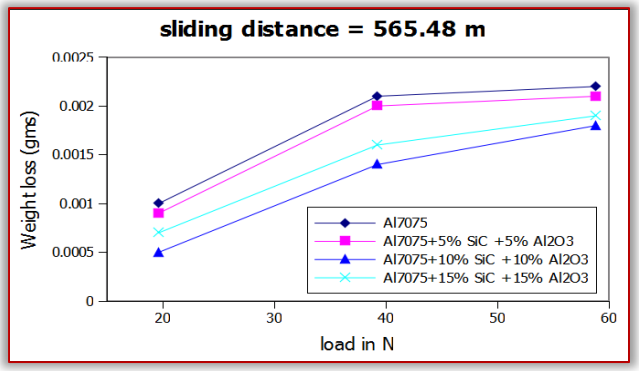

Figure 12b. Outcome of load on weight–loss of HAMMCs for a speed of 400 RPM [age hardening]

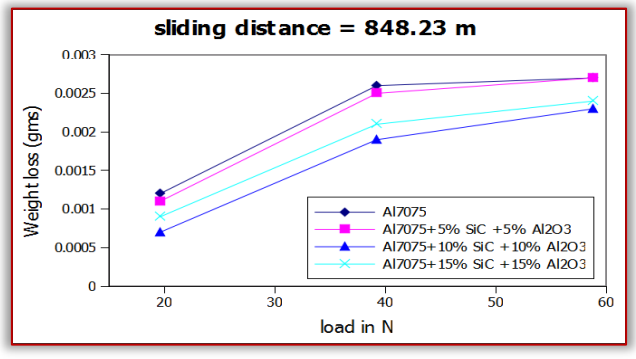

Figure 12c. Outcome of load on weight –loss of HAMMCs for a speed of 600 RPM [age hardening]

Friction coefficient reduced with an increment in percentage volume of Sic particles, wear and friction in Copper reinforced Al_2O_3 composites and reported the decreased coefficient of friction with increase in alumina content. From Figure 12a, for sliding velocity 0.9424m/s. The weight loss will be less for 10% reinforcement when 4kg of load is applied. From Figure 12b, for sliding velocity of 1.884 m/s, the weight loss will be less for 5% reinforcement compared to other percentages of reinforcement when 6kg load is applied. From Figure 12c, for sliding velocity 2.827m/s, the weight loss will be less for 5% reinforcement when 4kg of load is applied but when the load is increased to 6kg the weight loss is reduced for 10% reinforcement.

CONCLUSIONS

From the investigation the following conclusions were drawn on the mechanical and wear performance of as–cast and T6 aging of HAMMCs–Al7075–SiC–Al_2O_3. Wear resistance of Al7075/Al_2O_3+SiC composites incremented with weight percentage. The reduction in rate of wear with sliding distances, composition. It enhances with loads for age hardening & without age hardening. The age hardened Al–7075/Sic+Al_2O_3 Composite shows excellent resistance to wear while compare to Al7075/ Al_2O_3+SiC it has the distinctive property as addition of Silicon–carbide and Aluminium–oxide. The microstructural characterization discovered that the homogeneous circulation of the particle in the matrix system with minimal amount of porosity. The micro–structural study of SEM and EDX techniques shows the homogeneous distribution of the particulates in the hybrid composites.

In T6 heat treated (age hardening) Al7075–10wt%SiC+10wt% Al_2O_3 HAMMCs, improved the wear resistance was observed when compare with base alloy. Highest resistance to wear was observed in Al7075–10wt%SiC+10wt% Al_2O_3 due to the presence of reinforcements. Further decrement in wear rate with increment in weight percent of reinforcement for the desired sliding distances. From the investigation, it was concluded that, composites containing 10% weight of silicon carbide and 10% weight of aluminium oxide reinforcements with ageing exhibited superior mechanical and tribological properties.

Acknowledgement

We wish to thank University B.D.T. College of Engineering (Davangere), VGST–K FIST facility for melting and Material Testing (SJMIT, Chitradurga) for their support in providing facilities for various characterizations of materials and helped me to complete my research work. This research received no specific grant from any funding agency in the public, commercial, or not–for–profit sectors.

References

[1] ASM Handbook, "Composites", ASM International, 21 (2001).
[2] Sannino, A. P., Rack, H. J. (1995). "Dry sliding wear of discontinuously reinforced aluminum composites: review and discussion". Wear, 189(1): 1–19.
[3] Williams, J. A. (2005). "Wear and wear particles – Some fundamentals." Tribology International 38(10): 863–870
[4] Singla, M, Dwivedi, DD, Singh, L, Chawla, V. (2009). Development of aluminium based silicon carbide particulate metal matrix composite. Journal of Minerals & Materials Characterization & Engineering, 8(6), 455–467.
[5] Rajesh A M, Mohammed Kaleemulla, "Experimental investigations on mechanical behavior of aluminium metal matrix composites", Materials Science and Engineering 149 (2016) 012121. doi:10.1088/1757–899X/149/1/012121.
[6] Rajesh A M, Mohammed Kaleemulla, "Experimental investigations on mechanical and wear behavior of hybrid aluminium alloy", Volume: 05, Issue: 13, 2016, pp 128–131.
[7] Rajesh A M, Mohammed Kaleemulla, "Effect of heat treatment on hybrid aluminum metal matrix composites", International Journal of Emerging Research in Management &Technology, Volume–6, Issue–5, 2017, pp 548–551.
[8] M.K. Surappa, R.K. Uyyuru., S. Brusethaug, "Effect of reinforcement volume fraction and size distribution on the tribological behaviorof Al–composite/brake pad tribocouple", Wear260, 1248–1255, 2006.
[9] R.L. Deuis., C. Subramanina., J.M. Yellup., "Dry sliding wear of aluminium composites – a review", Compos Sci Technol., Vol. 57; 1997: pp. 415.
[10] Radhika N, Subramanian R, Venkat Prasat S 2011, „Tribological Behaviour of Aluminium /Alumina/Graphite Hybrid Metal Matrix Composite using Taguchi's Techniques", Journal of Minerals & Materials Characterization & Engineering, vol.10, no. 5, pp.427–443. 69.
[11] Radhika N, Subramanian R, Venkat Prasat S, Anandavel B 2012, „Dry sliding wear behaviour of aluminium/alumina/graphite hybrid metal matrix composites", Journal of Industrial Lubrication and Tribology, vol. 64, no. 6, pp. 359–366.
[12] Saleemsab Doddamani, Mohamed Kaleemulla, Yasmin Begum, Anand K J, "An Investigation on Wear Behavior of Graphite Reinforced Aluminum Metal Matrix Composites", JoRSTEM, Sp issue; 2017: pp. 1–6.
[13] Vencl, A., Bobic, I., Arostegui, S., Bobicd, B., Marinkovic, A., Babic, M. (2010) "Structural, mechanical and tribological properties of A356 aluminium alloy reinforced with Al_2O_3, SiC and SiC, graphite particles", Journal of Alloy and Compound, 506: 631–639.
[14] S Sawla, S Das "combined effect of reinforcement and heat treatment on the two body abrasive wear of aluminium alloy and aluminium particle composites", pp 555–561,2004.
[15] Gomes E.G., Rossi, Sept 2001, Key Engg. Materials, Vol.189–191, pp. 496–502.
[16] N Singh, Shweta Goyal, Kishore Khanna, July 2010. "Effect of Thermal Ageing on Al Alloy Metal Matrix Composite", Department of Mechanical Engineering, M.E. Thesis, ThaparUniversity, Patiala, India.
[17] Amro M. Al–Qutub, Effect of heat treatment on friction and wear behavior of Al6061 composite reinforced with 10% submicron Al_2O_3 particles, Department of Mechanical Engineering King Fahd University Of Petroleum And Minerals Dhahran, Saudi Arabia.
[18] Cui Y Geng, May 15 1997, journal of Materials Science Letters Vol. 16, N10, pp.788– 790.
[19] C.S. Ramesh, A.R. Anwar Khan, N. Ravikumar, P. Savanprabhu, (2005) "Prediction of wear coefficient of Al6061–TiO2 composites", Wear, Vol. 259, pp. 602–608.
[20] Abdulhaqq A. Hamid, P. K. Ghosh, S. C. Jain, Subrata Ray, (2008), "The influence of porosity and particles content on dry sliding wear of cast in situ Al(Ti)–Al2O3(TiO2) composite", Wear, Vol. 265, Issues 1–2, pp. 14–26.

ISSN: 2067-3809

[1.]Anca-Elena IORDAN

DESIGN AND IMPLEMENTATION OF A GAME USING ANDROID API

[1.] University Politehnica Timisoara, Faculty of Engineering Hunedoara, ROMANIA

Abstract: In this article are rendered the requisite stages for the accomplishment of a game. The design of the game is accomplished by the next two unified modelling language diagrams: use-case diagram and class diagram. By achieving these types of diagrams, the game is described in an obvious and concrete approach, without ambiguousness. There have been identified seven specific concepts of this game, and then there have been implemented corresponding classes for these concepts. For the game development on the Android platform it will be used computer science branches as object oriented programming and computational geometry, and as programming language it will be used Java Standard Edition with Android application programming interface. The CASE tool used to represent the diagrams was ArgoUML, and the source code was written in Eclipse integrated development environment.

Keywords: Game, UML, ArgoUML, Java SE, Android API, Eclipse IDE

INTRODUCTION

From the perspective of UML modelling language, the analysis of the software consists in the making of use-case diagram [1]. The games' options will be described in a clear manner by representing the use-cases. Each use-case presents the interactions between user (player) and the software (game). The representation of the use-case diagram is showed in figure 1.

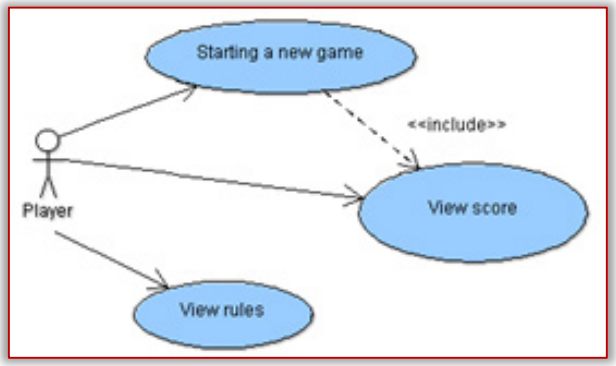

Figure 1. Use-case diagram

This diagram defines the software domain, allowing the visualisation of the dimension and the action sphere of the whole development process [2]. The diagram's structure contains:

- One actor that represents the user (player), this being the external entity which the software interacts with.
- Three use-cases which describe the functionality of the game.
- Relationships between user (player) and use-cases (association relations) and, also relations between use-cases (dependency relations).

THE DESIGN PHASE

The conceptual modelling allows identification of the most important concepts used in the game's implementation. There have been identified seven specific concepts of this game, and then there have been implemented corresponding classes [3] for these concepts. These classes are the following: "Peste", "Foc", "Animatie", "VizualizareJoc", "Joc", "Reguli" and "Principal".

The "Peste" class contains ten atributes: nine of "int" type and one atribute of "Bitmap" type defined in the *android.graphics* package [4]. Also this class has in its componence five methods. The structure of this class is showed in figure 2. It can be observed that an object of this class is made from a "Bitmap" object (composion relation), but it can be formed from a "Canvas" object defined in *android.graphics* package, two "Rect" objects defined in *android.graphics* package and a "Random" object defined in *java.util* [5] (aggregation relations).

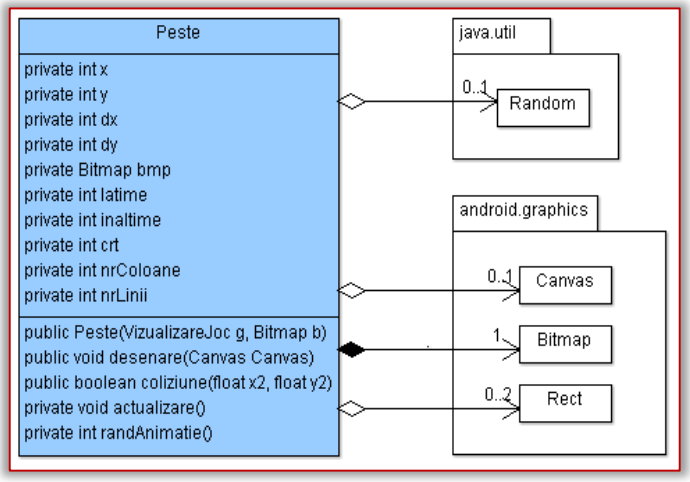

Figure 2. Structure of the "Peste" class

The "Foc" class has among its componence three atributes: two of "float" type and one atribute of "Bitmap" type defined in the *android.graphics* package. Also this class contains two methods. The representation of this class is showed in figure 3. It can be noted that an object of this class is composed of a "Bitmap" object (composition relation), but can be formed from a "Canvas" object defined in *android.graphics* package (aggregation relations).

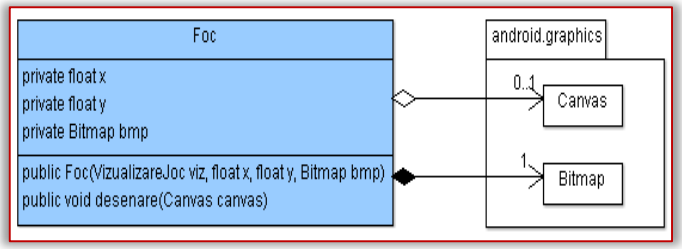

Figure 3. Structure of the "Foc" class

The "Animatie" class, which inherits the attributes and methods of the "Thread" class defined in the *java.lang* [6] package, has in its composition one attribute of "long" type and two methods. The structure of this class is showed in figure 4. It can be observed from the previous mentioned figure that an object of this class is formed from a "Canvas" object, a "Toast" object defined in the *android.widget* [7] package and an "Intent" object defined in *android.content* package. All of these three relations are aggregation relations.

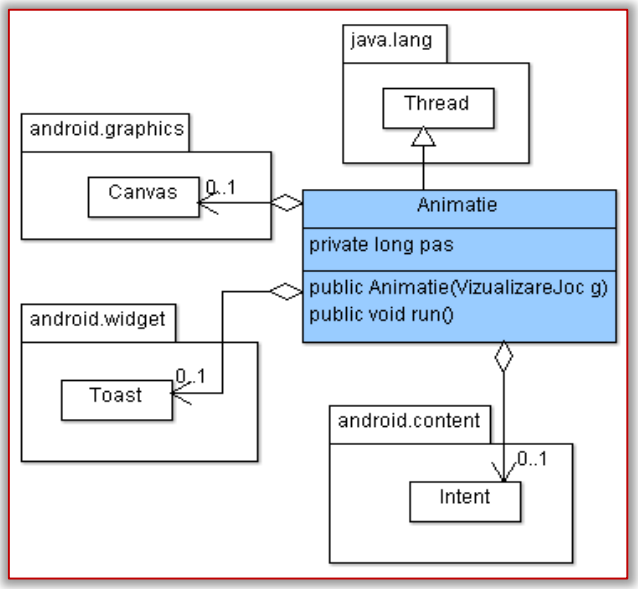

Figure 4. Structure of the "Animatie" class

The "VizualizareJoc" class, which inherits the "SurfaceView" class defined in the *android.view* package, has in its composition ten attributes: three attributes of "Bitmap" type, one attribute of "SurfaceHolder" type, two attributes of "List<Peste>" type, one attribute of "Foc" type, one attribute of "Animatie" type , one attribute of "long" type and one attribute of "int" type. The sequence from the class diagram which presents the structure of "VizualizareJoc" class is showed in figure 5. Due to the presence of the composition relations, it can be observed that an object of this class is composed of: three "Bitmap" objects, one "SurfaceHolder" object which corresponding class is defined in *android.view* [8] package, two object of the generic type "List" defined in *java.util* package, one "Animatie" object and one "Foc" object. Because of the aggregation relations existing in the class diagram, it can be observed that an object of this class is formed also from: one "MotionEvent" object defined in *android.view* package, one "Context" object defined in *android.content* [9] package, one "Random" object defined in *java.util* [10] package and one "Canvas" object defined in *android.graphics* package.

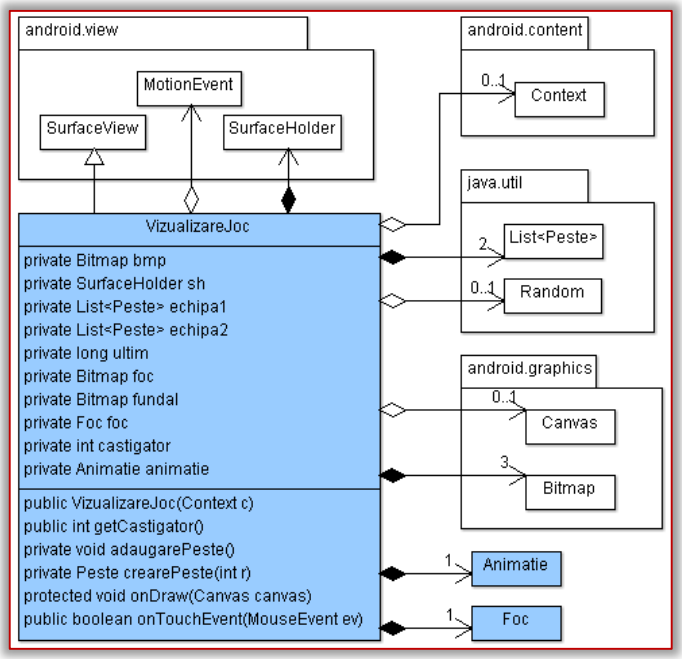

Figure 5. Structure of the "VizualizareJoc" class

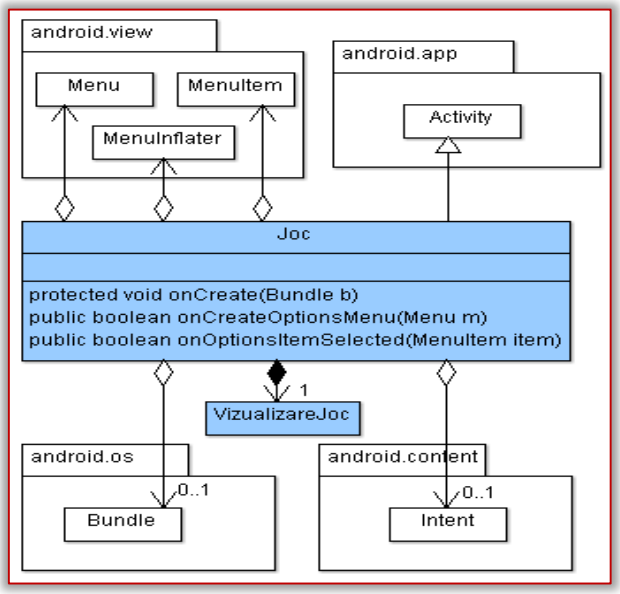

Figure 6. Structure of the "Joc" class

The "Joc" class, which inherits the attributes and methods of "Activity" class, defined in the *android.app* [11] package, has in its composition three methods. The structure of this class is presented in figure 6. Because of the presence of the composition relation, it can be noticed that an object of this class is composed from an object of "VizualizareJoc" type. Due to the presence of the aggregation relations, it can be observed that an object of "VizualizareJoc" type can be formed of an object of "Menu" type, an object of "MenuItem" type, an object of "MenuInflater" type, an object of tip "Bundle" type and an object of tip "Intent" type. The first three objects are defined in the *android.view* package, the forth object is defined in the *android.os* [12] package and the last (fifth) object is defined in the *android.content* package.

The "Principal" class, which inherits the attributes and methods of "Activity" class, has in its composition three attributes and three methods. The structure of this class is presented in figure 7. In this figure are represented the two existing composition relations, which means that an object of the "Principal" class is composed from an object of "Intent" type and two objects of "Button" type defined in the *android.widget* package. Also in the same figure are represented four aggregation relations. Their meaning consist in the fact that an object of the "Principal" class can contain: an object of "Menu" type, an object of "MenuItem" type, an object of "MenuInflater" type and an object of tip "Bundle" type.

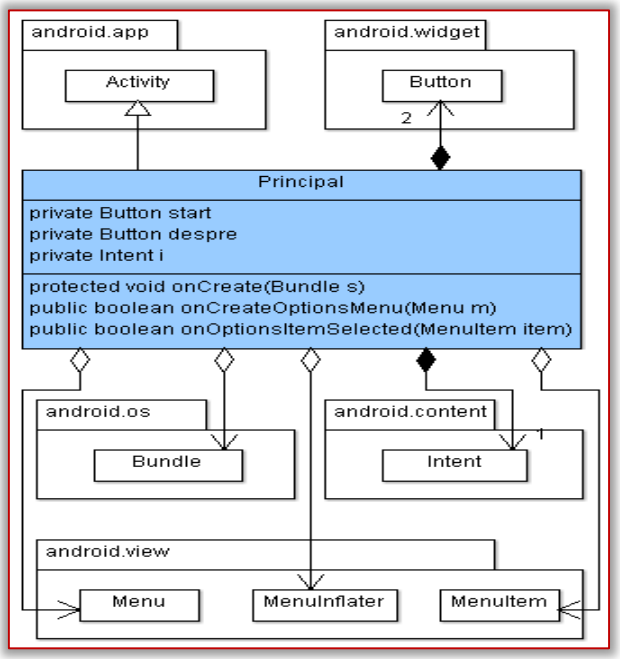

Figure 7. Structure of the "Principal" class

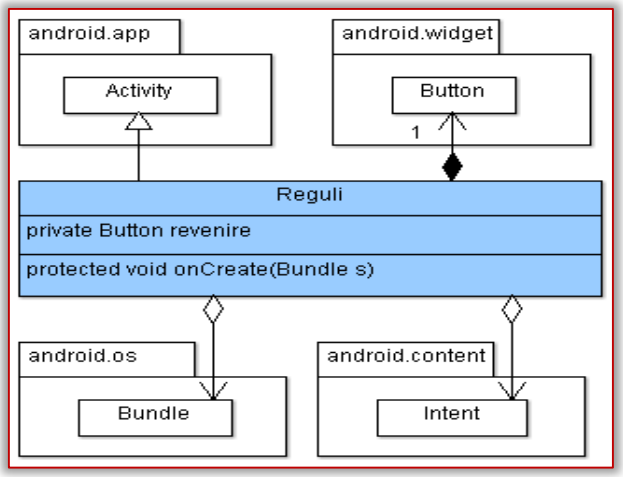

Figure 8. Structure of the "Reguli" class

The "Reguli" class, which inherits the attributes and the methods of the "Activity" class has in its composition one attribute of "Button" type and one method and it is represented in the figure 8. In this figure it can be observed that an object of this class is composed from an object of "Button" type due to the presence of the composition relation [13]. Because of the presence of the two aggregation relations [14], it can be noticed that an object of "Reguli" type can be formed from a "Bundle" type object and an "Intent" type object.

GRAPHICAL USER INTERFACE

The main user graphical interface of the game is an object of „Principal" type [15], having the graphical representation which is showed in figure 9.

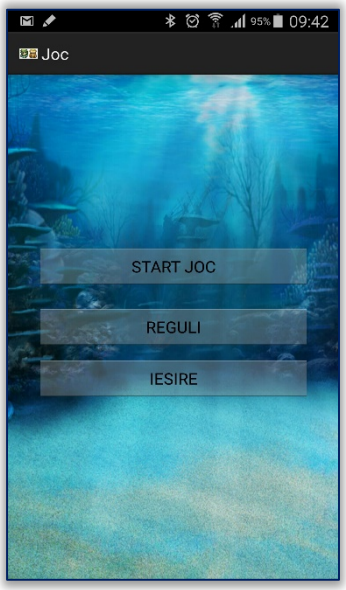

Figure 9. Main user graphical interface

By selecting the first option from the presented graphical interface, it is instantiated an object of "Joc" class, which allows the start of a new game (figure 9). To represent the two species of fish it is used an instance of "VizualizareJoc" class and to simulate the fish movement it is used an instance of "Animatie" class.

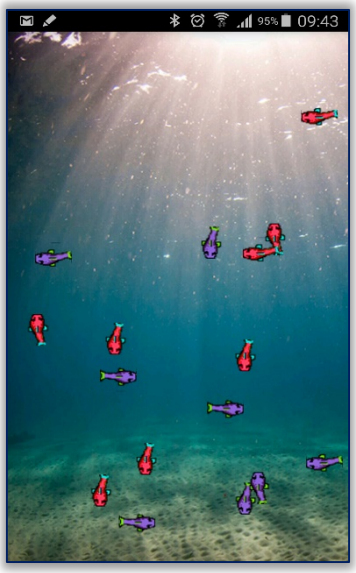

Figure 10. Graphical interface of the game

CONCLUSIONS

In this paper it was presented the development of a game based on UML design, Android API implementation, ArgoUML CASE tool and Eclipse interactive environment.

The Android SDK is a strong and full-featured set of APIs that Java developers will find usual and simple to utilize. Android

is a ripe, yet still growing, platform that many game developers have enfolded. Not only is Android a well-fixed platform, but the features of actual Android devices are starting to exceed the features of just those of latter generation console systems. The variety of users does Android an important platform for game development companies as respects the tools and services available.

Because the representation of the UML diagrams corresponding to all three phases: analysis, design and implementation, the puzzle game has been described in an obvious and objective manner, without ambiguity. The use of the unified modelling language for the achievement of the game is characterized by rigorous syntactic, rich semantic and visual modelling support.

References

[1] J. Hunt, Guide to the Unified Process featuring UML, Java and Design Patterns, Springer London Ltd, 2014
[2] B. Bruegge, A. Dutoit, Object Oriented Software Engineering Using UML, Patterns, and Java, Pearson Education, 2013
[3] A. Dennis, B. H. Wixom, D. Tegarden, Systems Analysis and Design with UML, John Wiley & Sons Ltd, 2012
[4] B. Hardy, C. Stewart, Android Programming, Pearson Education, 2015
[5] U. Roy, Advanced Java Programming, OUP India, 2015
[6] D. Vohra, Beginning Java Programming, John Wiley & Sons Ltd, 2015
[7] Z. Mednieks, G. Blake-Meike, M. Nakamura, Programming Android, O'Reilly Media Inc., 2016
[8] E. Hellman, Expert Android Programming, John Wiley & Sons Ltd, 2016
[9] B. Hardy, C. Stewart, Android Programming, Pearson Education, 2015
[10] J. Gosling, B. Joy, G. Steele, G. Bracha, A. Buckley, The Java Language Specification, Oracle, 2013
[11] W. M. Lee, Beginning Android Programming with Android Studio, John Wiley & Sons Ltd, 2013
[12] R. Rogers, Learning Android Game Programming, Pearson Education (US), 2011
[13] F. White, Object-Oriented Software Engineering: Practical Software Development using UML and Java, McGraw-Hill Education, 2015
[14] B. Rumpe, Modeling with UML, Springer International Publishing AG, 2016
[15] B. Burd, Java Programming for Android Developers, John Wiley & Sons Ltd, 2013

ISSN: 2067-3809

[1,2] Petinrin M. OMOLAYO, [1,3]Adegbola A. ADEYINKA

EFFECT OF VISCOUS DISSIPATION TERM ON A FLUID BETWEEN TWO MOVING PARALLEL PLATES

[1.]Department of Mechanical Engineering, University of Ibadan, Ibadan, NIGERIA
[2.]Prototype Engineering Development Institute, Ilesa, NIGERIA
[3.]Department of Mechanical Engineering, LadokeAkintola University of Technology, Ogbomoso, NIGERIA

Abstract: The fully developed laminar heat transfer of a Newtonian fluid flowing between two parallel plates where the bottom plate is fixed and the top plate is moving in an axial direction at constant speed was analyzed taking into account the viscous dissipation of the flowing fluid. Applying the velocity profile obtained for the plane Coutte-Poiseuille laminar flow, the energy equation with the viscous dissipation term was exactly solved for the boundary conditions of constant wall heat flux at one wall with the other insulated. Special attention is given to the shear produced by the movable top plate over and above the viscous dissipation due to internal fluid friction. The reason behind the behaviour exhibits by the temperature profile obtained at different velocities can be attributed to the effect of viscous dissipation coming into play due to the shear stress within the fluid layer induced by the movement of the upper plate.
Keywords: heat transfer, parallel plates, viscous dissipation, velocity profile, boundary conditions

INTRODUCTION

Deformation and flow of materials require energy. This mechanical energy is dissipated during the flow and is converted into internal energy of the material. The increase of internal energy is in form of temperature rise. Viscous dissipation is of interest for many applications: significant temperature rises are observed in polymer processing flows such as injection molding or extrusion at high rates. Aerodynamics heating in the thin boundary layer around high speed aircraft increases the temperature of skin. Viscous dissipation for a fluid with suspended particles is equated to the viscous dissipation in a pure Newtonian fluid, both being in the same flow (same macroscopic velocity gradient). The fluid flow in small devices and the corresponding heat transfer has received serious attention in recent past in view of the remarkable development in the field of microelectronics and MEMS. In small devices the effect of viscous dissipation that could play a vital role, result in inefficient heat dissipation leading to overheat problems. The understanding of the fluid flow phenomena has been critically reviewed [1] through micro scale devices and explored the physics of flow emphasizing the use of MEMS in different areas for flow control.

There has been an increase in research on flow and heat in microchannels recently due to the development in specific areas such as microfabrication technology, micro devices, micro electromechanical systems (MEMSs), the electronic Industry and the biomedical engineering. For a rarefied fluid flow at microscale a slip condition for the velocity and a jump condition for the temperature should be adopted [2]. Viscous dissipation is another parameter that ought to be taking into account at microscale. Viscous dissipation changes the temperature by behaving like an energy source due to a power generation induced by the shear stresses. Heat transfer and microscale fluid flow has a different behavior from that of macroscale case. At macroscale, a slip condition for the velocity and a jump condition for the temperature should be adopted. Gad-el-Hak [1] treated analysis for microchannel flows through study of microdevices fluid mechanics. Guo and Li [3] studied the size effects on micro scale single-phase fluid flow and heat transfer. Wu and Cherg[4] studied the friction factor and convective heat transfer in smooth silicon microchannels of trapezoidal cross-section. Zhang *et al.* [5] validated the Navier-Stokes equation for slip flow in transition region.

A numerical study [6] reported the influence of viscous dissipation for the flow of a Newtonian for the flow of a Newtonian fluid through a parallel plate channel. The effects of viscous dissipation on laminar forced convection through a pipe and channel have been studied [7] for the flow of a Phan-Thien Tanner fluid. The study has revealed that the viscous dissipation enhances the fluid elasticity. Performing an analytical study, using a functional analysis method, the effects of viscous dissipation on the heat transfer have been investigated [8] for a thermally-developing laminar Hartman flow through a parallel plate channel with the aid of a magnetic field. In a study of thermal development of forced convection in a parallel plate channel filled by porous medium, an investigation of the effects of viscous dissipation has been done [9] with the thermal boundary condition of uniform wall temperature including axial conduction effects. The analysis of laminar forced convection in a pipe for a Newtonian fluid of constant properties has been performed [10] by taking the effect of viscous dissipation into account. The analytical work by Aydin and Avci [11] has dealt with the convective heat transfer problem for the plane Poiseuille flow

with an emphasis given on the viscous dissipation effect. In a recent study, [12] the effects of viscous of viscous dissipation on heat transfer between two fixed parallel plates with constant heat flux boundary condition has been reported. Performing a numerical study, the influence of viscous dissipation on fully developed laminar heat transfer has been investigated [13] for a non-Newtonian fluid flowing between two parallel plates with the axial movement of one of the plates.

Problems that involve fluid flow and heat transfer with an axially moving core of solid body or fluid in an annular geometry can be found in many manufacturing processes, such as extrusion, drawing and hot rolling. In such processes, a hot plate or cylindrical rod continuously exchanges heat with the surrounding environment. For such case, the fluid involved may be Newtonian or non–Newtonian and the flow situations encountered can be either laminar or turbulent. In such industrial applications, it is of great importance to encounter the heat transfer from the moving boundary to the surrounding fluid and vice-versa.

In the previous report, the effect of viscous dissipation on fully developed Newtonian laminar heat transfer was discussed for the case of concentric annuli with axially moving cores. In this report, developed laminar heat transfer of a Newtonian fluid flowing between two parallel plates with one moving plate was analyzed taking into consideration the viscous dissipation of the flowing fluid. Applying the velocity profile obtained for the plane Coutte-Poiseuille laminar flow, the energy equation with the viscous dissipation term was exactly solved for the boundary conditions of constant wall heat flux at one wall with the other insulated. The objective of the paper is to investigate the effect of viscous dissipation on the heat transfer on a two parallel plates where one plate is moving and between two moving parallel plates.

NUMERICAL FORMULATION

The assumptions used in this analysis are:

1. The flow is incompressible and steady- laminar, and fully developed hydro-dynamically and thermally.
2. Either of two parallel plates is axially moving at a constant velocity.
3. The fluid is Newtonian and physical properties are constant.
4. The body forces and axial heat conduction are neglected.

The governing equations consist of continuity, momentum and energy equations. In order to get the velocity and temperature distributions between two plates, the governing equations have been derived based on the above-mentioned assumptions.

— Governing Equations

For steady, and two dimensional flow of an incompressible fluid with constant fluid properties, the continuity equation and momentum equations are given in equation (1) and (2) respectively [14]

$$\frac{\partial u}{\partial x} += 0 \tag{1}$$

$$\rho\left(u\frac{\partial u}{\partial x}+v\frac{\partial u}{\partial y}\right) = -\frac{\partial p}{\partial x}+\mu\left(\frac{\partial^2 u}{\partial x^2}+\frac{\partial^2 u}{\partial y^2}\right) + F_x \tag{2a}$$

$$\rho\left(u\frac{\partial v}{\partial x}+\frac{\partial v}{\partial y}\right) = -\frac{\partial p}{\partial y}+\mu\left(\frac{\partial^2 v}{\partial x^2}+\frac{\partial^2 v}{\partial y^2}\right) + F_y \tag{2b}$$

Also, the energy equation containing the viscous dissipation term μØ is given in equation (3)

$$\rho C_p\left(u\frac{\partial T}{\partial x}+v\frac{\partial T}{\partial y}\right) = -\left(\frac{\partial^2 T}{\partial x^2}+\frac{\partial^2 T}{\partial y^2}\right)+\mu Ø + q \tag{3}$$

where

$$\mu Ø = \mu\left[\left(\frac{\partial u}{\partial y}+\frac{\partial v}{\partial x}\right)^2+2\left[\left(\frac{\partial u}{\partial x}\right)^2+\left(\frac{\partial v}{\partial y}\right)^2\right]\right]$$

For a fully developed fluid flow between two parallel plates where one of the plates is set in motion and the other plates is kept stationary, the fluid between the plate is said to be subjected to coquette flow. Example of this flow can be found in journal bearing.

This fluid motion is also the case of parallel flow, in which the flow motion is only in one direction, which indicates that the velocity component in y-direction is zero (v=0). Therefore, from equations (1), the continuity equation reduces to

$$\frac{\partial u}{\partial x} = 0 \tag{4}$$

Also, from equations (1) and (2), the momentum equation reduces to

$$0 = -\frac{\partial p}{\partial x}+\mu\left(\frac{\partial^2 u}{\partial y^2}\right) \tag{5}$$

Neglecting the body forces F_x and F_y.

In couette flow, the fluid motion is sustained by the force provided by one of the plates and not by the pressure gradient, therefore, equation (5) further reduces to

$$0 = \frac{\partial^2 u}{\partial y^2} \tag{6}$$

Since uniform temperature field is going to be experienced on both plates, from equation (3), the convection term which has the temperature gradient, reduces to zero: Therefore, if the heat generation term, q is neglected, then equation (3) can be redefined as

$$k\frac{\partial^2 T}{\partial y^2}+\mu\left(\frac{\partial u}{\partial y}\right)^2 \tag{7}$$

— Boundary Conditions

The viscous domain considered is engine oil; which has a density, ρ= 888.2 kg/m3, thermal conductivity, k=0.145W/(m K), dynamic viscosity, μ=0.79938Pas and specific heat c_p=1870J/(kg K); and is bounded by two parallel plates of length 10mm each with a gap of 3mm. The lower plate velocity varies from 0 to 10m/s for each parametric run of upper plate velocity from 0 to 10m/s. The lower plate's

temperature is kept at 283.15K while the temperature of the upper plate is kept at 303.15K. Since it was assumed there is no heat flux to in direction of shear, thermal insulation was applied to the two boundaries of the gap between the plates with velocity symmetry boundary condition.

RESULTS AND DISCUSSION

The velocity distribution when upper plate velocity is at 10m/s and when both plates moves in opposite direction with velocities at 10m/s are shown in Figure 1 and Figure 2 respectively. In this paper, the effect of viscous dissipation term on a fluid between two moving parallel plates, where the bottom plate is fixed and the top plate is moving in an axial direction at a constant speed has been analysed. The velocity is an important parameter governing the heat transfer and fluid flow in a channel between two plates moving in opposite direction. Actually, it is a dimensional way of representing the effect of viscous dissipation.

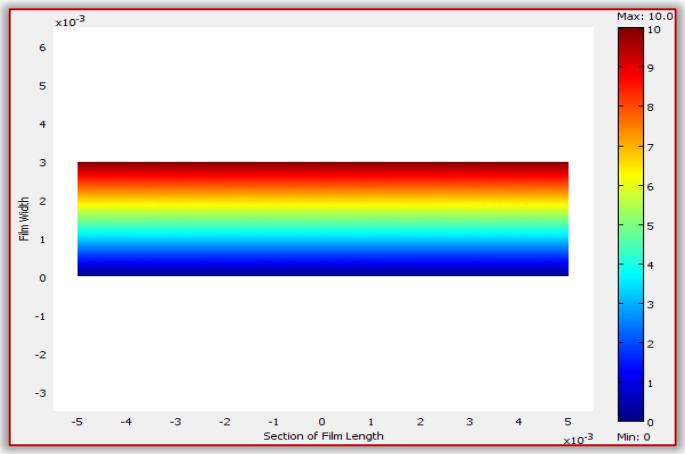

Figure 1: Velocity distribution
when upper plate velocity is at 10m/s

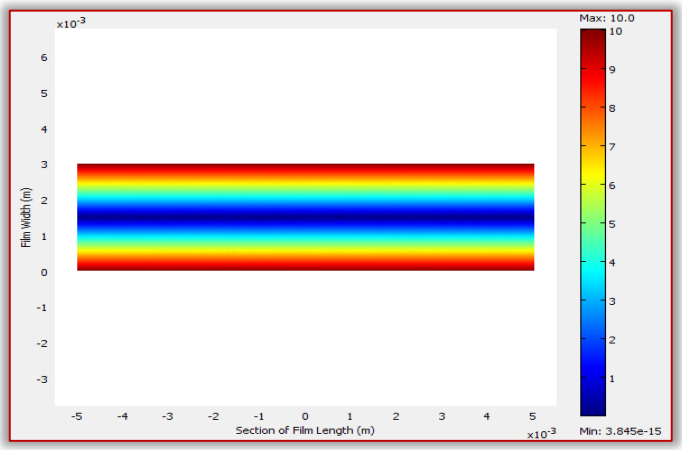

Figure 2: Velocity distribution when both plates moves
in opposite direction with velocities at 10m/s

Figure 3 and Figure 4 depict the variation of temperature profile for different velocities for the upper plate while keeping the lower plate at stationary position. Viscous dissipation acts as a source of energy in the flow and this severely affect the temperature distribution in Figure 3 and Figure 4. The reason behind such a behaviour exhibits by the temperature profile obtained at different velocities, can be attributed to the effect of viscous dissipation coming into play due to the shear stress within the fluid layer induced by the movement of the upper plate.

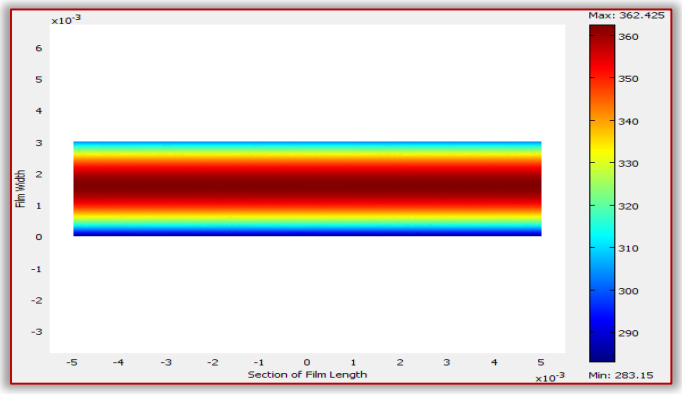

Figure 3: Temperature distribution
when upper plate velocity is at 10m/s

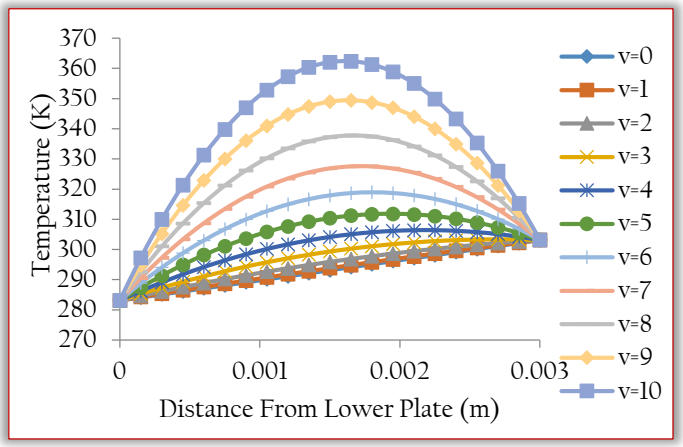

Figure 4: Temperature distribution between stationary lower plate
and moving upper plate with varying velocities

Viscous dissipation always generates a distribution of heat source stimulating the internal energy in the fluid, and hence the temperature profile gets distorted when both plates move in opposite direction as it is clear in Figure 5 and 6. It is observed that the velocity of the upper plate has great influence on the thermal behaviour of the film as the temperature rises towards the film centre with increase in velocity.

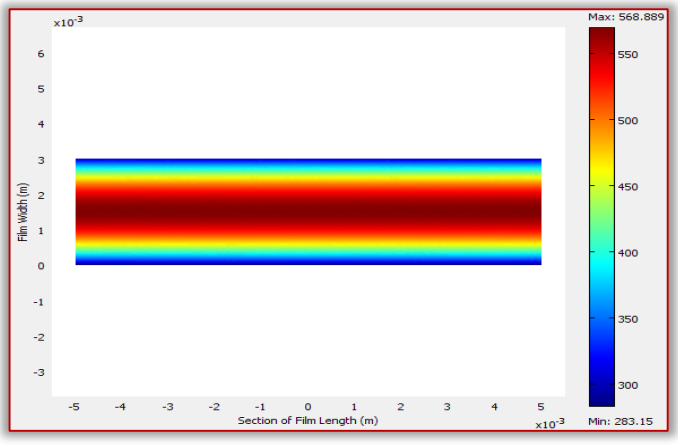

Figure 5: Temperature when both plates moves in opposite
direction with velocities at 10m/s

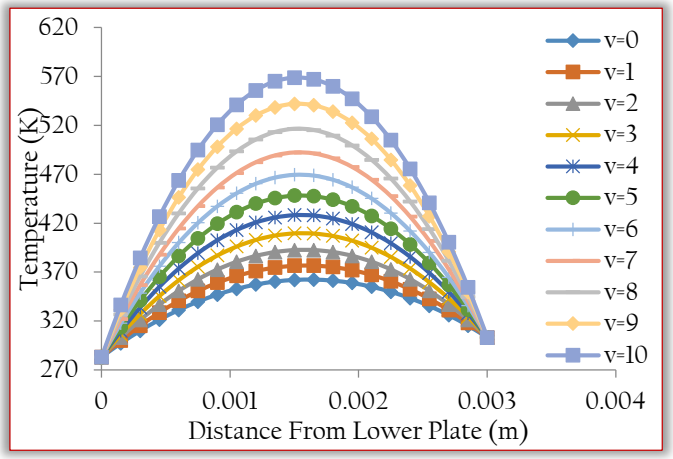

Figure 6: Temperature distribution between lower plate at 10m/s with varying upper plate velocities in opposite direction

CONCLUSION

In this present study, fully developed laminar heat transfer of a Newtonian fluid flowing between two parallel plates with one moving plate was analyzed taking into account the viscous dissipation for the thermal boundary conditions of constant wall heat flux at one wall with the other insulated. Apart from the effect of viscous dissipation due to internal fluid friction, an emphasis on viscous dissipation is given to include the effect of shear stress induced by the movement of the top plate. The reason behind such a behaviour exhibits by the temperature profile obtained at different velocities, can be attributed to the effect of viscous dissipation coming into play due to the shear stress within the fluid layer induced by the movement of the upper plate.

References

[1] M. Gad-el-Hak, Fluid mechanics of microdevices-the freeman scholar lecture, Journal of Fluids Engineering, 121(1), 1999, 5-33.

[2] A. El-Nahhas, Analytic Approximations for flows and Heat Transfer in Microchannels between Two Parallel Plates, Hindawi Publishing Corporation, 2012, 1-8.

[3] Z.Y. Guo, and Z.X. Li, Size effect on microscale single-phase flow and heat transfer, International Journal of Heat and Mass Transfer, 46(1), 2003, 149-159.

[4] H.Y. Wu, and P. Cheng, An experimental study of convective heat transfer in silicon microchannels with different surface conditions, International Journal of Heat and Mass transfer, 46(14), 2003, 2547-2556.

[5] Y. Zhang, R. Qin, and D. R. Emerson, Lattice Bolltzmann simulation of rarefield gas flows in microchannels, Physical Review E., 71(4), 2008, 047702/1-047702/4.

[6] K. C. Cheng, and R. S. Wu, Viscous Dissipation Effects on Convective Instability and Heat transfer in Plane Poiseuille-Couette Flow Heated From below, Appl.Sci Res., 32, 1976, 327-46.

[7] F.T. Pinho, and P.J. Oliveira, Analysis of Forced Convection in Pipes and Channels with the Simplified Phan-thien-tanner Fluid, Int.J. Heat Mass Transfer, 43, 2000, 2273-87.

[8] J. Lahjomri, K. Zniber, and A.A. Oubarra, Heat transfer by Laminar Hartmann's Flow in the Thermal Entrance-region with Uniform Wall Heat-Flux: The Graetz Problem Extended, Energy Conversion and Management, 44, 2003, 11-34.

[9] D.A. Nield, A.V. Kuznetzov, and M. Xiong, Thermally Developed Forced Convention in Porous Medium: Parallel-Plate Channel with Walls at a Uniform Temperature, with Axial Conduction and Viscous –dissipation Effects, Int.J. Heat Mass Transf., 46, 2003, 643-51.

[10] O. Aydin, Effects of Viscous Dissipation on the Heat Transfer in a Forced Pipe. Part1: Both Hydrodynamically and Thermally and Developed Flow, Energy Conversion and Management, 46, 2005, 757-69.

[11] O. Aydin, and M. Avci, Viscous-dissipation Effect on the Heat transfer in a Poiseuille Flow, Applied Energy, 83, 2006, 495—512.

[12] J. Sheela-Francisca, and C.P. Tso, Viscous Dissipation Effects On Parallel Plates with Constant Heat Flux Boundary Condition, Int. Commun. Heat MassTransf., 36, 2009, 249-254.

[13] G. Davaa, T. Shigechi, and S. Momoki, Effects of Viscous Dissipation On Fully-developed Heat transfer of Non-Newtonian Fluids in Plane Laminar Poiseuille-Couette Flow, Int.Commun. Heat Mass Transf., 31(5), 2004, 663-672.

[14] F. P. Incropera, and D. P. Dewitt, Fundamentals of Heat and Mass Tranfer, (5th edition, New York: John Wiley & Sons, 2005)

ISSN: 2067-3809

[1.]Ancuţa NEDELCU, [2.]Cristina COVALIU, [1.]Lucreţia POPA, [1.]Radu CIUPERCA,
[1.]Alexandra ANGHELET, [1.]Ana ZAICA, [1.]Mircea COSTIN

MODERN TECHNOLOGIES AND INSTALLATIONS DESIGNED TO INDUSTRIAL SCALE CULTIVATION OF MICROALGAE FOR OBTAINING ALGAL BIOMASS

[1.]National Institute of Research – Development for Machines and Installations Designed to Agriculture and Food Industry – INMA Bucharest, ROMANIA
[2.]University Politehnica Bucharest, Faculty of Biotechnical Systems Engineering, ROMANIA

Abstract: Nowadays, the biomass produced by the energetic plants is rather criticized, because these plants need large culture surfaces, thus competing with the agricultural land allotted to food production. One of the current trends of scientific biological researches with practical goal is the cultivation of algae designed to obtain the algal biomass as an important raw material used in biotechnologies for production of alternative fuel. This paper presents the most up-to-date technologies and installations for industrial cultivation of microalgae together with INMA researches results materialized in the installation of open culture systems growing, of waterfall type.
Keywords: algae, cultivation technologies, biomass, biofuels

INTRODUCTION

Production of vegetal biomass at large scale means to cultivate numerous species of plants. According to specialty literature (*R. Şumălan. 2011),* biomass is a very important component of carbon cycle and the carbon from atmosphere is turned into biological matter (biomass) by photosynthesis. By vegetal matter combustion, the carbon returns into the atmosphere as carbon dioxide. Biomass is biodegradable and renewable. Production of biomass is continuously extending due to increased interest in alternative energy sources.

Biomass is a renewable energy that supplies biofuels, generally of solid type and liquid biofuels. (*I.R. Pecingina. 2011*). Biofuels are fuels produced by bio-renewable sources coming from nature that, after their combustion in the engine produce less noxious emissions to the environment.

According to European and national laws and literature *(Carăuş I. 2007; I.R. Pecingina. 2011; M. Pavnutescu. 2011*) on improving environment quality, the general goal is to limit the quantity of fuel related to harvests and orient towards the biofuel coming from non-food sources, such as *waste and algae.*

The higher price of oil, as well as, the growing food crisis has led to an increased interest in algae culture, from which result vegetal oil, biodiesel, bioethanol, biobutanol and other fuels. This new energy source has many advantages among which the fact that it does not harm the environment, when storing it randomly and it does not affect fresh water stock, being biodegradable.

According to quantitative criterion, algal biomass represents about 20% out of world aquaculture production (*S. Dobrojan and. so on, 2016*). The advantages and very good results obtained by applying at different fields algal biomass make imperative the necessity of growing algae.

Recently, large quantities of red, brown and green and blue-green algae are being cultivated. Algae make efficiently use of solar energy conserving it in biomass. (*Marchin T.. s.a.. 2015*). More recently, algae industrial growing increased in the whole world as a source of renewable fuels. According to estimates, from the 50,000 of microalgae species cultivated, about 10 are being grown at industrial scale in order to obtain some products such as: Spirulina, Crypthecodinium cohnii, Chlorella, Dunaliella salina, Ulkenia sp, Haematococcus pluvialis, Schizochytrium, Aphanizomenon flos-aquae, Euglena and Odontella aurita.

Among the 10 species industrially cultivated, the species Chlorella, Spirulina and Cryptecodinium have the biggest contribution, as it results from the studies of specialists in domain. (*S. Dobrojan s.a.. 2016; Egardt J. Lie O. 2013*).

A strategic trend that is more and more spread lately is based on obtaining biodiesel and biogas from algal biomass.

MATERIAL AND METHOD

Large-scale cultivation of algae is achieved by means of various installations in terms of size, design and shape. There were designed very simple installations consisting of channels of small depth made in the soil, lined with polyethylene foil, but also special installations of big size were built, these ones comprising concreted circular or other shape basins endowed with systems of agitation of algal suspension, aerating systems, harvesting systems and even devices of adjusting the growing parameters (including automated systems).

Industrial-scale cultivation of microalgae is being achieved by different systems, as they are shown in the scheme from Figure 1.

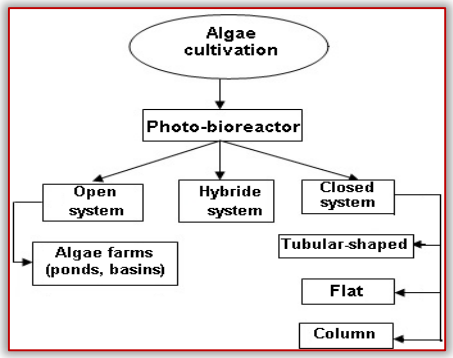

Figure 1 – Schematic representation of algae growing systems

— Open algaculture systems are recommended for areas of warm climate.

From practical reasons, algae should be grown in special farms and they should not be harvested in their natural environment, namely in the sea. Taking into account that the open systems might be contaminated by bacteria, biomass is mainly designed to obtain biofuel.

A large capacity farm endowed with circular basins, built in Taiwan is shown in Figure 2.

Its basins have approx. 45 meters diameter and the algal slurry depth is about 50cm; the algal culture is agitated by means of a mobile radial arm that also injects pressure air into the algae growth medium, where carbon dioxide of 20% was added for *Chlorella* and 10% for *Spirulina* culture.

Figure 2 – Industrial-scale installation for growing microalgae (from Hills, 1981)

— Closed systems of industrial scale algae culture consist of closed bioreactors placed vertically or horizontally, the algaculture being grown in recipients as sacks, bags, tubes, columns, flat constructions, etc.

Algae growth in closed cells (bags) and columns, Figure3 was developed as an alternative method of producing algae more rapidly and more efficiently than in the open systems.

Figure 3 – Algae cultivation in plastic bags

Within the system of algae culture on vertical, the algae are laid in transparent plastic bags, this way being exposed to sun rays on both sides. The bags with algae are hung from the ceiling and the roof protects them against the rain. Due to sunlight exposure algae productivity increases, as well as extracted oil yield. At the same time, algae contamination must be avoided. Another type of bioreactor is the tubular reactor, built of transparent pipes placed in parallel. In Figure 4 is presented a vertical tubular bioreactor *(M. Farieda. s.a.. 2017.)*

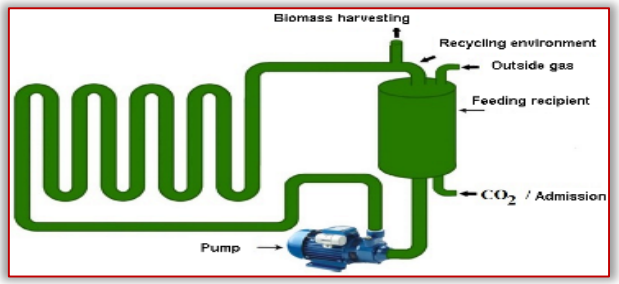

Figure 4 - Tubular photobioreactor with vertical tubes

The French-Dutch Company *Cloud Collective* (*Beverley Mitchell, 2014*) has transformed one strip of a Swiss highway in Geneva into an urban algae culture farm using the algal bioreactor with transparent pipes. (Figure5 a).

The installation was designed and manufactured in order to demonstrate that any urban scenery can be used as support for producing biomass. (Figure 5b). The algae liquid slurry circulates through the transparent pipes feeding with carbon dioxide coming from emissions generated by motorcars passing on the highway.

The process results in biomass-green fuel and environment air filtration using a simple method.

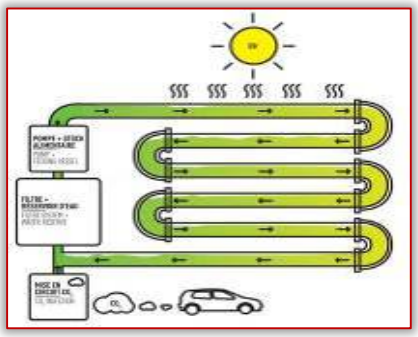

Figure 5 – Biomass production through a system of transparent pipes mounted on a viaduct
a) Highway overpass in Geneva; b) Production of algae biomass in transparent tubing reactors installed in urban areas

Another type of photobioreactor is the flat panel bioreactor as in Figure 6 (*M. Farieda s.a.. 2017. A.C. Apel s.a .2017*) The

method consists in passing a thin algae layer on a transparent panel made of glass, plexiglass or polycarbonate. A special attention was given to flat photobioreactors due to big ratio between surface-volume and high density of cells.

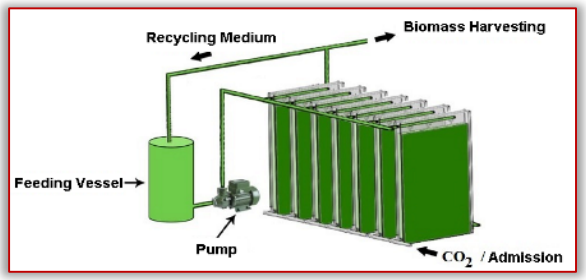

Figure 6 – Photobioreactor with flat vertical panels

Flat panels have generally the advantage of being able to be placed vertically or inclined towards sunlight, for a better illumination.

As a general rule, the algaculture installations of any type comprise: photobioreactors, energy sources, feeding systems, stirring systems, illuminating systems, harvesting systems, automating and control systems of working process.

RESULTS

In order to study an innovative technology for obtaining algal biomass in laboratory conditions, a functional model of installation for growing algae in open system of waterfall type, has been performed within INMA Bucharest.

Installation is made of one or several flat open reactors working in waterfall system, one collecting compartment, illuminating system, stirring system, algae recirculation system, as it is presented in Figure 7.

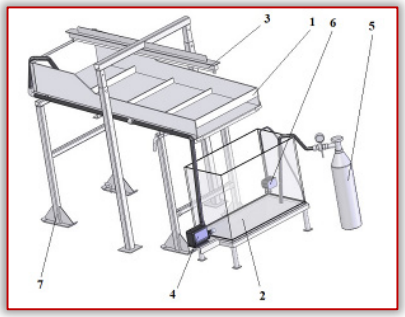

a)

b)

Figure 7 - Installation for open system growth of algae of waterfall type - ICA: 1. flat reactor; 2. collector; 3. illuminating system; 4. recirculation system; 5. CO_2 feeding and Ph control system; 6 agitators. a) appliance diagram; b) functional model ICA

In this type of reactor, the transparent panels made of glass, plexiglass or polycarbonate enable the sun direct radiation, light dissipation of heat, easy cleaning and maintenance. Algae culture is recirculated and slips on transparent panels in a thin layer of 3…35 mm.

Algae growing technology includes a series of processes, methods and techniques that must be respected and applied for obtaining algal biomass:

- Ensuring the nutritive environment;
- Algae inoculation is accomplished by special methods varying according to culture growing characteristics, level of adaptation to concrete cultivation conditions;
- Ensuring the conditions of cultivation-temperature, illumination, stirring;
- Biomass obtaining.

The researches on algaculture in the installation of waterfall type are being in course of developing.

A microalga cultivated in this installation is Chlorella. This microalgae is rich in proteins and essential fatty acids, minerals, vitamins, fibres. Chlorella is the richest source of chlorophyll known up to present, but it is cultivated also as a rich source of ribonucleic (RNA) and deoxyribonucleic acid (DRA).

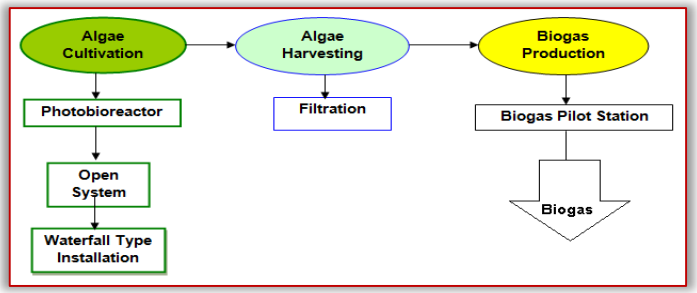

Figure 8 - Diagram-technology for obtaining biogas from algal biomass

Chlorella needs a specific medium of growing, namely a high purity and quality of water at which adds a great variety of natural minerals.

Culture of algae studied will grow in BBM (Bold Basal Medium) medium.

The innovative technology designed to obtain advanced biofuel from algae, proposed by INMA. Figure 8 consists in the following special technical equipment:

- Open growing system of algae using the waterfall type installation whose size is in accordance with the capacity of production desired.
- Algae harvesting-by filtration and centrifugal force.
- Obtaining biogas with pilot station by advanced dry and humid methanogenesis MGA endowed by INMA.

CONCLUSIONS

- In order to improve the environment quality one of the possible sources is to use the alternative energy.
- Unlike other alternative sources of energy, algae present a series of important advantages; they grow rapidly, do not compete with food sources for agricultural fields and do not need fresh water to develop.

- Microscopic algae could represent the newest and most viable and profitable generation of biofuels, outrunning the traditional fuels, natural oils and wood.
- Microalgae are microscopic aquatic organisms that feed by photosynthesis.
- In order to cultivate algae at industrial scale for obtaining biomass, three systems are viable: open, closed and hybrid systems, characterized by specific technologies and installations.
- Installation for algae growing in open system, of waterfall type can be appropriately sized according to production expected and is designed both to grow algae at lab-scale and industrial scale.
- Installation proposed is mainly made of one or several flat open reactors on which the algae culture slips in a thin layer, enabling the direct sunlight, light dissipation of heat, easy cleaning and maintenance. The advantage of system above is that to reach a high biomass density and a big productivity due to big ratio between surface and volume.
- Biomass will be capitalized through the pilot station for biogas production endowed by INMA.

Acknowledgement

The research work was funded by the NUCLEU Programme of the Ministry of Research and Innovation through financing contract no. 8 N / 09.03.2016 –Act.Ad.2/2017 for the project " *PN 16 24 04 04 „Researches regarding the development of an innovative technology for obtaining advanced biofuels from non-food bioresources.*

Note

This paper is based on the paper presented at ISB-INMA TEH' 2017 International Symposium (Agricultural and Mechanical Engineering), organized by University "POLITEHNICA" of Bucharest – Faculty of Biotechnical Systems Engineering, National Institute of Research-Development for Machines and Installations Designed to Agriculture and Food Industry – INMA Bucharest, Scientific Research and Technological Development in Plant Protection Institute (ICDPP), National Institute for Research and Development for Industrial Ecology – INCD ECOIND, Research and Development Institute for Processing and Marketing of the Horticultural Products "HORTING" and Hydraulics, Pneumatics Research Institute INOE 2000 IHP, University of Agronomic Sciences and Veterinary Medicine of Bucharest (UASVMB) – Faculty of Horticulture and Romanian Society of Horticulture (SRH), in Bucharest, ROMANIA, between 26 – 28 October, 2017.

References

[1] A.C. Apel. C.E. Pfaffinger, N. Basedahl. N. Mittwollen. J. Göbel. J. Sauter. T. Brück. D. Weuster-Botz. (2017). " Open thin-layer cascade reactors for saline microalgae production evaluated in a physically simulated Mediterranean summer climate". Algal Research. Issue 25. pp.381-390. Ed. Elsevier. London/U.K.

[2] Beverley Mitchell. Freeway Algae Garden Turns CO2 Emissions into Energy in Switzerland. (2014). http://inhabitat.com/overpass-algae-garden-turns-co2-emissions-into-combustible-biomass-in-switzerland/

[3] S. Dobrojan, V. Şalaru, V. Melnic, G. Dobrojan. (2016). Algae culture. Monography (Cultivarea Algelor. Monografie). State University from Moldavia. Laboratory of Scientific Research "Algology". Chisinau. ISBN 978-9975-71-736-6

[4] Egardt J., Lie O. (2013). Aulie J., Myhre P. Microalgae a market analysis carried out as part of the Interreg KASK IVA project: Blue Biotechnology for Sustainable Innovations. "Blue Bio". Sweden. 79 p.

[5] M. Farieda. M. Samera. E. Abdelsalam. R.S. Yousef. Y.A. Attia. A.S. Ali. (2017). Biodiesel production from microalgae: Processes. Technologies and recent advancements. Renewable and Sustainable Energy Reviews 79. pp. 893–913. Ed. Elsevier. London/U.K.

[6] Alternative fuels: biodiesel from algae Tag Archives: algaculture for fuel (Combustibili alternativi: biodiesel din alge. Tag Archives: cultivarea algelor pentru combustibil). http://inimafericita.ro/tag/cultivarea-algelor-pentru-combustibil/

[7] Marchin T., Erpicum M., Franck F.(2015). Photosynthesis of Scenedesmus obliquus in outdoor open thin-layer cascade system in high and low CO2 in Belgium. Journal of Biotechnology. Issue 215. pp.2-12. Ed. Elsevier. London/U.K.

[8] M. Pavnutescu. (2011). Exclusively GR: Green oil from sea algae. (Exclusiv GR: Petrol "verde" din alge marine). Green Report. http://www.green-report.ro/exclusiv-grnbsppetrol-ldquoverderdquo-din-alge-marine/

[9] I.R. Pecingina. (2011). Biotechnology for Obtaining Alternative Fuels From Seaweed. Annals of the „Constantin Brâncuşi" University of Târgu Jiu. Engineering Series. Issue 3/2011. pp. 418-426.

[10] R. Şumălan. (2011). Biomass-source of renewable energy. Agriculture Journal (BIOMASA-Sursă de energie regenerabilă. Gazeta de agricultură). https://www.gazetadeagricultura.info/eco-bio/565-energie-regenerabila/11375-biomasa-sursa-de-energie-regenerabila.html.

ISSN: 2067-3809

[1.]Bianca Ştefania ZĂBAVĂ, [1.]Gheorghe VOICU, [1.]Nicoleta UNGUREANU, [1.]Mirela DINCĂ,
[1.]Gigel PARASCHIV, [1.]Mariana MUNTEANU, [1.]Mariana FERDES

METHODS OF BIOGAS PURIFICATION – A REVIEW

[1.]University Politehnica of Bucharest. Faculty of Biotechnical Systems Engineering, ROMANIA

Abstract: Biogas is a product of anaerobic ferment of organic products. Among the fuels from vegetal biomass, biogas has a great importance and can successfully replace fossil fuels for obtaining electricity and heat; the use of biogas exists for a few years also in the field of transport. Biogas formed in the methane fermentation process contains about 50÷60% of methane. Other ingredients such as carbon dioxide, hydrogen sulfide, water, water vapour and small amounts of nitrogen and oxygen are compounds that lower the energy value of biogas. In this paper are presented the main methods of biogas purification.
Keywords: biogas, purification, methane

INTRODUCTION

A major concern for most people these days is the use and availability of energy. People spend a large portion of their earnings on gas, propane and oil. These fossil fuels are being continuously used to a large extent. Because these forms of energy are non-renewable, their availability will continue to decrease and costs will continue to go up. This has led to a search for new energy sources. One excellent source of energy is *biogas*.

Biogas originates from bacteria in the process of bio-degradation of organic material under anaerobic (without air) conditions. The natural generation of biogas is an important part of the biogeochemical carbon cycle. Methanogens (methane producing bacteria) are the last link in a chain of micro-organisms which degrade organic material and return the decomposition products to the environment. In this process biogas is generated, a source of renewable energy.

Biogas is a mixture of gases that is composed chiefly of:

- methane (CH_4): 40-70 vol.%
- carbon dioxide (CO_2): 30-60 vol.%
- other gases: 1-5 vol.% including
- hydrogen (H_2): 0-1 vol.%
- hydrogen sulfide (H_2S): 0-3 vol.%

Like those of any pure gas. the characteristic properties of biogas are pressure and temperature-dependent. They are also affected by the moisture content. The factors of main interest are:

- change in volume as a function of temperature and pressure.
- change in calorific value as a function of temperature, pressure and water-vapor content and
- change in water-vapor content as a function of temperature and pressure

The calorific value of biogas is about 6 kWh/m^3 - this corresponds to about half a litre of diesel oil. The net calorific value depends on the efficiency of the burners or appliances. Methane is the valuable component under the aspect of using biogas as a fuel (*Thomas H. et al.).*

Biogas offers a diversity of options for use. e. g. the decentralised production of electricity and heat, the distribution via heat networks, the feed-in of upgraded biogas into the natural gas grid and its follwing use as a natural gas substitute for energy, as fuel or in the chemical industry – figure 1. Independently of the use selected, the objective is to make the energy utilisation as efficient as possible.

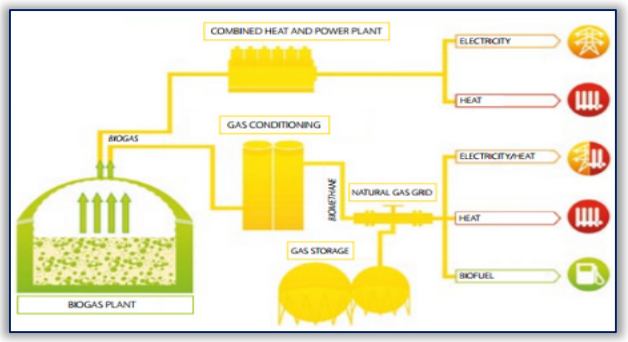

Figure 1 - Various options for using biogas

MATERIAL AND METHOD

Biogas is a product of anaerobic fermentation of organic products. Of the biomass fuel, biogas is of particular importance and can successfully replace fossil fuels for electricity and heat. In order to obtain biogas in a productive and profitable way, it must be processed before use. Thus, prior to use, raw biogas is subjected to conditioning (purification) operations, resulting in the properties required by users.

Biogas purification is the operation of retention of unwanted biogas components before it is used in the combustion process. Whatever the ultimate way of using biogas, it is impossible to use it in the raw state. The only recyclable component is methane. To enable the use of biogas by cogeneration, the substances to be eliminated are: water, organohalogen, carbon dioxide and sulfur *(Ioan B. and Minciuc E., 2003).*

The most important reasons for improving the quality of biogas include the need to meet the requirements of the installations in which it is used (engines, boilers, fuel cells, etc.)

increasing its calorific value but also for standardizing the quality *(Krzysztof B. et al..2011)*.

There are small amounts of biogas present in certain compounds that due to their oxidising or incombustible properties have to be eliminated to favor a good combustion process. During the conditioning process, these compounds that inhibit the combustion process are reduced in quantity or totally eliminated, depending on the final use of biogas.

Figure 2 shows the most commonly used methods of biogas conditioning: pressure adsorption, biogas purification with water under pressure, physical and chemical absorption, membrane separation and cryogenic separation. These methods largely involve the removal of hydrogen sulfide, carbon dioxide and water vapor.

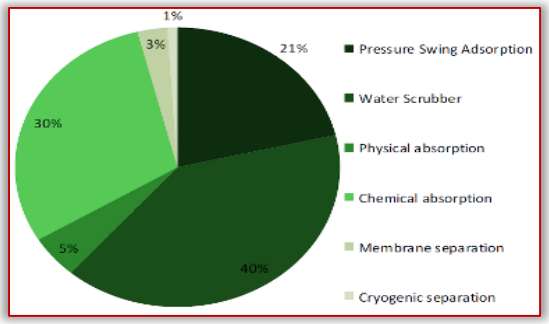

Figure 2 - Methods of biogas conditioning

Biogas can be used as a substitute for household and industrial gas or can be used as a renewable and sustainable energy source to produce heat or electricity in co-generation units (CHP) *((Krischan J. et al.,2011)*.

Table 1 highlights biogas components that are removed depending on how they are used.

Table 1. Removal of biogas components according to its final use

Use	H_2S	CO_2	H_2O
Gas station (boiler)	< 1000 ppm	No removal required	No removal required
Stove	Removal required	No removal required	Removal required
Cogeneration of heat and electricity	< 1000 ppm	No removal required	Removal required
Fuel for cars	Removal required	Removal required	Removal required
Fuel for the gas network	Removal required	Removal required	Removal required

The method of conditioning the raw biogas must be determined from the construction of the biogas plant for the fact that it may require some specific details in the construction of the plant.

RESULTS

Raw biogas needs to be cleaned to remove toxic and harmful constituents (e.g.. hydrogen sulfide, ammonia, VOCs. Halides, moisture, siloxanes, particulates, AB 1900 COCs, etc.) to meet regulatory and technical standards. The principle of cleaning techniques used currently includes adsorption, biofiltration, water scrubbing (an absorption process) and refrigeration.

— Biofiltration

Biofiltration relies upon the natural biological metabolism of sulfur-oxidizing bacteria species to convert hydrogen sulfide into elemental sulfur or sulfate. These systems are designed to ensure a high-density microbial community and maximize contact between the microorganisms and the feed gas *(Y. Zhu, 2001)*.

A biological filter combines water scrubbing and biological desulfurization. As with water scrubbing, the biogas and the separated digestate meet in a counter-current flow in a filter bed. The biogas is mixed with 4% to 6% air before entry into the filter bed.

Biofiltration systems can be set up in three different configurations: bioscrubber, biofilter, and biotrickling filter (Figure 3).

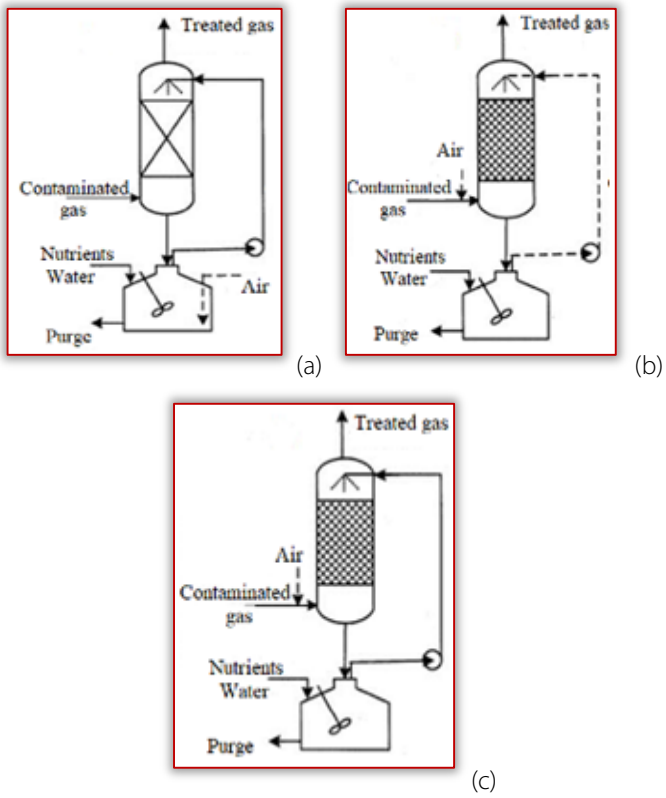

Figure 3 - Biofiltration Process Schematic
A) Bioscrubber. B) Biofilter. C) Biotrickling Filter

In a bioscrubber, pollutants are absorbed into liquid flowing counter-currently through an absorption column, similar to a water scrubber. The liquid is then sent to a bioreactor for microbes to degrade the contaminants.

A biofilter consists of a packed bed of organic material that stimulates biofilm growth through which humidified biogas is pumped. Contaminants in the biogas contact absorb and adsorb into the biofilm and interact with the microbes.

Biofiltration systems are effective for treating low and high H_2S concentrations from 50-100 ppm to 2000-4000 ppm, resulting in a H_2S removal of 89-99.9% at a rate of 20-125 g H_2S / m3 / h. Most bacteria grow and function optimally at a temperature of about 35 ° C and a neutral pH.

— Adsorption

Adsorption is the adhesion of compounds onto a solid surface. When biogas is flushed through an adsorbent bed, contaminant molecules will bind to the adsorbent's surface, removing the contaminants from the gas stream. Effective

adsorbents are generally highly porous with high surface area which greatly increases their removal capacity.

Pressure swing adsorption (PSA) is a method for the separation of carbon dioxide from methane by adsorption/desorption of carbon dioxide on zeolites or activated carbon at alternating pressure levels. Commonly used adsorbents are zeolite, carbon molecular sieve, silicagel and activated carbon, due to their low cost, large specific area and pore volume and excellent thermal stability (*Siriwardane RV. Et al., 2003)*. These adsorbents are designed to have a specific pore size thus enabling selective adsorption of molecules that are smaller than the designed pore size. Figure 4 shows a four-vessel swing adsorption adsorption system using carbon molecular sieves that circulate between absorption and regeneration *(Zhao Q. ei al.. 2010)*.

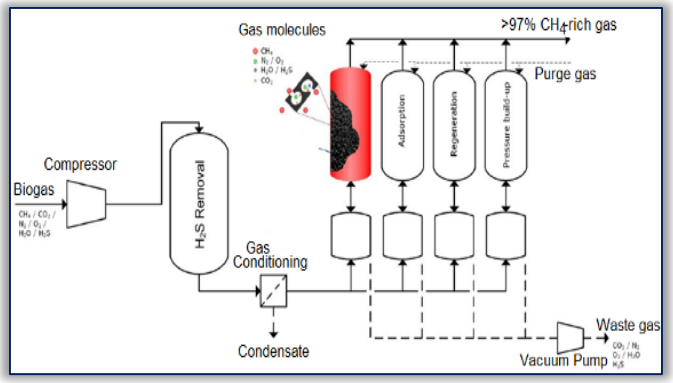

Figure 4 - Pressure Swing Adsorption Process Diagram

The adsorbent must be replaced once it is filled or can be regenerated a limited number of times. This contributes to operational cost.

— Pressurized Water Scrubbing

Purification of biogas by pressure water is one of the most widely used biogas treatment methods. Pollutant compounds can be physically adsorbed (or dissolved) in a liquid solution.

A schematic diagram of this method is shown in figure 5. To enhance the absorption of CO_2 and H_2S, biogas is usually compressed to 900–1200k Pa and a high surface area packing media is used.Inside the scrubber,biogas flows counter-currently to water that is sprayed from the top of scrubber and the absorption primarily occurs on the surface of the packing media. The raw biogas is introduced at the bottom of the column and flows upward, while fresh water is introduced at the top of the column, flowing downward over a packed bed. The packed bed (typically a high-surface-area plastic media) allows for efficient contact between the water and gas phases in a countercurrent absorption regime.

It is important that the H_2S be removed prior to the removal of the CO_2. as H_2S is highly corrosive and would result in decreased life and higher maintenance of the subsequent compressors required in the CO_2-removal step. Cleaned biogas can contain > 96% CH_4 after drying (*Liangcheng Y. et al., 2014*).

The disadvantage of water scrubbing is that it is less efficient than other processes, both in terms of CH_4 loss and energy. However, some of the energy inefficiency of the process may be offset by the use of a single-pass water scrubbing system, since other processes require a regeneration stage. Water scrubbing is the most applicable CO_2 scrubbing process for use in an agricultural setting because of its simplicity, low cost and low toxicity.

Another advantage of water scrubbing over some other processes is that water is fairly easy to dispose of whereas the chemicals used in some of the other processes may require special handling and disposal when spent.

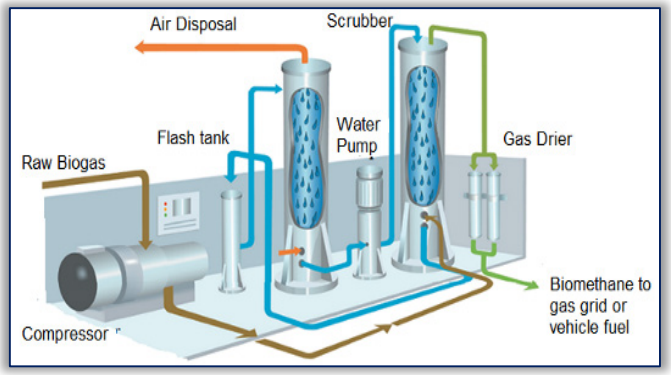

Figure 5 - The process of purifying biogas in a pressurized water system

— Refrigeration/Chilling

Refrigeration, or gas cooling provides a simple means for removing moisture from biogas. When the gas is cooled (typically to between -18 – 2 °C), water vapor condenses on the cooling coils and can be captured in a trap. Some ammonia will also be removed given the high solubility of ammonia in water. Insignificant trace amounts of other compounds may also be absorbed into the water. At lower temperatures of < -73 °C. VOCs will condense and can be removed too. At -70 °C. 99% removal of siloxane can be achieved as well, but it is costly to operate at such low temperatures.

H_2S should be removed prior to refrigeration to significantly lengthen the life of the refrigeration unit.

Raw biogas contains a variety of compounds aside from methane. These include hydrogen sulfide (H2S), oxygen (O2), nitrogen (N2), volatile organic compounds (VOCs), siloxanes and moisture (H2O). To remove these contaminants, adsorption, water scrubbing, biofiltration and/or refrigeration processes are employed *(Matthew D. et al.. 2014*).

Tabel 2. Contaminants removed by different biogas cleaning technologies

Biogas Cleaning Process	H_2S	O_2	N_2	VOCs	NH_3	Siloxanes	H_2O
Adsorption	**	/	-	**	*	**	**
Water Scrubbing	**	--	--	**	**	**	--
Biofiltration	**	--	--	**	/	/	--
Refrigeration	/	-	-	/	**	*	**

Legend: ** High removal (intended) * High removal (pre-removal by other cleaning technology preferred) / Partial removal - Does not remove -- Contaminant added R Must be pretreated

Next, a comparison is made between three methods of eliminating undesirable compounds from the biogas composition. Each of these technologies is able to treat different contaminants in different degrees (Table 2).

CONCLUSION

Biogas is a product of anaerobic ferment of organic products. Among the fuels from vegetal biomass, biogas has a great importance and can successfully replace fossil fuels for obtaining electricity and heat; the use of biogas exists for a few years also in the field of transport. Biogas formed in the methane fermentation process contains about 50÷60% of methane. Other ingredients such as carbon dioxide, hydrogen sulfide, water, water vapour and small amounts of nitrogen and oxygen are compounds that lower the energy value of biogas.

Biogas purification is the operation of retention of unwanted biogas components before it is used in the combustion process. Whatever the ultimate way of using biogas, it is impossible to use it in the raw state. The only recyclable component is methane.

Raw biogas needs to be cleaned to remove toxic and harmful constituents (e.g.. hydrogen sulfide, ammonia, VOCs, halides, moisture, siloxane, particulates,. etc.) to meet regulatory and technical standards. The principle cleaning techniques used currently include adsorption, biofiltration, water scrubbing (an absorption process) and refrigeration.

The method of conditioning the raw biogas must be determined from the construction of the biogas plant for the fact that it may require some specific details in the construction of the plant.

Note

This paper is based on the paper presented at ISB-INMA TEH' 2017 International Symposium (Agricultural and Mechanical Engineering), organized by University "POLITEHNICA" of Bucharest – Faculty of Biotechnical Systems Engineering, National Institute of Research-Development for Machines and Installations Designed to Agriculture and Food Industry – INMA Bucharest, Scientific Research and Technological Development in Plant Protection Institute (ICDPP), National Institute for Research and Development for Industrial Ecology – INCD ECOIND, Research and Development Institute for Processing and Marketing of the Horticultural Products "HORTING" and Hydraulics, Pneumatics Research Institute INOE 2000 IHP, University of Agronomic Sciences and Veterinary Medicine of Bucharest (UASVMB) – Faculty of Horticulture and Romanian Society of Horticulture (SRH), in Bucharest, ROMANIA, between 26 – 28 October, 2017.

References

[1] Bejan Mircea, Rusu Tiberiu. (2007) A renewable energy source - the biogas of organic waste (O sursă de energie regenerabilă – biogazul din deşeurile organice). Buletinul AGIR nr. 1;

[2] Dilea M., Paraschiv G., Voicu Gh., Biriş S.Şt., Ungureanu N., Toma L. Ionescu M.(2013). Biogas. The most effective technology for biomass. Bulgaria;

[3] Ioan Bitir Istrate, Eduard Minciuc. (2003). Utilization of biogas for the production of electric and thermal energy (Valorificarea biogazului pentru producerea energiei electrice si termice). Cartea Universitară.

[4] Krischan J., Makaruk A., Harasek M. (2012). Design and scale-up of an oxidative scrubbing process for the selective removal of hydrogen sulfide from biogas. J Hazard Mater 2012;215–216:49–56;

[5] Krzysztof BIERNAT, Izabela SAMSON-BRĘK.(2011). Review of technology for cleaning biogas to natural gas quality. Automotive Industry Institute PIMOT. Warsaw;

[6] Liangcheng Yang, Xumeng Ge, CaixiaWan, FeiYuc, YeboLi. (2014) Progress and perspectives in converting biogas to transportation fuels. Renewable and Sustainable Energy Reviews;

[7] Matthew D. Ong..Robert B. Williams. Stephen R. Kaffka DRAFT. (2014). Comparative Assessment of Technology Options for Biogas Clean-up. California Biomass Collaborative University of California. Davis;

[8] Paraschiv G., Dincă M.N., Ungureanu N., Moiceanu G., Toma M.L. (2017). Waste recycling plants (Instalaţii pentru reciclarea deşeurilor). Editura POLITEHNICA PRESS. Bucureşti;

[9] Siriwardane RV. Shen MS. Fisher EP (2003). .AdsorptionofCO2. N2. And O2 on natural zeolites. EnergyFuels2003;17:571–6.

[10] Thomas Hoerz, Pedro Krämer, B. Klingler, C. Kellner, Thomas Wittur, F. v. Klopotek, A.Krieg. H. Euler. Biogas Digest Volume I Biogas Basics. Information and Advisory Service on Appropriate Technology

[11] Y. Zhu. (2001). The Environmental and Industrial Gas Purification Technology. Chemical Industry Press. Beijing;

[12] Zhao. Q., E. Leonhardt., C. MacConnell, C. Frear and S. Chen. (2010). PurificationTechnologies for Biogas Generated by Anaerobic Digestion. Climate Friendly Farming Puyallup. WA: Center for Sustaining Agriculture and Natural Resources.

[13] ***BIOGAS an introduction. Fachagentur Nachwachsende Rohstoffe e.V. (FNR) Agency for Renewable Resources. 2013

[14] http://www.edu.pe.ca/agriculture/biogas.pdf

ISSN: 2067-3809

[1.]Ruzena KRALIKOVA, [2.]Lydia SOBOTOVA

ENVIRONMENTAL MANAGEMENT SYSTEM - A WAY TO SUSTAINABLE DEVELOPMENT IN UNIVERSITIES

[1.]Technical University of Kosice, Faculty of Mechanical Engineering,
Department of Process and Environmental Engineering, Kosice, SLOVAKIA

Abstract: Traditionally EMSs are implemented across all operations at a facility simultaneously. This way of implementation works well for industry and smaller businesses and offices where operations are easily delineated and there is a simple chain of command structure in place. The University is able to implement the EMS strategy similarly. Environmental Management System is an integrated organized set of policies and procedures under which the University can remain compliant with applicable environmental regulations, and in addition, manage and lessen our impacts on the environment, thereby improving the University's overall environmental performance. The University's EMS will require continual evaluation of the University's activities to ensure the University is doing as much as possible to reduce its impact on the environment and to remain environmentally compliant. This paper describes present situation and approach of universities to implementation of EMSs in Slovakia and into university management in abroad. The main principles and key requirements of the organisation management in accordance with the sustainable development are not only safety and quality managing of all activities in organisation in both manufacturing and services (education) but also environmental appropriate access.

Keywords: Environmental Management System (EMS) strategy, continual evaluation, implementation

INTRODUCTION

The University is made up of a variety of under-graduate, graduate, and professional schools, each comprised of many departments with unique specialties. In addition to academics, the University maintains a large laboratories, a large educational and research departments, lecture halls and facilities maintenance staff that maintain the infrastructure of the University, such as utilities and building [7]. With so many diverse operations, University-wide implementation is exceedingly difficult. To more effectively communicate the tasks and goals of the environmental management system (EMS) to all the faculty, staff, and students, as well as getting the required support of the EMS from all departments, the EMS is being implemented incrementally on a much smaller scale [2].

ENVIRONMENTAL MANAGEMENT AS TOOL FOR SUSTAINABLE DEVELOPMENT

The main principles and key requirements of the organization management are not only safety and quality managing of all activities in organization in both manufacturing and services (i.e. education) but also environmental appropriate access in accordance with the sustainable development [5]. Modern pro-environmental oriented management approaches (as BS 8555 standard, EMS, EMAS etc.) emphasizes the principle of continuous improvement, based on the Deming Cycle, Figure 1.

Implementation of environmental management system influences the growing interest of the public, pressure from customers and business partners, and especially aware of own responsibility for the state of the environment. This system is implemented voluntarily and the enterprise can actively monitor and manage the impact of its activities on the environment, enterprise can gradually reduce all its negative environmental impacts.

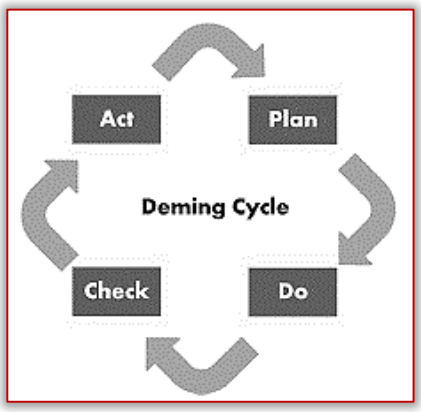

Figure 1. Deming cycle

Figure 2. Continual Improvement model [9]

The most commonly used framework for an EMS is ISO 14001 standard. An integral part of the EMS is the detailed systematic control of all documents including policies, procedures, training records, reports, permits, and all other relevant environmental information, Figure 2.

APPLICABLE OF ENVIRONMENTAL MANAGEMENT SYSTEM INTO UNIVERSITY ORGANIZATION

Environmental management system is an integrated organized set of policies and procedures under which the University can remain compliant with applicable environmental regulations, and in addition, control and lessen our impacts on the environment, thereby improving the University's overall environmental performance. This may sound complicated, but the concept is relatively simple. As coordinated teams, Environmental Health & Safety (EHS) and each department at the University systematically and regularly evaluate the department's operations for environmental regulatory compliance and environmental impacts. Operations are modified as necessary to meet the requirements of the regulations. Identified environmental impacts are ranked and investigated to find ways to prevent, lessen, or eliminate these impacts.

Policy and strategy

An EMS enables an organization to manage its environmental performance in a comprehensive, systematic and documented manner. It serves as a tool to reduce the impact, both immediate and long-term, of an organization's operations on the environment. It encourages the allocation of resources, assignment of responsibility, and ongoing evaluation of practices, procedures and processes with a view to continual improvement of the system [4].

For universities, the introduction of EMS mean improving the image of the public and it also may be proof of its quality and social responsibility. It can reform the education of the students to a better and also open up new opportunities for obtaining research grants and supporting cooperation between faculties [2].

Eco Campus

One of the schemes, which enables to colleges and universities to be recognized for addressing key issues of environmental sustainability is Eco Campus [1]. Eco Campus is a scheme which offers a flexible phased approach to implementing an environmental management system for the higher and further education sector.

Eco Campus provides a modular, phased, incremental approach to developing an EMS in line with both BS8555 & ISO 14001. Participants gain recognition at each stage of the process through a series of awards from bronze through silver, gold and platinum. The platinum award conforms to the requirements of the international environmental management standard ISO 14001 (see the Figure 3).

The scheme enables colleges and universities to be recognized for addressing key issues of environmental sustainability 6]. Eco Campus provides awards relating to 4 levels of achievement, linked to each stage of EMS development:

Phase 1: Planning (Bronze)
- Senior management commitment
- Environmental awareness training
- Baseline environmental review
- Draft environmental policy

Phase 2: Implementing (Silver)
- Legal & other requirements
- Significant environmental aspects
- Objectives, targets & programs
- Environmental policy

Phase 3: Operating (Gold)
- Resources, roles, responsibility & authority
- Competence, training & awareness
- Communication
- Documentation
- Control of documents
- Operational control
- Emergency preparedness and response

Phase 4: Checking & Correcting (Platinum)
- Monitoring & measurement
- Evaluation of compliance
- Nonconformity, corrective action & preventative action
- Control of records
- Internal audit
- Management review

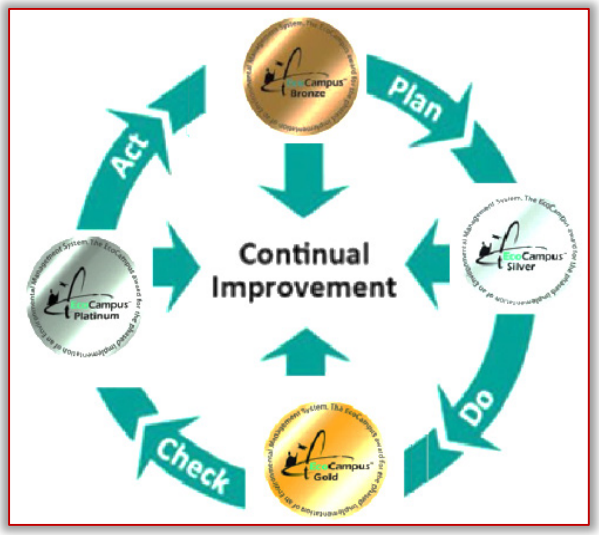

Figure 3. Stage of the process Eco Campus

BS 8555

Eco Campus is closely aligned to ISO 14001, the international environmental management standard, and BS 8555, the British guidance standard.

The British Standard BS8555 (full title: Guide to the phased implementation of an environmental management system including the use of environmental performance evaluation, Figure 4) describes how to implement a generic EMS and can be used as a route towards ISO14001 and EMAS.

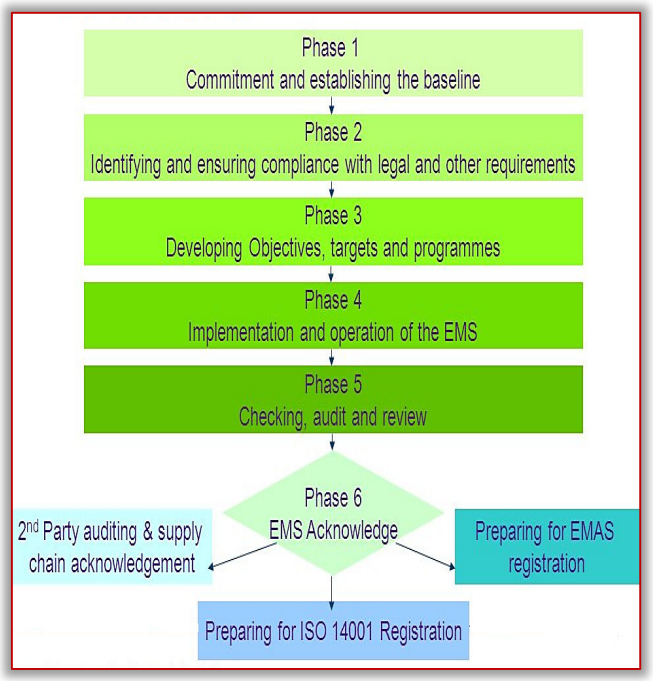

Figure 4. BS8555 Model

FOREIGN UNIVERSITY ENVIRONMENTAL MANAGEMENT SYSTEM

As an example of the existing EMS in foreign universities is Manchester Metropolitan University (MMU). This University has implemented an Environmental Management System that is certified by ISO14 001 and awarded Eco campus Platinum as one of only 28% of Eco Campus-registered Universities that have Eco Campus Platinum. The Environmental Management System is implemented by using the phased approach of the Eco Campus scheme, which provides a structured approach to work towards the ISO14001:2015 standard. In 2016, MMU was the first University to achieve the new and more challenging ISO14001:2015 standard. EMS incorporates all of the University's business activities, including estates and operations, leadership and governance, learning, teaching and research and engagement activities. Environmental Sustainability Strategy 2014–2020 sets out the actions MMU needs to take to achieve our aims and become a Sustainable University [8]:

- Placing environmental sustainability alongside graduate employability
- Use of sustainable modes of transport that minimize environmental impact
- Embed sustainable design principle
- Grow sustainability-themed research activity by 2020
- Ambitious targets to reduce carbon emissions by 50% by 2020
- Prevent, reduce, reuse and recycle
- Reuse and recycle 85% of waste by 2020
- Protect and enhance biodiversity across the university
- Offer opportunities to develop skills and knowledge to live and work sustainability
- Zero waste to landfill policy commitment
- Use alternative water sources and reduce water consumption by 25% by 2020.

MMU is an example for other universities which illustrates as to implement and realize the environmental policies and plans into university concept. It's vital that staff, students, trade union representatives should be have the enthusiasm and interest to engage in the development of environmental policies, strategies and management plans of their university.

CONCUSION

Currently, there is no university in Slovakia, which would have introduced a certified environmental management according ISO 14001. According scheme EMAS II, while efforts to introduce environmental education into university teaching process, especially in terms of sustainable development and the establishment of EMS in the next step. This scheme was planning to introduce the issue of sustainable development in relevant study program as well as the introduction of at least one subject on that topic at all levels of higher education.

The next phase is a scheme EMAS III, which is used in the step of introducing of environmental management system and schemes Green University of Slovakia and also for higher education of institutions [3]. The aim for the future is to certify the EMS in the Slovak universities the same as universities abroad that they have been successfully practiced with positive results already in the process of system integration

Acknowledgment

The research in this paper was solved in framework of grants: KEGA No 045TUKE -4/2018 (50%) and KEGA No 041TUKE-4/2018 (50%), supported by Slovak Research and Development Agency.

References

[1] Alshuwaikhat and Abubakar: An integrated approach to achieving campus sustainability. Assessment of the current campus environmental management practices, Journal of Cleaner Production. Vol.16, 2008, pp. 1777 - 1785. ISSN 0959-6526.

[2] Krasny, E. M., Lundholm, C., Plummer, R.: Environmental ecudation, resilience, and learning: reflection and moving forward. Environmental Education Research. Vol. 16(5-6), 2010, pp. 665-672, ISSN 1350-5622.

[3] Procházková, D., Rusko, M.: Relation between human system safety management and environmental management. Journal of Environmental Protection, Safety, Education and Management. Vol. 5 (9), 2017, p. ISSN 1339-5270.

[4] Rusko, M., Procházková, D.: Solution to the problems of the sustainable development management. Research papers Faculty of Materials Science and Technology Slovak University of Technology in Trnava. Vol. 19 (31), 2011, p.77-84. ISSN 1336-1589.

[5] Newman L.: Change, uncertainty, and futures of sustainable development. Futures. Vol. 38(5). 2006. pp. 633 -637.
[6] Nicolaides, A.: The implementation of environmental management towards sustainable universities and education for sustainable development as an ethical imperative, International Journal of Sustainability in Higher Education. Vol. 7 (4), 2006, pp. 414 – 424, ISSN: 1467-6370.
[7] Rands, G. P.: A principle-Attribute matrix for Environmentally Sustainable Management. Education and Its Application. The case for Change-Oriented Service-Learning Projects. Journal of Management Education. Vol. 33 (3), 2009, pp. 296-322, ISSN 1052-5629.
[8] http://www.mmu.ac.uk/environment/ems/index.php
[9] http://ems.iema.net/emsexplained

ISSN: 2067-3809

[1.]Emeka Segun NNOCHIRI, [2.]Oluwaseun Adedapo ADETAYO

GEOTECHNICAL PROPERTIES OF LATERITIC SOIL STABILIZED WITH CORN COB ASH

[1.]Department of Civil & Environmental Engineering, Afe Babalola University, Ado-Ekiti, NIGERIA
[2.]Department of Civil Engineering, Federal University, Oye-Ekiti, NIGERIA

Abstract: This study assesses geotechnical properties of lateritic soil using corn cob ash (CCA). Preliminary tests were carried out on the soil sample for classification purposes. California Bearing Ratio (CBR), Unconfined Compressive Strength (UCS) and compaction tests were performed on both the soil sample and the stabilized lateritic soil, which was stabilized by adding CCA in percentages of 2, 4, 6, 8 and 10 respectively by weight of the soil. The results showed that the addition of CCA reduced the values of Maximum Dry Density (MDD) from 1345kg/m^3 at 0% CCA to 1284kg/m^3, the Optimum Moisture Content (OMC) increased from 14.95% to 20.20%, both at 10% CCA. The unsoaked CBR values increased from 9.25% at 0% CCA to 28.20%, the UCS values increased from 495kN/m^2 to 560kN/m^2, for both CBR and UCS, the peak values were at 8% CCA. It was therefore concluded that CCA performs satisfactorily as a cheap stabilizing agent for stabilizing lateritic soil especially for subgrade purposes.
Keywords: Atterberg limits, corn cob ash, lateritic soil, stabilization, strength tests

INTRODUCTION

Many researchers have come up with various definitions of laterites, of note to this study is as posited by Ola (1983), where laterites is defined as the product of tropical weathering with red, reddish brown and dark brown colour, with or without nodules or concreting and generally (but not exclusively) found below hardened ferruginous crust or hard pan. Fundamentally, soils having a ratio of silica to sesquioxide (SiO_2/Fe O_3 + Al_2 O_3) which are less than 1.33 are regarded as laterites, between 1.33 and 2.00 are as regarded as lateritic soil and those above 2.00 are as non-lateritic soils. Though, this definition is not convenient from the engineering point of view especially where there is a lack of adequate laboratory facilities. According to Maignien (1966) and Gidigasu (1976) have three stages have been identified in the process of laterization. The first stage, decomposition is characterized by physico-chemical breakdown of primary mineral and the release of constituent elements. The second stage involves leaching under appropriate drainage condition of combined silica and bases and the relative accumulation and enrichment from outside sources (absolute accumulation) of oxides and hydroxides of sesquioxides (mainly Al_2O_3 and Fe_2O_3), the most resistant to leaching. The third stage which is the hydration or desiccation involves partial or complete dehydration (sometimes involving hardening) of the sesquioxide rich materials or secondary materials. There are five major factors that influence the formation of soils and they are: parental material, climate, topography, vegetation and time, of these primary factors, climate in considered to be the most important factor (Ola, 1978).

Laterite, a sedimentary rock deposit arising from the weathering of rocks, is one of the most common and readily available road building materials that can be sourced locally in Nigeria (Joel and Edeh, 2015). According to Bello et al. (2015), lateritic soils are generally used for road construction in Nigeria. Lateritic soil in its natural state more often, have low bearing capacity and low strength as a result of high content of clay. If lateritic soil contains a substantial amount of clay materials, its strength and stability cannot be guaranteed under load especially in the presence of moisture. The presence of high plastic clay in lateritic soil, causes soil cracks and damage on pavement, road ways, building foundations or any civil engineering construction projects. The need to improve the strength and durability of lateritic soil in recent time has become imperative, consequently, this has led researchers towards using stabilizing materials that can be sourced locally at very a cheap cost. These local materials can be categorized as either agricultural or industrial wastes. The capability to blend the naturally occurring lateritic soil with some chemical additives to give it better engineering properties in both strength and water proofing is very important.

Stabilization, according to Ogundipe (2013), is the process of blending and mixing materials with a soil to improve certain properties of the soil. The process may include the blending of soils to achieve a desired gradation or the mixing of commercially available additives that may alter the gradation, texture or plasticity or act as a binder for cementation of the soil. There are three purposes of stabilization, these include; strength improvement, dust control and soil water proofing (Amu and Adetuberu, 2010).

According to Mujedu et al.,(2014), corncob is the hard thick cylindrical central core of the maize, it is also described as the agricultural waste product obtained from corn or maize which is the most important cereal crop in Sub-Sahara Africa, 589 million tons of maize was produced worldwide in the year 2000 and the United States was reported to be the

largest maize producer having 52 % of world production. Africa produced 7% of the world maize. Corn cob ash can be obtained by drying the cobs thoroughly and burning them intensively using open air burning. Thereafter, the product would be sieved using sieve number 200.

Figure 1: Corn Cob

LOCATION AND GEOLOGY OF THE STUDY AREA

According to Ogunribido (2011), the study area Akure lies within longitude 7^0 18^1 N and 7^0 16^1 N North of Equator and between latitude 5^0 09^1 E and 5^0 11.5^1 E of Green Winch meridian. The study area occurred within the Precambrian Crystalline rocks of the basement complex of Southwestern Nigeria. The predominant rock types in the study area are charnockites, granite, gneiss and migmatitic rocks. In some places in the study are these rocks have undergone deep weathering.

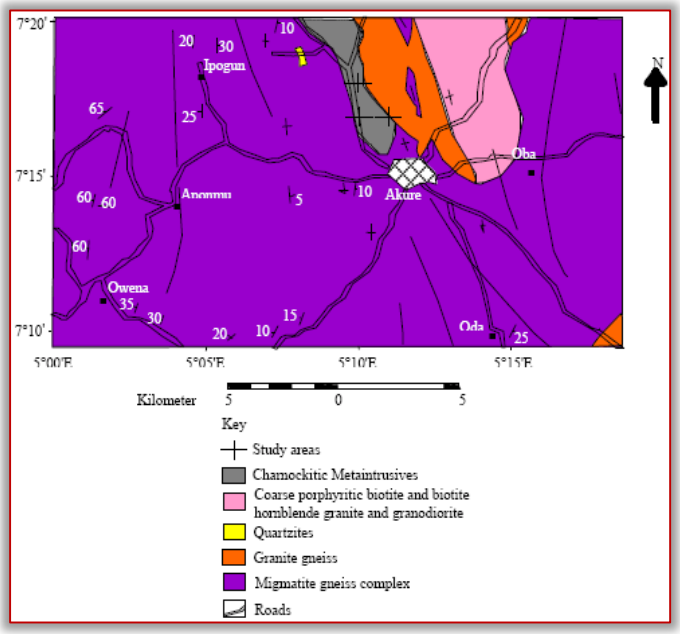

Figure 2: Geological map of Akure showing study area. Source: Ademeso (2009).

MATERIALS

The materials used for this research work were lateritic soil, Corn Cob Ash (CCA) and potable water.

The lateritic soil was collected from at burrow pit in Akure, Ondo State at depths representative of the soil stratum and not less than 1.2m below the natural ground level.

The corncob was collected from a large corn farmland. The cobs were dried thoroughly, cut into smaller sizes and burnt for about ten hours using open air burning at 600^0C. Finally the product was sieved through BS Sieve 75µm Sieve.

Potable water was gotten from the running taps in the laboratory.

METHODS

The soil sample was air-dried for two weeks at the Geotechnical Laboratory of Federal University of Technology, Akure before analyzing the soil sample. The Corn Cob Ash (CCA) was added to the natural soil sample at varying proportion of 2,4,6,8 and 10% by weight of soil, the following tests were carried out on the mixes: Atterberg limits test, compaction tests, unconfined compressive strength and the California Bearing ratio tests. The procedures for the various tests were carried out in accordance with BS 1377 (1990) and BS 1924 (1990).

DISCUSSIONS

The sum of SiO_2, Al_2O_3 and Fe_2O_3 for Corn Cob Ash gives 80.44%, which is greater than 70% recommended by ASTM C618 (2003), for the classification of pozolanic materials.

Table 1. The chemical composition test results of Corn Cob Ash

Elemental oxides	Weight percentages
CaO	10.24
SiO_2	64.90
MgO	2.08
Na_2O	0.43
Al_2O_3	10.79
Fe_2O_3	4.75
SO_3	2.53
K_2O	4.23

Source: Owolabi et al., (2015)

Table 2. The preliminary test results of lateritic soil

Property	Amount
Natural moisture content (%)	13.20
Percentage passing BS No 200 Sieve	52
Liquid limit (%)	53
Plastic Limit (%)	18
Plasticity Index (%)	35
Specific gravity	2.70
Maximum Dry Density (kg/m^3)	1345
Optimum moisture content (%)	14.95
California bearing ratio (Unsoaked) (%)	9.5
Unconfined Compressive Strength (kN/m^2)	495
AASHTO Classification	A-7-6

Preliminary tests (such as Atterberg limits, specific gravity and particle size analysis) were carried out on the soil sample. According to Garber and Hoel (2009), for a soil to be classified into A-7 group, it must have a minimum liquid limit value of 41%, percentage passing through BS No 200 sieve must be greater than 35% and the Plasticity Index must be greater than 11%, all these conditions were met by the Soil Sample. Also for a soil to be classified into the A-7-6 subgroup, it must satisfy the following requirement, P.I > L.L -30, therefore 35 > 53-30 = 23.

Table 3: Strength test results

CCA (%)	MDD (kg/m^3)	OMC (%)	UCS (kN/m^2)	CBR (Unsoaked) (%)
2	1340	15.80	510	11.10
4	1335	16.70	525	18.05
6	1320	18.10	542	24.64
8	1301	19.10	560	28.20
10	1284	20.20	550	26.10

— Compaction

With the increased addition of CCA, the Maximum Dry Density (MDD) reduced. This reduction may be attributable to the replacement of soils by the CCA in the mixture which has lower specific gravity of 1.05, this is less than that of the lateritic soil (2.70). The CCA therefore fills the voids in the lateritic soil. The reduction in MDD may also be attributed to coating of the soil by the CCA which result to large particles with larger voids and hence less density (Fattah et al., 2013).

With the increased addition of CCA to the lateritic soil sample, the Optimum Moisture Content increased in value this may be attributed to the addition of CCA, which decreases the quantity of free silt and clay fraction and coarser materials with larger surface areas were formed, these process need water to take place. This implies also that more water is needed in order to compact soil-CCA mixtures (Fattah et al., 2013).

— California Bearing Ratio (CBR) tests

It was observed that the gradual increase in addition of CCA led to increase in value of Unsoaked CBR till it got to its optimum value of 28.20% at 8% CCA.

With the further addition of CCA that is at 10% the value in CBR reduced. The increase in CBR may be because of the gradual formation of cementitious compounds in the soil by reaction between CCA and some amounts of Calcium hydroxide present in the soil. The decrease in CBR at 10% CCA may be due to extra CCA that could not be mobilized for the reaction which occupies spaces within the sample. This reduces the bond in the soil-CCA mixture (Okafor and Okonkwo, 2009).

— Unconfined Compressive Strength (UCS) tests

As more CCA ash was being added to the soil, the values of Unconfined Compressive Strength (UCS) increased to its optimum value at 8% CCA by weight of soil. Thereafter, it reduced at 8% CCA. Increase in values of UCS and decrease at 10% CCA can be explained as it was in the case of California bearing ratio.

— Atterberg limit

Figure 3, shows the relationship between the addition of CCA to the lateritic soil and its effects on the Atterberg limits (Liquid limit, Plastic limit and Plasticity Index). It was observed that there was a general reduction in values of liquid limit, and Plasticity Index. While the plastic limit values increased. According to Fattah et al., (2013), decrease in liquid limit and plasticity index is an indication of improvement of the soil, since CCA reaction forms compound possessing cementitious properties calcium silicate cement with soil particles.

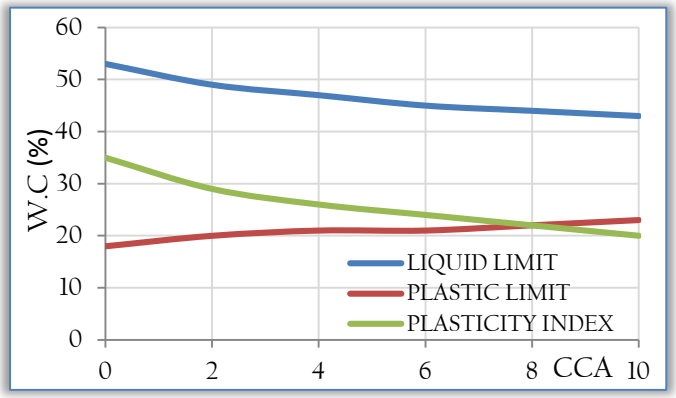

Figure 3: Graph showing effects of CCA on Water Content (W.C.)

CONCLUSIONS

From the results of the investigation carried out in this study, the following conclusions can be drawn:

— The lateritic soil was classified under A-7-6 group.

— Liquid Limit and Plasticity Index values reduced considerable from 53% at 0% CCA to 43% at 10% CCA and from 35% at 0% CCA to 20% at 10% CCA respectively.

— The treatment of the lateritic soil resulted to the decrease in Maximum Dry Density (MDD) and increase in Optimum Moisture Content (OMC) with the addition of CCA.

— The Unsoaked CBR values increased with the addition of CCA to the lateritic soil sample to an optimum value of 28.20% at 8% CCA by weight of soil from 9.25% at 0% CCA.

— The UCS values increased with the addition of CCA to the lateritic soil sample to an optimum value of 560kN/m^2 at 8% CCA by weight of soil.

As a consequence, one can conclude that the Corn Cob Ash (CCA) performs satisfactorily as a cheap agent for stabilizing lateritic soil especially for sub-grade purposes in road construction.

References

[1] Ademeso, O. A. (2009) Deformation Traits in Charnockitic Rocks of Akure Area, Southwestern Nigeria. Asian Journal of Earth Sciences, 2: 113-120.

[2] American Society of Testing and Materials (ASTM) C618 (2003). Standard Specification for Coal Fly Ash and raw or calcined natural pozzolan for use in Concrete. American Society for Testing and Materials, ASTM International: West Conshohocken, PA.

[3] Amu, O. O. and Adetuberu, A. A. (2010) Characteristics of Bamboo Leaf Ash Stabilization of Lateritic Soil in Highway Construction. International Journal of Engineering and Technology, Vol. 2(4), Pp 212-219.

[4] Bello, A.A. Ige, J.A. and Ayodele, H. (2015) Stabilization of Lateritic Soil with Cassava Reel Ash. British Journal of Applied Science and Technology, 2015, 7 (6): 642-650, 2015, Article no BJAST.

[5] British Standards (BS) 1377 (1990) Methods of Test for Soils for Civil Engineering Properties. London: British Standard Institution.

[6] British Standards (BS) 1924. (1990) Methods of Test for Stabilized Soils. British Standard Institute, London.
[7] Fattah, M.Y., Rahil, F.H. and Al-Soudany, K.Y.H. (2013) Improvement of Clayey Soil Characteristics Using rice Husk Ash, Journal of Civil Engineering and Urbanism, Vol. 3, Issue 1: 12-18.
[8] Garber, N.J. and Hoel, L.A. (2009) Traffic and Highway Engineering. 4th Edition, CENGAGE Learning, United States, 2009.
[9] Gidigasu, M.D. Lateritic Soil Engineering. Pedogenesis and Engineering Principles. Elsevier, Amsterdam. 535 pp, 1976.
[10] Joel, M. and Edeh, J.E. Comparative Analysis of Cement and Lime Modification of Ikpayongo Laterite for Effective and Economic Stabilization. Journal of Engineering Trends in Engineering and Applied Sciences (JETEAS), 6 (1): 49-56, 2015.
[11] Maignien, R. Review of Research on Laterites. National Resources Research, V, UNESCO, Paris. Pp 1-148, 1966.
[12] Mujedu, K. A., Adebara, S.A. and Lamidi, I.O. The Use of Corncob Ash and Sawdust Ash as a Cement Replacement in Concrete Works. International Journal of Engineering and Science (IJES), Vol. 3, Issue 4, Pp 22-48, 2014.
[13] Ogundipe, O.M. An Investigation into the Use of Lime Stabilized Clay as Sub-grade. International Journal of Scientific and Technology Research. Vol. 2, Issue 10, 2013.
[14] Ogunribido, T. H. T. Potentials of Sugar Cane Straw Ash for Lateritic Soil Stabilization in Road Construction. International Journal of Science Emerging Technology, 2011, Vol. 3 No. 5, 2015.
[15] Okafor F.O. and Okonkwo, U.N. Effects of Rice Husk Ash on some Geotechnical Properties of Lateritic Soil. Leonardo Electronic Journal of Practices and Technologies. ISSN 1583-1078, Issue 15. P. 67-74, 2009.
[16] Ola, S.A. Tropical Soils of Engineering Practice. Balkenia Publishers, Rotterdam, Netherlands, 1983.
[17] Ola S.A. Geotechnical Properties and Behaviour of some Stabilized Nigerian Lateritic Soil. Q.T.J. Engr. Geo. London. Vol. III, 1978. Pp. 148-160, 1978.
[18] Owolabi, T.A., Oladipo, I.O. and Popoola, O.O. Effect of Corn Cob Ash as a Partial Substitute for Cement Cement in Concrete. New York Science Journal, 8 (11), 2015.

ISSN: 2067-3809

[1.]Eugen MARIN, [1.]Marinela MATEESCU, [1.]Dragoş MANEA, [1.]Gheorghe GHEORGHE

TECHNICAL EQUIPMENT FOR WORKING THE SOIL IN THE ROW OF FRUIT TREES SIMULTANEOUSLY WITH ROOT CUTTING TO MODERATE SHOOTS GROWTH AND PRECISION FOLIAR FERTILISATION

[1.]National Institute of Research – Development for Machines and Installations Designed to Agriculture and Food Industry – INMA Bucharest, ROMANIA

Abstract: INMA Bucharest designed, produced and tested an experimental model of technical equipment for working the soil in the row of fruit trees along with root cutting to moderate shoots growth and precision foliar fertilization, within the innovative technology of fruit plantation maintenance in the rural areas. The paper presents experimental research with the aggregate of the TD 80D New Holland tractor and the ETR technical equipment for determining the qualitative working indexes of soil working and root cutting. The results obtained generate valid solutions for the achievement of a significantly improved product within the fruit plantation maintenance technology and offer to the interested economic agents an efficient product, adapted to the specific heavy conditions in the country.
Keywords: soil working, root cutting, fruit trees

INTRODUCTION

The objectives of world fruit growing in general and in Europe, in particular, are directed to reduce the growing vigour of cultivated fruit species (apple, pear, cherry, sour cherry and walnut) by mechanical interventions on the root system in order to establish intensive and super-intensive fruit plantations with high tree density per area unit (ha). On these small-scale plantations, technological works such as cuttings, phytosanitary treatments, fruit harvesting etc, can be made easier, with greater efficiency, less workforce and maintaining the same production (Hoying. 2017).

Worldwide research in fruit growing has shown that cutting a part of the tree root system, correlated with crown cutting, is beneficial, helping to keep trees down and maintaining root growth within the nutritional space of each tree.

The area of nutrition may be a field with herbicide applied and/or worked on a 1-1.4 m band under the tree rows where one can apply norms of localized irrigation (drip, micro-spraying) and fertilization (fertigation) of which only trees can benefit (Dorais et Ehret. 2008).

A root cutting equipment at a distance of 50-60-cm from the trees trunk (row axis) with high quality working indexes maintains root growth only in the nutrition space and is a control operation of fruit trees growth.

Root cuttings must be made in the side of the row by mechanically reducing their length during vegetation, on both sides of the row, alternatively, one year on one side and in the second year on the other side, in order not to compromise the stability of the fruit trees. The cut of a root should be like that of a branch, be straight, without fringes and keeps the required distance.

MATERIAL AND METHOD

The experimental researches were carried out with a technical equipment for soil working on the row of fruit trees. Together with root cuttings to moderate shoots growth and precision foliar fertilization. ETR (figure 1) was made by INMA and intended for the maintenance of fruit plantations in order to increase fructification efficiency by performing a single-pass ploughing on a strip at a distance from the trunk to maintain loose soil to the surface, cutting the root at a distance from the trunk to moderate the shoots growth and foliar fertilization.

Figure 1 - Technical equipment for working the soil in the row of fruit trees along with root cutting to moderate shoots growth and precision foliar fertilization, ETR

ETR technical equipment is designed to perform proper root cutting works in all soil types where fruit plantations are located, ranging from mild to hard and with a stony structure soil, specific to plantations located on hill areas; it is robust and has stability in the working direction by maintaining the same distance from the tree axis (Marinela Mateescu et al.. 2016).

It performs the following works in the same time:

- ploughing on a strip at a distance from the trunk to maintain a loose soil to the surface;
- root cutting at a distance from the trunk to moderate shoots growth;
- precision foliar fertilization.

The ETR technical equipment consists of a metal frame fitted with a coupling system at the three-point suspension mechanism of a wheeled tractor, a wheel for copying the soil

and adjusting the working depth of a right plough body for ploughing, a support for an articulated guide and means for adjusting the cutting depth and blocking in the vertical cutting direction of a disc-type working part with a large diameter for root cutting (Marin E. et al.. 2015) and a device for precision foliar fertilization.

The main technical characteristics of the ETR technical equipment are:

- power source: 80 HP wheeled tractor
- strip width, 250 mm
- strip depth, 150..200 mm
- working depth of the large diameter disc knife, 10...250 mm
- cutting distance from the trunk, 500...600 mm

The experiments made in laboratory-field conditions to determine the qualitative and energetic indices of ETR technical equipment, were performed on the INMA Bucharest experimental plot according to the specific test procedure made for this purpose. The following measuring and control equipment and instruments were used to test the ETR equipment: metallic tape, mechanical timer, device for measuring plow depth, rulers, set squares, poles, stakes. etc.

The following qualitative working indexes were determined under laboratory conditions:

- root cutting depth;
- distance from the trunk to the root cutting disc;
- soil working depth;
- distance from the trunk to the soil working plough body.

RESULTS

- *The root cutting depth* was determined using the measuring tape by measuring the distance between the surface of the non-worked field and the rim of the large diameter disc knife active part (Figure 2).

Table 1. Average values of root cutting depth

Repetition	a cm	a_m cm	S – standard deviation cm	Cv- variation coefficient %
Working speed: 3 km/h				
1	19.6	19.42	0.29	1.49
2	19.4			
3	19.4			
4	19.2			
5	19.5			
Working speed: 5 km/h				
1	19.4	19.36	0.27	1.39
2	19.3			
3	19.6			
4	19.3			
5	19.2			
Working speed: 7 km/h				
1	19.2	19.20	0.37	1.95
2	19.3			
3	19.4			
4	18.9			
5	19.2			

Measurements were made in 5 points at intervals of 2 m between them, for three working speeds (small, medium and maximum) of the ETR technical equipment. Based on the measurements, the *average depth of root cutting* was calculated. Table 1 shows the average values of root cutting depth. The coefficient of variation is defined as the ratio between the value of the standard deviation and the average value and is given as percentage (Marin E. et al.. 2012).

Figure 2 – Measuring root cutting depth

- *The Distance from the trunk to the root cutting disc* was determined by means of measuring tape by measuring the distance between the trunk and the rim of the large diameter disc knife active part (Figure 3). Measurements were made in 5 points at intervals of 4 meters between trees for three working speeds (small, medium and maximum) of the ETR technical equipment. Based on the measurements, the *average distance from the trunk to the root cutting disc* was calculated.

Table 2 shows the average values of the distance from the trunk to the root cutting disc.

Table 2. Average values of the distance from the trunk to the root cutting disc

Repetition	d cm	d_m cm	S-standard deviation cm	Cv- variation coefficient %
Working speed: 3 km/h				
1	58	56.4	3.33	5.90
2	56			
3	54			
4	58			
5	56			
Working speed: 5 km/h				
1	60	59.3	4.51	7.61
2	58			
3	56			
4	62			
5	60			
Working speed: 7 km/h				
1	54	53.5	4.51	8.47
2	52			
3	50			
4	56			
5	54			

Figure 3 - Measuring the distance from the trunk to the root cutting disc

- *Soil working depth* was determined by means of measuring tape by measuring the distance from the level of the soil resulting from the work to the bottom of the furrow (Figure 4). Measurements were made in 5 points at

intervals of 2 m between them for three working speeds (small, medium and maximum) of the ETR technical equipment. Based on the measurements, the *average soil working depth* was calculated. Table 3 shows the average values of the soil working depth.

Table 3. Average values of soil working depth

Repetition	a_i cm	a_{im} cm	S-standard deviation cm	Cv-variation coefficient %
Working speed: 3 km/h				
1	16.2	16.12	0.45	2.80
2	16.0			
3	15.8			
4	16.4			
5	16.2			
Working speed: 5 km/h				
1	16.0	16.02	0.33	2.10
2	15.8			
3	15.6			
4	16.0			
5	15.8			
Working speed: 7 km/h				
1	15.6	15.44	0.36	2.33
2	15.4			
3	15.8			
4	15.6			
5	15.2			

Figure 4 - Measuring soil working depth

— *The distance from the trunk to the soil working plough body* was determined by means of measuring tape by measuring the distance between the trunk and the furrow wall made by the soil working plough body. Measurements were made in 5 points at intervals of 4 m between trees for three working speeds (small, medium and maximum) of the ETR technical equipment. Based on the measurements, the *average distance from the trunk to the soil working plough body* was calculated.

Table 4 shows the average values of the distance from the trunk to the soil working plough body.

Table 4. Average values of the distance from the trunk to the soil working plough body

Repetition	d_t cm	d_{tm} cm	S-standard deviation cm	Cv-variation coefficient %
Working speed: 3 km/h				
1	130	126.4	5.03	3.98
2	124			
3	124			
4	126			
5	128			
Working speed: 5 km/h				
1	128	126	3.61	2.86
2	126			
3	124			
4	128			
5	124			
Working speed: 7 km/h				
1	126	125.2	4.51	3.60
2	128			
3	124			
4	122			
5	126			

The energetic indexes determined were:

— Effective working speed V_e. in km/h

A linear space *s* was measured by means of measuring tape on the test field and the beginning and end of this space was marked with 2 stakes. When the aggregate became operational in the test field, the timer was switched on and at the exit of that respective space it was stopped and the time *t* for passing the space *s* was read out on the timer. Determinations for three working speeds were made. The operation was repeated 5 times for each working speed and based on this, the arithmetic mean was calculated.

With recorded data, the travel speed *v* was calculated with the following relation (*Tecusan et Ionescu. 1982*):

$$V_e = \frac{3.6 \times s}{t}. \text{ km/h}$$

— The theoretical working capacity $W_{ef.}$ in ha/h

The theoretical working capacity was calculated with the relation (Caba et al. 2013):

$$W_{ef} = 0.1 \times B_l \times V_e. \text{ ha/h}$$

where: B_l is the working width of the technical equipment, in m; V_e – working speed, in km/h.

Energetic indexes for the aggregate TD 80D New Holland tractor (http://agriculture.newholland.com. 2011) + ETR technical equipment are shown in Table 5.

Table 5. Energetic indexes for the aggregate TD 80D New Holland tractor + ETR technical equipment

Parameters determined	Value				
Travel speed, km/h	3.0	3.1	3.2	4.9	5.0
Theoretical working capacity $W_{ef.}$ ha/h	0.66	0.68	0.70	1.07	1.1

Figure 5 shows an aspect during the determination of energetic indexes for the aggregate TD 80D New Holland tractor + ETR technical equipment.

Figure 5 - Aspect during the determination of energetic indexes for the aggregate TD 80D New Holland tractor + ETR technical equipment during root cutting and soil processing works

CONCLUSIONS

— The qualitative working indexes achieved during the experimentation of the ETR technical equipment fall

within the agrotechnical requirements corresponding to each individual work. The values of the variation coefficients were below 10%. which is admitted by the agrotechnical requirement, as follows:

— Variation coefficient values of root cutting depth depending on the working speed are graphically represented in Figure 6;

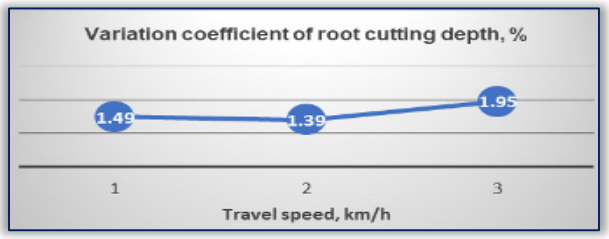

Figure 6 - Variation coefficient of root cutting depth depending on the working speed

— Variation coefficient values of the distance from the trunk to the root cutting disc, depending on the working speed, are graphically represented in Figure 7;

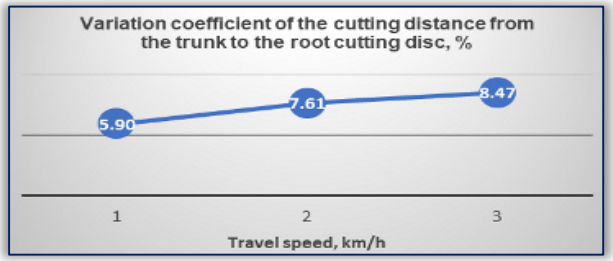

Figure 7 - Variation coefficient of the distance from the trunk to the root cutting disc depending on the working speed

— Variation coefficient values of soil working depth depending on the working speed are graphically represented in Figure 8;

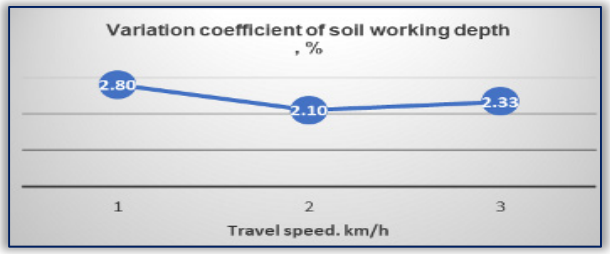

Figure 8 - Variation coefficient of soil working depth depending on the working speed

— Variation coefficient values of the distance from the trunk to the soil working plough body depending on the working speed, are graphically represented in Figure 9.

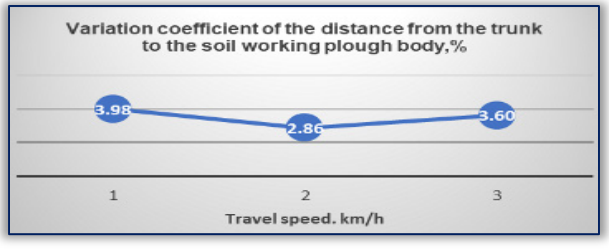

Figure 9 - Variation coefficient of the distance from the trunk to the soil working plough body depending on the working speed

— The energetic indexes achieved during the experimentation of the ETR technical equipment fall within the agrotechnical requirements corresponding to each individual work.

— Experimental research has enabled the technical and technological validation of the solutions addressed when designing the components of the ETR technical equipment;

— Experimental results make it possible to develop a useful recommendation for farmers applying innovative maintenance technology for fruit plantations.

Acknowledgement: The results presented were achieved with the support of the Ministry of Research and Innovation. Programme NUCLEU, contract no. 8N/09.03.2016. Addendum no. 2/2017. Project PN 16 24 02 04 – "Innovative technology for fruit plantations maintenance in the rural areas by soil works, root cutting and precision foliar fertilisation".

Note: This paper is based on the paper presented at ISB-INMA TEH' 2017 International Symposium (Agricultural and Mechanical Engineering), organized by University "POLITEHNICA" of Bucharest – Faculty of Biotechnical Systems Engineering, National Institute of Research-Development for Machines and Installations Designed to Agriculture and Food Industry – INMA Bucharest, Scientific Research and Technological Development in Plant Protection Institute (ICDPP), National Institute for Research and Development for Industrial Ecology – INCD ECOIND, Research and Development Institute for Processing and Marketing of the Horticultural Products "HORTING" and Hydraulics, Pneumatics Research Institute INOE 2000 IHP, University of Agronomic Sciences and Veterinary Medicine of Bucharest (UASVMB) – Faculty of Horticulture and Romanian Society of Horticulture (SRH), in Bucharest, ROMANIA, between 26 – 28 October, 2017.

References

[1] Caba I.L., Biriş S., Selvi K.C., Bungescu S., Vlăduţ V., Nițu M. (2013). Researches on improvement of working process of fibrous forages shredding parts. INMATEH Agricultural Engineering. Vol. 39. No. 1. Bucharest. Romania;

[2] Dorais M., Ehret D.L. (2008). Improving the Health-Promoting Properties of Fruit and Vegetable Products. A volume in Woodhead Publishing Series in Food Science. Technology and Nutrition. Agriculture and Agri-Food Canada. Research Branch. pages 346–391. Canada;

[3] Hoying A. (2017). Orchard Crops. Encyclopedia of Applied Plant Sciences (Second Edition). Pages 246-254. Vol. 3. Cornell University. Ithaca. NY. USA;

[4] Marin E., Toderaşc P., Manea D., David A. (2015). Technical equipment for tilling the soil and root pruning row of trees. Patent application RO-BOPI 6/2015;

[5] Marin E., Sorica C., Manea. D. (2012). The establishing of corn with the equipment for soil tillage and sowing in narrow strips. Actual Tasks on Agricultural Engineering: Proceedings of the 40. International Symposium on Agricultural Engineering. Opatija. Croatia. 21-24 February 2012 2012 pp.231-241 ref.9;

[6] Mateescu M., Marin E., Vlăduţ V., Manea D., Gheorghe G., Cârdei P., Tudor A., Boruz S., Sărăcin I., Stoian F.. (2016). Solidworks 3d parametric modelling technique for root cutting equipment declining growth of shoots in orchards. Annals of the University of Craiova - Agriculture. Montanology. Cadastre Series. Vol. XLVI. Craiova;

[7] Tecusan N., Ionescu E. (1982). Tractors and motor cars. Didactic and Pedagogic Publishing House. Bucharest. Romania;

[8] http://agriculture.newholland.com/uk/en/Products/Tractors . 2011.

[1.]Mihaela Elena NAGY, [1.]Constantin COȚA, [1.]Nicolae CIOICA,
[1.]Zoltán GYÖRGY, [2.]Lucian FECHETE-TUTUNARU

INVESTIGATIONS REGARDING DEGRADATION BY HYDRATION-DRYING OF SOME BIOCOMPOSITES REINFORCED WITH NATURAL FIBER

[1.]National Institute of Research – Development for Machines and Installations Designed to Agriculture and Food Industry – INMA, Branch Cluj-Napoca, ROMANIA
[2.]Technical University of Cluj-Napoca, Faculty of Mechanics, ROMANIA

Abstract: Biocomposite materials with improved properties can be obtained by reinforcing a biodegradable matrix with natural fibers. In order to obtain the biodegradable matrix a viable solution are thermoplastic starch based polymers. A method to avoid the inconveniences of using thermoplastic starch (poor mechanical properties and low resistance to moisture) can also be the reinforcement with natural fibers. The composite material studied was obtained by the reactive extrusion of various mixtures of starch, glycerol, poly (butylene adipate-co-terephthalate) (PBAT) and Miscanthus fibers as reinforcing material. This paper presents the results of water uptake and FT-IR spectroscopy investigations for 4 samples of composite material with thermoplastic starch matrix and reinforced with Miscanthus fibers in different concentrations (up to 20%).
Keywords: composite, thermoplastic starch, Miscanthus fibers, degradation

INTRODUCTION

Extending the use of composite materials in almost all areas of activity is influenced by a multitude of factors such as the need for materials with less weight but with certain mechanical properties, environmental and health concerns, the need to reduce energy consumption, sustainable achievement. etc. [5]

The use of renewable materials both as reinforcement elements and as matrix for composite materials contributes to the mitigation of some environmental pollution problems due to synthetic composite materials. Degradable composite materials are composite materials made of a polymer matrix derived from renewable sources (polysaccharides, vegetable oils) or from fossil sources (synthetic polymers such as polyethylene, polypropylene, polyesters, etc.) with natural fiber reinforcement or by-products from agriculture.

One of the most used and studied bio-composite materials is one that uses starch as a matrix [2.6]. To improve the properties of starch based materials biobased polyesters or synthetic biodegradable polyesters such as poly (butylene adipate-co-terephthalate) (PBAT) [7] can be added.

The use of natural fibers (flax, jute, hemp, Miscanthus) to reinforce the biodegradable matrix ensures improved properties of the composite, good mechanical properties, low weight and certain environmental benefits.[1.3.4].

Generally, the manufacturing technologies of degradable composite materials involve machines and processes for obtaining the matrix, preparing the reinforcement components, impregnating or treating the fibers, cutting the fibers, making the reinforcement (different shapes: network, fabric, braid, etc.) injection molding, compression and extrusion, compression-molding, or other processes.

MATERIAL AND METHOD

The samples in this study were prepared by reactive extrusion with a laboratory twin-screw extruder with co-rotating intermeshing, self-wiping screws ZK 25. Collin. (Germany). The raw materials used were: native corn starch obtained from SC ROQUETTE SA Calafat, Romania, having water content of 12.01 %, a density of 0.561 g/cm^3 and an amylose content of 21%. glycerol purchased from SC Nordic Invest SRL Cluj-Napoca with a concentration of 99.5% and a density of 1.262 g/cm^3. Poly(butylene adipate-co-terephthalate) (PBAT) purchased from BASF Company - product code is Ecoflex F Blend C1200 with mass density of 1.25-1.27 g/cm^3, melting point 110-120 °C and melt flow 2.7 - 4.9 g/10 min. and Miscanthus fibers obtained from Arge Miscanthus Romania.

Table 1 shows the ratio of the components used in the formula for the composite material reinforced with fibers.

Table 1. The components ratio in the composite formula

Composite sample	Starch (%Starch+PBAT+ Glyc)	PBAT (%Starch+PBAT+ Glyc)	Glycerol (%Starch+PBAT+ Glyc)	Miscanthus fibers (%Starch+PBAT+ Glyc))
P0	64	13	23	0
P5	64	13	23	5
P10	64	13	23	10
P20	64	13	23	20

The samples were cut into rectangular pieces (Figure 1) and was added distilled water. For each sample we measure the water uptake using a Partner WLC 0.6/B1 analytical balance with a precision of 0.1 g after the excess water was removed by placing the sample on absorbant paper for 1 minute. The modification induced by hydratio/drying processes could have effects on the vibration of the molecular bonds. FT-IR

measurements can reveal this kind of modifications. To study degradation due to hydration-drying processes, the samples were hydrate by submerging them in distilled water for 48 hours (Figure 2), after which they were dried for 6 days at 25°C. The FT-IR absorption spectra were recorded with JASCO FTIR 4100 spectrometer in spectral range 400 - 4000 cm^{-1}, resolution 4 and accumulation 100.

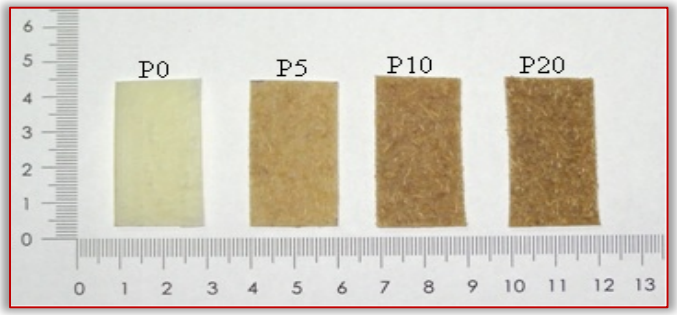

Figure 1 – Composite material samples with different fibers content

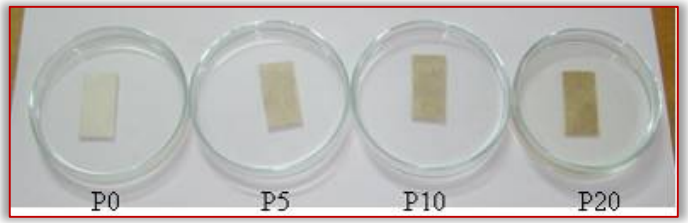

Figure 2 –Samples after 48 h of submerging in distillate water

RESULTS

Table 2 presents the samples mass with uptake water absorbed after 24/48/72 h of hydration by four composite materials samples with different formula presented in Table 1. The sample P0 which has the formula with no fibers (0%) reached the maximum water uptake with higher velocity (in 24 h) and that started to degrade.

The sample P5 which has the formula with lower fibers content (5%) absorbed the highest amount of water (~28% of sample mass) in 48 h and then started to degrade. The lowest quantity of water (~16% of sample mass) was absorbed by the sample P20 (with 20% Miscanthus fiber) in 48 h.

Table 2. The sample mass after hydration and water uptake

Sample	P0	P5	P10	P20
Dry sample [g]	2.17	1.59	1.58	1.55
Distilled water [g]	20	20	20	20
Sample after 24 h	2.63	2.01	1.97	1.79
Sample after 48 h	2.62	2.03	1.98	1.80
Sample after 72 h	2.60	2.02	1.98	1.80
Water uptake [g]	0.46	0.44	0.40	0.25

As can be seen from Figure 3. B, all samples regardless of the fiber content absorb most of the water in the first 3 hours, but the samples reinforced with Miscanthus fibers absorbed the highest amount of water slower than the sample with no fibers (P0).

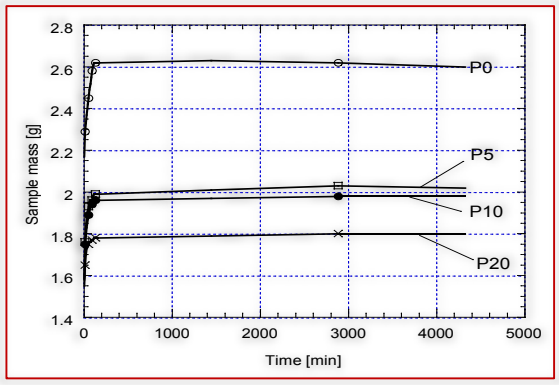

a)

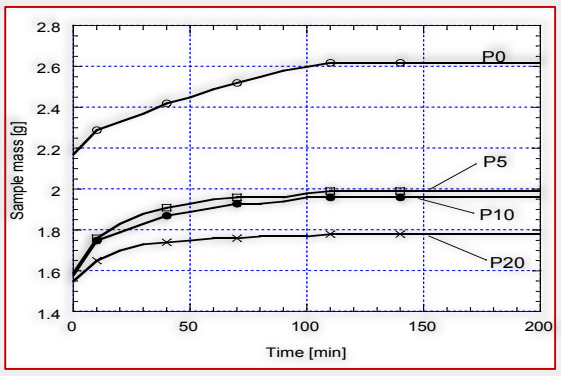

b)

Figure 3 –Sample mass with water uptake after 72 h – a; detailed view for the first 3 hours – b

Also the sample with higher fiber content absorbed the lowest amount of water. The samples reinforced with different ratio of fibers keep their integrity for 72 h but the sample P0 (no fibers reinforcement) start to degrade after 24 h (Figure 3.a) Also the sample with higher fiber content absorbed the lowest amount of water. The samples reinforced with different ratio of fibers keep their integrity for 72 h but the sample P0 (no fibers reinforcement) started to degrade after 24 h (Figure 3.a)

In order to study the samples by FTIR spectroscopy we recorded and compared the IR spectra of samples P0-P20 before and after hydration-drying. Due to the observation regarding water uptake, we analyzed the spectra of samples P0 (no fiber content). P5 (5% fibers absorbed the highest amount o water) and P20 (20% fibers absorbed the lowest amount o water).

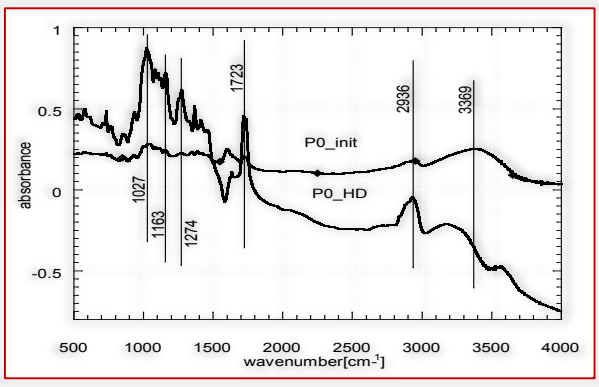

Figure 4 – FT-IR spectra of P0 sample: initial state-P0_init and after hydration-drying

CONCLUSIONS

- Biocomposite materials with improved properties can be obtained by reinforcing a biodegradable matrix with natural fibers.
- Samples were prepared by reactive extrusion with a laboratory twin-screw extruder.
- Raw materials used are: native corn starch, glycerol, PBAT and Miscanthus fibers.
- All the samples regardless of the fiber content absorb most of the water in the first 3 hours.
- Miscanthus fiber content decrease the speed of water uptake.
- The sample with higher fiber content absorbed the lowest amount of water.

Note

This paper is based on the paper presented at ISB-INMA TEH' 2017 International Symposium (Agricultural and Mechanical Engineering), organized by University "POLITEHNICA" of Bucharest – Faculty of Biotechnical Systems Engineering, National Institute of Research-Development for Machines and Installations Designed to Agriculture and Food Industry – INMA Bucharest, Scientific Research and Technological Development in Plant Protection Institute (ICDPP), National Institute for Research and Development for Industrial Ecology – INCD ECOIND, Research and Development Institute for Processing and Marketing of the Horticultural Products "HORTING" and Hydraulics, Pneumatics Research Institute INOE 2000 IHP, University of Agronomic Sciences and Veterinary Medicine of Bucharest (UASVMB) – Faculty of Horticulture and Romanian Society of Horticulture (SRH), in Bucharest, ROMANIA, between 26 – 28 October, 2017.

References

[1] Averous L., Fringant C., and Moro L. (2001). Plasticized starch-cellulose interactions in polysaccharide composites. Polymer vol. 42. pp.6565-6571

[2] Bastioli C. (1998) Biodegradable materials—present situation and future perspectives. Macromol Symp. Vol.130. pp.379-391.

[3] Carvalho A. J. F., Curvelo A. A. S. and Agnelli J. A. M.. (2002). Wood pulp reinforced thermoplastic starch composites. Int. J. Polym. Mater. Vol.51. pp. 647-660

[4] J. Gironès. J. P. López. P. Mutjé. A. J. F. Carvalho. A. A. S. Curvelo and F. Vilaseca. (2012).Natural fiber-reinforced thermoplastic starch composites obtained by melt processing. Key. Eng. Mater. Vol.72. pp.858-863.

[5] Hanselka H. (1998) Fiber composites of raw renewable materials for the ecological lightweight design. Materialwiss Werkst vol.29. pp. 300-311

[6] Hermann A.S., Nickel J., Riedel U. (1998) Construction materials based upon biologically renewable resources. Polym.Degrad.Stab. vol.59. pp.251-261

[7] Yeh J. T. , Tsou C. H. et all.(2010). Compatible and crystallization properties of poly(lactic acid)/poly(butylene adipate-co-terephthalate) blends. J. Appl. Polym. Sci. Vol.116. pp.680-687

ISSN: 2067-3809

Fascicule 1

[January - March]

t o m e XII

[2019]

ACTA Technica CORVINIENSIS
BULLETIN OF ENGINEERING

ISSN: 2067-3809

[1.]Gheorghe VOICU, [1.]Gabriel Alexandru CONSTANTIN, [1.]Elena-Mădălina STEFAN,
[1.]Paula TUDOR, [1.]Mariana Gabriela MUNTEANU, [2.]Tomasz ŻELAZIŃSKI

ASPECTS REGARDING THE ASEPTIC PACKAGING OF FOOD PRODUCTS

[1.]University Politehnica Bucharest. Faculty of Biotechnical Systems Engineering, ROMANIA
[2.]Warsaw University of Life Sciences– SGGW, POLAND

Abstract: Aseptic packaging of food products is necessary to prolong their validity and to preserve their original qualities, but also for obtaining higher quality products. Aseptization must be done both for the product to be packaged and for packaging, but also for the enclosure where packaging takes place (the packing machine). There are many ways to sterilize package, but the sterilization procedure usually begins with the packaging material which must be maintained under sterile conditions until the package is made, but also during filling and closing. For the product to be packaged, the most used sterilization methods are thermal treatments, while for packing machines both thermal treatments are used (with steam and hot air) but also combined treatments (thermal and chemical). For packaging material, the most commonly used sterilization procedure is spraying with hydrogen peroxide or peracetic acid solution.
Keywords: food products, aseptic packaging, sterilization

INTRODUCTION

Aseptic packaging is defined as the filling of a sterile food product intended for marketing in sterile containers, under sterile conditions and closing the containers so that reinfection is prevented (hermetic closure). It is obtained, therefore, high quality products with a high shelf life.

Aseptic packaging involves both sterilization of the product and of the materials and package used. Sterilization of products for aseptic packaging is carried out, in general, by HTST or UHT procedures which allow both the destruction of microorganisms and the inactivation of enzymes *(Turtoi M., 2003; Ramos et al. 2015; Tran et al. 2008; Nema & Ludwig, 2010))*.

Aseptic term implies absence or removal of any unwanted micro-organism from the package, product or other characteristic areas, while the term hermetic is used to indicate mechanical properties corresponding to the exclusion of penetration phenomenon of microorganisms into a package, but also of water vapor or gas in / out of the packaging.

Aseptic packaging is used for many reasons:

- the use of unsuitable packages for sterilization in the package;
- thermal treatments used allow achieving of a high temperature for a relatively short time, thus increasing the efficiency of treatment in comparison to lower temperature but long-term treatments;
- prolonging the shelf life of food products stored at normal temperatures.

At aseptic packaging, the product is transported to the packaging machine in a closed system, presterilized and then aseptically dosed in packages that is formed inside the machine. Filling takes place in the aseptic area of the machine, packages sterilization being performed with sterile air under pressure. The aseptic area of the machine in which is realized the filling is small with few moving elements. This is a very important factor which contributes to the integrity of the entire system. The packages are closed under the liquid level, filling is thus complete and, in this way, the content is completely protected against oxidation and at the same time the package is used with maximum efficiency. For products that require agitation, filling may be incomplete.

MATERIAL AND METHODS – ASEPTIC PACKAGING PRINCIPLES

The food products are altered depending on the speed at which the micro-organisms multiply. Multiplication of micro-organisms occurs rapidly in a warm environment and slows at low temperatures. It results that, when the food product is frozen, micro-organisms cannot multiply at all, being completely destroyed when a very high temperature is applied (*Okawara. 2008*; *Office of Compliance, 2004*).

By controlling and destroying micro-organisms, the food products are kept longer. Sterilization methods used in aseptic processing of food are HTST (high temperature - short time) or UHT (ultra-high temperature).

The HTST process is defined as being sterilization by heating the product at an elevated temperature between a few seconds and a few minutes depending on the temperature value. The UHT process is a thermal sterilization treatment in continuous flow to a temperature that may vary between 130-150°C with a maintenance time of 2-8 seconds. The maximum temperature is used for products with low viscosity, (for example milk) and the minimum value is used for products with high viscosity. Thermal treatment must reach 135°C for a period of one or more seconds (*Ramos et al. 2015; Tran et al. 2008)*.

Milk products and fruit juices must be packaged under aseptic conditions to preserve the microbiological qualities conferred by the thermal treatment applied.

When sterilizing food products through processes HTST or UHT problems with inadequate enzyme inactivation may occur. This is specific especially to vegetal enzymes (ex. peroxidases), namely proteases and bacterial lipases.

It is noteworthy that, bacterial enzymes have a much higher resistance to temperature as compared to spores of *Bacillus stearothermophilu,* which are reference spores in thermal treatment.

Aseptic packaging is used for food products such as:

- whole milk / partially skimmed / dietetic milk pasteurized or sterilized (UHT);
- milk based drinks (milk with flavours, milk with cocoa, milk with chocolate);
- milk enriched with vitamin and mineral salts for children, athletes and future mothers;
- consumer cream, sweet or fermented;
- acid dairy products, such as yoghurt, beaten milk, etc.;
- natural mineral water with flavours or purified water;
- specific beverages for athletes;
- simple or mixed fruit juices;
- beverages based on fruit juice;
- alcoholic beverages;
- cold tea;
- coffee and coffee based drinks with added milk;
- soups, flavoured sauces;
- vegetable oil and oil based products (creams, mayonnaise, liquid margarine, dessert sauces).

Tetra Pack aseptic packaging consists of successive cardboard layers, aluminium foil and polyethylene. This combination provides safety and convenience in the use of the product. Each type of packaging material has its specific function in protecting the food. Combination of cardboard, polyethylene and aluminium foil varies according to the product to be packaged; in all cases, however, the only material that comes in direct contact with the food is polyethylene for food use.

Thus, for a product packaged in Tetra Brik Aseptic, there is the following combination of materials:

- 75% paper from renewable sources that gives firm packages and stability;
- 25% polyethylene to prevent reinfection of the product with micro-organisms, which confers resistance to the aggression of external factors;
- 5% aluminium, which is a barrier to air and light, helping to preserve the taste and nutritional qualities of the food product.

Aseptic packages have different shapes and are accessible to any type of consumer. It is necessary, however, that everything is sterile in the manufacturing process, food products, packaging material, equipment and environment in which packaging is carried out. Aseptic packaging is UHT sterilized before heat-treated food product is introduced, resulting in a food with a life span of over 3 months.

As a method of sterilization, the passage of the packaging material can be used through a hydrogen peroxide bath, in concentration of 30%, heated to 70°C for 5-6 seconds. Hydrogen peroxide is then removed from the packaging by pressing rollers or hot air. The environment in which foods are thermally processed and sealed must be, also, lacking bacteria, which means that packaging machines must be sterile as before and after the packaging process is completed.

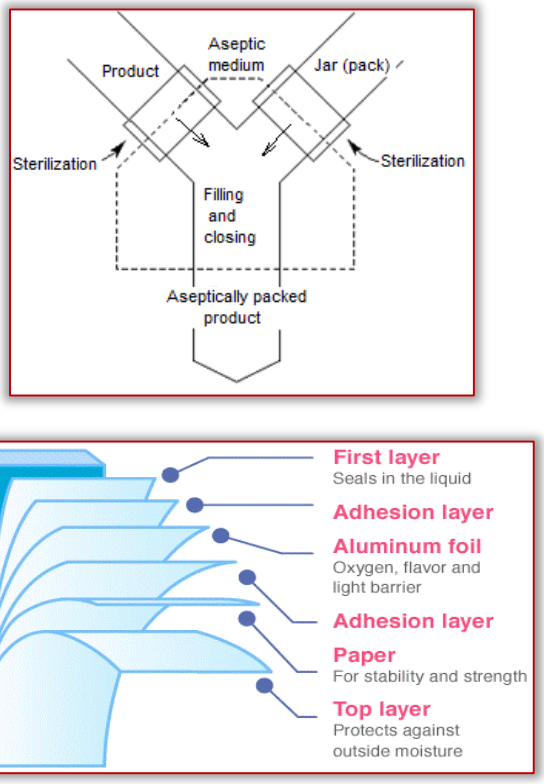

Figure 1 – Principle of aseptic packaging (a) *(Turtoi. 2003)* and complex material for aseptic packaging (b)

RESULTS

— Sterilization of the surface of packaging material in contact with food products

For the sterilization of packaging material used in aseptic packaging three methods can be used, singular or in combination: thermal treatment, chemical treatment and irradiation.

A. Sterilization of the surface of the packaging by thermal treatments

a. Sterilization with saturated steam

The safest thermal agent for sterilization is saturated steam. When using it, the following problems may occur:

- an enclosure is required in which the packaging must be kept under pressure in order to reach sufficiently high temperatures at which sterilization can take place in a few seconds;
- avoid the penetration of fake air into the sterilization space as far as possible otherwise it can influence heat transfer from the steam to the surface of the packaging;
- steam condensation may remain on the surface of the packaging by diluting the food product.

b. Steam sterilization with superheated steam

Overheated steam can be used for sterilization of aluminium metal cans and tin plate.

It has the advantage that it can be used for sterilization of packaging, as well as packaging materials under normal pressure conditions, reaching temperatures of 220-225°C, for

35–45 s depending on the material from which they are made.

c. Hot air sterilization

As with overheated steam, hot air sterilization has the advantage that the necessary temperatures can be obtained at atmospheric pressure. This simplifies the problems of mechanical design of the sterilization system.

This process is used for the sterilization of complex aseptic cartons made from cardboard / aluminium foil / plastic material. At the surface of the material, the temperature 145°C can be reached for 180 s. under the conditions in which the hot air used for sterilization has a temperature of 315°C. Even if the working temperature is high, hot air treatment can only be used for packaging where acidic food is packaged.

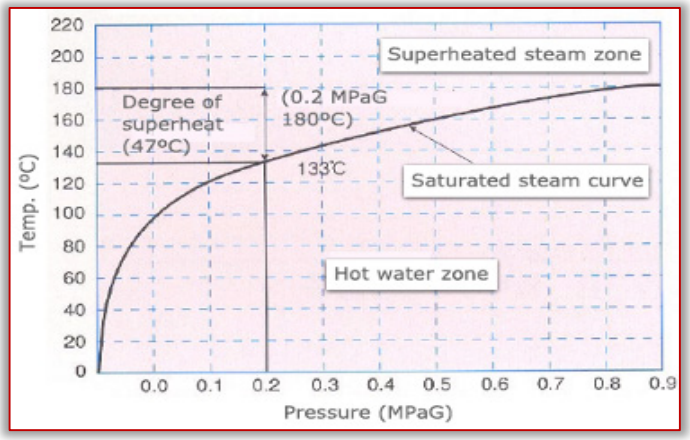

Figure 2 – State Diagram of Water (Pressure - Temperature) *(Okawara. 2008)*

d. Sterilization with hot air and steam

It is a combined process that is used to sterilize packages from stable materials to lower temperatures (about 160°C),, such as the sterilization of the inner surfaces of glasses and caps made from polypropylene, in which case the hot air blows inside the glasses through a nozzle that evenly heats both the bottom and the walls of the glass (*Akers. 2010*).

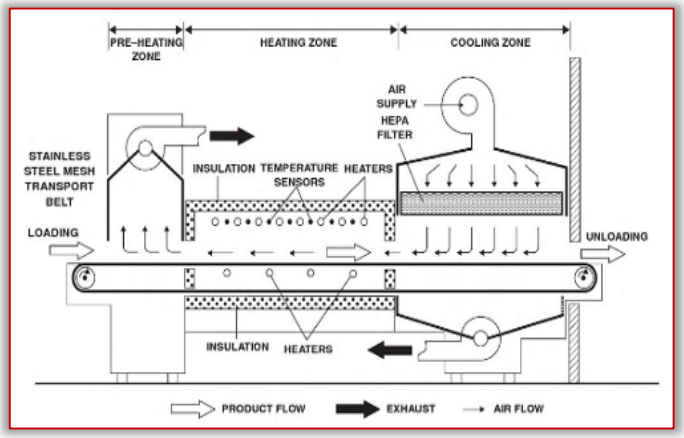

Figure 3 – Dry heat sterilization / depyrogenation tunnel. Schematic *(Akers. 2010)*

e. Sterilization by extrusion in the manufacture of packaging

In the process of extruding preforms for obtaining plastic containers (polyethylene, polyethylene terephthalate, polypropylene etc.) can be reached temperatures of 180-230°C, which are kept for up to 3 minutes so that the packaging is sterilized. Variations in retention time of the granules inside the extruder and uneven temperature distribution cannot guarantee, however, the sterility of all the particles.

For this reason no reduction in microbial spores greater than 3-4 D can be achieved and the packaging thus obtained can only be used for acidic food products with a pH below 4.5. If after the extrusion a sterilization with hydrogen peroxide is made of the packages, they can also be used for products with a pH> 4.5.

B. Sterilization of the packaging surface through chemical treatments

a. Sterilization with hydrogen peroxide

Hydrogen peroxide (H_2O_2) is used for a long time in treating the surface of the packaging to destroy the micro-organisms in combination with the effect of heat, because at the ambient temperature neither the concentrated solutions have a fatal effect. For the short-term destruction of the most resistant spores on the packaging material, the minimum temperature must be at least 80 ° C. and the concentration is at least 30%. There is also the danger that hydrogen peroxide used to sterilize packaging and packaging material will reach the food.

The packaging material is sterilized, mostly, by immersion in hydrogen peroxide with concentration 30-33% or by spraying on the surface of the packaging, followed by hot air drying in both cases.

To reduce the amount of oxygenated water used and increase the efficiency of treatment, we can use a series of combinations of heat and / or radiant or irradiated energy. Thus, for lethal effects of 3-5 D. the hydrogen peroxide concentration drops below 5% for which the possibility of hydrogen peroxide in the packaged product decreases.

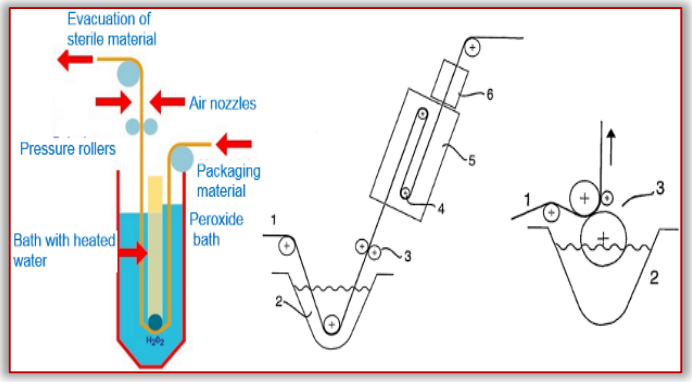

Figure 4 – Sterilization of the packaging material by immersion (chemical treatments)

b. Sterilization with peracetic acid

Peracetic acid has increased destructive efficiency in combination with hydrogen peroxide, even at 20°C. a 1% solution removing over 100 species of resistant spores in just 5 minutes. The duration of sterilization is reduced, in this case about 5 times, and the maximum working temperature is 40°C.

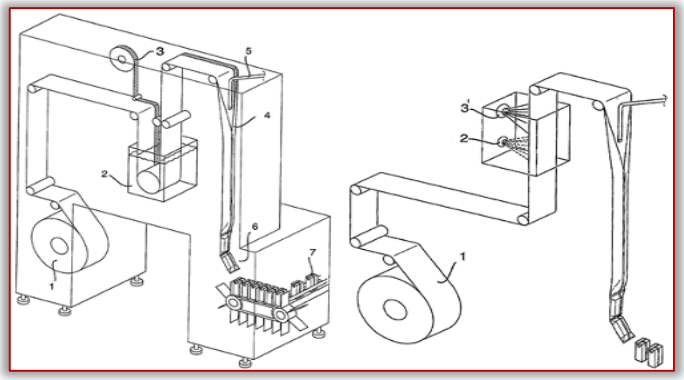

Figure 5 – Chemical treatments applied to packaging materials for forming, filling and closing
1 – roll with packaging material; 2 – immersion area in sterilizing solution; 3 – packaging accessory; 4 – packaging formation; 5 – filling the packaging; 6 – packaged product; 7 – full packaging disposal; 2' – splash area; 3' – hot air drying area

C. Sterilization of the packaging surface by irradiation

Surface of packaging or packaging materials used in aseptic packaging can be sterilized by irradiation with ultraviolet radiation, infrared, ionizing or pulsed light (*Bhavya and Umesh-Hebbar. 2017; Falguera et al. 2011; Reineke et al. 2015; Tanino et al. 2007*).

a. Irradiation with ultraviolet radiation

Ultraviolet radiation with a wavelength of 200-280 nm has the effect of destroying microorganisms, the optimal value being 253.7 nm. To inactivate microorganisms, the energy density of the radiation treatment must be at least 400 J/cm^2 *(Falguera et al. 2011)*.

The conditions for good efficacy of sterilization of ultraviolet radiation surfaces are:

— the irradiated materials to be smooth, UV-resistant and non-adhering dust to avoid the shading effect of surfaces;
— the irradiation intensity should be uniform and suitable for sterilization of the entire package, even if it has a complex form.

The method is used, in general, commercially available in combination with hydrogen peroxide.

b. Irradiation with infrared radiation

Infrared Radiation (IR) is converted into heat by contact with an absorbent surface resulting in an increase of surface temperature. Like UV irradiation, irradiation with IR is used only for smooth and regular surfaces. IR is used to treat the interior of the aluminium caps on which a plastic lacquer was deposited. Due to the possibility of soaking the lake, maximum temperature should be less than 140°C.

c. Irradiation with ionizing radiation

Radiation techniques using gamma radiation of Co60 or Cs139 are used to sterilize the inside of the packaging, usually made of materials that do not withstand sterilization temperatures or cannot be sterilized efficiently by other means, due to the shape they have, such as laminated plastic bags used in bag-in-box aseptic packaging.

They irradiate with at least doses of 25 kGy (2.5 Mrad), which are sufficient to ensure sterility. The bags are enclosed in microorganism impermeable boxes before irradiation. A dose of 20 kGy ensures the sterilization of a 9 mm polyethylene strap infected with approximately 105 spores *Bacillus stearothemophilus*.

d. Treatment with light pulses

Light pulses (PL) are obtained from the "flash" lamp and their effect is sufficient to destroy the microorganisms on the surface of a package. Light pulses have a duration of 10-1–10-6 s. a spectrum of wavelengths of 170–2600 nm, providing an energy density of 0.01–50 J/cm^2. When sterilizing packaging material, the pulse lamp is inserted into the tube that is formed in packs of complex materials type pillow pack to a packaging machine in the formation - filling - closing system *(Bhavya and Umesh-Hebbar. 2017)*.

— Food sterilization

Sterilization is the process by which all living microorganisms are removed or destroyed on the surface of the packaging and inside the food. The sensitivity of micro-organisms must be taken into account in the choice of sterilization methods used in relation with the action of external environmental factors and the physical and chemical qualities of the product subjected to sterilization.

Sterilization is intended to destroy all microorganisms present in the food, both vegetative forms, as well as those sporulated. When sterilizing, some of the microbial and toxins are also destroyed, likewise, some of the enzymes are inactivated (tissues and microbes) (*Barbosa-Canovas and Juliano. 2008*).

In order to be commercially stable the food, it should be heated for a certain time at a pre-determined temperature, depending on the nature of the food (*Cumings. 2004*).

Liquid products less acidic, like milk, are more likely to develop microorganisms and bacteria than strong acid products (for example, fruit juices).

UHT thermal treatment (Ultra High Temperature) or Ultra Pasteurization takes place before packaging, with optimized heat exchangers (*Ramos et al. 2015; Tran et al. 2008)*

Through this controlled process which allows the action of heat for a very short period of time (between 2 and 4 seconds) – followed by an equally rapid cooling, minimal nutritional losses are minimized.

A combined application of electric pulse treatment (PEF) with heat treatment can lead to an accelerated inactivation of endospore in comparison to a pure thermal inactivation in an identical temperature field. This treatment could be used as an alternative treatment technique at ultra-high temperatures of liquid foods with a high pH value, such as milk, vegetable juices or soups (*Reineke et al. 2015)*. The PEF treatment parameters applied resulted in energy inputs of 60.92-257.14 kJ kg^{-1} and thermal loads of 94.61-136.25°C.

Also, food products (in general, vegetables and fruits) can be sterilized with ionizing radiation. Still, conservation with ionizing radiation destroys vitamins, minerals and lack the food from taste and smell. The method has the benefit that the food remain "fresh" for a long time. This treatment

involves exposing the food to a stream of ionizing rays that can be generated by a radioactive source. Foods can be irradiated with gamma or with X ray. Radiation-beam technology uses radioactive substances. ^{60}Co or ^{137}Cs. Here, the processors should however have a great responsibility, because doctors draw attention to the danger of these treatments (*Bogdan et al. 2011*).

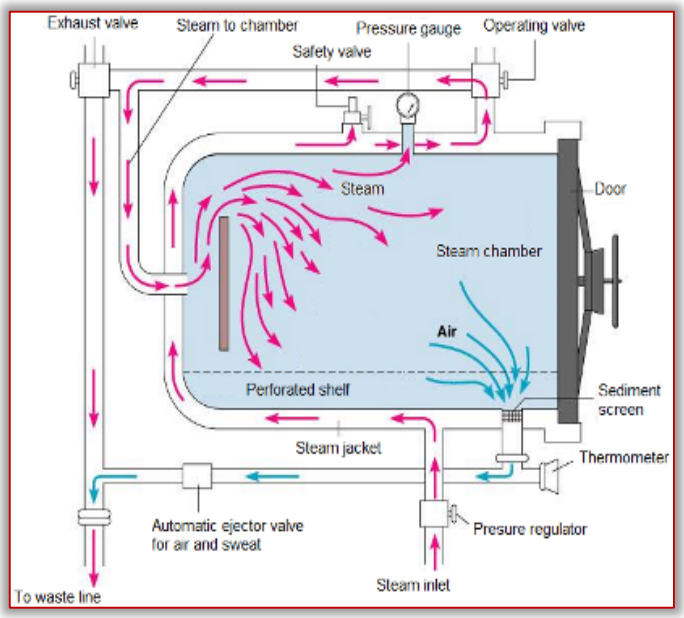

Figure 7 – The principle of sterilizing autoclaves of preserved foods (Cumings. 2004)

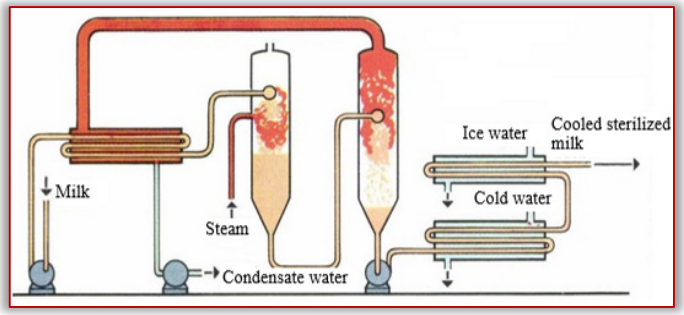

Figure 8 – Sterilization of milk with steam injection

CONCLUSIONS

To ensure high quality food products and preserve its quality for a long time, processors are forced to use aseptic packaging technology lines. It is necessary to sterilize both food product, before filling the packages, as well as sterile packaging, but for aseptic packaging it is also necessary to sterilize the packing machines and the enclosure where filling and closure takes place.

There is an essential difference between hermetic and aseptic. The aseptic term implies the absence or elimination of any unwanted organism in the product, packaging or other specific areas, while the term hermetic is used to indicate mechanical properties corresponding to the exclusion of the microorganism penetration into a packaging and of the gases or water vapours into and out of the packaging. So, it is not sufficient to seal the packing to ensure the quality of packaged products, but also the sterilization of the three elements involved in the packaging process: product, packaging, packaging environment.

Both processors, as well as manufacturers of packaging or packaging materials together with manufacturers of packaging machines must work together to meet the goal of producing aseptic food products with a longer conservation period and improved qualities.

Note

This paper is based on the paper presented at ISB-INMA TEH' 2017 International Symposium (Agricultural and Mechanical Engineering), organized by University "POLITEHNICA" of Bucharest – Faculty of Biotechnical Systems Engineering, National Institute of Research-Development for Machines and Installations Designed to Agriculture and Food Industry – INMA Bucharest, Scientific Research and Technological Development in Plant Protection Institute (ICDPP), National Institute for Research and Development for Industrial Ecology – INCD ECOIND, Research and Development Institute for Processing and Marketing of the Horticultural Products "HORTING" and Hydraulics, Pneumatics Research Institute INOE 2000 IHP, University of Agronomic Sciences and Veterinary Medicine of Bucharest (UASVMB) – Faculty of Horticulture and Romanian Society of Horticulture (SRH), in Bucharest, ROMANIA, between 26 – 28 October, 2017.

References

[1] * * * - (2004). Sterile drug products produced by aseptic processing — Current good manufacturing practice. Office of Compliance in the Center for Drug Evaluation and Research (CDER) in cooperation with the Center for Biologics Evaluation and Research (CBER) and the Office of Regulatory Affairs (ORA). Rockville. USA;

[2] * * * - (2008). Sterilizing technology by superheated steam. Okawara MFG. Co..Ltd.. Japan

[3] Akers M.. (2010). Sterile drug products: Formulation. Packaging, manugacturing and quality. Informa Healthcare. New York.

[4] Barbosa-Cánovas G.V. and Juliano P.. (2008). Food sterilization by combining high pressure and thermal energy. Food Engineering: Integrated Approaches. Springer. XXIV. Hardcover;

[5] Bhavya M.L., Umesh-Hebbar H. (2017). Pulsed light processing of foods for microbial safety. Food Quality and Safety. Vol.1. Iss. 3. pp.187–202.

[6] Bogdan A. et al. (2011). Elements Microbiology. Editura Asclepius Publishing, Bucharest.

[7] Cumings B. Sterilization process: Water steam spray batch retort, batch autoclave sterilizer. Pearson Education. Inc.. 2004

[8] Falguera V., Pagán J., Garza S., Garvín A., Ibarz A. (2011). Ultraviolet processing of liquid food: A review. Part 2: Effects on microorganisms and on food components and properties. Food Research International. Vol.44. pp.1580–1588;

[9] Nema S., Ludwig J. (2010). Pharmaceutical dosage forms: Parenteral medications. Vol.2: Facility design, sterilization and processing. Informa Healthcare. London.

[10] Ramos M., Wurlitzer N., Machado T., Sucupira N., Modesto A. (2015). Validation of an aseptic packaging system of liquid

foods processed by UHT sterilization. Chemical Engineering Transactions. Vol. 44. 6.pg.;
[11] Reineke K., Schottroff F., Meneses N., Knorr D. (2015). Sterilization of liquid foods by pulsed electric fields–an innovative ultra-high temperature process. Frontiers in Microbiology. vol.6. art.400. University of Natural Resources and Life Sciences, Vienna. Austria;
[12] Tanino M., Xilu W., Takashima K., Katsura S. and Mizuno A.. (2007). Sterilization using dielectric barrier discharge at atmospheric pressure. International Journal of Plasma Environmental Science & Technology. Vol.1. No.1. 102-107;
[13] Tran H., Datta N., Lewis M.J., Deeth H.C. (2008). Prediction of some product parameters based on the processing conditions of ultra-high-temperature milk plants. International Dairy Journal 18
[14] Turtoi M. (2003). Principles of aseptic packaging of food products. Bulletin AGIR. no. 3. pp.60-65.

ISSN: 2067-3809

[1.]Gabriela Cristina SIMION, [1.]Mirela Nicoleta DINCĂ, [1.]Georgiana MOICEANU, [1.]Mihai CHITOIU

RENEWABLE ENERGY IN CONTEXT OF SUSTAINABLE DEVELOPMENT

[1.]University Politehnica of Bucharest, Faculty of Biotechnical Systems Engineering, ROMANIA

Abstract: At the basis of the evolution and development of modern human society lies the energy, being one of the input components for most production processes and comfort offered to people. Energy can be analyzed from a safety perspective through the availability of energy resources for the economy, sustainability, the impact of using different energy sources on the environment and competitiveness, at the level of attracting energy sources. The paper explores the analysis of renewable energy resources: biomass, wind, solar energy and its current development at national and European level.
Keywords: renewable energy, biofuels, biomass, wind energy, solar energy, biogas, fermentation

INTRODUCTION

The concept of energy security is in connection with sustainable development by identifying and exploiting alternative energy sources, reducing environmental pollution, upgrading and modernizing existing transport routes. The European Union is increasingly exposed to instability and rising prices on international energy markets, as well as, to the consequences of the fact that hydrocarbon reserves are gradually being mobilized by a small number of holders.

Renewable energy refers to forms of energy obtained through energetic transfer of the resulting energy from natural renewable processes. Therefore, solar energy, wind energy, flow waters energy, that of biological processes and geothermal heat can be taken by humans using different procedures. The types of energy that are not renewable include nuclear energy, as well as, the energy generated through burning of fossil fuels, like oil, charcoal and natural gases. These resources are, evidently, not renewable, as they are found harder each year. From the renewable energy sources we can find-wind energy, solar energy, water energy, biofuels and biogas. All of these forms of resources are been used for generating biofuels, electric current, hot water, etc.

Wind energy is generated through the transfer of wind energy by a wind turbine. Winds form because the Earth is heated unevenly by the energy radiated by the Sun which reaches our planet. This variable warming of the air layers produces different air density zones, which, in turn, creates movement of the air. The kinetic energy of wind can be used by the wind turbines, which are capable of generating electricity. Some wind turbines are capable of producing up to 5 MW of electric energy, even though they require a constant speed of the wind of about 5.5 m/s. or 20 km/h. There are only a few areas on Earth which have those attributes, especially at high altitude and oceanic areas.

The concept of solar energy refers to the energy that is directly produced through transfer of solar energy radiated by the sun. This can be used to generate electric energy or to warm the air inside a building. Even though this type of energy is reusable and easy to produce, the main problem is that the Sun doesn't offer constant energy in any place on Earth.

Not to mention the rotation of the planet, the day-night temperature difference, the solar light can be used for energy only for a short part of every day. Another setback of using this type is that of the cloudy days, when the energy potential drops because of the blocking of the solar light.

Hydro-energy represents the capacity of a system (water) to make energy from the passing from one state to another. In practice, this is the energy produced in hydro stations with the help of the movement of water, caused by the level difference between the accumulation lake and the station.

Biomass represents the renewable resource which is most abundant on our planet. This includes absolutely all the organic matter produced through metabolically processes of the living organisms. Biomass is the first form of energy used by man, once with the discovery of fire.

At the present day, in the European Union, the Renewable Energy Directive sets rules for the EU to achieve its 20% renewables target by 2020. http://ec.europa.eu/energy/en/topics/renewable-energy.

MATERIAL AND METHOD

From the 1990, the UE has put itself in an ambitious plan to become a worldwide leader in the renewable energy domain. For example, the UE disposes at the present day of a capacity to create wind energy the equivalent of 50 coal based factories, to which their costs have been reduced to half in the past 15 years. The renewable energy market of the UE has an annual business number if 15 billion EURO (half of the entire worldwide market), an average of 300000 workers and is an important exporter. At the present day, the renewable energy is beginning to compete, from the cost point of view, with fossil fuels.

In 2001, EU decided that the electricity percent produced from renewable resources should reach 21% by 2010. In 2003, it was decided that at least 5.75% of the entire quantity of gas and diesel should be made from bio-fuels by 2010. A few countries record a rapid rise in usage of renewable energy through support national policies. But

according to the actual times< EU will be around 1-2 percent below the fixed targets.

For the EU to fulfill its long term objectives of climatic changes and reduce its dependency for the import of fossil fuels, it must reach and even top those objectives. The renewable energy occupies the third place for producing electricity and still has risen potential, with all the advantages for the environment.

An efficient measure for preventing climatic changes represents an urgency and the EU must continue to keep control as a leader through examples and act for extending as much as 92possible the international action. Europe must be ambitious and act in an integrate way and promote the Lisbon objectives.

The EU made already its first steps in the direction of limiting the economic rise from the energy usage increment. The EU initiative combined legislative initiatives and energy efficiency programs which encourage competition and the efficient usage of renewable energy. The EU engagement of preventing climatic changes is a long term one.

For reducing the rise of global temperature to a maximum of 2 degrees over the pre-industrial levels, the gas emissions with greenhouse effect should reach the maximum value until 2025 and then they should be reduced by at least 15%, preferably at most 50% comparative to those levels from 1990. This challenge means that Europe should react now, especially in the fields of energetic efficiency and renewable energy.

Aside from the prevention of climatic changes, measures regarding renewable resources and the energetic efficiency will contribute to the rising of this energy usage and lowering the UE dependency to average energy. Also this policy will create numerous workplaces of good quality in Europe and will maintain the no.1 place as a leader in technology, for a worldwide sector in full development.

From this perspective, the UE plan of Emission Commercialization creates a flexible frame from the point of view of costs for a cleaner production of energy. This plan is also the nucleus for the worldwide market of CO2.

The maximum potential will be exploited only through a long term engagement for development and installation of renewable energy.

Table 1. A synthetic analysis of the resources and their potential on the market in Romania

Technology	Level of resource existence	Market Potential
Wind	2-3	2
Solar Photovoltaic	2-3	1
Solar Thermal	2-3	2-3
Micro-hydro	3	3
Biomass	3	3
Geothermal	3	2-3
Energy valued waste	2	2

In Romania there is a technical and scientifically experience important in the domain of renewable resources, but that remained at the theory levels. In present the market conditions do not favor their direct competition. The closest to a commercial use are applications that use biomass, micro-hydro, geothermal resources.

In the present day, the electric energy that comes from renewable sources is 42.29%. Therefore, hydro is 29.88%, wind is 11.07%, solar photovoltaic is 1.18% and biomass is 0.16% [www.agerpres.ro/economie/2017/04/19].

Both the energy law and the energy efficiency law stimulate the development of renewable energy and the ANRE has in plan the completion of a specific program.

RESULTS

Renewable energy resources that compete directly with fossil fuel are biomass and wastes from agriculture.

Since biomass is the only carbon-based renewable fuel, its application becomes more and more important for climate protection. Among the thermochemical conversion technologies (i.e.. combustion, gasification and pyrolysis), combustion is the only proven technology for heat and power production. Biomass combustion systems are available in the size range from a few kW up to more than 100 MW. The efficiency for heat production is considerably high and heat from biomass is economically feasible[14]

Biomass represents the renewable resource which is most abundant on our planet. This includes absolutely all the organic matter produced through metabolically processes of the living organisms. Biomass is the first form of energy used by man, once with the discovery of fire.

Biomass has a worldwide interest as a renewable energy resource that can make a big contribution to rural development and to the implementation of sustainable energy supply systems at local, regional and global level. The current primary energy conversion technologies contained in biomass are the following: direct burning, gasification, pyrolysis, biological fermentation.

Energy security and climate change mitigation are core elements in current European energy policy. The EU countries are mandated to meet by 2020 a target of 20% renewable resources in the energy supply and 10% renewable resources in energy in the transport sector [4]. The latter corresponds to a replacement of 50 billion liters of fossil transportation fuels. The Energy Strategy 2020 [3] of the European Commission calls for increased use of renewable resources in the energy system and the European Council has presented a long term target for the EU and other industrialized countries of 80 to 95% cuts in greenhouse gas emissions by 2050. A cornerstone in renewable energy projections of the European Union is biomass, which is expected to account for 56% of the renewable energy supply in the EU by 2020

When biomass is used as a fuel, instead of fossil, the same amount of carbon dioxide is released into the atmosphere. If the use of biomass is to produce energy, it is considered a neutral carbon fuel, due to the drastic reduction of gas emissions into the atmosphere by producing methane instead of CO2. Carbon represents about 50% of the dry

vegetal mass and is part of the atmospheric carbon cycle. Biomass fixes CO2 from the atmosphere during growth after carbon dioxide is released as a mixture of carbon dioxide (CO2) and methane (CH4), depending on the last use of the plant material.[1]

Almost all the resulting agricultural residues can be used as resource for renewable energy, but considering the possibilities of collection and baling for transportation, only the following types of agricultural residues are considered:

» straw
» maize stalks
» corn hammers
» sunflower – strains, capite and seed husks
» vineyards
» flax and hemp pocketing

In the category of "straw" were included the residues resulting from the harvesting and treatment of the main crops of grain cereals – wheat, barley, rye, oats. It is obvious that depending on the species and the variety, the weight of the straw in relation to the weight of the grain varies widely. Under these conditions it was considered that an average of straw weight is about 90% of the grain weight. [4]

Corn stalks are the plant, as harvested less. The weight of the maize strains is very varied depending on the maize variety and the humidity at harvest. Corn ham is the support of corn grains in the pot. The weight of corn ham is on average equal to the weight of the grain. The flakes and hemp are the remains of the plant stems after the fibers have been extracted. The weight of the cases is approx. 50% of the weight of the plants. [20]

Table 2. The biomass potential by sorts, regions

Region	Forestry biomass thousand tones/year	Wood waste thousand tones/year	Agricultural biomass thousand tones/year	Biogas ml.mc/year	Urban waste thousand tones/year	TOTAL TJ
Dobrogea	54	19	844	71	182	29,897
	451	269	13,422	1,477	910	
Moldova	166	58	2,332	118	474	81,357
	1,728	802	37,071	2,462	2,370	
Carpatic Region	1,873	583	1,101	59	328	65,415
	19,552	8,049	17,506	1,231	1,640	
Transilvania	835	252	815	141	548	43,757
	8,721	3,482	12,956	2,954	2,740	
Vest Plain	347	116	1,557	212	365	60,906
	3,622	1,603	24,761	4,432	1,825	
Subcarpatic Region	1,248	388	2,569	177	1,314	110,198
	13,034	5,366	40,849	3,693	6,570	
South Plain	204	62	3,419	400	1,350	126,639
	2,133	861	54,370	8,371	6,750	
TOTAL	4,727	1,478	12,637	1,178	4,561	518,439
	49,241	20,432	20,093	24,620	22,805	

Starting from the above, the total biomass production used for fuel is:

» straw – 3,357 thousand t / a
» maize stalks and corn hammers – 17,286 thousand tons / year
» sunflower – 7,350 thousand t / a
» vineyards – 255 thousand tons / year
» flax and hemp pocket – 5,590 thousand t / a

The resulting agricultural biomass traditionally has three possible uses, namely:

» re-use in agriculture (animal husbandry)
» raw materials in the pulp and paper industry
» fuel

What is not consumed by one of these forms is burnt in the field, embedded in soil or stored for biological degradation. In areas with a lot of arable land, biomass can play an essential role in energy production.

Table 3. Energy potential of biomass

Parameter	UM	Technical	Economical
a) Vegetal biomass			
Thermal/ electrical energy	TJ/year	471,000	289,500
	Thousant tep/year	11,249	6,915
b) Biogas			
Thermal/ electrical energy	TJ/year	24,600	14,800
	Thousand tep/year	587	353
c) Urban waste			
Thermal/ electrical energy	TJ/year	22,800	13,700
	Thousand tep/year	544	327
TOTAL	TJ/year	518,400	318,000
	Thousand tep/year	12,382	7,595

CONCLUSIONS

From the 1990, the EU has put itself in an ambitious plan to become a worldwide leader in the renewable energy domain. For example, the EU disposes at the present day of a capacity to create wind energy the equivalent of 50 coal based factories, to which their costs have been reduced to half in the past 15 years. The renewable energy market of the UE has an annual business number if 15 billion EURO (half of the entire worldwide market), an average of 300,000 workers and is an important exporter. At the present day the renewable energy is beginning to compete, from the cost point of view, with fossil fuels.

In 2001, EU decided that the electricity percent produced from renewable resources should reach 21% by 2020. In 2003, it was decided that at least 5.75 % of the entire quantity of gas and diesel should be made from bio-fuels by 2010. A few countries record a rapid rise in usage of renewable energy through support national policies. But according to the actual times, EU will be around 1-2 percent below the fixed targets. For the EU to fulfill its long term objectives of climatic changes and reduce its dependency for the import of fossil fuels, it must reach and even top those objectives. The renewable energy occupies the third place for producing electricity and

still has rise potential, with all the advantages for the environment.

For the potential to be reached, the web of policies must support and stimulate competitiveness of such sources of energy. Some internal sources of low CO2 emission are already available, others, such as wind energy, wave energy still require support for entering the market.

The maximum potential will be exploited only through a long term engagement for development and installation of renewable energy.

Note

This paper is based on the paper presented at ISB-INMA TEH' 2017 International Symposium (Agricultural and Mechanical Engineering), organized by University "POLITEHNICA" of Bucharest – Faculty of Biotechnical Systems Engineering, National Institute of Research-Development for Machines and Installations Designed to Agriculture and Food Industry – INMA Bucharest, Scientific Research and Technological Development in Plant Protection Institute (ICDPP), National Institute for Research and Development for Industrial Ecology – INCD ECOIND, Research and Development Institute for Processing and Marketing of the Horticultural Products "HORTING" and Hydraulics, Pneumatics Research Institute INOE 2000 IHP, University of Agronomic Sciences and Veterinary Medicine of Bucharest (UASVMB) – Faculty of Horticulture and Romanian Society of Horticulture (SRH), in Bucharest, ROMANIA, between 26 – 28 October, 2017.

References

[1] www.gazetadeagricultura.info/.2011Biomass Renewable energy resource Sursa de energie regenerabila;

[2] Commission E: Energy (2010).2020 A strategy for competitive, sustainable and secure energy. European Commission. Brussels. BE;

[3] Bentsen N.S., Felby C. (2012). Biomass for energy in the European Union- A review of bioenergy resources assessments. Biotechnology for Biofuels;

[4] Ros V., Chira T., Balc G., Fechete L. (2004). Method for evalation of energetic potential in a farm Metoda de evaluare a potentialului energetic dintr-o ferma agricola. vol.5. ISSN 1312-5443

[5] http://www.minind.ro/domenii_sectoare/energie/studii/potential_energetic.pdf (2006) Studiul privind evaluarea potentialului energetic actual al surselor regenerabile de energie in Romania(solar. vant. biomasa. microhidro. geotermie). identificarea celor mai bune locatii pentru dezvoltarea investitiilor in producerea de energie electrica neconventionala. ICEMENERG SA. Bucuresti;

[6] http://leg-armonizata.minind.ro/leg_armonizata/energie/Directiva_2009_28_CE.pdf(2009) Directiva 2009/28/CE privind promovarea utilizarii energiei din sursele regenerabile. Jurnalul oficial al Uniunii Europene. L140/6;

[7] Chum H.L,. Overend R.P.(2001). Biomass and renewable fuels. Fuel Processing Technology 71 2001. 187–195;

[8] Hovelius K. (1997)- Eneregy and analysis of biomass production/Energia si analiza productiei de biomasa. Raport 222. Suedia. Universitatea de stiinte agricole. Uppsala. ISSN 0283-0086;

[9] http://www.renascc.eu/documente/sa33134ro_1282ro.pdf(2011) Treaty regarding the EU functioning. European Directive2009/28/CE regarding the promoting of renewable sources energy /Tratatul privind funcționarea Uniunii Europene Directiva 2009/28/CE privind promovarea utilizării energiei din surse regenerabile European Comission Bruxelles;

[10] Bent Sørensen.(2004) Renewable Energy. Its physics, engineering, use, environmental impacts, economy and planning aspects. Third Edition. Elsevier Science;

[11] EUROPEAN COMMISSION - EUR 21350 (2005). Biomass - Green energy for Europe. Luxembourg: Office for Official Publications of the European Communities. 2005;

[12] Demirbas A.. Combustion characteristics of different biomass fuels.(2004) Progress in Energy and Combustion Science 30 (2004) 219–230;

[13] Van Loo S. and J. Koppejan (2002) Handbook of Biomass Combustion and Co-firing. Twente University Press. 2002;

[14] Thomas Nussbaumer (2003) Combustion and Co-combustion of Biomass: Fundamentals. Technologies and Primary Measures for Emission Reduction Energy & Fuels 2003. 17. 1510-1521.

ISSN: 2067-3809

[1.]Loganathan PARASURAMAN, [2.]Deepa KRISHNAMURTHY

PRANDTL BOUNDARY LAYER FLOW OF A CASSON NANOFLUID PAST A PERMEABLE VERTICAL PLATE

[1-2.]Department of Mathematics, College of Engineering, Guindy, Anna University, Chennai-25, Tamilnadu, INDIA

Abstract: This paper demonstrates the non-Newtonian flow behavior of a nanofluid under the permeability of a porous medium. In particular, this investigation focused on the flow properties of Silica (SiO_2) nanofluid subject to the buoyancy driven Casson fluid flow. The volume fraction of nanoparticles influences the velocity and temperature field. The higher percentage of volume fraction thickens the thermal boundary layer which in turn reduces the growth of velocity boundary layer. The effects of rheological parameters such as Prandtl number, thermal Grashof number, permeability, Casson parameter, Nusselt number and skin friction coefficient has been explored abundantly. The quantitative comparison of this study with the already existing results produces an excellent correlation.

Keywords: Casson fluid; Moving vertical plate; Silica; Nanofluid; Porous medium

INTRODUCTION

Non-Newtonian fluids are processed under laminar flow conditions owing to their high consistency. The wide ranges of applications are found in the non-Newtonian fluids which unveil a pseudoplastic flow. In other words, the fluid exhibits a decrease in viscosity with increasing rate of shear. The paint, printing inks and disperse systems are the most renowned examples of this kind of flow behavior. However, on account of poor flow at low shear rate, the pseudoplasticity is objectionable in some way [Cross (1965)].

The yield stress of a non-Newtonian fluid involves in the rheological characteristics. A substance driven by a yield stress and generating a nonlinear flow curve is often called as the yield-pseudo plastic material. This type of material exhibits infinite apparent viscosity with zero shear rate. At very low apparent viscosity, the rate of shear drastically achieves an infinite value. This viscoplastic behavior associated with the Casson fluid model. Consequently, Casson fluid is described as a non-Newtonian shear thinning fluid with a yield stress. Also, this model has been used for expounding the shear stress and shear rate behaviour of blood, yoghurt, tomato puree, molten chocolate, many food stuffs and biological materials [Chhabra and Richarson (1999)].

The Casson flow model was invented by Casson. The constitutive equation which is formulated for this model is used to effectively illustrate the flow curves for suspension of pigments in printing inks and silicon suspensions. By virtue of its possible applications, many researchers made their focus of attention on this flow model. Hussanan et al. (2014) derived the exact solution of Newtonian heating Casson fluid over an oscillating vertical plate. The notable conclusion of this article is that an increase in the value of Prandtl number and Casson fluid parameter regulate the flow separation. Venkatesan et al. (2014) developed a numerical modelling of Casson fluid through a mild bell shaped stenosis at lower shear rates. It was analyzed that the larger blood vessel with the elevated rate of shear demonstrates the Newtonian characteristics of the fluid; whereas the smaller diameter arteries uplift the apparent viscosity and betraying the non-Newtonian characteristics.

Over the years, nanofluids drew attention of many scientists. Choi initiated the term called nanofluid; accordingly nano technology based heat transfer was evolved [Das et al. (2007), Choi et al. (1995)]. Silica nanofluids have enormous findings in the literature. Generally, this kind of fluid serves as a flow agent in powdered foods and pharmaceutical products. Hydrated silica can be utilized as a rough material in removal of plaques. Theoretically, Blasius and Sakiadis problem for nanofluids was explained by Ahmad et al. (2011). Das et al. (2015) examined the hall current and thermal radiation effects on a water based nanofluid containing Al_2O_3, Cu and Ag nanoparticles under rotating frame of reference over an oscillating porous plate. Noghrehabadi et al. (2011) and Noghrehabadi et al. (2012) inspected the heat transfer enhancement in SiO_2 water nanofluid under the variation of volume fraction and compared the results with Ag water nanofluid over a stretching sheet.

According to Shi et al. (2017), the thermal resistance of miniature heat pipe radiators was lowered for the 0.6% volume fraction of SiO_2 water nanofluid and this nanofluid has strengthen the performance of radiators comparing to the results of DI (Deionized) water. Ullah et al. (2016) studied the effects of chemical reaction and thermal radiation on MHD free convective Casson nanofluid flow past a nonlinearly stretching sheet saturated in a porous medium with slip and convective boundary conditions. Casson nanofluid flow through a cone which is rotated and fixed in a rotating frame filled with ferrous nanoparticles was numerically studied by Raju and Sandeep (2017). Haq et al. (2014) concentrated on the MHD effects with suction/injection of Casson nanofluid past a shrinking sheet and the numerical results were

discussed for the flow properties. Meybodi et al. (2015) centralized their priority to viscosity. Least squares support vector machines method is adopted to predict the viscosity in this analyzes. Muthucumaraswamy et al. (2011) found the exact solution of incompressible viscous fluid flow over an oscillating plate with thermal radiation and chemical reaction. Rayleigh's problem described the fluid flow along a moving horizontal plate. On account of practical applications, convective flow over an impulsively started vertical plate has been studied in this article. The most prominent distinctive aspect distinctive aspect of this work is the non-Newtonian flow configuration that has been dealt with the SiO_2 -water nanofluid past a permeable impulsively started semi-infinite vertical plate. The complexities pertaining to the non-linearity of the rheological characteristics are represented graphically. To assure the reliability and accuracy of the solution, the investigation is directed towards the comparison with the results of Soundalgekar (1977). Certainly, the correlation discloses an appreciable and extremely good match.

MATHEMATICAL ANALYSIS

Consider a convective Casson fluid flow over a nanofluid past a permeable moving semi-infinite vertical plate. Assume that the plate is at rest initially. Hence, it is evident that the fluid temperature remains ambient temperature. The plate suddenly starts to accelerate vertically upwards with a constant speed u_0 at $t^* > 0$. This impulsive motion results in the velocity and temperature. At this time level the temperature of the plate raised to T'_w $(> T'_\infty)$. Eventually, the fluid encounters the heat transfer near wall. For the case that the flow is far away from the plate, the velocity and temperature gradually drops to zero. The fluid motion is taken along x direction vertically and the y direction is normal to the plate. The velocities u and v are described along vertical and horizontal directions respectively. The schematic representation is shown in figure 1.

The effect of viscous dissipation is negligible in the energy balance equation. The expression for the flow configuration of Casson fluid can be defined by a constitutive relation [Makanda et al. (2015), Arthur et al. (2015), Raju et al. (2016) and Ullah et al. (2016)].

$$\tau_{ij} = \begin{cases} 2\left(\mu_B + \frac{P_y}{\sqrt{2\pi}}\right)e_{ij}, & \pi > \pi_c \\ 2\left(\mu_B + \frac{P_y}{\sqrt{2\pi_c}}\right)e_{ij}, & \pi \le \pi_c \end{cases}$$

Here, $\pi = e_{ij}e_{ij}$ and e_{ij} is the $(i, j)^{th}$ component of the shear rate. π_c is the critical value of π concerned with the model. μ_B is the plastic dynamic viscosity and P_y is the yield stress of the fluid.

The governing boundary layer equations of the mathematical model that encompasses the above assumptions, constitutive equation, Boussinesq approximation and the flow equations mentioned in [Tiwari et al. (2007)] can be expressed as

$$\frac{\partial u}{\partial t^*} = \frac{\mu_{nf}}{\rho_{nf}}\left(1+\frac{1}{\beta}\right)\frac{\partial^2 u}{\partial y^2} + g\frac{(\rho\beta^*)_{nf}}{\rho_{nf}}(T' - T'_\infty) - \frac{\mu_{nf}}{k\rho_{nf}}u \quad (1)$$

$$\frac{\partial T'}{\partial t^*} = \frac{k_{nf}}{(\rho c_p)_{nf}}\frac{\partial^2 T'}{\partial y^2} \quad (2)$$

Suitable initial and boundary conditions of the problem are

$$\begin{aligned} &t^* \le 0,\ u = 0, T' = T'_\infty \quad \text{for all } y \\ &t^* > 0,\ u = u_0, T' = T'_w \quad \text{for } y = 0 \\ &u \to 0, T' \to T'_\infty \quad \text{as } y \to \infty \end{aligned} \quad (3)$$

where β^* is the thermal expansion coefficient, μ_{nf} and ρ_{nf} are the dynamic viscosity and density of nanofluid respectively.

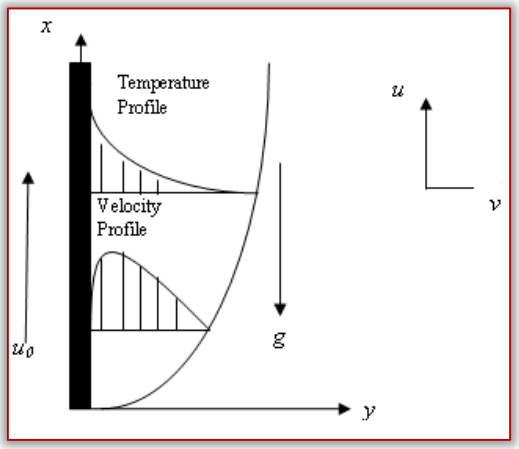

Figure 1. Schematic representation of the flow model

The expressions for the nanofluid parameters are defined as [Ahmad et al. (2011)]

$$\mu_{nf} = \frac{\mu_f}{(1-\phi)^{2.5}},\ \rho_{nf} = (1-\phi)\rho_f + \phi\rho_s,$$
$$(\rho c_p)_{nf} = (1-\phi)(\rho c_p)_f + \phi(\rho c_p)_s,$$
$$(\rho\beta^*)_{nf} = (1-\phi)(\rho\beta^*)_f + \phi(\rho\beta^*)_s$$

Effective thermal conductivity is described by [Oztop et al. (2008), Hamilton and Crosser (1962)]

$$\frac{k_{nf}}{k_f} = \frac{(k_s + 2k_f) - 2\phi(k_f - k_s)}{(k_s + 2k_f) + \phi(k_f - k_s)}$$

Here ϕ is the volume fraction coefficient, ρ_s is the nanoparticle density, ρ_f is the density of the base fluid, $(c_p)_f$ and $(c_p)_s$ are respectively the heat capacity of base fluid and nanoparticle. The thermophysical properties of various materials at 25^{0}C are taken from [Hussein et al. (2013)] and the nanoparticles considered in this investigation are spherical shaped nanoparticles. Non dimensional quantities employed on the coupled partial differential equations (1), (2) and (3) are taken as

$$U = \frac{u}{u_0},\ Y = \frac{yu_0}{\upsilon_f},\ t = \frac{t^* u_0^2}{\upsilon_f},\ T = \frac{T' - T'_\infty}{T'_w - T'_\infty}$$

$$Gr = \frac{\upsilon_f g\beta_f^*(T_w' - T_\infty')}{u_0^3},\ Pr = \frac{\upsilon_f(\rho c_p)_f}{k_f},\ K = \frac{ku_0^2}{\upsilon_f^2}$$

where U, Y, t and T are the dimensionless velocity, horizontal direction, time and temperature respectively. Gr is the thermal Grashof number, Pr is the Prandtl number, K is the permeability parameter and υ_f is the kinematic viscosity of the base fluid.

Non dimensional form of (1), (2) and (3) are

$$\frac{\partial U}{\partial t} = \left(1+\frac{1}{\beta}\right)B_1\frac{\partial^2 U}{\partial Y^2} - B_1\frac{U}{K} + B_2 Gr\,T \qquad (4)$$

$$\frac{\partial T}{\partial t} = \frac{1}{Pr}B_3\frac{\partial^2 T}{\partial Y^2} \qquad (5)$$

Appropriate initial and boundary conditions are

$$\begin{aligned} &t \le 0,\ U = 0, T = 0 \quad \text{for all } Y \\ &t > 0,\ U = 1, T = 1 \quad \text{for } Y = 0 \\ &U \to 0,\ T \to 0 \text{ as } Y \to \infty \end{aligned} \qquad (6)$$

Solutions of the equations (4) and (5) together with the initial and boundary conditions (6) are acquired by Laplace transform technique. The expressions which explicate the flow characteristics are obtained as follows.

— Temperature distribution

$$T(Y,t) = \text{erfc}\left[\frac{Y}{2\sqrt{B_3}}\sqrt{\frac{Pr}{t}}\right]$$

— Velocity distribution

Case (i):

If K is finite

$$U(Y,t) = \frac{Gr\,B_2}{B_5}\left\{\begin{array}{l} \frac{e^{B_6 t}}{2}\left[\begin{array}{l} F_1(Y,t)+F_2(Y,t) \\ -F_3(Y,t)-F_4(Y,t)\end{array}\right] \\ -\frac{1}{2}\left[F_5(Y,t)+F_6(Y,t)\right] \\ +\text{erfc}\left(\frac{\sqrt{B_4}\,Y}{2\sqrt{t}}\right)\end{array}\right\}$$

$$+\frac{1}{2}\left[F_5(Y,t)+F_6(Y,t)\right]$$

where $F_1(Y,t) = e^{-y\sqrt{\frac{B_5+B_6}{aB_1}}}\ \text{erfc}\left(\frac{Y}{2\sqrt{aB_1 t}} - \sqrt{(B_5+B_6)t}\right)$

$$F_2(Y,t) = e^{y\sqrt{\frac{B_5+B_6}{aB_1}}}\ \text{erfc}\left(\frac{Y}{2\sqrt{aB_1 t}} + \sqrt{(B_5+B_6)t}\right)$$

$$F_3(Y,t) = e^{-y\sqrt{B_4 B_6}}\ \text{erfc}\left(\frac{\sqrt{B_4}\,Y}{2\sqrt{t}} - \sqrt{B_6 t}\right)$$

$$F_4(Y,t) = e^{y\sqrt{B_4 B_6}}\ \text{erfc}\left(\frac{\sqrt{B_4}\,Y}{2\sqrt{t}} + \sqrt{B_6 t}\right)$$

$$F_5(Y,t) = e^{-y\sqrt{\frac{B_5}{aB_1}}}\ \text{erfc}\left(\frac{Y}{2\sqrt{aB_1 t}} - \sqrt{B_5 t}\right)$$

$$F_6(Y,t) = e^{y\sqrt{\frac{B_5}{aB_1}}}\ \text{erfc}\left(\frac{Y}{2\sqrt{aB_1 t}} + \sqrt{B_5 t}\right)$$

Case (ii):

As $K \to \infty$, the permeability becomes infinitely large which is the case that there is no porous medium.

$$U(Y,t) = \text{erfc}\left(\frac{Y}{2\sqrt{aB_1 t}}\right)$$

$$+\frac{Gr\,B_2 t}{(aB_1B_4 - 1)}\left(\begin{array}{l} \text{erfc}\left(\frac{Y}{2\sqrt{aB_1 t}}\right) - \frac{Y}{\sqrt{\pi aB_1 t}}e^{-\frac{Y^2}{4aB_1 t}} \\ +\frac{Y^2}{2aB_1 t}\text{erfc}\left(\frac{Y}{2\sqrt{aB_1 t}}\right) \\ -\text{erfc}\left(\frac{Y\sqrt{B_4}}{2\sqrt{aB_1 t}}\right) \\ +\frac{Y\sqrt{B_4}}{\sqrt{\pi aB_1 t}}e^{-\frac{Y^2 B_4}{4B_1 t}} \\ -\frac{Y^2 B_4}{2aB_1 t}\text{erfc}\left(\frac{Y\sqrt{B_4}}{2\sqrt{aB_1 t}}\right)\end{array}\right)$$

where

$$B_1 = \frac{1}{(1-\phi)^{2.5}\left((1-\phi)+\phi\left(\frac{\rho_s}{\rho_f}\right)\right)},\ B_2 = \frac{(1-\phi)+\phi\left(\frac{(\rho\beta^*)_s}{(\rho\beta^*)_f}\right)}{(1-\phi)+\phi\left(\frac{\rho_s}{\rho_f}\right)},$$

$$B_3 = \frac{k_{nf}}{k_f\left((1-\phi)+\phi\left(\frac{(\rho C_p)_s}{(\rho C_p)_f}\right)\right)}$$

$$B_4 = \frac{Pr}{B_3},\ B_5 = \frac{B_1}{K},\ B_6 = \frac{B_5}{aB_1B_4 - 1},\ a = 1+\frac{1}{\beta}$$

Heat transfer can be analysed from the Nusselt number expression with the various values of Pr.

$$Nu = \frac{k_{nf}}{k_f}\sqrt{\frac{Pr}{\pi B_3 t}}$$

Skin friction coefficient is given by

$$C_f = -\frac{1}{(1-\phi)^{2.5}}\left(1+\frac{1}{\beta}\right)\left.\frac{\partial U}{\partial Y}\right|_{Y=0}$$

RESULTS AND DISCUSSION

To establish the validation of the current results, an extensive comparison has been done with the solution of Soundalgekar (1977) for $t = 0.2, Pr = 0.71, Gr = 5\ \&\ 10, K \to \infty,\ \beta \to \infty,\ \phi = 0$ and $\eta = \frac{Y}{2\sqrt{t}}$. The exact solution obtained in this study manifests the wonderful match which is illustrated in figure 2.

Figure 3 demonstrates the effects of K, t, Pr and Gr on the velocity of SiO_2 nanoparticles with the fixed volume fraction $\phi = 0.02$. The rise in the permeability leads to the increase in velocity. Physically, this is due to the bulk behaviour of the fluid which is strongly depending on the porous medium structure. Velocity is uplifted by the larger time level due to the impulsive motion of the plate with constant velocity. The higher values of Prandtl numer exhibit decrease in the velocity boundary layer as a result of resistance in the fluid flow caused by the viscosity. The greater external cooling of the plate improves the flow speed.

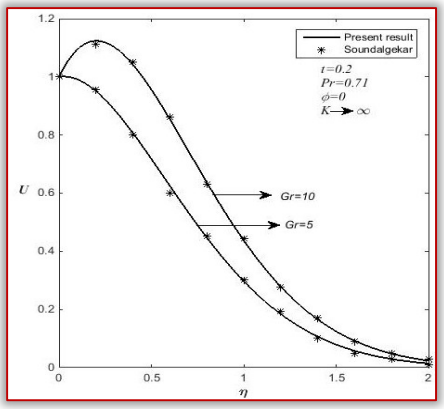

Figure 2. Comparison of velocity profiles with the results of Soundalgekar (1977)

Figure 3. Influence of $K, t, \Pr, Gr$ and β on velocity distribution of SiO_2

As mentioned previously, the Casson parameter depends on the viscosity and yield stress of the fluid. By lowering the yield stress, the rise in the values of Casson parameter achieved. This fluid flow resembles the Newtonian fluid flow in default of the yield stress. From figure 3 and 4 the complexities occur in the velocity distribution as a result of elevation in β has been illustrated. Chhabra and Richardson (1977) pointed out that the physical properties of non-Newtonian fluids are normally temperature dependent. The temperature difference is likely to be important in improving the Gr values. The greater values of Gr and β evidently increase the non linearities of the flow curve.

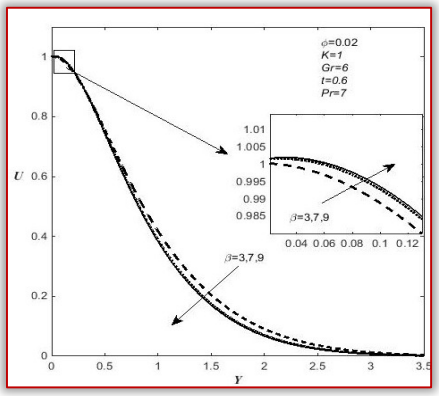

Figure 4. Velocity distributions of SiO_2 for different values of Casson parameter

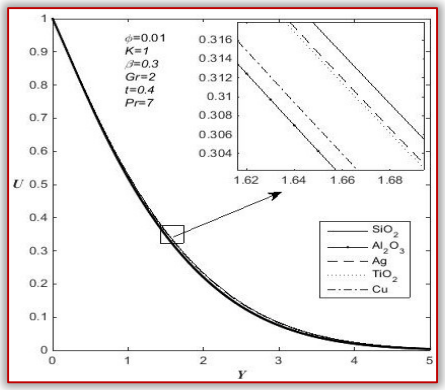

Figure 5. Velocity distributions of various nanoparticles

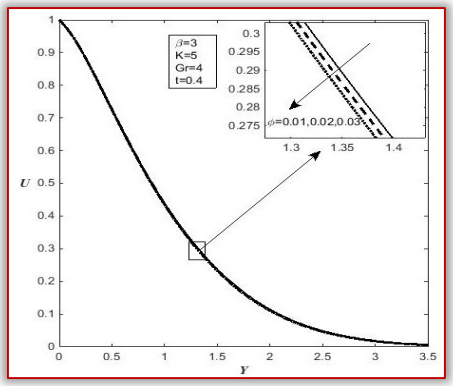

Figure 6. Effect of ϕ on velocity distribution

In figure 5 and 7, the velocity and temperature profiles of various nanoparticles SiO_2, Al_2O_3, Ag, TiO_2 and Cu are discussed. SiO_2 nanoparticles produce the highest velocity distribution and the lowest temperature distribution.

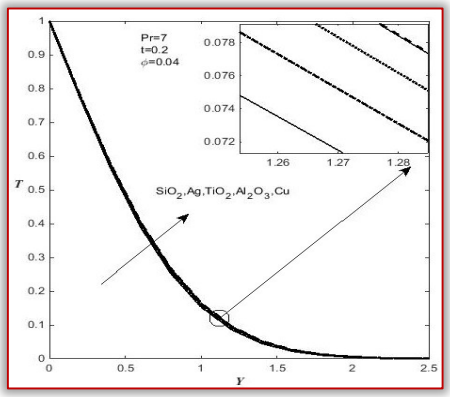

Figure 7. Temperature distribution of various nanoparticles

Figure 8 explains the influence of Prandtl number, ϕ and time. Increasing the values of Prandtl number, results in the temperature drop. This is because of the less physical strength in the thermal conductivity. On the other hand, temperature shoots up rapidly for the elongated time.

Rise in the amount of nanoparticle concentration elevates the thermal conductivity of the base fluid. Due to high thermal conductivity, the thinner momentum boundary layer and thicker thermal boundary layer are observed. These circumstances reduce the speed of the flow and increase the temperature in SiO_2 nanofluid which is depicted in figure 6 and 8.

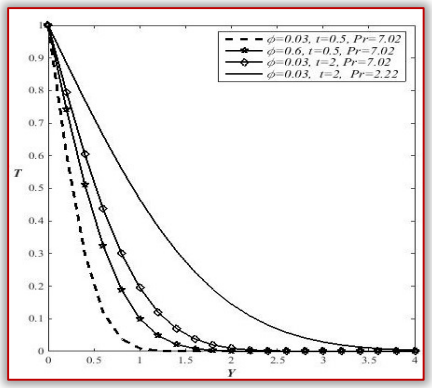

Figure 8. Influence of ϕ, t and Pr on temperature distribution of SiO_2

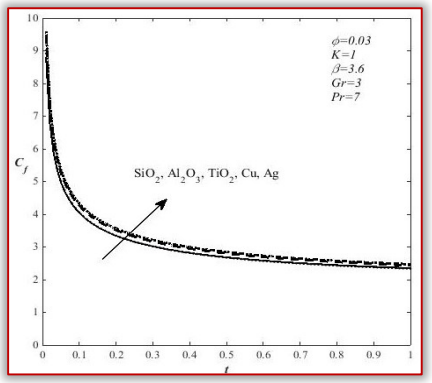

Figure 9. Skin friction coefficient for different nano particles

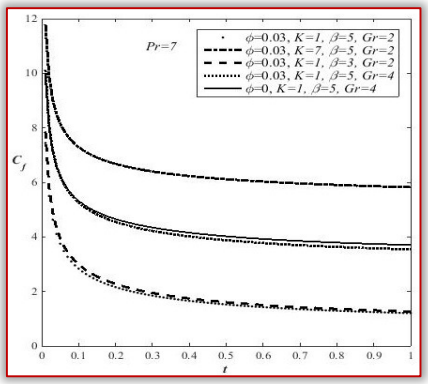

Figure10. Influence of ϕ, K, β and Gr on Skin friction coefficient of SiO_2

The shear stress of the flow towards the plate experiences the velocity gradient and fluid flow retardation. From figure 9, SiO_2 nanoparticles exhibit the lowest skin friction comparing to the other nanoparticles on account of viscosity fluctuation at 3% volume fraction, $\mathrm{K}=1,\ \beta=3.6,\ \mathrm{Gr}=3$ and $\mathrm{Pr}=7$.

Figure 10 depicts the influence of different parameters on the skin friction coefficient. Thermal conductivity of the conventional fluid greatly improved when the large amount of nanoparticles dispersed. Consequently, there is a drop in the viscous drag. Rise in the permeability leads to the increase in the number of pores or the size of pores in the porous medium. Owing to this fact, the fluid approaches the plate surface easily which improves the friction between the plate and the fluid. An increase in the Grashof number results in the elevation of skin friction coefficient. Higher values of Casson parameter display the growth in viscous drag due to the significant change in dynamic viscosity.

Figure 11 emphasizes the influence of Nusselt number on SiO_2 nanoparticles with 2% volume fraction and Prandtl number values enhance the energy transport from high temperature region to low temperature region. Thus it is evident that there is a remarkable increase in the Nusselt number values.

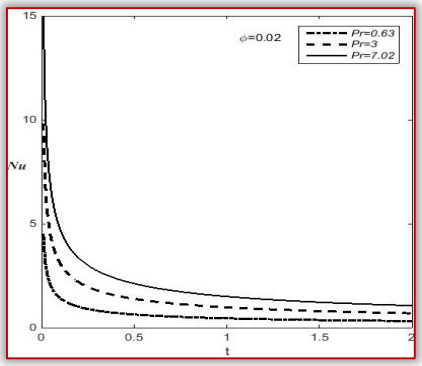

Figure 11. Variation in the Nusselt number in SiO_2 for different Pr

CONCLUSIONS

A bulk of theoretical and experimental investigation carried out on nanofluids. However, very few researchers reviewed the SiO_2 –water nanofluids. In addition to that there is no contribution in non-Newtonian (Casson fluid) behaviour of nanofluids through a porous medium. This study analyses this phenomena and concludes with the following stupendous inferences.

- Among the five nanoparticles including metallic and non-metallic nanoparticles, SiO_2 displays the highest velocity, lowest skin friction and temperature.
- Enhancing Prandtl number values produce the greatest improvement in the Nusselt number but lessen the temperature and velocity field.
- Uplifting Grashof number and Casson parameter provides some irregularities in the flow pattern. Near to the plate surface, it is noted that the velocity is growing and it is decaying while the fluid far away from the surface.
- Volume fraction of nanoparticles (amount of nanoparticles dispersed in the conventional fluid) escalate the temperature and slow down the speed.
- Velocity and temperature field rapidly increases for a large time scale.
- The flow speed is stimulated when the permeability is getting larger. Increment in K, β and Gr display the rise in viscous drag. When there is an increase in the volume fraction coefficient, the skin friction is significantly reduced.

Acknowledgement

One of the authors, K. Deepa immensely expresses the gratitude to Anna University, Chennai for supporting this research work with the financial assistance through "Anna Centenary Research Fellowship".

References

[1] Ahmad, S; Rohni, A.M; Pop, I; Blasius and Sakiadis problems in nanofluids: Acta Mech, Vol.218, pp.195–204, 2011.
[2] Arthur, E.M; Seini, I.Y and Bortteir, L.B; Analysis of Casson fluid flow over a vertical porous surface with chemical reaction in the presence of magnetic field: Journal of Applied Mathematics and Physics, Vol.3, pp.713-723, 2015.
[3] Chhabra, R.P. and Richardson, J.F: Non-Newtonian flow in the process industries; fundamentals and engineering applications, Butterworth-Heinemann publishing, 1999.
[4] Choi, U.S.S. and Eastman, J.A: Enhancing thermal conductivity of fluids with nanoparticles, ASME International Mechanical engineering congress & Exposition, San Francisco, CA, 1995.
[5] Cross, M.M: Rheology of non-Newtonian fluids: A new flow equation for pseudo plastic systems, Journal of colloid science, Vol. 20, pp.417-437, 1965.
[6] Das, S.K; Choi, U.S.S; Yu, W and Pradeep, T: Nanofluids science and technology, A John Wiley & Sons, Inc., Publication, 2007.
[7] Das, S; Jana, R.N, Makinde, O.D: Magnetohydrodynamic free convective flow of nanofluids past an oscillating porous flat plate in a rotating system with thermal radiation and hall effects, Journal of Mechanics, pp.1-14, available at: doi:10.1017/jmech.2015.49, 2015.
[8] Hamilton, R.L and Crosser, O.K: Thermal conductivity of heterogeneous two component systems, I & EC fundamentals, Vol.1 No.3, 1962.
[9] Haq, R.U; Nadeem, S; Khan, Z.H and Okedayo, T.G: Convective heat transfer and MHD effects on Casson nanofluid flow over a shrinking sheet, Central European Journal of Physics, Vol.12 (12), pp.862-871, 2014.
[10] Hussanan, A; Salleh, M.Z; Tahar, R.M and Khan, I: Unsteady boundary layer flow and heat transfer of a Casson fluid past an oscillating vertical plate with Newtonian heating, PLOS ONE, VoL.9(10), 2014.
[11] Hussein, M.A; Bakar, R.A; Kadirgama, K and Sharma, K.V: Experimental measurement of nanofluids thermal properties, International Journal of automotive and mechanical engineering, Vol.7, pp.850-863, 2013.
[12] Makanda, G; Shaw, S and Sibanda, P: Effects of radiation on MHD free convection of a Casson fluid from a horizontal circular cylinder with partial slip in non-Darcy porous medium with viscous dissipation, Boundary Value Problems, Vol.75, 2015.
[13] Meybodi, M.K; Naseri, S; Shokrollahi, A; Daryasafar, A: Prediction of viscosity of water-based Al_2O_3, TiO_2, SiO_2 and CuO nanofluids using a reliable approach, Chemometrics and Intelligent Laboratory Systems, Vol.149, pp.60-69, 2015.
[14] Muthucumaraswamy, R; Nagarajan, G; Subramanian, V.S.A: Thermal radiation and MHD effects on flow past a vertical oscillating plate with chemical reaction of first order, Acta Technica Corviniensis-Bulletin of Engineering, 2011.
[15] Noghrehabadi, A; Ghalambaz, M and Ghalambaz, M: A Theoretical investigation of SiO_2-water nanofluid heat transfer enhancement over an isothermal Stretching sheet, International journal of multidisciplinary sciences and engineering, Vol.2(9), 2011.
[16] Noghrehabadi, A; Ghalambaz, M; Ghalambaz, M and Ghanbarzadeh, A: Comparing thermal enhancement of Ag-water and SiO_2-water nanofluids over an isothermal stretching sheet with suction or injection, Journal of computational and applied research in mechanical engineering, Vol.2(1), pp.37-49, 2012.
[17] Oztop, F.H; Abu-Nada, E: Numerical study of natural convection in partially heated rectangular enclosures filled with nanofluids, International Journal of Heat and Fluid Flow, Vol.29, pp.1326-1336, 2008.
[18] Raju, C.S.K and Sandeep, N: Unsteady Casson nanofluid flow over a rotating cone in a rotating frame filled with ferrous nanoparticles: A numerical study, Journal of Magnetism and Magnetic Materials, Vol.421, pp.216-224, 2017.
[19] Raju, C.S.K; Sandeep, N; Sugunamma, V; Jayachandra Babu, M and Ramana Reddy, J.V: Heat and mass transfer in magnetohydrodynamic Casson fluid over an exponentially permeable stretching surface, Engineering Science and Technology, An International Journal,Vol.19, pp.45-52, 2016.
[20] Shi, J; Zhao, W; Li, J and Liu, Z: Heat transfer performance of heat pipe radiator with SiO_2/Water nanofluids, Heat transfer-Asian research, Vol.46(7), 2017.
[21] Soundalgekar, V.M: Free convection effects on the stokes problem for an infinite vertical plate, Journal of Heat Transfer, Vol.99, pp.499-501, 1977.
[22] Tiwari, R.K; and Das, M.K: Heat transfer augmentation in a two-sided lid-driven differentially heated square cavity utilizing nanofluids, International Journal of Heat and Mass Transfer, Vol.50, pp.2002-2018, 2007.
[23] Ullah, I; Khan, I and Shafie, S: MHD natural convection flow of Casson nanofluid over nonlinearly stretching sheet through porous medium with chemical reaction and thermal Radiation, Nanoscale research letters, Vol.11, 2016.
[24] Ullah, I; Bhattacharyya, I; Shafie, S and Khan, I: Unsteady MHD mixed convection slip flow of Casson fluid over nonlinearly stretching sheet embedded in a porous medium with chemical reaction, thermal radiation, heat generation/absorption and convective boundary conditions, PLOS ONE, 2016.
[25] Venkatesan, J; Sankar, D.S; Hemalatha, K and Yatim, Y: Mathematical analysis of Casson fluid model for blood rheology in stenosed narrow arteries, Journal of Applied Mathematics, Hindawi, 2014.

ISSN: 2067-3809

[1.]Oluwayomi Ife AKINYEMI, [1.]Titus Adeyemi ALONGE,
[1.]Olumuyiwa Idowu OJO, [2.]Oyetola OGUNKUNLE

GEO-SPATIAL TREND MAPPING OF SOME ANNUAL CLIMATE VARIABLE FOR SOUTH WEST NIGERIA

[1.]Agricultural Engineering Department, Ladoke Akintola University of Technology, Ogbomoso, NIGERIA
[2.]Mechanical Engineering Science Department, University of Johannesburg, SOUTH AFRICA

Abstract: The concept of climate has gained much relevance because of its dynamic and complex nature and the significant influence it has on various aspects of the environment including the increasing threat of global climate change. The varying pattern does not encourage the stable practice of agriculture, thereby causing an increase or decrease in their yield. Data were collected from Nigeria Meteorological Agency (NIMET) for rainfall, temperature and relative humidity data for the period of 38 years and were analyzed in order to generate geo-spatial trend maps of climate variability to aid smart agricultural crop production. The mean temperature, average rainfall and average relative humidity for each year of the study period were calculated. Imagery shape file was also extracted from South West Nigeria maps. The weather data and Imagery shape file were then imported into Arc GIS 9.0 for geo-spatial maps for Rainfall, Temperature and Relative Humidity. The analysis showed prolonged variability in average annual rainfall received over the climatic zone across the three climatic factors. The results indicated a temperature higher than 27°C cause under-development of anthers and loss of viability of pollen. Higher temperature disturbs the photosynthesis and respiration and these may result in low production. Rainfall pattern reveals that rainfall in South West has been highly varied. Relative humidity pattern between the years tends to either increase or decrease in the result by (±3) with a relative stability in the last 5 years of this study period thereby aiding the easy prediction of the shelf life of agricultural products.
Keywords: climate factors; climatic variability; agricultural production; south-west of Nigeria

INTRODUCTION

The last several decades have witnessed warmer temperatures across the globe, with more rapid warming observed during the last half of the 20th century compared with the first (Jones *et al*., 2001). Agriculture in Nigeria is a branch of the economy in Nigeria providing employment for about 30% of the population as at 2010 (Sanusi, 2010). Heavy rainfall events have increased, longer and more intense droughts have occurred.

The adverse effects of food insecurity have already been felt in the South Western of Nigeria. Currently, and over the next few decades, climate change impacts on agriculture are more likely to arise from increased climate variability and increased frequency and intensity of extreme events, rather than from changes in mean climatic conditions. It has produced several effects on food security thereby resulting in scarcity of some items not produced in this part of the country. With all these adverse effect of climate on agriculture been stated, addressing climate concerns through adaptation will be advantageous to agriculture (FAO, 2006).

The Intergovernmental Panel on Climate Change (IPCC) notes that adaptability through changes in "processes, practices or structures" is a crucial element in reducing potential adverse impacts or enhancing beneficial impacts of Climate change (IPCC 2001). Adaptation is regarded as a vital component of climate change impacts and vulnerability assessment (Skinner *et al*., 2001). In the context of development, Burton (1996) asserts that a practical response strategy is to improve adaptation to climate variability, including extreme events. Smith (1997) maintains that adaptation is necessary to avoid impacts that can otherwise occur gradually and may be irreversible. That is, increasing the robustness of infrastructure designs and investments can reap immediate benefits through improved resilience to climate variability and extreme atmospheric events. Adaptation is viewed as a crucial step to strengthen local capacity to deal with forecasted and unexpected climatic conditions (Smith *et al.,* 1996).

Nigeria, by virtue of its location, enjoys a warm tropical climate with relatively high temperatures throughout the year and two seasons; the rainy or wet season that lasts from mid-March to November in the south and from May to October in the north; and the dry season that occupies the rest of the year. However in a country where the temperatures do not fluctuate regularly, constant elements such as rainfall and relative humidity are heavily relied on to differentiate between the season and climate zones.

The climate of the country is influenced by the interaction of two air masses: the relatively warm and moist tropical marine mass which originates over the Atlantic ocean and is associated with southwest winds in Nigeria and the relatively cool, dry and relatively stable tropical continental air mass that originates from the Sahara Desert and is associated with the dry, cool and dusty North-East Trades (harmattan).

In the south, it's a different case as the long wet season that starts in mid-March and last till July is a season of heavy rains and high humidity. Plants and pasture are fresh and green grasses and weeds grow rapidly and look attractive. Plant development depends on high atmospheric humidity in the sense that many plants have the ability to directly absorb moisture from unsaturated air of high humidity.

This percentage tells how close the air is to being saturated. If the relative humidity is 50%, the air contains half the water vapour required for it to be saturated. If the amount of water vapour in the air increases, the relative humidity increases, and if the amount of water vapour in the air decreases, the relative humidity decreases. However, relative humidity is dependent on air temperature, too. If the water vapour content stays the same and the temperature drops, the relative humidity increases. If the water vapour content stays the same and the temperature rises, the relative humidity decreases. This is because colder air doesn't require as much moisture to become saturated as warmer air (Monteith and Unsworth, 2008).

According to 2004 estimate the value of agriculture production constituted 30.8%; industry, 43.8% and services 25.4%, of the nation GDP, respectively. The nation's GDP real growth rate stood at 7.1% (CIA World Factbook, 2004). Temperature rise is likely to result in reduced food production within the next couple of decades in regions already facing food insecurity. To determine the correlating effects of these two climatic factors, a model will be used to study the processes taking place in the soil-plant-atmosphere continuum and carry out scenario testing. This approach permits revisiting of the past, simulating the present and predicting the future, thus, made it flexible in all situations.

With an upgraded capability to environmental parameters, proper management intervention could be done to minimize risk in the future. The rainfall pattern can simply be accessed using simulation models. Another issue is the spatial and temporal dimension of water productivity. A spatio-temporal analysis could broaden the role of models in exploring improved water use in agriculture (Ines *et al.,* 2002). The use of Geographic Information System (GIS) and crop models permits more efficient analysis because the temporal and spatial dimensions could be examined at once.

This study focused on the assessment of climate variation in South Western region of Nigeria based on the variations in rainfall, relative humidity and temperature within the period 1970-2007. The aim is to assess climate change in south-west of Nigeria as it may likely affect agricultural crop production.

This study helps to address the research gap by providing an assessment of the overall effect of climatic variability on agricultural production through analysis of some climatic conditions data associated with crop production.

Rainfall, temperature and relative humidity seems to be the main contributor to agricultural crop production in the south western part of Nigeria. The analysis will help farmers on how to cope with the environmental changes in the context of farm management and precision farming.

DATA AND METHODOLOGY

— Description of study area

South West Nigeria, as shown in Figure 1, constitute of six states namely, Ogun, Oyo, Osun, Ekiti, Ondo and Lagos. The area falls between longitude 2° 31' and 6° 00' East and latitude 6° 21' and 8° 37' North with a total land area of 77,818 Km^2 and a projected population of 28,767,752 in 2002. The states are part of few states that participated in Agricultural production in Nigeria. The study area is bounded in the East by Edo and Delta states, in the North by Kwara and Kogi states, in the west by the Republic of Benin and in the south by the Gulf of Guinea (Agboola, 2004). Between March and October, the prevalent winds in the region is the moist maritime South-west monsoon which blows inland from the Atlantic Ocean, this is the period of rainy season. November to February is the period of dry season when the dry laden winds blow from the Sahara desert. The mean annual rainfall of about 1,205 mm, fell within an approximate period of 109 days with two rainfall peaks in June and September.

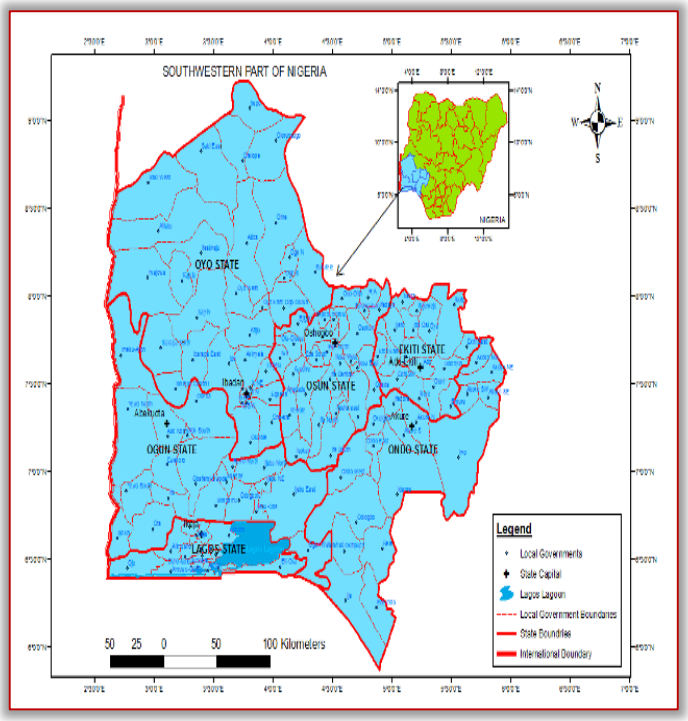

Figure 1: Map of the study area (Southwest, Nigeria).
Adapted from Ojo and Olawale, 2014

— Data collection and analysis

The data used for this project were secondary and were collected from Nigeria Meteorological Agency (NIMET). The data cover relative humidity, temperature and rainfall of the south-west of Nigeria from 1970 to 2007. The data were recorded on monthly basis, that is, from January to December. Imagery shape file was also extracted for the study area. Rainfall data was subjected to various statistical techniques to arrive at valuable result.

The correlation analysis was used to determine the pattern in total rainfall over time for the weather station in the study area. The data were processed using Microsoft Excel software. Microsoft Excel was used to calculate mean of maximum and minimum temperature, average rainfall and average relative humidity for each year from 1970 to 2007 respectively. Imagery shape file was also imported into Arc GIS 9.0 for map productions for rainfall, temperature and relative humidity.

Correlation analysis was also carried out using temperature data of 38 years to determine the variations in temperature and establish the temperature trend in the study area.

RESULTS AND DISCUSSION

— Variations in rainfall, temperature and relative humidity in South West Nigeria

The impact of climate change on crop yield is generally estimated from a combination of the effects of climate models on the physical crop growth pattern (Müller *et al.*, 2011). Climate change, if not properly assessed, will obviously jeopardize farming sustenance of the rural people in Africa, particularly where inadequate access to agricultural knowledge and technology of climate will hamper their ability to adapt and plan (Lobell *et al.*, 2008, Salami and Matthew, 2009).

Trend analysis of the data set over the study time was therefore obtained to determine the recent and current trend in temperature as it provides indication of the increase or decrease of good climatic conditions.

— Rainfall Pattern

The result of this study show that rainfall variations and pattern in South west is worthy of close examination, as its variations over time is remarkable.

The results showed that there was a high variation of precipitation in the Southwest. The trend of total annual rainfall for the periods is shown in Figure 2a.

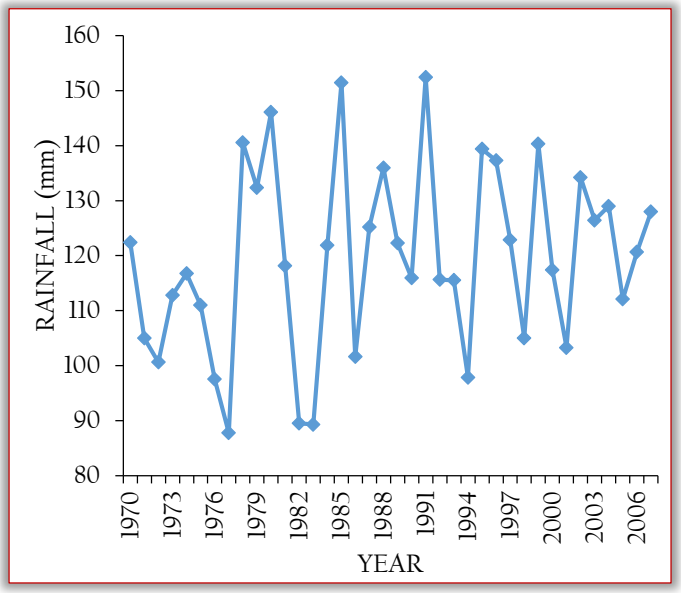

Figure 2a: Trend line for yearly mean rainfall variation

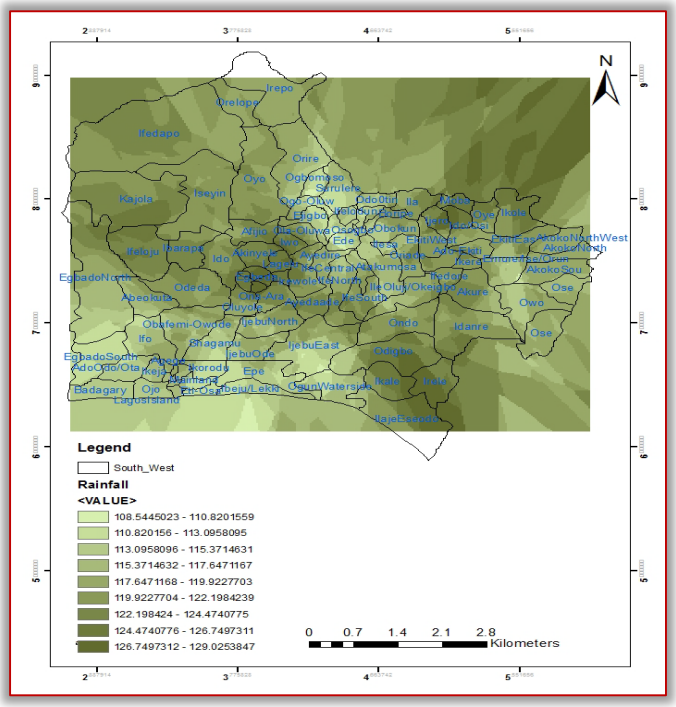

Figure 2b: Geo-spatial variation map of annual Rainfall for South West of Nigeria

Total rainfall of the area was characterized by two distinct peaks: one in 1985 and the other (highest) peak in 1991. This shows that these years were the wettest year within the period under study.

Generally, the total rainfall of the area decreased in the period 1970-1973 and increase in year 1974. There was also slight decline in years 1976, 1977, 1982, 1983 and 1994. There was a sharp increase after year 1978; this was more experienced in year 1985 till about year 1992 with a sharp decline in year 1993. Within this period there was an interesting variation of rainfall as it experienced a rise and fall. The total rainfall continued to increase and decline in the period 1994-2007.

The geo-spatial variation map of annual rainfall for the study area is shown in Figure 2b. The mean total annual rainfall is highest for year 1991 (152 mm) while it is lowest for year 1977 (88 mm). The implication of this is that rainfall in South west varies in amount from year 1970-2007. Therefore, it is not expected that equal amount of rainfall can fall from one year to another. Annual rainfall range indicates the variability of annual rainfall and hence denotes how reliable the rainfall is in terms of its persistence as a constant and stable replenishing source of water in south western region. It was also observed that there was decreased crop production in the years with less precipitation.

Agricultural produce were very scarce and the yields were reduced as compared to the years with high precipitation rates. Agricultural production in South Western part of Nigeria is largely fed by rainfall; any decrease in precipitation rate will have unfavourable impact on agricultural production and largely reduce the crop yields as relatively reported by Chikezie *et al.*, 2015).

— Temperature Pattern

The mean yearly temperature variation is shown in Figure 3a. The lowest average temperature value of 23°C was recorded within the period under study in year 2007. The minimum value of 26°C was recorded in years 1971, 1974, 1975, 1976, 1978 and 1980, which shows that these years were relatively cooler.

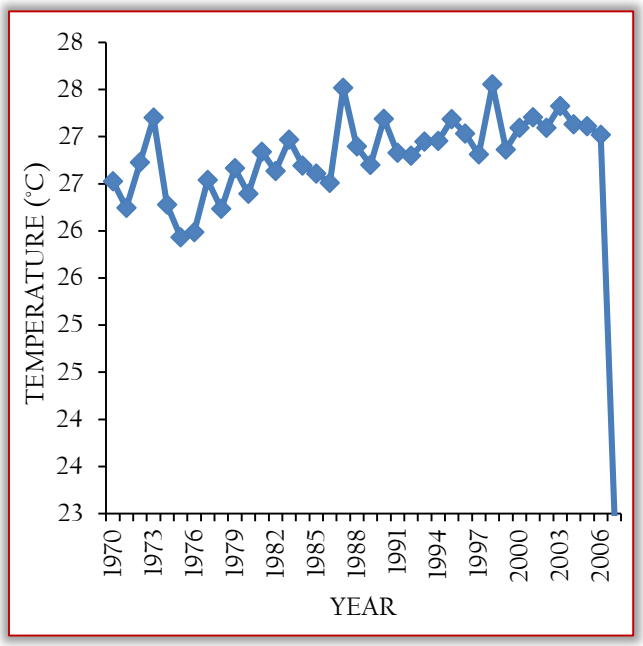

Figure 3a: Trend line for mean yearly temperature variation

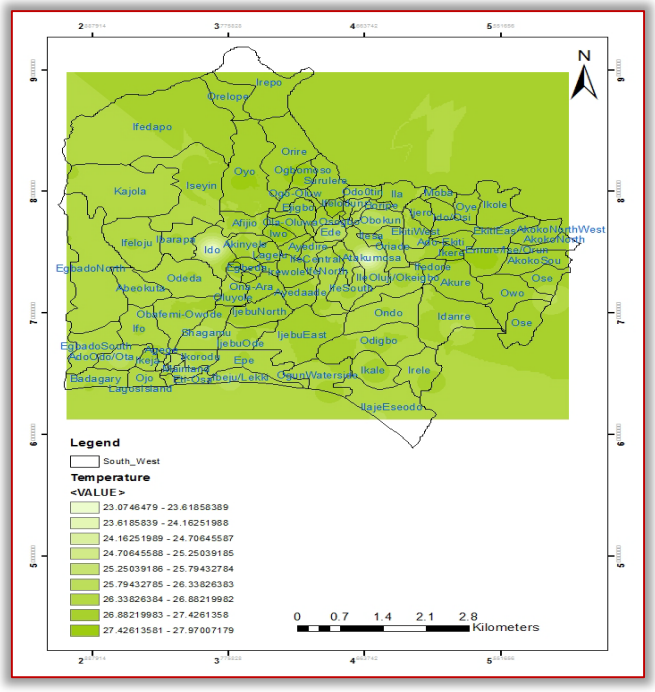

Figure 3b: Geo-spatial variation map of annual temperature for South West Nigeria

The maximum value of 28°C was however recorded in years 1987 and 1998, indicating that it was a relatively warmer years. Temperature in south west has been slightly varied. The varying period was the early years of the study period 1970-1980. The geo-spatial variation map of annual temperature for South West Nigeria is shown in Figure 3b. In general, the mean annual temperature of the study area was stable with slight fluctuations in years 1987, 1998 and 2007 within the period.

— Relative humidity pattern

The relative humidity trend is shown in Figure 4a. It can be observed that there is a slight difference in the trend pattern from year to year. However, the trend of relative humidity varies at the early stage of the study period 1970-1972. There was a stable trend over the period 1973-1975. The (highest) peak relative humidity was in year 1979, with other high values recorded in the year 1976 and 1978. Also the lowest years were years 1983, 1992, 1993, 1998, 2000 and 2002 relatively 79%. Other varies trend falls within the highest value and the lowest. This shows the variation of relative humidity within a predictable range for agricultural practices. The geo-spatial variation of map of annual relative humidity for South West is shown in Figure 4b.

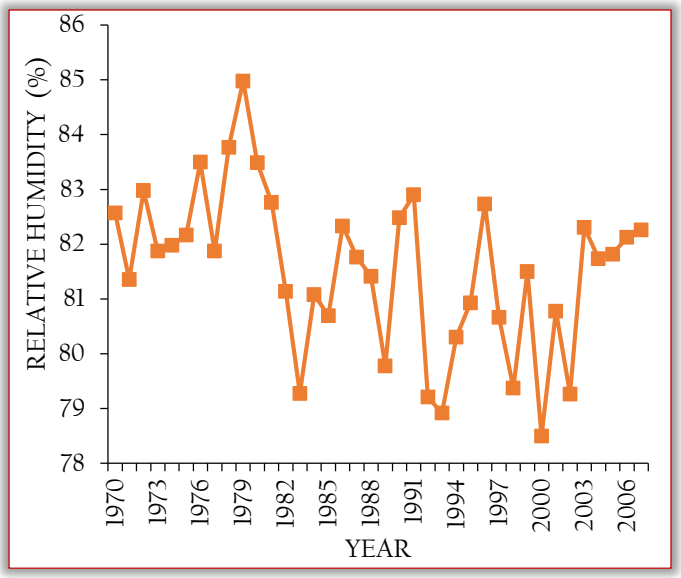

Figure 4a: Trend line for mean yearly relative humidity variation

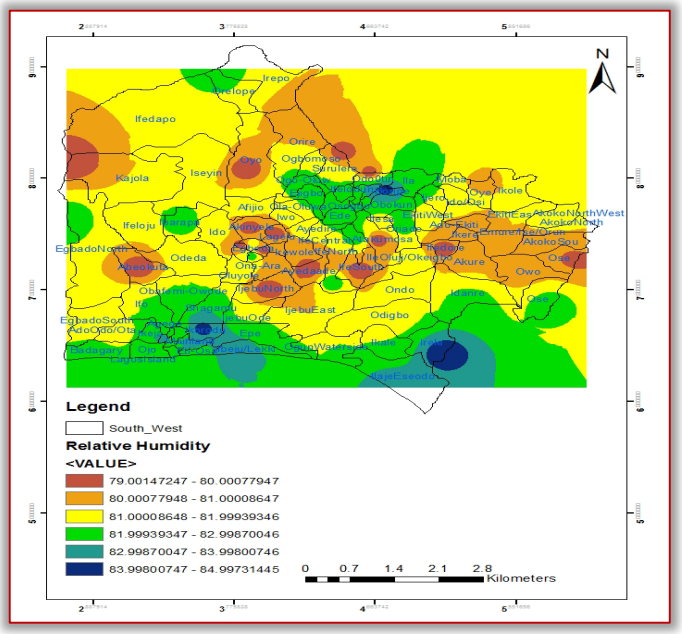

Figure 4b: Geo-spatial variation of map of annual relative humidity for South West

CONCLUSION AND RECOMMENDATION

The results establish variability and change in zonal rainfall, temperature and relative humidity experienced in agricultural production in Nigeria.

The study has revealed the effects that climatic variables, such as rainfall, relative humidity, temperature have on agriculture in the study area. The analyses have shown prolonged variability in average annual rainfall received over the climatic zone across the three climatic factors considered and such variation and changes were statistically established. Such prolong variability also extend its socioeconomic importance to the ground water resources and hydrological sector.

Rainfall, temperature and relative humidity showed transitions from dry to wet conditions in the change point analyses between 1970 and 2007 as there were observed jumps with no imbalance in averaged zonal rainfall distribution, temperature and relative humidity across the climatic periods.

The results will assist in planning ahead in order to avert problems such as early drought associated with climatic variables in the study area. Besides reducing over dependence on rain-fed agriculture, it is recommended that farmers should plant drought resistant crops or early maturing crop varieties especially in the extremely southern zone. The farmer should be tutored on how to cope with the environmental changes in the context of farm management and precision farming.

References

[1] Agboola S.A. (1979): An Agricultural Atlas of Nigeria, Oxford University Press, Nigeria pp. 248.

[2] Burton, I., (1996). The growth of adaptation capacity: practice and policy. In: Adapting to Climate Change: An International Perspective [Smith, J., N. Bhatti, G. Menzhulin, R. Benioff, M.I. Budyko, M. Campos, B. Jallow, and F. Rijsberman (eds.)]. Springer- Verlag, New York, NY, USA, pp. 55–67.

[3] Chikezie C, Ibekwe U. C, Ohajianya D. O, Orebiyi J. S, Ehirim N. C, Henri-Ukoha A, Nwaiwu I.U.O, Ajah E. A, Essien U.A, Anthony G and Oshaji I.O. (2015). Effect of Climate Change on Food Crop Production In Southeast, Nigeria: A Co-Integration Model Approach. International Journal of Weather, Climate Change and Conservation Research; 2(1): pp.22-31.

[4] CIA (2004). Central Intelligence Agency World Factbook. Cited 16th June 2004, https://www.cia.gov/library/publications/download.html. Accessed on: 28 Jan. 2016.

[5] Estimating Water Productivity. Agric. Water Manage. 54 (3), 205–225.

[6] FAO. Food and Agriculture Organization FAOSTAT Database (on-line) (2006). Disponivel em: <http://faostat.fao.org> Accessed on: 28 Jan. 2016.

[7] Ines, A.V.M., Gupta, A.D., Loof, R., (2002). Application of GIS and crop growth models in

[8] IPCC, 2001: Climate Change (2001). The Scientific Basis. Contribution of Working Group I to The Third Assessment Report of the Intergovernmental Panel on Climate Change [Houghton, J.T., Y. Ding, D.J. Griggs, M. Noguer, P.J. van der Linden, X. Dai, K. Maskell, and C.A. Johnson (Eds.)]. Cambridge University Press, Cambridge, United Kingdom and New York, NY, USA, pp. 881.

[9] Lobell D B, Burke M B, Tebaldi C, Mastrandrea M D, Falcon W P and Naylor R L. 2008. Prioritizing climate change adaptation needs for food security in 2030 Science 319 607–10.

[10] Monteith, J. and Unsworth, M. 2008. Principles of environmental physics. Academic Press, California, USA. 3rd Edition. pp 116 - 139.

[11] Müller C, Cramer W, Hare W L and Lotze-Campen H. 2011. Climate change risks for African agriculture Proc. Natl Acad. Sci. USA 108 4313–5.

[12] Olumuyiwa Idowu Ojo and Saheed Olabanjo Olawale (2014). Assessment of Weather Variability Impact on Cassava Yield in South Western Nigeria. LAUTECH Journal of Engineering & Technology, Vol. 9, number 2. ISSN: 1597-0000.

[13] P. D. Jones, T. J. Osborn, K. R. Briffa. 2001. The Evolution of Climate over the Last Millennium. Science; 292(5517): 662 – 667. DOI: 10.1126/science.1059126.

[14] Salami AT, Matthew OJ (2009). Challenges of Effective Climate Change Adaptation and Mitigation in Nigeria: The Role of Education. A paper presented at 5th World Environmental Education Congress (WEEC), May 10 -14, at Montreal, Canada.

[15] Sanusi Lamido Sanusi. 2010. Growth Prospects for the Nigerian Economy. Convocation Lecture delivered at the Igbinedion University Eighth Convocation Ceremony, Okada, Edo State, November 26, 2010.

[16] Skinner, M. and Smith, B. (2001). Adaptation options in Agriculture to Climate Change: A typology, mitigation and Adaptation Strategies for Global Change. African Journal of Agriculture and Resource Economics 3(5) pp. 78-82

[17] Smith, J.B. (1997). "Setting priorities for adaptation to Climate change." Global Environmental Change 7:251-264.

[18] Smith, J.B., Bhatti, N., Menzhulin, G., Benioff, R., Budyko, M.I., Campos, M., Jallow, B., Rijsberman, F., (1996). Adapting to Climate Change: Assessments and Issues. Springer, Berlin. Springer- Verlag, New York, NY, USA, 475 pp.

ISSN: 2067-3809

Fascicule 1

[January - March]

t o m e XII

[2019]

ACTA Technica CORVINIENSIS
BULLETIN OF ENGINEERING

ISSN: 2067-3809

[1.]Galina PATAMANSKA, [2]Elena GRANCHAROVA

HYDRAULIC MODELING FOR BETTER OPERATIONAL PERFORMANCE OF EXISTING IRRIGATION CANAL

[1-2.]Institute for Soil Science, Agrotechnologies and Plant Protection „N. Pushkarov", Sofia, BULGARIA

Abstract: Mathematical simulation model is a suitable tool for understanding the hydraulic behavior of an open irrigation canal and obtaining information on actual hydraulic parameters of water flow. In this paper, a simulation model of an open irrigation canal created using hydraulic software HEC-RAS is presented. The model was calibrated with observed flow data in steady state conditions and optimal roughness value and actual canal carrying capacity were determined. Computer simulations for different values of roughness and operating discharge were carried out in order to diagnose the condition of the lining and defining the limits of the hydraulic parameters of the studied canal.

Keywords: irrigation canal, simulation model, hydraulic modeling, diagnostics, analysis

INTRODUCTION

In irrigation systems the flow parameters are measured in a limited number of points along the canal course, which does not provide sufficient information for effective management - supply of needed water for irrigation of the agricultural crops without deficiency or excess spillage.

Mathematical simulation model is a suitable tool for understanding the hydraulic behavior of the open irrigation canal and for obtaining information about the actual values of the flow parameters. As a result of the hydraulic analysis of the flow in the canal carried out with a model, complete information is obtained about the changes in water levels along the canal occurring after each change of water supply at the head of the canal and/ or change of the water discharge in the canal off takes (Baume et al,.1994). The roughness factor is an essential parameter of the mathematical models of the open canals as it participates in the calculations of the friction slope and influences the hydraulic parameter determination accuracy. Models should be calibrated by roughness parameter.

Computer analysis can be very useful in assessing the existing situation of an old irrigation system with open canals and in searching for possible solutions to improve water management. With the calibrated steady flow model, in terms of roughness hydraulic studies and assessing the influence of operating conditions can be carried out.

In this paper, a simulation model of an open irrigation canal created using hydraulic software HEC-RAS is presented. The model was calibrated with observed flow data in steady state conditions and optimal roughness value and actual canal carrying capacity was determined. Computer simulations for different values of roughness and operating discharge were carried out in order to diagnose the condition of the lining and defining the limits of the hydraulic parameters of the studied canal.

MATERIALS AND METHODS

— Description of software used

In this study, the freeware software HEC-RAS, Version 4.1 (Hydrologic Engineering Center - River Analysis System) developed by U.S. Army Corps of Engineers, is selected to create a simulation model of the study canal. Using this software, one-dimensional hydraulic calculations are performed in a branched network of natural and / or artificial channels. The software system includes a user interface, steady flow model, unsteady flow model and modules that provide graphical and tabular presentation of the results. It can simulate steady and unsteady flows in open channel. For the steady state conditions, water surface profile can be simulated in critical, supercritical and mixed flow regimes (US Army Corps of Engineers, 2010).

For conducting hydraulic modeling and simulation of the water surface profile in irrigation canal data are required for its geometry, the boundary conditions, the water discharge, the canal roughness, geometric description of the hydraulic structures along the canal course, such as gates, culverts, weirs. Introducing the geometry of the canal includes defining the profile of the canal bed of the study reach by setting series of cross-sections that longitudinally define its shape.

For the calculation of the longitudinal water surface profile at steady flow, the one-dimensional equation of energy (Bernoulli equation) is integrated by the standard step method. In order to be able to start the calculation, a discharge upstream of the canal and a stage downstream are set as boundary conditions. For the interior points the stage is estimated keeping the water discharge constant.

As results of canal flow simulation the following hydraulic parameters: depth/ water surface elevation, energy grade line elevation, friction slope, flow velocity, critical depth/critical depths line elevation, water volume in the canal and others can be determined.

The roughness coefficient cannot be measured directly and therefore it is necessary to determine it by other methods. One of the methods used to assess the roughness is by simulation with a mathematical model. The classic approach for evaluation and calibration of the parameter roughness is associated with modeling of the steady flow in the canal (Malaterre et al, 2010).

The computational procedure is iterative and simulations with the irrigation canal model are carried out for a series of roughness values. For the determination of the roughness coefficient, the values of the hydraulic parameters in the observation points along the irrigation canal course and the numerical results of the computer experiments are compared according to a certain criterion. Nguyen and Fenton investigate the application of three main types of target function and show that least squares minimization gives the best results (Nguyen and Fenton D., 2004). The best match between the observed and calculated values for the hydraulic parameter, according to the selected criterion, determines the optimal roughness value.

— Description of the studied canal

The studied canal is a first part of an existing irrigation canal - the main canal M1-1 of „Sredna Tundja" irrigation system, in length 7.586 km, which starts from an attachment facility from the Binkus bent on the Tundzha river from an elevation of 185 m to a distribution shaft in the region of village Gavrailovo 7.586 km in length (fig. 1.) The canal is designed up to discharge 41 m^3/s.

The canal has trapezoidal cross-section and consists of 3 sections, two of them lined with concrete 2.642 km and 3.403 km in length with 2 m bottom width, a side slope of 1.5, the average bottom.

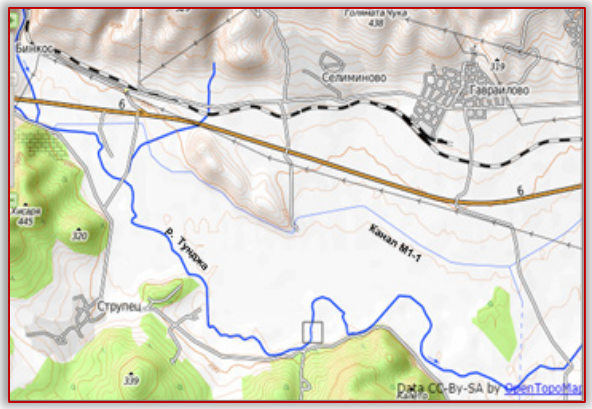

Figure 1 - Map of main canal M-1-1 of „Sredna Tundja" irrigation system and vicinity area (www.topomaps.info)

RESULTS

Hydraulic simulation model of the studied canal was created using hydraulic software HEC-RAS. It was built on the basis of the design parameters of main irrigation canal M 1-1. When creating the simulation model a realistic representation of the existing situation was sought. To reproduce the real geometry of the canal, three cross sections are set - at the canal inlet, at the head of rocky canal section and at the head of lined canal section in the canal end. The irrigation canal has a simplified geometry and the cross sections can be introduced with four points and a value of the coefficient of roughness. Since two of the canal sections are not completely lined, they were introduced with six points and changes in the lining are recorded by entering two values of the roughness coefficient for the lined and unlined part of the bank (Figure 2a). As boundary conditions rating curve at the head of the canal and critical depth at the end were set.

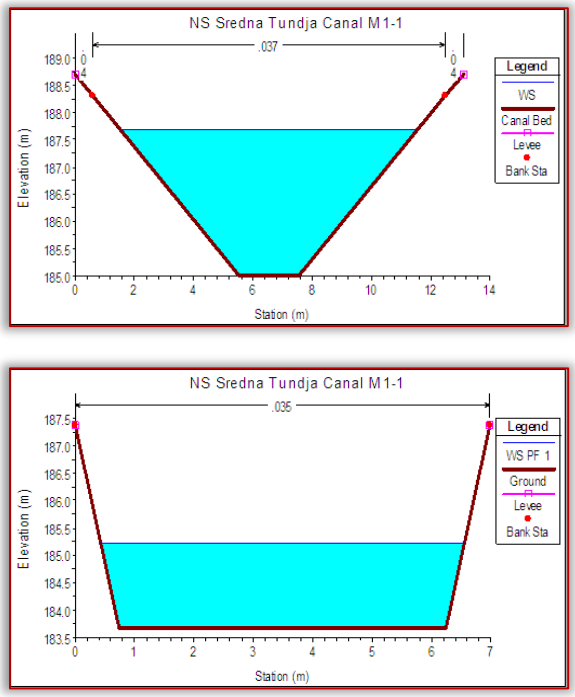

Figure 2 - Canal cross sections

Calibration of HEC-RAS model of the M1-1 canal for roughness coefficient n.

The HEC-RAS model of the M1-1 canal was calibrated using data for observed inlet water discharge and one depth at the end of the canal before the distribution shaft in the area of the village of Gavrailovo. Calibration data was selected from the daily operational information for canal depth measurements during the period from 14th of May to 29th of July 2012 under steady state of canal conditions.

The model has been used to simulate the steady flow in the canal M1-1 for increasing values of the roughness coefficient of the lined part of the canal cross sections in the range of 0.014 to 0.04 and the roughness coefficient equal to 0.035 for the unlined part and the rocky section in the steady state conditions. The initial value of the roughness for concrete lined canal and grassed surface of unlined part of the banks were selected in tables published in (Chow, 1959). A total of 20 experiments were conducted.

The simulated and measured values of the depth in the end of the canal for different values of the roughness coefficient are presented in Table 1. The simulated depth hydrographs were compared with observed depth hydrograph using linear regression. No significant deviation between the measured and estimated values is available and high correlation (R^2>0.9) between the observed and simulation depths was achieved for the respective water discharges. An

optimum value of the roughness n = 0.037 is determined for which the correlation coefficient is the highest (Figure 3).

Table 1. Measured and simulated depth hydrographs for different values of the roughness coefficient
Q_{in} - inlet discharge, h_o - measured depth in canal end, h_s - simulated depth in canal end, n- roughness coefficient

Q_{in}, m^3/s	h_o, m	h_s, m			
		n=0.014	n=0.025	n=0.035	n=0.037
3.5	0.83	0.69	0.76	0.81	0.82
9.5	1.39	1.15	1.24	1.31	1.33
12.5	1.61	1.33	1.42	1.49	1.51
15.68	1.66	1.48	1.58	1.65	1.67
18.44	1.78	1.59	1.69	1.77	1.78

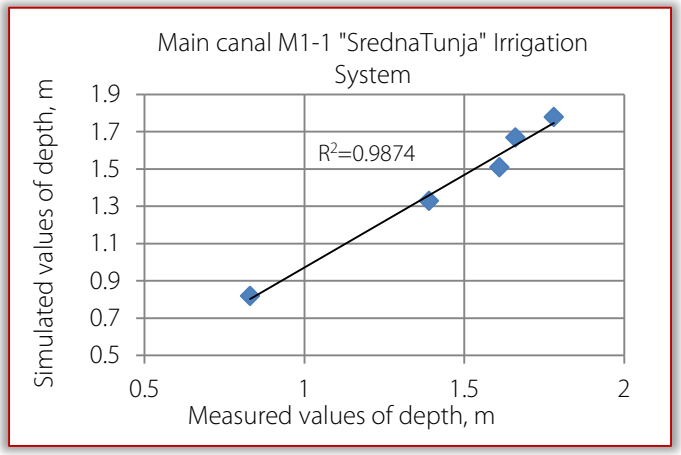

Figure 3 - Comparison of measured values of depth in the tail of canal versus simulated values for roughness coefficient n =0.037 using linear regression

By simulations of steady flow in the canal for estimated optimum value of the roughness n = 0.037 and increasing values of the inlet water discharge the current canal carrying capacity of 20 m^3/s is determined, as water discharge for which the depth in the lined canal section reaches the maximum 3.3 m, determined by the height of the lining. A 50% reduction in capacity shows a significant worsening of the operational performance of the canal.

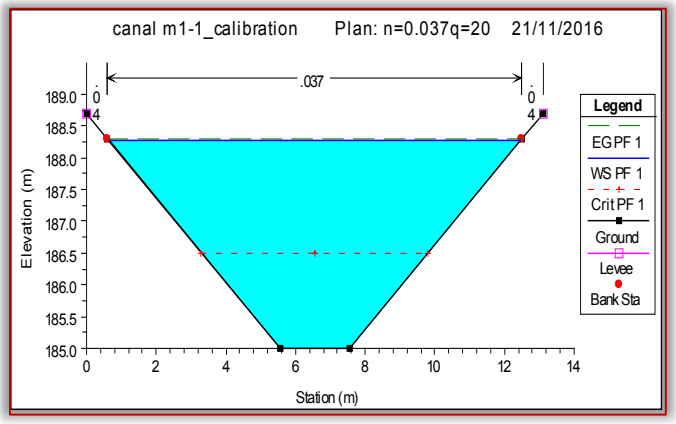

Figure 4 - Canal cross section plot for roughness coefficient n =0.037and inlet discharge Q_{in} =20 m^3/s.

Simulation of steady flow in the canal for different value of roughness coefficient n.

With the model of canal M1-1 simulations were conducted for different values of roughness in order to diagnose the condition of the lining and study the parameters of flow in canal and determining their limits. For several values of the roughness coefficient of the lined part of the cross section: n=0.017, 00.025, 0.035, 0.037 and inlet water discharge 18.5 m^3/s, a steady flow in the canal was simulated.

The analysis of the modeling results shows the influence of the roughness on the flow parameters in the irrigation canal. Figure 5 shows a longitudinal profile along the canal axis and water surface profiles for the different values of roughness coefficient. Increasing the roughness in the canal leads to an increase in canal depths. With further increases in roughness, the depths in the canal will reach the maximum of 3.3 m, set at design with the height of the lining. Therefore, in the poor condition of the irrigation canal lining the operating discharge should be reduced.

The simulated water surface profiles obtained can be used as reference for estimating the roughness in the presence of updated data for observed depths at characteristic points along the canal course.

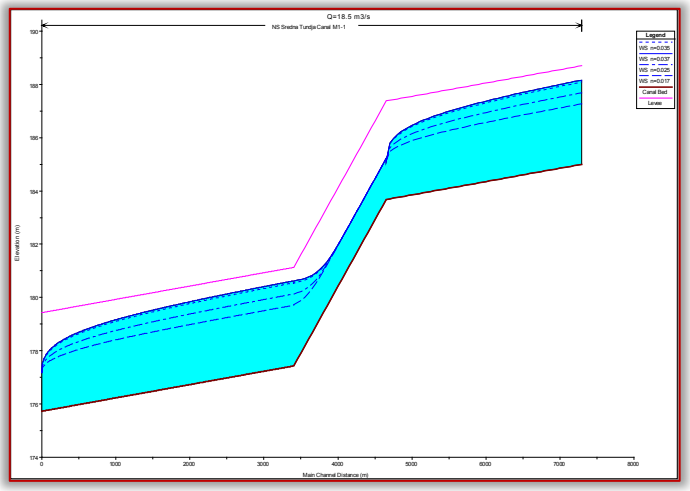

Figure 5 - Water surface profiles for different values of roughness coefficient n= 0.017, 0.025, 0.035, 0.037 and water discharge Q = 18.5 m^3/s

CONCLUSIONS

Using the HEC-RAS hydraulic software, a simulation model of the M-1-1 canal of „Sredna Tundja" irrigation system was established, which was calibrated under steady-state conditions with available operating data for observed depths. The results obtained in the hydraulic model studies have shown:

For roughness coefficient equal to 0.037 there is a good match to the simulated with the measured values of the depth at the end of the canal at a high degree of correlation (R^2= 0.987).

By determining the estimated value of the canal roughness, an actual value of the canal carrying capacity 20 m^3/s can be determined. A 50% reduction in capacity shows a significant worsening of the operational performance of the canal.

With the increase of the coefficient of roughness, which simulates the deterioration of the lining, the depth in the canal increases and it can reach the maximum determined during design.

The results of computer analysis can be used in the redesign and rehabilitation of existing canals and to select the appropriate procedure for the operational management.

Note

This paper is based on the paper presented at ISB-INMA TEH' 2017 International Symposium (Agricultural and Mechanical Engineering), organized by University "POLITEHNICA" of Bucharest – Faculty of Biotechnical Systems Engineering, National Institute of Research-Development for Machines and Installations Designed to Agriculture and Food Industry – INMA Bucharest, Scientific Research and Technological Development in Plant Protection Institute (ICDPP), National Institute for Research and Development for Industrial Ecology – INCD ECOIND, Research and Development Institute for Processing and Marketing of the Horticultural Products "HORTING" and Hydraulics, Pneumatics Research Institute INOE 2000 IHP, University of Agronomic Sciences and Veterinary Medicine of Bucharest (UASVMB) – Faculty of Horticulture and Romanian Society of Horticulture (SRH), in Bucharest, ROMANIA, between 26 – 28 October, 2017.

References

[1] Baume, J. P., Hilmy S., Malaterre P.-O., Jacques R., (1994), Development and Field-Installation of a Mathematical Simulation Model in Support of Irrigation Canal Management. IIMI, Research Paper, Colombo, Sri Lanka.
[2] Chow, V. T. 1959. Open channel hydraulics. McGraw-Hill, Inc. New York, N.Y.
[3] US Army Corps of Engineers, (2010). HEC-RAS User Manual. Hydrologic Engineering Center, Version 4.1.
[4] US Army Corps of Engineers, (2010), HEC-RAS Hydraulic Reference Manual. Hydrologic Engineering Center, Version 4.1.
[5] Mishra, A., Anand A., Singh R., N. S. Raghuwanshi (2001). Hydraulic modelling of Kangsabati main canal for performance assessment. J. Irrig. Drain. Eng, ASCE 127(1) 27-46.
[6] Malaterre, P.O., Baume J.P., Jean-Baptiste N., Sau J. (2010). Calibration of open channel flow models: a system analysis and control engineering approach. In Proc. SimHydro 2010:"Hydraulic modeling and uncertainty", 2-4 June 2010.
[7] Nguyen T. H, Fenton, D. J. (2004) Identification of roughness in open channels. Proc. of 6th International Conference on Hydro-Science and Engineering, Brisbance, Australia, June 2004.
[8] Timbadiya, P. V., Patel P. L., Porey R.D, (2012), Calibration of HEC-RAS model prediction of flood for lower Tapi River, Journal of Water Resource and Protection, 4, pp. 847-850.

ISSN: 2067-3809

[1.]Cosmin SPIRCHEZ, [1.]Alina LUNGULEASA, [2.]Maria PRUNĂ, [1.] Liviu GACEU,
[1.]Raluca FORFOTĂ, [1.]Irina DUMITRACHE

RESEARCH ON THE CALORIFIC VALUE OF THE HARDWOOD SPECIES

[1.]Transilvania University of Braşov, ROMANIA
[2.]Institute for Research in Construction Technology and Equipment Bucharest, ROMANIA

Abstract: Romania is a country with a great potential in the field of biomass energy. At the level of 2016, an area of 229973 km^2 was used for agricultural and forestry purpose of which the forest area was 4.7%. The lands covered by the forest are widely exploited and the waste resulting from the processing of cut wood is often left to degrade producing water pollution. Renewable energy resources represent one of the replacement variants for fossil fuels in Romania and worldwide with high development perspectives in the future. Presently, biomass contributes by approximately 12% to the production of primary energy in worldwide and in the developing countries this occupies 40-50% of the necessary energy. Biomass resources presently represent the raw material resulted from wood processing, agricultural, municipal waste and animal dejections. The determination of the calorific value for wood is similar to that of coal (as solid fuel) and with little differences as compared to liquid fuel (benzene) or gaseous one (natural gas, biogas).
Keywords: biomass, hardwood, calorimetric bomb, calorific value

INTRODUCTION

In the year 2000, the estimated contribution of the biomass to the European Union's energy supply was of 1900 PJ. This contribution was of approximately two thirds of the entire energy production achieved by renewable resources in the European Union.

For bioenergy, the following tendencies have been observed:

- Heat: In the year 1990, the production of thermal energy from biomass was of approximately 1500 PJ;
- Electricity: the production of electric energy from biomass was of 54 PJ in the year 1990 and increased to 166 PJ in 1999 (an increase of 9% per year);
- Fuel: the present contribution of biofuels is of approximately 25 PJ, almost negligible in the overall production of bio-energy.

Despite the modest role of bio-fuel in terms of energy, the production and use of biomass increased rapidly in the last 10 years. The production of bio-diesel increased from 80 Ktons in 1993 to 780 Ktones in 2001. The production of ethanol in the European Union increased from 48 to 216 ktones in the same period. France, Spain and Sweden are the three main players on the European energy market (*Berkesy. 2011*).

Up to the present, six member states of the European Union wish to enforce tax programs to support the use of bio-fuel (Austria, Belgium, Germany, Spain, Italy and Sweden). In these charts biofuels are exempt from taxes, as compared to fossil fuels used for transportation.

Renewable energy resources represent one of the replacement variants for fossil fuels in Romania and worldwide with high development perspectives in the future. In Romania, it is estimated an energy consumption of 34.9 Mtoe (million tones oil equivalent) until 2020. Biomass covers more than 60% of the entire renewable energy sources, respectively 190-200 PJ/year. (Gherghicescu,1997).

Presently, a great part of the energy necessary for humankind is produced from fossil fuels. Fuel can be found under three forms, respectively fossil fuel, nuclear fuel and renewable fuel. Researchers from all countries applied a multitude of projects in order to reduce carbon dioxide emissions (*Astburg. 2000*) .

In approximately 50 years, according to European Union statistics, all fossil fuels in the world will be exhausted. It is predicted that the entire world will suffer from a huge energy deficit which must be covered by production of alternative energy (*Eisentraut. 2012*). The biggest risk of fossil fuel use is represented by the toxic emission discharged in the atmosphere.

The production and consumption of fuel materials ensured the quality of living necessary for humankind. The biomass reserves differ throughout the territory of the European Union, as well as worldwide. The forest spreading area varies from 27. 6 million hectare in Sweden to 117 hectares in Cyprus. Worldwide, the forest fund occupies approximately 4 billion hectares, the biggest quantity being distributed on the territory of the Russian Federation- 809 million hectares, Brazil 478 million hectares, Canada 310 million hectares, U.S.A. 303 million hectares, China 197 million hectares.

Biomass is a renewable energy source by its renewal year after year; it is widely spread worldwide and possesses great costs as compared to fossil fuel. Biomass resources of which fuel material is produced. It may include wood, wood waste, agricultural cereals and waste resulted from their production, municipal waste, and animal dejections (*Beldean. 2004*).

Biomass under vegetal form is a complex compound and differs from a species to another. It contains all form of vegetal matter, growing on the surface of the earth, in the water or above the water, as well as substances produced by biological development (*Lunguleasa 2007.2008*).

Research performed in the field of energy proves that electrical energy and heat can be produced from biomass by conversion processes. In 2009, biomass ensured approximately 10% (50 EJ) (1EJ=10^{18} J) of the entire primary energy produced worldwide.

Biomass takes part in the carbon cycle in nature by use of carbon dioxide. Carbon dioxide participates to the photosynthesis processes during the growth, but it is the component determining a more complete burning during wood combustion (*Aghamohammadi. 2011*).

Presently, biomass contributes by approximately 12% to the production of primary energy in worldwide and in the developing countries this occupies 40-50% of the necessary energy.

Romania holds a surface of 6300 thousand hectares representing 27% of the existing territory.

Biomass resources presently represent the raw material resulted from wood processing, agricultural, municipal waste and animal dejections (Cleveland. 2009).

Biomass differs from the other renewable sources by the fact that it represents a rich raw material which can be transformed by various conversion processes in liquid, gaseous and solid fuel. Biomass is divided in 4 categories described in the Regulation SR EN 14961-1:

- Forestry production: wood, waste resulted from wood cutting, sawdust, shrubs;
- Waste resulted from agricultural production, cereal waste.
- Energetic cereals: crops from short term processing, starch crops (corn, wheat, barley), sugar crops (sugarcane, sugar beet), fodder crops (grass, alfalfa), oleaginous crops (sunflower, soy, safflower)

MATERIAL AND METHOD

The determination of the calorific value for wood is similar to that of coal (as solid fuel) and with little differences as compared to liquid fuel (benzene) or gaseous one (natural gas, biogas).

The equipment used for the determination of the calorific value of the wood biomass was the calorimeter with explosive burning type XRY-1C, manufactured by Shanghai Changji Geological Instrument Co. din China (Fig1).

Before performing the proper said attempt, the calorimetric bomb is calibrated with benzoic acid with a known calorific value (usually 26 463 kJ/kg (1kJ/kg=1J/g) with slight differences of maximum ±3% as compared to this value) in order to assess the *k* calorific coefficient of the calorific equipment.

$$PCS_s = k \cdot \left(\frac{(t_f - t_i)}{m_l}\right) - q_s - q_b [kJ/kg]; \quad (1)$$

where: k – calorific coefficient determined by calibration with benzoic acid, expressed in kJ/grad; t_f – final temperature, in degrees; t_i – initial temperature, in degrees; m_l – wood mass, in kg; q_s – heat consumed for the burning of the nickeline wire in kJ; q_b – heat obtained by burning of the cotton thread, in kJ.

The assessment procedure of the calorific value of the wood mass refers first to all to the preparation of the raw material and the equipment, then to the proper said assessment and finally to the obtainment of the final result. The preparation of the wood mass for testing consists of sampling a small part of a approximately 0.6 – 0.8 grams of the entire material weighted with a precision of 0.0002 g. The sample must be clean originating from freshly cut wood because old wood does not have all volatile and flammable substances, fact that might influence its calorific value. This sample is placed in a porcelain crucible and placed in a laboratory autoclave to allow drying at a temperature of 103±2 °C.

The obtainment of the anhydric state of the wooden mass is checked by successive weighting until the difference between the two successive weightings becomes smaller than the double of weighting precision or covers for a piece of such size of at least 2 hours of keeping the piece in the autoclave.

After drying, the samples are kept in exsiccator to cool down and maintain the humidity content until its placement into the calorimetric bomb.

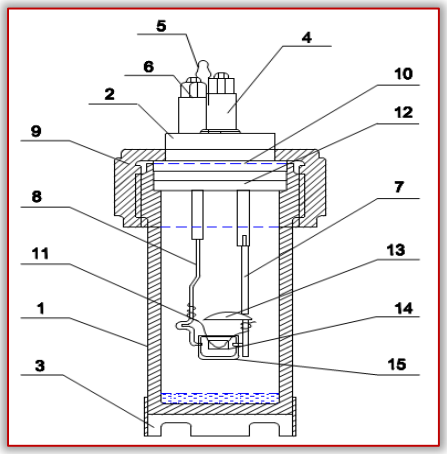

Figure 1 - Equipment for the assessment of the calorific value of the wood biomass with calorimetric bomb with own soft

In industrial practice there are manufacturing by remains from all wood species that can be processed. Therefore, in the research process the indigenous broadleaf category was used: Acer Pseudoplatanus and Salix Alba.

The inferior calorific value of wood is determined on basis of higher calorific value: by means of the ratio:

$$PCI_i = PCS_s - 6 \cdot (U + 9 \cdot h) [kJ/kg] \quad (2)$$

where: PC_s- superior calorific value (kJ/Kg); U- dampness of the wood sample (Kg/Kg); h- hydrogen content of the wood sample (3.6%).

The preparation of the equipment for the trial refers to the checking of the water quantity from the calorimeter or hod Cu (so as not to exceed by 1-2 mm the lid of the calorimetric bomb). The water Ap agitator A from the hod, the computer software C. the exterior thermometer of the calorimeter T and the gas pressure in the oxygen tank Bo. The test sample 1 is connected to the cotton thread 2 and placed in the calorimeter crucible 3. The nickeline spiral thread is tied 4 to the cotton thread after which the protection lid is properly

placed. 5. The crucible is connected to the calorimetric bomb's lid 6 by means of two electrodes 7 and 8 which continue with the connective electric wires of the calorimetric bomb 9 and 10. By screwing in the lid of the calorimetric bomb, the bomb is connected 11 by screw 12 to the oxygen tank, entering 30 atmospheres. The bomb is placed in the equipment calorimeter Cu, it is connected by means of the two electric wires. The calorimeter's lid is closed and the thermostat T is placed inside to determine the temperature (Figure1).

Next, the computer software is accessed filling in the type of test (assessment or calibration), sample name, sample mass of the nickeline and cotton thread, as well as further necessary information. After this, the operation for the assessment of the calorific value begins by selection and activation of the "START" button from the computer program displayed on the computer display (Figure2). This is the start moment of the calorific value assessment.

The final result of wood biomass burning is expressed by calorific value, notion by which is understood the quantity of heat obtained by burning of the mass unit. For combustible materials with high hydrogen and water content such as the wood biomass, two calorific values can be distinguished, namely the superior calorific (PCS) and inferior calorific value (PCI). PCS is determined directly by means of the calorimetric bomb where the water vapors are formed by burning of the hydrogen contained in the wood, as well as the ones formed by decomposition of the water are condensed in the bomb. Discharging approximately 2 510.4 kJ (600 kcal) for every kilo of condensed water vapors (the so-called condensation heat). PCS cannot be used, practically due to the fact that the water vapors are discharged outside by a funnel and only the PCI can be used effectively.

RESULTS

The test contains three distinct stages (Figure2), namely:

- the fore period ("fore"). Its purpose being the determination of the temperature variations in the calorimetric pot due to heat exchange with the exterior before the burning. During this period, usually lasting 5 minutes, the temperature is displayed and read every minute using the precision thermocouple meter. The last temperature from the fore period represents in fact the first temperature from the main period. The values of the recorded temperature in this period are usually seven. After recording the sixth value, the burning of the material takes place (Figure 2) and it is displayed on the menu bar ("Burning time").
- The main period ("main") starts by ignition of the sample having as consequence the temperature rise in the calorimetric pot due to burning of the wood particle and heat discharge. In order to determine the final temperature, the temperature values are displayed every minute. The final temperature is given by the maximum value of the temperature, because after its decrease, the calorimetric pot is not receiving heat from the bomb. The values recorded during this period vary depending on the burning time of the combustible material in the calorimetric bomb. The number of values may vary in the range of 19-42 temperature values recorded during this period.
- The after period ("after") has the purpose of determining the average temperature variation in the calorimetric pot due to heat exchange with the exterior after the burning. Just like in the fore period, the temperature is displayed every half minute for a period of 4-5 minutes, being recorded an average of 8-10 temperature variation values.

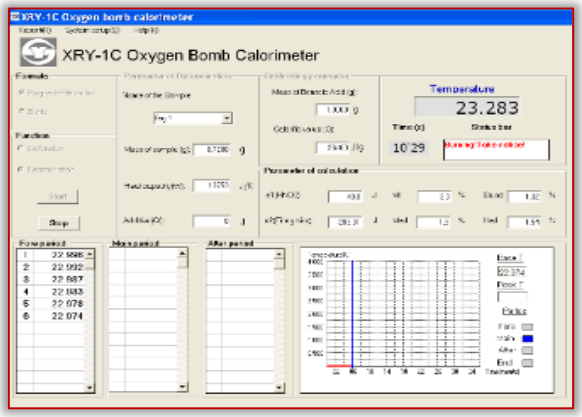

Figure2 - Description of the process for determining the calorific value

For acer pseudoplatanus for 0% humidity was obtained the superior calorific value 18802 kJ/kg. and inferior calorific value 18336 kJ/kg; for 10% humidity was obtained the superior calorific value 16805 kJ/kg and inferior calorific value 16618 kJ/kg; for 20% humidity was obtained the superior calorific value15041 kJ/kg and inferior calorific value 14668 kJ/kg; for 50% humidity was obtained the superior calorific value 9749 kJ/kg and inferior calorific value 9166 kJ/kg.

In Figure 3, is presented the variation calorific value function moisture content for Acer pseudoplatanus.

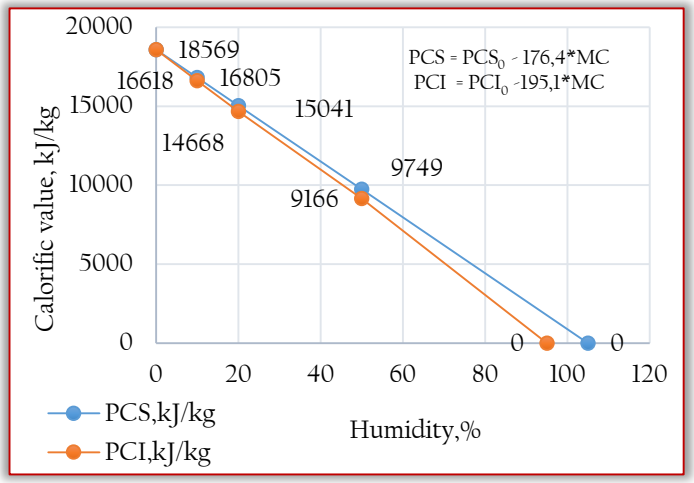

Figure 3 - The graphic calorific value for Acer pseudoplatanus

For salix alba for 0% humidity was obtained the superior calorific value 20830 kJ/kg. and inferior calorific value 20224 kJ/kg; for 10% humidity was obtained the superior calorific

value 17846 kJ/kg and inferior calorific value 17259 kJ/kg; for 20% humidity was obtained the superior calorific value14862 kJ/kg and inferior calorific value 14294 kJ/kg; for 50% humidity was obtained the superior calorific value 6364 kJ/kg and inferior calorific value 4944 kJ/kg.

In figure 4 is presented the variation of calorific value function moisture content for Salix Alba.

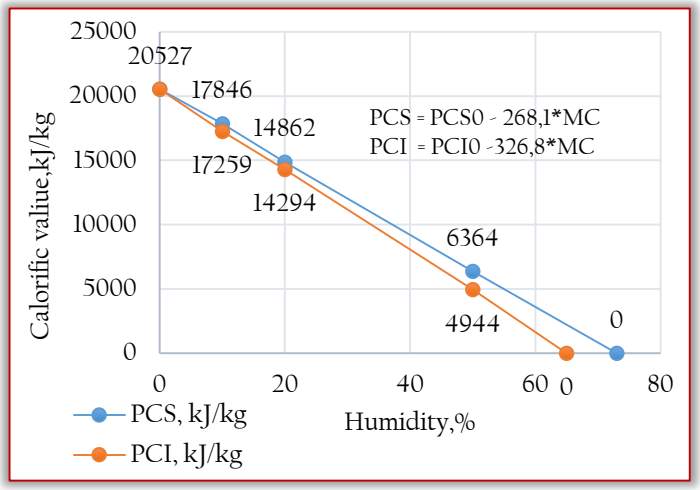

Figure 4 - The graphic of calorific value for Salix alba

CONCLUSIONS

- The wood biomass burning is a non-ecological process, but indispensable to human activity due to the thermal energy it produces;
- Wood biomass is twice renewable, first by being part of the vegetal world obtained by photosynthesis and secondly by trees recycling the carbon in the nature;
- For Acer Pseudoplatanus for 0% humidity the superior calorific value is 18802 kJ/kg and for 50% humidity the superior calorific value is 9749 kJ/kg; for Salix Alba for 0% humidity the superior calorific value is 20224 kJ/kg; for 50% humidity the superior calorific value is 6364 kJ/kg;
- The research shows that as the humidity of the wood is lower the superior calorific value is higher.

Note: This paper is based on the paper presented at ISB-INMA TEH' 2017 International Symposium (Agricultural and Mechanical Engineering), organized by University "POLITEHNICA" of Bucharest – Faculty of Biotechnical Systems Engineering, National Institute of Research-Development for Machines and Installations Designed to Agriculture and Food Industry – INMA Bucharest, Scientific Research and Technological Development in Plant Protection Institute (ICDPP), National Institute for Research and Development for Industrial Ecology – INCD ECOIND, Research and Development Institute for Processing and Marketing of the Horticultural Products "HORTING" and Hydraulics, Pneumatics Research Institute INOE 2000 IHP, University of Agronomic Sciences and Veterinary Medicine of Bucharest (UASVMB) – Faculty of Horticulture and Romanian Society of Horticulture (SRH), in Bucharest, ROMANIA, between 26 – 28 October, 2017.

References

[1] Abbasi S.A., Nipaney P.C., Schaumberg G.D. (1990) Bioenergy potential of eight common aquatic weeds, Biological Wastes, vol.3, No.4, pp. 359-366;
[2] Aghamohammadi N., Sulaiman N., Aroua M.K. (2011) Combustion characteristics of biomass in South East Asia, Biomass and bioenergy, vol.35;
[3] Astbury G.R. (2000) A review of the properties and hazards of some alternative fuels. Process safety and environment protection, vol. 86, pp. 397-414, 2008.
[4] Beldeanu C.E. (1999) Forestry products and wood study. Ed. Universităţii "Transilvania", Publishing Braşov;
[5] Beldeanu C.E. (2004) Sanogene characteristic species from forestry fund. Ed. Universităţii "Transilvania" Publishing, Braşov;
[6] Berkesy C., Begea A., Berkesy L., Crăciun M., Andreica M., Someşan M. (2011) Aspects of biomass production cominf from forests. Ecoterra. No.28;
[7] Cleveland J.C. (2009) Dictionary of energy. University of Boston Press;
[8] Dănilă A., Prună M., Spîrchez C. (2014) Dynamic models identification of the fireproofing wooden waste burning process, International Symposium Istanbul, 28-30 April 2014. Turkey
[9] Eisentraut A., Brown A. (2012) Technology Roadmap-Bioenergy for Heat and Power, Ed. Corlet, Paris;
[10] Lunguleasa A., Costiuc L., Paţachia S., Ciobanu V. (2007) Ecological combustion of wood biomass, Ed. Universităţii "Transilvania" Publishing, Braşov;
[11] Lunguleasa A. (2008) Management of wood biomass quality, Ed.Universităţii "Transilvania" Publishing, Braşov;
[12] Swithenbank J., Chen Q., Zhang X., Sharifi V., Pourkashamiani M. (2011) Wood would burn, Biomass and bioenergy, vol.3.

ISSN: 2067-3809

[1.]Marius Remus OPRESCU, [2.]Sorin Ştefan BIRIŞ , [1.] Eugen MARIN, [1.]Cristian SORICĂ,
[2.]Nicoleta UNGUREANU, [1.] Elena SORICĂ, [1.]Iulian DUMITRU, [1.]Ion GRIGORE, [3.]Vică BĂLAN

CONSIDERATIONS ON MECHANICALLY ACTIVE EQUIPMENT FOR OPENING INTERRUPTED FURROW USED IN TECHNOLOGY OF HOEING PLANT CULTURES, FRUIT AND VINE PLANTATIONS

[1.]National Institute of Research – Development for Machines and Installations
Designed to Agriculture and Food Industry – INMA Bucharest, ROMANIA
[2.]University "POLITEHNICA "Bucharest, Faculty of Biotechnical Systems Engineering, ROMANIA
[3.]Mido Rom Electronic SRL, ROMANIA

Abstract: Lately, there is a decrease in arable land surface while the population grows, therefore the need to increase agricultural production per unit of surface is a must to meet food needs. Water resources are reduced and therefore it is important to promote techniques and technologies that efficiently utilize water from various sources with low energy consumption. In sapling crops, directing water along the plant line or uniform storage is achieved with continuous or interrupted (compartmentalized) furrows. The paper aims to analyse the construction and operation of several types of equipment for opening compartmentalized furrows and how they work.
Keywords: efficient capitalization of water, technical equipment, interrupted furrow

INTRODUCTION

For soil supply with additional water to those naturally received by precipitation, quantities established according to the pedoclimatic conditions and plant requirements, it is necessary to establish additional works in the respective technologies.

Due to the fact that the arable area is decreasing as the population grows, the increase in agricultural production per unit of surface remains the main solution to meet the growing demands and better quality of food.

The achievement of large agricultural output is influenced by several factors (mechanization, fertilization, weed control, pests, biological soil potential, seed quality), each with its importance, but lack of soil water over periods overlapping the critical phases in plant development, diminishes the harvest even compromises it as a result of the drought.

In Romania, the area with economic irrigable potential is estimated at 3 million hectares, of out of which 1.5 million ha with high economic efficiency. In this context, irrigation will become the most important water consumer in agriculture and one of the main consumers nationwide, demanding on average 35-45% of the country's exploitable water resources. Water resources in Romania are low with a value of about 1660m3 / inhabitant and in other countries in Europe they are 2.5 times bigger and, therefore, it is important to promote techniques and technologies that efficiently capitalize water from various sources with low energy consumption, soil water and its circulation. About 41% of our country's arable land is affected at some times of the year by excessive humidity on about half of the arable area and in the same year longer or shorter droughts are recorded and watering with variable rules is required; soil erosion phenomena are manifested on 35% of the total agricultural area. Water resources in Romania are modest compared to other countries in Europe (11th place for local resources and 21st place for the ones formed on its territory) [1]

Due to the fact that for the watering of the plants an important amount of fresh water is used and their needs are higher in dry periods, other sources of water (groundwater, drainage, wastewater, precipitation water etc.) are needed which by their chemical composition qualitatively corresponds to plant requirements.

The effects of the watering process are felt both economically and socially and in environment protection. Watering ensures the normal development of agricultural crops which leads to stable revenues, by increasing the photosynthesis process to enriching the atmosphere in oxygen and reducing the carbon dioxide content, allowing the development of microbial activity in the soil and increasing the humus content by producing a quantity of increased by vegetal debris, avoiding the deterioration of the ecological balance by improving the drought-affected microclimate. Gravitation is the oldest form of irrigation. The surface leakage consists in the fact that water is distributed on the ground by free flowing on the furrows or strips, while the drain and the infiltration of water into the soil, take place. In general, the lands for watering are modelled by shaping them to ensure a continuous slope imposed by the general characteristics of the leakage, the watering method or the requirements of the agricultural exploitation.

The modelling of irrigable agricultural land is of particular importance because this work ensures a uniform distribution of water in the soil, whether it is conducted through furrows or strips on the surface of the land, or it is sprayed. Opening the interrupted furrows is necessary in the following situations:

- on landscaped lands for sprinkling with fixed or mobile installations and with uneven or sloping streams causing water leakage and pouring into microdepreses;
- on lands with kneaded microrelief with small slopes, not arranged for irrigation and in which rainwater flows rapidly downstream, being not used by the plant and producing the phenomenon of erosion [2].

MATERIAL AND METHOD

Watering is both an important technological sequence in the crop culture agro technology, as well as the most important technical means of eliminating the water of the soil, constituting the infrastructure of sustainable development. Technologies to combat the effects of climate change have evolved to reduce the water consumption of plants (dripping, micro-spraying). of the superior capitalization of water by reducing losses and associating with other works (fertilization, herbicides, etc.) and using other sources of water waste from animals or rural, urban and industrial environment).

To meet water requirements, it is necessary to adopt new technologies that reduce water consumption by associating with other works, storing water from other sources, distributing water near plant roots, increasing watering efficiency etc. The rational use of water in agriculture implies prioritization of water use in critical situations (droughts. etc.), the adoption of measures to impose the application of reference models, the application of innovative solutions for reducing water losses, the quality control of water for the reduction of environment pollution. A superior valorisation of the water from the rainfall and also of the water obtained by the sprinkler irrigation method is obtained by modelling the soil surface.

In the case of continuous or interrupted furrows, it is intended to obtain as many sections of the furrow as necessary to carry and accumulate as much water as possible. Interrupted brasses are executed to reduce the erosion phenomenon resulting from rainfall, slope or creep. Depending on the sowing scheme, interrupted watering grooves can be performed on sowing crops between plant rows, alternately or on each interval.

Furrows used in agriculture are of great importance for agricultural production and are a major component of the agricultural ecosystem [3] [4] [5] and [7].

It is estimated an increase in agricultural production per hectare by 20% in agricultural crops with broken furrows. This is explained by the infiltration of a larger amount of water at the plant roots and by the reduction of the soil erosion phenomenon [1]. Water management along the plant line or uniform storage is achieved with continuous or interrupted furrows (compartments).

For the constructive and functional analysis of mechanically operated equipment for open furrows used in owing crops technology and viticol and fruit plantations, it is necessary to study the constructive characteristics of these equipments, the functioning of the working parts and the working process carried out by them so that at the end to be able to recommend the best constructive solution that can be considered.

RESULTS

The open furrow work is known as soil processing by ridgeplowing (soil modelling) and was initially made with the help of some trailed animals.

This operation is done with a machine that works in aggregate with a tractor, the machine on which is mounted equipment for continuous furrows or specialized equipment for making interrupted furrows.

The machine equipped for the execution of the continuous furrows is made up of ridgeplows which make the tringhiular section of the furrow and the modifiers that make the parabolic section and the finishing of the furrow; the machine equipped for the execution of the interrupted furrows is composed of the same ridgeplows, the rotors with blades and a mechanism for controlling the rotors for interruption of the furrows and the execution of some digestions (plugs); both equipment is mounted on a frame with supporting wheels. The number of workstations is selected based on the sowing pattern, the section spacing and the row between the processed rows (on each interval or at two intervals). The most commonly used seed sowing scheme is 6 or 8 rows and the maximum number of machined intervals is 5 and 7 respectively, which must coincide with the number of workstations.

In the case of continuous or interrupted furrows, it is important to obtain an enlarged section of the furrow (Figure 1) to transport and accumulate a larger volume of water respectively.

Figure 1 - Continuous compartmented furows after rain [2]

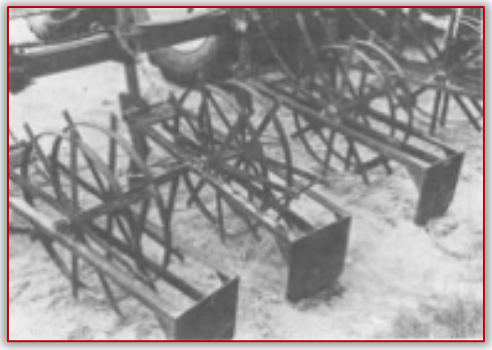

Figure 2 - Equipment for continuous open furrows [2]

Aspects during working with a broken open furrow are shown in Figure 3-6.

Figure 3 - Open furrow machine compartmented into each row interval [6]

Figure 4 - The open-beam machine is divided into three ranges

Figure 5 - Open furrow machine divided over a single interval [8]

Figure 6 - Open furrow machine compartimented over a single interval [9]

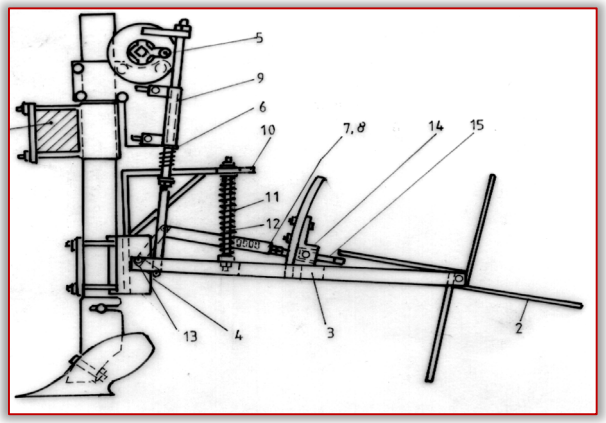

Figure 7 - Work unit with splitting furrow equipment [10]:
1. Equipment frame for opening watering furrows; 2. Pallets rotor; 3. Support arm; 4. Lever system; 5. Roller cam; 6. Resort traction; 7. Adjusting pipe; 8. Adjustment nut; 9. Guide; 10. Surface support; 11.Rod; 12. Compression resort; 13. Joint; 14. Lock bolt guide; 15. Bolt lock

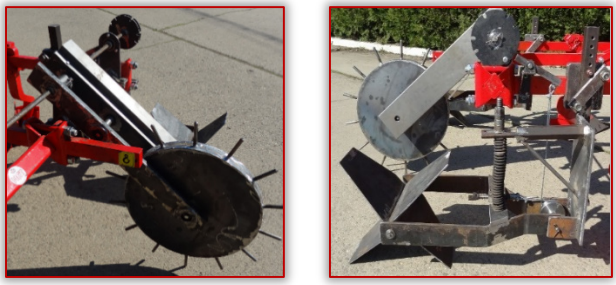

Figure 8 - Driving mechanism [6]

The adriving mechanism aims to unlock the pallet rotor to form the ground plug on the furrow. It consists of the following main parts:

- camshaft support;
- camshaft;
- lever / cable and locking bolt.

The control mechanism of the rotor blades in order to interrupt the furrows on variable lengths correlated with the slope of the ground is driven by the rotating wheel (Figure 8). The rotation motion is transmitted by means of a chain transmission (Figure 9) to a cam shaft positioned next to each work section.

During the rotation movement, the camshaft will operate the lever / cable mechanism from each section in the direction of unlocking the blade by means of the locking bolt and by rotating the blade, the furrow plug will be made at predetermined distances. The rotors will have three or four pallets of trapezoidal shape being pressed on the bottom of the furrow by two spring-mounted bends or spring-loaded spring bends. The time when the rotation of one of the pallets will be blocked by a bolt it will scrape the bottom and the side walls of the furrow by mobilizing a quantity of soil in front of it.

When the eccentric cam is operating the lever mechanism, the bolt retracts. releases the rotor with the blades, which rotates one step leaving a ground plug with a base width between 20 and 40 cm and the height equal to the depth of the furrow . While the blade rotor rotates with a 90 ° bolt released by the camming action, it returns to the previous position blocking the next rotor blade and then repeating the cycle. The device provides for the modelling of the watering compartments on the intervals between the plant ranges in two ways: alternatively a range with a furrow and a furrow interval or consecutive interval, depending on the sowing pattern, the soil type and the root zone [6].

Figure 9 - Chain transmission for driving the rotor control mechanism [6]

Since lately. temperatures have been growing at increasing intervals, watering of trees and vines is becoming a necessity. In FIGURE 10 is presented the equipment for modelling the soil in furrows divided into vineyard plantations, simultaneously in two furrows per interval PCMV2.2 + EMBC2-0. at a distance of 20-40 cm in order to accumulate water from precipitation in the soil on the surface to which the droplets fall, avoiding water leakage outside the cultivated perimeter or accumulation in depression areas on land with a slope of up to 5% on mild, medium or heavy texture, showing a depth of at least 250 mm at a near humidity by the minimum ceiling. The equipment consists of the following main components: 2 plows (left. right), a device for making split compartments provided with a control mechanism and optionally with two knife arrows if the simultaneous carrying of the pigs is desired. The plows are mounted on the plow frame in the lateral sides corresponding to the plowing in the bellows with the furrow overhanging inside the row, having the support of the deformed bodies towards the inside of the frame.

The device for making compartmented furorows consists of the following main parts: the control mechanism, the rotor support. the blade rotor and the presser mechanism of the rocker blades. The adjustment of the swath compartmenting mechanism will allow the creation of soil plugs along the furrow at different distances (1.5. 3 or 6 m).

The driving mechanism consists of spur gear, transmission and drive mechanism. The spur gear is provided with steel spurs on the belt to increase the grip on the ground, avoiding skidding. For the transport position, the spur gear will be locked in a vertical position. The transmission is of the chain type and has the role of transmitting the movement from the spur gear to the camshaft. The driving mechanism is designed to block the blade rotor to form the ground plug on the furrow.

Figure 10 - Equipment for soil modelling in furrows compartmented on fruit and vineyard plantations. simultaneously in two furrows per interval. PCMV2.2 + EMBC2-0 [6]

CONCLUSIONS

In order to provide the soil with additional water to those naturally received by precipitation, it is necessary to develop technologies adapted to the new pedoclimatic conditions.

Technologies to combat the effects of climate change have evolved to reduce the plants water consumption (dripping, micro-spraying), high water utilization by reducing losses and associating with other works (fertilization, herbicides. etc.) and using other sources of water waste from animals or rural, urban and industrial).

A superior capitalization of water from precipitation, as well as of water obtained by sprinkler irrigation method is obtained by shaping the soil surface in the form of continuous or interrupted furrows. It is estimated an increase in agricultural production per hectare by 20% in agricultural crops with lands so shaped.

Note: This paper is based on the paper presented at ISB-INMA TEH' 2017 International Symposium (Agricultural and Mechanical Engineering), organized by University "POLITEHNICA" of Bucharest – Faculty of Biotechnical Systems Engineering, National Institute of Research-Development for Machines and Installations Designed to Agriculture and Food Industry – INMA Bucharest, Scientific Research and Technological Development in Plant Protection Institute (ICDPP), National Institute for Research and Development for Industrial Ecology – INCD ECOIND, Research and Development Institute for Processing and Marketing of the Horticultural Products "HORTING" and Hydraulics, Pneumatics Research Institute INOE 2000 IHP, University of Agronomic Sciences and Veterinary Medicine of Bucharest (UASVMB) – Faculty of Horticulture and Romanian Society of Horticulture (SRH), in Bucharest, ROMANIA, between 26 – 28 October, 2017.

References

[1] Biolan I., Serbu I., Mardare F., Biolan C.(. 2015) – Modern techniques of irrigation of agricultural crops. AGIR Publishing House;
[2] Biolan I.. Serbu I.. Tusa G.C.. Mardare F.(.2016) - Agricultural Irrigation-Technology. AGIR Publishing House;
[3] Guo X.N., Hu T.S., Tan G.M., (2009) - Farmland drainage standard based on multi-attribute analysis. Transactions of the Chinese Society of Agricultural Engineering. 25(2009) 64-70;
[4] He X.C., Shao D.G., Liu W.Y. (2006) - Research progress and prospect of resource utilization of farmland drainage.Transactions of the Chinese Society of Agricultural Engineering. 22(2006) 176-179;
[5] Li Y.H. (2016) - A review of environmental effect and ecosystem function of farmland drainage ditch.Heilongjiang Science and Technology Information. (2016) 244;
[6] AQUAPROIECT S.A. (2017) - Project: Device for modelling the soil in compacted furrows in two constructive solutions. Contract no. 4639/2017-I.N.M.A;
[7] Song C.J., Li Q., Wang Y.,(2014) - Research overview of ecosystem effect of farmland drainage ditch.Modern Agricultural Sciences and Technology. 2(2014) 201-203.
[8] www.elsevier.com/locate/agwat
[9] http://ac.els-cdn.com/S0378377409000754/1-s2.0-S0378377409000754-main.pdf?_tid=8d834490-623d-11e7-8b80-00000aab0f02&acdnat=1499340396_162626dd2180dbed58d5727f8eaf263c
[10] http://www.revagrois.ro/PDF/2009_1_502.pdf

[1.]Mirela Nicoleta DINCĂ, [1.]Mariana FERDEŞ, [1.]Gigel PARASCHIV, [1.]Nicoleta UNGUREANU,
[1.]Bianca ZĂBAVĂ, [1.]Mariana IONESCU, [1.]Georgiana MOICEANU

RECOVERY OF ORGANIC WASTE THROUGH COMPOSTING PROCESS

[1.]University Politehnica of Bucharest, Faculty of Biotechnical Systems Engineering, ROMANIA

Abstract: Waste treatment involves all chemical, physical and biological processes that have the role of modifying certain characteristics of the waste in order to reduce their volume and hazardousness, thus facilitating their recovery. Among the available technologies, composting is presented as one of the most promising options for recycling the organic fraction into a valuable organic fertilizer called compost. In the present paper are presented the main composting methods, namely: passive composting in piles, turned windrow composting, passive aerated windrows, aerated static pile and in – vessel composting.
Keywords: waste treatment, composting methods, aerobic fermentation, organic waste

INTRODUCTION

Today, the most urgent environmental problem is global warming, the main challenge in the waste management sector being waste avoidance. Solid waste management, especially the organic fraction, has become one of the major challenges of the 21st century from an economic, social and environmental protection point of view (*Fernandez et al.*. 2016). Organic waste, such as agricultural and forestry residues and municipal solid waste, has become a major issue in both developed and developing countries (*Rashad et al.*. *2010*). Waste treatment involves all the chemical, physical and biological processes which have the role to modify certain features of the wastes in order to reduce their volume and hazardous character, thus facilitating their recovery *(Căpățână & Simonescu. 2006)*. According to Eurostat statistics, at the level of EU member states, 15% of the municipal wastes generated by one person in 2013 were treated by composting (*http://ec.europa.eu/eurostat*).

Among the methods of biological waste treatment, composting is the simplest and most efficient technology for treating the organic fraction. Composting can be defined as an aerobic process of biochemical decomposition of organic matter resulting in a stable product without pathogenic germs that can be used in agriculture (*Haug. 1993*; *Zhang & Sun. 2014*). The substrate used in the composting process consists of different sources of organic waste, such as: biodegradable waste collected from dwellings and households (kitchen waste, garden waste - cut grass, leaves, tree bark, debris from trimming trees and hedges, animal manure). residues from the processing of vegetables and fruits, residues from meat and fish processing, biodegradable municipal waste (sludge from wastewater treatment plants, newspapers, cardboard), waste from wood processing (sawdust, wood chips) and residues from agricultural crops (*Francou et al..2005*).

Transformation of organic matter during the composting consists of two complex processes, namely: *degradation* and *humification*. Over time, special attention has been given to the humification process, especially the formation of humic substances (humic and fulvic acids), due to their efficiency in improving soil fertility and stimulating plant growth (*Fornes et al.. 2012; Zhao et al. 2016*). During the first phase of the process, the simple organic carbon compounds are easily mineralised and metabolised by the microorganisms, producing CO_2, NH_3, H_2O, organic acids and heat. The optimum temperature range for composting is 40–65°C but temperatures above 55°C are required to kill pathogenic microorganisms. The temperature variation during composting plays an important role in the development of microbial communities. During the various stages of the biodegradation phase, the organic compounds are decomposed into CO_2 and NH_3 with O_2 consumption (*Bernal et al.. 2009*). In Figure 1, it can be seen the temperature curve during the composting process.

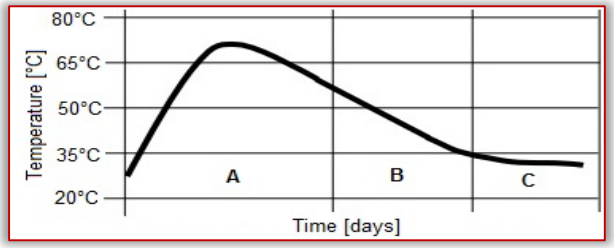

Figure 1 – The temperature curve during the composting process (Bachert et al.. 2008)
A – degradation; B – transformation; C – maturation

The pH level of the raw materials used in composting pile is also very important. The optimum pH range for microbial activity is between 6.5 and 8.0 (*Graves et al.. 2010*). Water is another important parameter for the survival of composting micro-organisms. The moisture content of the compost pile fluctuates during the composting as water is lost in evaporation process. If the substrate subject to composting is too dry, sprinkling with water must also be ensured during the decomposition process (*Paraschiv et al.. 2017*, *Graves et al.. 2010*).

Aeration is another key factor in the composting technology. A correct aeration controls the temperature, eliminates excess humidity and CO_2 and provides the O_2 required for biological processes. Optimal O_2 concentration is between 15 - 20% (*Bernal et al.. 2009*).

Maturation phase of substrate is the most important operation in the composting technique. The process is taking place in several phases and is decisively influenced by the composition, homogeneity and humidity of the organic substrate used and by the amount of air used in the decomposition process. The start-up phase of the maturing phase is the production of raw compost, the purpose of the operation being on the one hand ventilation and on the other hand the mixing of the raw materials at different stages of decomposition. In this phase, fresh compost is in a state of advanced decomposition, being semi mature. The mature compost is obtained after all organic components have been transformed into soil and humus aggregates, appearing in the form of black, loose and fine soil *(http://www.icpa.ro/documente)*.

Properly storing the finished compost product is the final step of the composting process. The finished compost should be stored in a manner that prevents dust or odours from developing and prevents contamination of the product from weeds, leachate or other contaminants (*http://www.compost.org*).

This paper was aimed to present the main composting methods used for organic waste treatment, namely: passive composting in piles, turned windrow composting, passive aerated windrows, aerated static pile and in – vessel composting.

MATERIAL AND METHOD

Composting methods differ in duration of decomposition, the potential for stability and maturity, depending on the type of substrate used (*Mengistu et al.. 2017*). The main five methods of composting developed for use in large-scale are passive composting piles, turned windrow composting, passive aerated windrows, aerated static pile and in-vessel systems.

RESULTS

Passive composting pile is the simplest form of composting and does not require special equipment, being used in principle for composting the leaves. The compost pile should be periodically turned for determining the porosity of the substrate. Aeration is done by passive air movement through the compost pile (Figure 2). This method requires that the pile be small enough to allow the passive air movement, otherwise the anaerobic zones will form (*Graves et al.. 2010*).

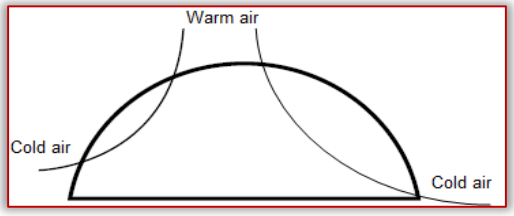

Figure 2 - Passive composting in pile (*Graves et al.. 2010*)

Turned windrow composting involves arranging the substrate in long and narrow furrows. The width of the compost pile is established depending on the size of the machine used to turn the organic material. The time required to finish the active phase of composting process using the windrow method ranges from 3 to 9 weeks (depending on the composted material), after that the maturation phase begins (Figure 3) (*http://esrd. alberta.ca/waste/composting-at-home, http://www.swrcb.ca.gov*).

Figure 3 - Turned windrow composting (*Bachert et al.. 2008*)

Passive aerated windrows does not require turning, the aeration being accomplished by passive air movement through the perforated pipes placed in the porous layer (peat moss, straw or matured compost) at the base of the pile (Figure 4). The porous layer can have a height of 15-20 cm and a width of 3 m. The main feature of this porous layer is to allow a uniform distribution of air in the pipes, but also to insulate the pile, which will ensure the optimum temperature during substrate degradation. The top layer (aprox. 15 cm) consists of peat moss or matured compost, which has the role of retaining moisture and unpleasant odors released during the decomposition process (*Graves et al.. 2010; http://esrd.alberta.ca/waste/composting-at-home).*

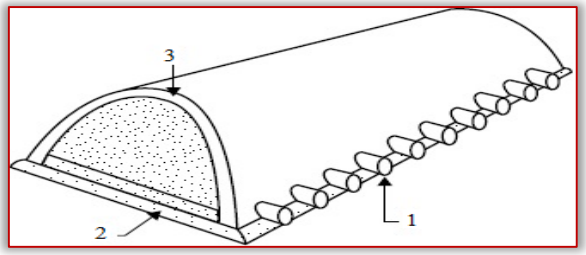

Figure 4 - Passive aerated windrow (*Graves et al.. 2010*)
1 – perforated pipe; 2 – base layer (compost. peat moss or straw base); 3 – coating layer (compost or peat moss)

Aerated static pile is one of the most used methods for composting and can last from 3 to 6 months, depending on the substrate used (Figure 5). The main difference between passive aerated windrow and aerated static pile is that the aerated static pile uses blowers that either suction air from the pile or blow air into the pile using positive pressure (*Stentiford. 1996*).

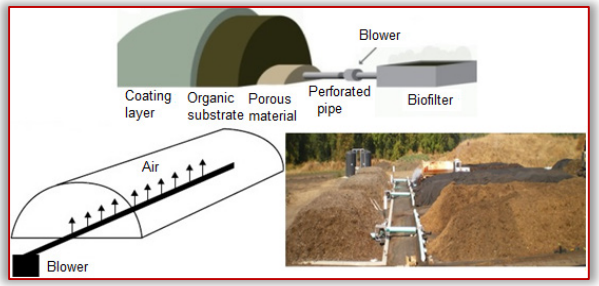

Figure 5 - Aerated static pile (*Graves et al.. 2010; http://compostingtechnology.com*)

At the base of the composting pile there are located perforated pipes for aeration connected to blowers that introduce or suck air from the composted substrate. The pipes are covered with a porous material made of wood chips or straw to allow a uniform air distribution in the pile. The final coating layer (15 cm) of the compost pile is often made of mature compost or sawdust to absorb unpleasant odors and moisture (*Graves et al.. 2010; http://compostingtechnology.com/)*. In this case, the composting pile is not turned. The dimensions of such a compost pile are: height between 1.5 and 2.5 m, the width of 3 – 5 m, while the length of the pile is limited by the air distribution in the pipes, but it should not be more than 21 - 27 m.

In – vessel composting involves the closure of organic waste in a container. Composting process can be done in bins (Figure 6) provided with aeration systems similar to those of aerated static piles or in bins without aeration systems to which it is necessary the regular turning of the substrate in order to maintain the aerobic conditions (*Graves et al.. 2010).*

Figure 6 – Composting process in bins (*Storino et al.. 2016*)

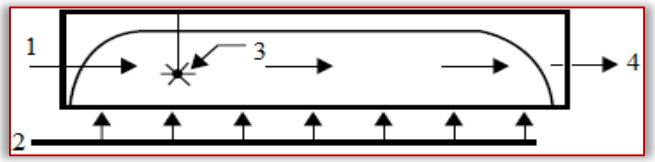

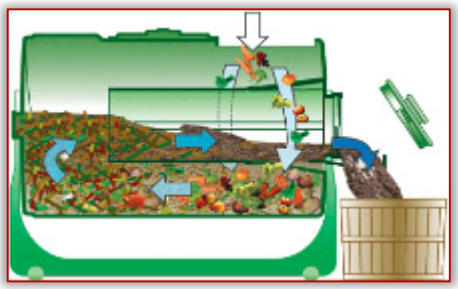

Figure 7 - Rectangular agitated bed (*Graves et al.. 2010*) and rotating drum composting (http://mtlion.com/gardencomposter/technology.html)
1 – organic substrate; 2 – air; 3 – turning device; 4 – compost

Another *in – vessel systems* are represented by rectangular agitated bed and rotating drum composting (Figure 7). The rectangular agitated bed system uses long and narrow beds where the composting taking place and an automated turner for periodic turning. In the case of rotating drum, the composting time is reduced to 2 – 3 weeks. These two systems require less work than windrows because they use an automated turning process or a self-turning mechanism (*Graves et al.. 2010*).

CONCLUSIONS

Composting cannot be considered a new technology, but amongst the waste management methods it is gaining interest as a suitable option for organic waste with economic and environmental benefits. This process reduces the risk of spreading pathogens and weed seeds and the final product, called compost, can be used to improve soil quality and fertility.

Note

This paper is based on the paper presented at ISB-INMA TEH' 2017 International Symposium (Agricultural and Mechanical Engineering), organized by University "POLITEHNICA" of Bucharest – Faculty of Biotechnical Systems Engineering, National Institute of Research-Development for Machines and Installations Designed to Agriculture and Food Industry – INMA Bucharest, Scientific Research and Technological Development in Plant Protection Institute (ICDPP), National Institute for Research and Development for Industrial Ecology – INCD ECOIND, Research and Development Institute for Processing and Marketing of the Horticultural Products "HORTING" and Hydraulics, Pneumatics Research Institute INOE 2000 IHP, University of Agronomic Sciences and Veterinary Medicine of Bucharest (UASVMB) – Faculty of Horticulture and Romanian Society of Horticulture (SRH), in Bucharest, ROMANIA, between 26 – 28 October, 2017.

References

[1] Bachert C., Bidlingmaier W., Wattanachira S. (2008). Handbook on compost production in uncovered piles (rows) (Manual privind producerea compostului în grămezi (şiruri) neacoperite). European Compost Network ECN/ORBIT Publishing House. ISBN 3-935974-23-X. Germania;

[2] Bernal M.P., Alburquerque J.A., Moral R. (2009). Composting of animal manures and chemical criteria for compost maturity assessment. A review. Bioresource Technology. Vol. 100. pp. 5444–5453. Elsevier Science Publisher;

[3] Căpăţână C., Simonescu C.M. (2006). Storage, treatment and recycling of recoverable waste and materials (Depozitarea. tratarea şi reciclarea deşeurilor şi materialelor recuperabile). Matrix Rom Publishing House. ISBN (10) 973-755-058-7. Bucureşti/România;

[4] Fernandez C., Mateu C., Moral R., Sole–Mauri F. (2016). A predictor model for the composting process on an industrial scale based on Markov processes. Environmental Modelling & Software. Vol. 79. Iss. C. pp.156 – 166. Elsevier Science Publisher. Amsterdam/The Netherlands;

[5] Fornes F., Mendoza-Hernandez D., Garcia-de-la-Fuente R., Abad M., Belda R.M. (2012). Composting versus vermicomposting: A comparative study of organic matter evolution through straight and combined processes. Bioresource Technology. Vol. 118. pp. 296–305. Elsevier Science Publisher;

[6] Francou C., Poitrenaud M., Houot S. (2005). Stabilization of organic matter during composting: influence of process and feedstocks. Compost Science & Utilization. Vol. 13. Iss. 1. pp. 72 – 83. Taylor & Francis Publisher. Philadelphia/USA;
[7] Graves R.E., Hattemer G.M., Stettler D., (2010). National Engineering Handbook. Chapter 2: Composting. Part 637 Environmental Engineering. pp. 1-67. United States Department of Agriculture;
[8] Haug R.T. (1993). The practical handbook of compost engineering. Lewis Publishers. ISBN 0-87371-373-7. United States of America;
[9] Mengistu T., Gebrekidan H., Kibret K., Woldetsadik K., Shimelis B., Yadav H. (2017). Comparative effectiveness of different composting methods on the stabilization, maturation and sanitization of municipal organic solid wastes and dried faecal sludge mixtures. Environmental Systems Research. Vol. 6. Iss. 5. pp. 1 – 16. Springer Open Publisher;
[10] Paraschiv G., Dinca M.N., Ungureanu N., Moiceanu G., Toma M.L. (2017). Installations for waste recycling (Instalații pentru reciclarea deşeurilor). Politehnica Press Publishing House. 289 pages. ISBN 978-606-515-750-7. Bucureşti/România;
[11] Rashad F.M., Saleh W.D., Moselhy M.A. (2010). Bioconversion of rice straw and certain agro-industrial wastes to amendments for organic farming systems: 1. Composting. quality. stability and maturity indices. Bioresource Technology. Vol. 101. Iss.15. pp. 5952–5960. Elsevier Science Publisher;
[12] Stentiford E.I. (1996). The Science of Composting Part 1(Marco de Bertoldi. Ed.). Composting Control: principles and practice. pp.51 – 54. Springer Science + Business Media Dordrecht Publishing House. ISBN 978-94-010-7201-4. England/United Kingdom;
[13] Storino F., Arizmendiarrieta J.S., Irigoyen I., Muro J., Aparicio – Tejo P.M. (2016). Meat waste as feedstock for home composting: Effects on the process and quality of compost. Waste Management. Vol. 56. pp. 53 – 62. Elsevier Science Publisher;
[14] Zhao X.I., Li B.Q., Ni J.P., Xie D.T. (2016). Effect of four crop straws on transformation of organic matter during sewage sludge composting. Journal of Integrative Agriculture. Vol. 15. Iss. 1. pp. 232–240. Elsevier Science Publisher;
[15] Zhang L., Sun X., (2014). Changes in physical, chemical and microbiological properties during the two-stage co-composting of green waste with spent mushroom compost and biochar. Bioresource Technology. Vol. 171. pp. 274–284. Elsevier Science Publisher;
[16] ***Alberta Environment. The Composting Council of Canada. (1999). Mid-scale Composting Manual. 1st edition. no. T/506. ISBN 0-7785-0943-5 (on-line), http://esrd.alberta.ca/waste/composting-at-home/documents/MidscaleCompostingManual-Dec1999.pdf;
[17] *** Environment in the EU. 54/2015, http://ec.europa.eu/eurostat/documents/;
[18] *** Institutul Național de Cercetare-Dezvoltare pentru Pedologie. Agrochimie și Protecția Mediului. ICPA Bucureşti. (2006). Composting guide of household waste from periurban farms (Ghid de compostare a deşeurilor menajere din fermele periurbane). Estfalia Publishing House. Bucureşti/România, http://www.icpa.ro/documente/Ghid%20compostare%20deseuri%20menajere.pdf;
[19] *** Technical Document on Municipal Solid Waste Organics Processing. Environment Canada. 2013. http://www.compost.org/English/PDF/Technical_Document_MSW_Organics_Processing_2013.pdf. ISBN: 978-1-100-217079;
[20] *** http://www.swrcb.ca.gov/rwqcb5/board_decisions/tentative_orders/0705/dairies/dairies-baykeeper-att-g-7.pdf;
[21] *** http://compostingtechnology.com/aerated-pile-systems/aerated-static-pile-asp-system/;
[22] *** http://compostingtechnology.com/aerated-pile-systems/aerated-static-pile-asp-system/;
[23] *** http://mtlion.com/gardencomposter/technology.html.

ISSN: 2067-3809

[1.]M.J. AMBALI, [2.]B.O. SHITTU, [3.]A.O. BAMBE

IMPROVED PICTURE ARCHIVING AND COMMUNICATION MODEL FOR MEDICAL IMAGE MANAGEMENT

[1-3.]Department of Computer Engineering Technology Federal Polytechnic Offa, Kwara State, NIGERIA

Abstract: Picture Archiving and Communication Systems (PACS) is a technology employed in collection, storage, processing and retrieval of medical imaging data within the medical world like hospitals and medical diagnostic facilities across separate geographic locations. PACS breaks down the physical and time barriers associated with traditional film-based image retrieval, distribution and display. Added features may include compression of the captured images: without losing its functionality and hence enhance speed of transfer and time of communication, reduced storage space and memory usage. This feature is observed to be absent in the present model and implementation of picture archiving and communication system. Furthermore, images are store away with little description of the features and observation of practitioners on the image so stored; this has made PACS very limited in its uses in telediagnosis and distance teaching (education) of young radiologist. With the identified limitations with the existing model of PACS, an improved model for PACS was developed. This work developed an improved model for PACS with the incorporation of new features into the existing model. Its objectives were achieved implementing multimedia PACS; a reduction in transmission time and storage space requirements of radiological images was noticeable when compared with the existing model of PACS.

Keywords: medical images; teleradiology; Computed Tomography (CT); telediagnosis; work stations

INTRODUCTION

Picture Archiving and Communications System, abbreviated as PACS, enables medical images from imaging modalities such as x-rays and scans to be stored electronically and viewed on screens, so that medical practitioners and other health professionals can access the information. In th past, film has been almost the only medium for capturing, storing, and displaying radiological images. Film is a fixed medium with usually only one set of images available.

Electronic images and reports are transmitted digitally via PACS; this eliminates the need to manually file, retrieve or transport film jackets (Wagner, Morrison, Carrino, Schweitzer and Nothnagel, 2002). The medical images are stored in independent formats such as AVI, portable document file (PDF) and DICOM. The most common format for image storage is DICOM (Digital Imaging and Communications in Medicine).

In the past, film has been almost the only medium for capturing, storing, and displaying radiological images. Film is a fixed medium with usually only one set of images available. A PACS consists of four major components: the imaging modalities such as Computed Tomography (CT) and Magnetic Resonance Imaging (MRI), a secured network for the transmission of patient information, workstations for interpreting and reviewing images, and long and short term archives for the storage and retrieval of images and reports.

BACKGROUND

The principles of PACS were first discussed at meetings of radiologists in 1982. Various people are credited with the coinage of the term PACS. Cardiovascular radiologist Dr Andre Duerinckx reported in 1983 that he had first used the term in 1981. Dr Samuel Dwyer, though, credits Dr Judith M. Prewitt for introducing the term. Dr Harold Glass, a medical physicist working in London in the early 1990s secured UK Government funding and managed the project over many years which transformed Hammersmith Hospital in London as the first filmless hospital in the United Kingdom. Dr Glass died a few months after the project came live but is credited with being one of the pioneers of PACS (Bauman, Gell and Dwyer, 1996).

METHODOLOGY

— Architecture

Essentially, a PACS network consists of a central server which stores a database containing the images as shown in figure 1. This server is connected to one or more clients via a LAN or a WAN that provide or utilize the images. Web-based PACS is becoming more and more common: these systems utilize the Internet as their means of communication (Taira, Breant, Chan, Huang, and Valentino, 1996).

The software (thin or smart client) is loaded via ActiveX, Java, or .NET Framework. PACS workstations offer means of manipulating the images (crop, rotate, zoom, brightness, contrast and others). Modern radiology equipment, modalities, feed patient images directly to the PACS in digital form. For backwards compatibility, most hospital imaging departments and radiology practices employ a film digitizer.

The medical images are stored in an independent format. The most common format for image storage is DICOM (Rosslyn, 2001). (Digital Imaging and Communications in Medicine), a NEMA standard (Hori, 1996). As shown in the figure below, we have a central database which stores the images for a short or long time as the case may be, the database is populated by

different imaging modalities through the database gate way and acquisition gateway, the flow of data is controlled by the PACS controller and archive server, the users or client can then log on to use the stored images and data for the purpose of research or consultation or teaching of students as the case may be. This is achieved via a webserver and application software installed for such purposes.

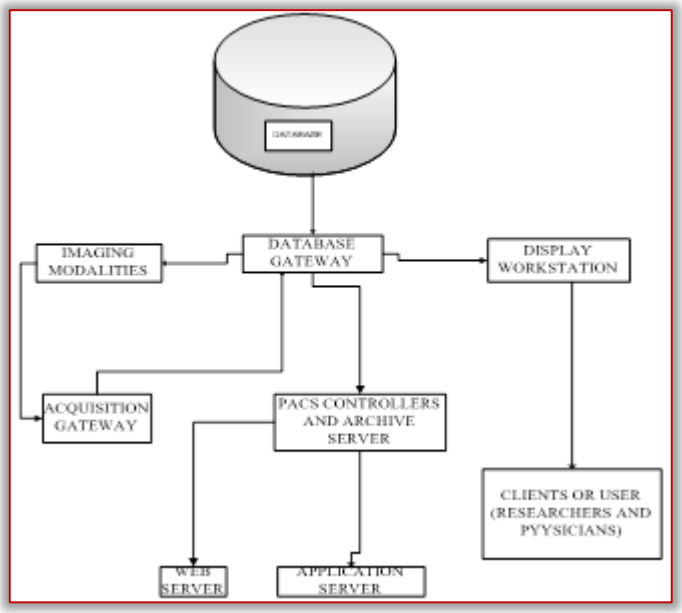

Figure 1: Basic Architecture of a PACS (Rosslyn, 2001)

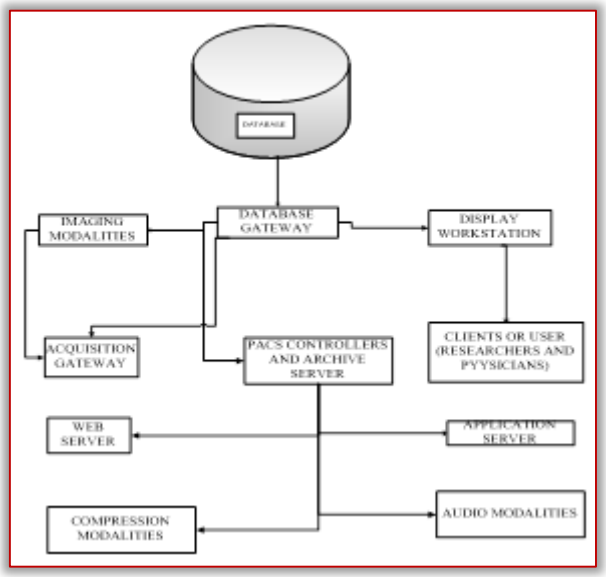

Figure 2: Proposed research framework

— Model Formulation

An evaluation of the model of the PACS led to the development of a robust model. An improved model was proposed and implemented to verify the assumptions acquired from the analysis of the scheme. During this stage, a further comparison of existing schemes and their architectures, and the new proposed solution were compared to extract similarity on the design and the improvement by this work. Analysis of selected cases was achieved from intensive study of related cases or examples of past activities.

WORKINGS OF THE PROPOSED MODEL

The physical layout of PACS as shown in figure 3 is the physical representation of how several modalities interacts to form the Picture Archiving and Communication System. The input modality comprises of the scanners, digitizers, CT scan, MIR scan and other means of capturing images. The images are captured from any of the clients or server and are stored on a dedicated database. Any user at a remote area can have access to these images wirelessly.

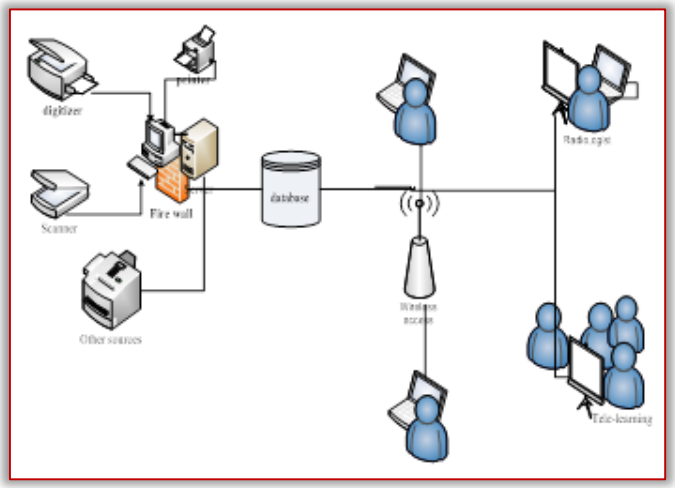

Figure 3: Physical layout of PACS (Alamu. 2011)

The conceptual frame work of PACS depicts the abstraction of the whole interaction of individual component of PACS as shown in figure 4. Abstraction is the ability of a researcher to bring to light what he thinks in his mind to tangible representation. In figure 4, all the modalities are grouped into sections like the, imaging modalities which includes the CT, MIR and Ultra Sound scanning machines, remote hospital which is made up of the local server, local client and gadgets for effective communication, central image archives which serves as a coordinating points for all the entry and exit of images in to the PACS. It contains the storage server clusters and routers to send images to the correct locations. Another section is the Image display and hard copy printing, this serves to display the images so stored on the database, and on extreme situation a print of the image may be ordered. All these functional parts and their communication is depicted in Figure 4.

The flow of work in the Picture Archiving and Communication System is depicted in figure 5, the imaging modalities are used for capturing the images and are stored in the database of PACS, the doctors and radiologist input their comment on the image and diagnosis is done based on the comment of the medical practitioners. If the image captured is to be frequently used (i.e. by an unstable patient that is it is frequently used for consultation), then the image is stored in a nearline storage device else it is stored permanently. From the nearline storage, the images can be used for referrals or

for teaching purposes during ward round, the referrals are done on a secured network.

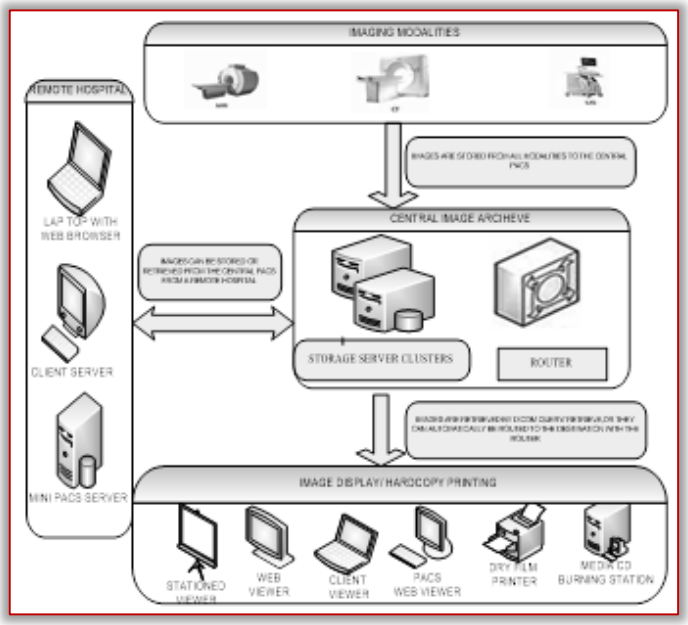

Figure 4: Conceptual frame work of PACS

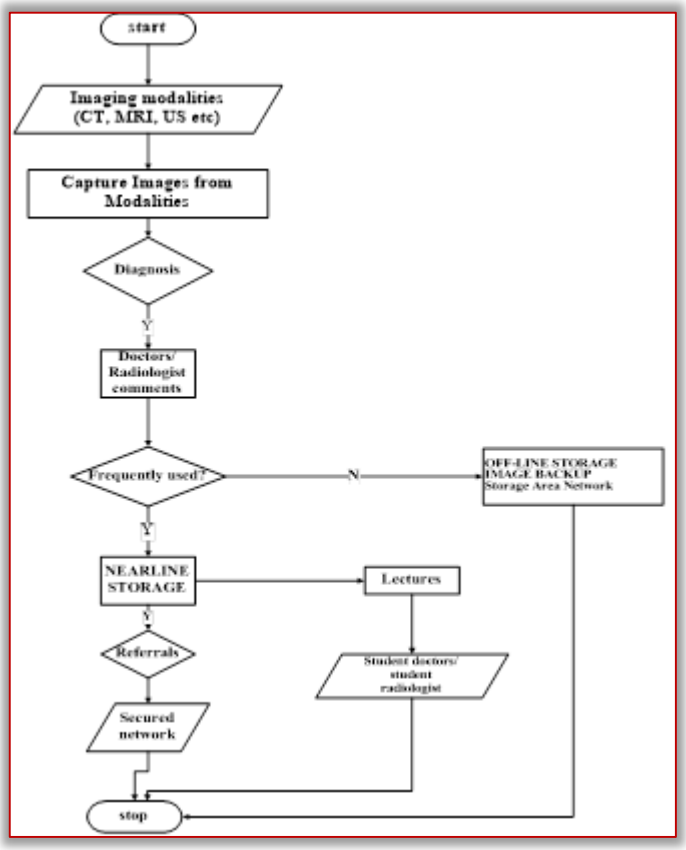

Figure 5: Flow chart of the operation of PACS

CONCLUSIONS

Picture archiving and communication systems (PACS) are responsible for solving the problem of acquiring, transmitting, and displaying radiologic images. The major benefit of PACS resides in its ability to communicate images and reports to referring physicians in a timely and reliable fashion.

The technical evolution toward more integrated systems and the shift toward Web-based technology are rapidly merging the two concepts of PACS and teleradiology in global image management and communication systems. PACS has been of tremendous help by helping to show patients their radiology images, by reducing the time spent finding images for review, by reducing the time spent finding radiology reports, by making consultations more time efficient. For clinicians whose practice is heavily dependent on radiology images, such as orthopedic surgeons and respiratory physicians, the advent of MPACS has made a substantial difference to the conduct of their clinics. PACS has made tremendous changes on the conduct of ward rounds.

References

[1] Alamu F. O. (2011). Development of a Robust Model for Picture Archiving and Communication System (M. Tech Thesis)," Submitted to Department of Computer Science and Engineering, Faculty of Engineering and Technology, Ladoke Akintola University of Technology Ogbomoso, Nigeria.

[2] Bauman R.A, Gell G, & Dwyer S.J. (1996). Large picture archiving and communication systems of the world Part 2. J Digit Imaging, 9, 172–7.

[3] Hori S.C., (1996), Image acquisition," Sites, technologies, and approaches". Radiol Clin North Am. 34, 469–94.

[4] Rosslyn (2001), "Digital Imaging and Communications in Medicine (DICOM)," National Electrical Manufacturers Association, PS 3.1-2001, pp iii–iv, 4–12.

[5] Taira R.K., Breant C.M., Chan H.M., Huang L., & Valentino D.J., (1996). Architectural design and tools to support the transparent access to hospital information systems, radiology information systems, and picture archiving and communication systems. J Digit Imaging, 9, 1-10.

[6] Wagner S.C., Morrison W.B., Carrino J.A., Schweitzer M.E. & Nothnagel H (2002). Picture archiving and communication system: Effect on reporting of incidental findings. Radiology, 225, 500–5.

ISSN: 2067-3809

Fascicule 1

[January - March]

t o m e XII

[2019]

ACTA Technica CORVINIENSIS
BULLETIN OF ENGINEERING

ISSN: 2067-3809

MANUSCRIPT PREPARATION – GENERAL GUIDELINES

Manuscripts submitted for consideration to ACTA TECHNICA CORVINIENSIS – Bulletin of Engineering must conform to the following requirements that will facilitate preparation of the article for publication. These instructions are written in a form that satisfies all of the formatting requirements for the author manuscript. Please use them as a template in preparing your manuscript. Authors must take special care to follow these instructions concerning margins.

INVITATION

We are looking forward to a fruitful collaboration and we welcome you to publish in our ACTA TECHNICA CORVINIENSIS – Bulletin of Engineering. You are invited to contribute review or research papers as well as opinion in the fields of science and technology including engineering. We accept contributions (full papers) in the fields of applied sciences and technology including all branches of engineering and management.

ACTA TECHNICA CORVINIENSIS – Bulletin of Engineering publishes invited review papers covering the full spectrum of engineering and management. The reviews, both experimental and theoretical, provide general background information as well as a critical assessment on topics in a state of flux. We are primarily interested in those contributions which bring new insights, and papers will be selected on the basis of the importance of the new knowledge they provide.

Submission of a paper implies that the work described has not been published previously (except in the form of an abstract or as part of a published lecture or academic thesis) that it is not under consideration for publication elsewhere. It is not accepted to submit materials which in any way violate copyrights of third persons or law rights. An author is fully responsible ethically and legally for breaking given conditions or misleading the Editor or the Publisher.

ACTA TECHNICA CORVINIENSIS – Bulletin of Engineering is an international and interdisciplinary journal which reports on scientific and technical contributions. Every year, in four online issues (fascicules 1–4), ACTA TECHNICA CORVINIENSIS – Bulletin of Engineering [e-ISSN: 2067-3809] publishes a series of reviews covering the most exciting and developing areas of engineering. Each issue contains papers reviewed by international researchers who are experts in their fields. The result is a journal that gives the scientists and engineers the opportunity to keep informed of all the current developments in their own, and related, areas of research, ensuring the new ideas across an increasingly the interdisciplinary field. Topical reviews in materials science and engineering, each including:

- ✓ surveys of work accomplished to date
- ✓ current trends in research and applications
- ✓ future prospects.

As an open-access journal ACTA TECHNICA CORVINIENSIS – Bulletin of Engineering will serve the whole engineering research community, offering a stimulating combination of the following:

- ✓ Research Papers – concise, high impact original research articles,
- ✓ Scientific Papers – concise, high impact original theoretical articles,
- ✓ Perspectives – commissioned commentaries highlighting the impact and wider implications of research appearing in the journal.

ACTA TECHNICA CORVINIENSIS – Bulletin of Engineering encourages the submission of comments on papers published particularly in our journal. The journal publishes articles focused on topics of current interest within the scope of the journal and coordinated by invited guest editors. Interested authors are invited to contact one of the Editors for further details.

BASIC INSTRUCTIONS AND MANUSCRIPT REQUIREMENTS

The basic instructions and manuscript requirements are simple:

- ✓ Manuscript shall be formatted for an A4 size page.
- ✓ The all margins of page (top, bottom, left, and right) shall be 20 mm.
- ✓ The text shall have both the left and right margins justified.
- ✓ Single-spaced text, tables, and references, written with 11 or 12-point Georgia or Times New Roman typeface.
- ✓ No Line numbering on any pages and no page numbers.
- ✓ Manuscript length must not exceed 15 pages (including text and references).
- ✓ Number of the figures and tables combined must not exceed 20.
- ✓ Manuscripts that exceed these guidelines will be subject to reductions in length.

The original of the technical paper will be sent through e-mail as attached document (*.doc, Windows 95 or higher). Manuscripts should be submitted to e-mail: redactie@fih.upt.ro, with mention "for ACTA TECHNICA CORVINIENSIS".

STRUCTURE

The manuscript should be organized in the following order: Title of the paper, Authors' names and affiliation, Abstract, Key Words, Introduction, Body of the paper (in sequential

headings), Discussion & Results, Conclusion or Concluding Remarks, Acknowledgements (where applicable), References, and Appendices (where applicable).

THE TITLE

The title is centered on the page and is CAPITALIZED AND SET IN BOLDFACE (font size 14 pt). It should adequately describe the content of the paper. An abbreviated title of less than 60 characters (including spaces) should also be suggested. Maximum length of title: 20 words.

AUTHOR'S NAME AND AFFILIATION

The author's name(s) follows the title and is also centered on the page (font size 11 pt). A blank line is required between the title and the author's name(s). Last names should be spelled out in full and succeeded by author's initials. The author's affiliation (in font size 11 pt) is provided below. Phone and fax numbers do not appear.

ABSTRACT

State the paper's purpose, methods or procedures presentation, new results, and conclusions are presented. A nonmathematical abstract, not exceeding 200 words, is required for all papers. It should be an abbreviated, accurate presentation of the contents of the paper. It should contain sufficient information to enable readers to decide whether they should obtain and read the entire paper. Do not cite references in the abstract.

KEY WORDS

The author should provide a list of three to five key words that clearly describe the subject matter of the paper.

TEXT LAYOUT

The manuscript must be typed single spacing. Use extra line spacing between equations, illustrations, figures and tables. The body of the text should be prepared using Georgia or Times New Roman. The font size used for preparation of the manuscript must be 11 or 12 points. The first paragraph following a heading should not be indented. The following paragraphs must be indented 10 mm. Note that there is no line spacing between paragraphs unless a subheading is used. Symbols for physical quantities in the text should be written in italics. Conclude the text with a summary or conclusion section. Spell out all initials, acronyms, or abbreviations (not units of measure) at first use. Put the initials or abbreviation in parentheses after the spelled-out version. The manuscript must be writing in the third person ("the author concludes... ").

FIGURES AND TABLES

Figures (diagrams and photographs) should be numbered consecutively using Arabic numbers. They should be placed in the text soon after the point where they are referenced. Figures should be centered in a column and should have a figure caption placed underneath. Captions should be centered in the column, in the format "Figure 1" and are in upper and lower case letters.

When referring to a figure in the body of the text, the abbreviation "Figure" is used Illustrations must be submitted in digital format, with a good resolution. Table captions appear centered above the table in upper and lower case letters.

When referring to a table in the text, "Table" with the proper number is used. Captions should be centered in the column, in the format "Table 1" and are in upper and lower case letters. Tables are numbered consecutively and independently of any figures. All figures and tables must be incorporated into the text.

EQUATIONS & MATHEMATICAL EXPRESSIONS

Place equations on separate lines, centered, and numbered in parentheses at the right margin. Equation numbers should appear in parentheses and be numbered consecutively. All equation numbers must appear on the right-hand side of the equation and should be referred to within the text.

CONCLUSIONS

A conclusion section must be included and should indicate clearly the advantages, limitations and possible applications of the paper. Discuss about future work.

Acknowledgements

An acknowledgement section may be presented after the conclusion, if desired. Individuals or units other than authors who were of direct help in the work could be acknowledged by a brief statement following the text. The acknowledgment should give essential credits, but its length should be kept to a minimum; word count should be <100 words.

References

References should be listed together at the end of the paper in alphabetical order by author's surname. List of references indent 10 mm from the second line of each references. Personal communications and unpublished data are not acceptable references.

- ✓ *Journal Papers:* Surname 1, Initials; Surname 2, Initials and Surname 3, Initials: Title, Journal Name, volume (number), pages, year.
- ✓ *Books:* Surname 1, Initials and Surname 2, Initials: Title, Edition (if existent), Place of publication, Publisher, year.
- ✓ *Proceedings Papers:* Surname 1, Initials; Surname 2, Initials and Surname 3, Initials: Paper title, Proceedings title, pages, year.

ISSN: 2067-3809

ACTA TECHNICA CORVINIENSIS – Bulletin of Engineering is an international and interdisciplinary journal which reports on scientific and technical contributions.

The ACTA TECHNICA CORVINIENSIS – Bulletin of Engineering advances the understanding of both the fundamentals of engineering science and its application to the solution of challenges and problems in engineering and management, dedicated to the publication of high quality papers on all aspects of the engineering sciences and the management.

You are invited to contribute review or research papers as well as opinion in the fields of science and technology including engineering. We accept contributions (full papers) in the fields of applied sciences and technology including all branches of engineering and management. Submission of a paper implies that the work described has not been published previously (except in the form of an abstract or as part of a published lecture or academic thesis) that it is not under consideration for publication elsewhere. It is not accepted to submit materials which in any way violate copyrights of third persons or law rights. An author is fully responsible ethically and legally for breaking given conditions or misleading the Editor or the Publisher.

The Editor reserves the right to return papers that do not conform to the instructions for paper preparation and template as well as papers that do not fit the scope of the journal, prior to refereeing. The Editor reserves the right not to accept the paper for print in the case of a negative review made by reviewers and also in the case of not paying the required fees if such will be fixed and in the case time of waiting for the publication of the paper would extend the period fixed by the Editor as a result of too big number of papers waiting for print. The decision of the Editor in that matter is irrevocable and their aim is care about the high content-related level of that journal.

The mission of the ACTA TECHNICA CORVINIENSIS – Bulletin of Engineering is to disseminate academic knowledge across the scientific realms and to provide applied research knowledge to the appropriate stakeholders. We are keen to receive original contributions from researchers representing any Science related field.
We strongly believe that the open access model will spur research across the world especially as researchers gain unrestricted access to high quality research articles. Being an Open Access Publisher, Academic Journals does not receive payment for subscription as the journals are freely accessible over the internet.

GENERAL TOPICS

ENGINEERING
- ✓ Mechanical Engineering
- ✓ Metallurgical Engineering
- ✓ Agricultural Engineering
- ✓ Control Engineering
- ✓ Electrical Engineering
- ✓ Civil Engineering
- ✓ Biomedical Engineering
- ✓ Transport Engineering
- ✓ Nanoengineering

CHEMISTRY
- ✓ General Chemistry
- ✓ Analytical Chemistry
- ✓ Inorganic Chemistry
- ✓ Materials Science & Metallography
- ✓ Polymer Chemistry
- ✓ Spectroscopy
- ✓ Thermo-chemistry

ECONOMICS
- ✓ Agricultural Economics
- ✓ Development Economics
- ✓ Environmental Economics
- ✓ Industrial Organization
- ✓ Mathematical Economics
- ✓ Monetary Economics
- ✓ Resource Economics
- ✓ Transport Economics
- ✓ General Management
- ✓ Managerial Economics
- ✓ Logistics

INFORMATION SCIENCES
- ✓ Computer Science
- ✓ Information Science

EARTH SCIENCES
- ✓ Geodesy
- ✓ Geology
- ✓ Hydrology
- ✓ Seismology
- ✓ Soil science

ENVIRONMENTAL
- ✓ Environmental Chemistry
- ✓ Environmental Science & Ecology
- ✓ Environmental Soil Science
- ✓ Environmental Health

AGRICULTURE
- ✓ Agricultural & Biological Engineering
- ✓ Food Science & Engineering
- ✓ Horticulture

BIOTECHNOLOGY
- ✓ Biomechanics
- ✓ Biotechnology
- ✓ Biomaterials

MATHEMATICS
- ✓ Applied mathematics
- ✓ Modeling & Optimization
- ✓ Foundations & Methods

ACTA TECHNICA CORVINIENSIS – Bulletin of Engineering has been published since 2008, as an online, free-access, international and multidisciplinary publication of the Faculty of Engineering Hunedoara.

We are very pleased to inform that our international and interdisciplinary journal ACTA TECHNICA CORVINIENSIS – Bulletin of Engineering completed its eleven years of publication successfully [issues of years 2008 –2018, Tome I–XI]. In a very short period it has acquired global presence and scholars from all over the world have taken it with great enthusiasm.

Every year, in four online issues (fascicules 1 – 4), ACTA TECHNICA CORVINIENSIS – Bulletin of Engineering [e-ISSN: 2067-3809] publishes a series of reviews covering the most exciting and developing fields of science and technology. Each issue contains papers reviewed by international researchers who are experts in their fields. The result is a journal that gives the scientists and engineers the opportunity to keep informed of all the current developments in their own, and related, areas of research, ensuring the new ideas across an increasingly the interdisciplinary field.

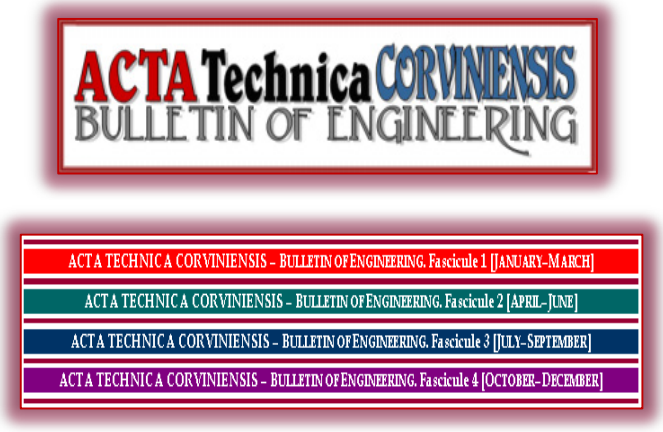

Now, when we celebrate the tenth years anniversary of ACTA TECHNICA CORVINIENSIS – Bulletin of Engineering, we are extremely grateful and heartily acknowledge the kind of support and encouragement from all contributors and all collaborators!

On behalf of the Editorial Board and Scientific Committees of ACTA TECHNICA CORVINIENSIS – Bulletin of Engineering, we would like to thank the many people who helped make this journal successful. We thank all authors who submitted their work to ACTA TECHNICA CORVINIENSIS – Bulletin of Engineering.

ACTA TECHNICA CORVINIENSIS – Bulletin of Engineering exchange similar publications with similar institutions of our country and from abroad.

ISSN: 2067-3809

INDEXES & DATABASES

We are very pleased to inform that our international scientific journal ACTA TECHNICA CORVINIENSIS – Bulletin of Engineering completed its eleven years of publication successfully [2008–2018, Tome I–XI].
In a very short period the ACTA TECHNICA CORVINIENSIS – Bulletin of Engineering has acquired global presence and scholars from all over the world have taken it with great enthusiasm.
We are extremely grateful and heartily acknowledge the kind of support and encouragement from all contributors and all collaborators!

ACTA TECHNICA CORVINIENSIS – Bulletin of Engineering is accredited and ranked in the "B+" CATEGORY Journal by CNCSIS – The National University Research Council's Classification of Romanian Journals, position no. 940 (http://cncsis.gov.ro/).
ACTA TECHNICA CORVINIENSIS – Bulletin of Engineering is a part of the ROAD, the Directory of Open Access scholarly Resources (http://road.issn.org/).

ACTA TECHNICA CORVINIENSIS – Bulletin of Engineering is also indexed in the digital libraries of the following world's universities and research centers:

WorldCat – the world's largest library catalog
https://www.worldcat.org/
National Lybrary of Australia
http://trove.nla.gov.au/
University Library of Regensburg – GIGA German Institute of Global and Area Studies
http://opac.giga-hamburg.de/ezb/
Simon Fraser University – Electronic Journals Library
http://cufts2.lib.sfu.ca/
University of Wisconsin – Madison Libraries
http://library.wisc.edu/
University of Toronto Libraries
http://search.library.utoronto.ca/
The University of Queensland
https://www.library.uq.edu.au/
The New York Public Library
http://nypl.bibliocommons.com/
State Library of New South Wales
http://library.sl.nsw.gov.au/
University of Alberta Libraries – University of Alberta
http://www.library.ualberta.ca/
The University of Hong Kong Libraries
http://sunzi.lib.hku.hk/
The University Library – The University of California
http://harvest.lib.ucdavis.edu/

ACTA TECHNICA CORVINIENSIS – Bulletin of Engineering is indexed, abstracted and covered in the world–known bibliographical databases and directories including:

INDEX COPERNICUS – JOURNAL MASTER LIST
http://journals.indexcopernicus.com/
GENAMICSJOURNALSEEK Database
http://journalseek.net/
DOAJ – Directory of Open Access Journals
http://www.doaj.org/
EVISA Database
http://www.speciation.net/
CHEMICAL ABSTRACTS SERVICE (CAS)
http://www.cas.org/
EBSCO Publishing
http://www.ebscohost.com/
GOOGLE SCHOLAR
http://scholar.google.com
SCIRUS – Elsevier
http://www.scirus.com/
ULRICHSweb – Global serials directory
http://ulrichsweb.serialssolutions.com
getCITED
http://www.getcited.org
BASE – Bielefeld Academic Search Engine
http://www.base-search.net
Electronic Journals Library
http://rzblx1.uni-regensburg.de
Open J–Gate
http://www.openj-gate.com
ProQUEST Research Library
http://www.proquest.com
Directory of Research Journals Indexing
http://www.drji.org/
Directory Indexing of International Research Journals
http://www.citefactor.org/

ISSN: 2067-3809